Design and Synthesis of Novel Coumarin-based Lignans as Pro-inflammatory Cytokine Inhibitors for the Treatment of Chronic Inflammatory Diseases

THESIS

Submitted in partial fulfillment

of the requirements for the degree of

DOCTOR OF PHILOSOPHY

by

SANTHOSH KUMAR S

ID. No. 2012PHXF0538H

Under the Supervision of

Prof. A. Sajeli Begum

BITS Pilani

Pilani | Dubai | Goa | Hyderabad

BIRLA INSTITUTE OF TECHNOLOGY AND SCIENCE, PILANI

2018

BIRLA INSTITUTE OF TECHNOLOGY AND SCIENCE, PILANI

CERTIFICATE

This is to certify that the thesis entitled "Design and Synthesis of Novel Coumarin-based Lignans as Pro-inflammatory Cytokine Inhibitors for the Treatment of Chronic Inflammatory Diseases" and submitted by SANTHOSH KUMAR S ID No 2012PHXF0538H for award of Ph.D. of the Institute embodies original work done by him under my supervision.

Signature of the Supervisor :

Name in capital letters : **A. Sajeli Begum**

Designation : **Associate Professor**

Date :

ACKNOWLEDGEMENTS

It is a great pleasure to utilize this unique opportunity to express my deep sense of gratitude and humble regards to ***Birla Institute of Technology and Science-Pilani, Hyderabad Campus.***

I am extremely grateful to my beloved research supervisor ***Prof. A Sajeli Begum****, Dept. of Pharmacy, for her support, patient guidance and cheerful encouragement throughout the research work at BITS-Pilani Hyderabad Campus, Hyderabad. A great human being, a holistic teacher, who took me under her wings, like how a parent takes and shielded me from all the weakness that I have encountered. It was my shear fortune, or may be a gift from above, that I was under her leadership, this feeling of delight and fullness that I am experiencing today in me, wouldn't had been possible without her immense efforts, skills, encouragement and excellent direction. Her broad knowledge, passion, visionary thinking, and invaluable advices have influenced me in so many ways. She was unparalleled in her critical assessment of methods, evaluation and interpretation of the results of this work. To me, she has become a model of good supervisor, mentor and a successful researcher.*

With great respect and honor, I would like to express my gratitude to our HOD ***Prof. D. Sriram,*** *Department of Pharmacy, BITS-Pilani Hyderabad Campus, Hyderabad for his knowledge, ever-willing help, valuable suggestion and constant presence to be a source of inspiration and motivation to carry out this research work. I deem my great privilege to thank DAC member,* ***Prof. P. Yogeeswari****, Associate Dean, Sponsored Research and Consulting Division, BITS-Pilani Hyderabad Campus, Hyderabad for her knowledge, ever-willing help, kind support, valuable suggestion, inspiration and constant encouragement throughout our project work.*

It's my privilege to express our deep sense of gratitude to ***Prof. Souvik Bhattacharyya****, Vice Chancellor,* ***Prof. S.C. Sivasubramanian****, Registrar,* ***Prof. G Sundar****, Director,* ***Prof. Sanjay Kumar Verma****, Dean,* ***Prof. Vidya Rajesh****, Associate Dean, Academic Research Division, BITS-Pilani Hyderabad Campus, for their support to do my research work.*

*I am thankful to **Dr. Onkar P. Kulkarni**, for his kind nature, disciplined technical advice, priceless intellectual guidance, uncompromising commitment, innovative and constructive ideas and perfection throughout the animal work. Truly my words and actions will not be enough in applauding him, but will surely make an attempt today saying, sir I am blessed and my whole life will never be able to repay for what I have received from you.*

*I am greatly acknowledge the help rendered by faculty members **Dr. Vamsi Krishna Venuganti, Prof Punna Rao Ravi, Dr. Arti Dhar, Dr. Balaram Gosh, Dr. Swati Biswas, Prof N Rajesh, Prof R Krishnan, Prof G Ramakrishnan** at BITS-Pilani Hyderabad Campus, Hyderabad. I express sincere thanks to **Prof. B.R. Prashantha Kumar**, JSS College of Mysore, JSS University, Mysore, for allowing us to carry out molecular docking studies with their facilities. I am extremely thankful to **Dr. Ameer Basha**, Scientist, PJTSAU, Hyderabad for his caring nature.*

*I am very much thankful to all of my friends **S. Mahibalan**, **Rukaiyya Khan**, **Poornachandar Rao**, **Ramya**, **Kirti Hira**, **Pragya**, **Samrun**, **V. Muralidharan, G. Susiharan, Sivan .C, Bobesh K Andrews**, **Manoj .C**, **Anup Jose, Praveen kumar .M**, **R. Reshma Srilakshmi**, **Nikhila .M**, **Prashanthi .M**, **V. Siva Krishna**, **E. Madhu Rekha**, **Girdhari Roy, Sudeep Kumar Gade, Rajaram, Kalyani, Kavitha, Pravesh**, **Sarfaraj Niazi, Madhu**, **Srikanth**, **Shubam Dwivedi**, **Barathi .M**, **A. Santhanakrishna Kumar, Mr. A. Praveen** for their whole hearted help, enthusiasm, valuable suggestions and best wishes during my research work.*

*I express my sincere thanks to non-teaching staff members **Mrs Baghyalakshmi**, **Mr. Praveen**, **Mr. Rajesh, Mrs. Saritha**, **Mr. Ramkishore, Mr. Srinivas**, **Mrs. Rekha, Mrs. Sunitha** and all central analytical laboratory technicians especially **Mr. Ramana Babu, Mr. Uppalaiah, Mr. K. Kumar, Mr. Mallesh G, Mr. Narasimha K, Mr. K. Swamy** for their kind co-operation even during odd hours during my research studies. And I express my sincere thanks to **mice**, who sacrificed their life to complete my project.*

Thesis work is dedicated to my family members. Last but not the least, I bow my head and thank to the Almighty God for blessing me with all the factors which summed up to complete my dissertation work successfully. I thank all whom I have not mentioned by name but nevertheless have been instrumental in the successful completion of this dissertation.

Santhosh kumar. S

ABSTRACT

The present thesis work discloses some potentially active coumarin-based lignan derivatives that are small molecule pro-inflammatory cytokine inhibitors for the treatment of chronic inflammatory conditions. In phase **I**, natural product derivatives like 7,8-dihydroxy-4-methyl coumarin (**1a**) and phenyl propanoids (**3b**, **4b**, **5b**) were identified to be significantly active against cytokines such as Tumor necrosis factor – alpha (TNF-α), Interleukin-1 Beta (IL-1β) and Interleukin-6 (IL-6) through synthesis and in-vitro lipopolysaccharides (LPS)-induced cell based assays (ELISA). Based on these observations, some structural analogues (**1a-7c**) of coumarins and phenyl propanoids were designed and docking studies were performed over TNF-α, IL-1β and IL-6 proteins using GOLD 5.2 software. Cinnamic acid derivatives displayed higher GOLDScore_fitness and more number of non-bonding interactions with TNF-α, IL-1β, and IL-6 target proteins as compared to coumarins, especially the ethyl cinnamates possessing acetyl units. With this background, the coumarins (**1a** and **1b**) and cinnamic acid derivatives (**3-7c**) were fused in different permutations and combinations to generate sixty novel fused-cyclic coumarin-based lignans (**8-13k**), which mimicked natural coumarinolignans. Docking studies on **8-13k** unravelled some interesting compounds which had high GoldScore_fitness, interesting active site interactions and distinctive π-π interactions when compared to the standards (cleomiscosin A, diclofenac sodium and prednisolone).

In phase **II**, some representative hit molecules (**9d**, **10d**, **11d** and **11e**) from phase I were selected for synthesis and pharmacological studies. Compounds **9d**, **10d**, **11d** and **11e** were synthesized

by oxidative coupling of 7,8-dihydroxy-4-methyl coumarin (**1a**) and ethyl cinnamate ester derivatives (**3b**, **4b** and **5b**) using diphenyl selenoxide as catalyst. All the compounds were found to show excellent inhibition effect under in-vitro TNF-α, IL-1β and IL-6 protein estimation assay by ELISA using LPS-stimulated RAW 264.7 cell lines, compared to the natural compound cleomiscosin A (**15**), which was isolated and characterized from the seeds of *Cleome viscosa* seeds for the study. Noticeably compound **10d** showed IC_{50} values of 8.5 µM, 22.48 µM and 47.57 µM against TNF- α, IL-1β and IL-6 proteins, respectively. Additionally, all the compounds decreased the LPS-induced nitric oxide (NO) levels significantly and possessed very weak cytotoxicity. Further, the effect of the coupled products (**9d**, **10d**, **11d** and **11e**) was found to be synergistic when compared to individual compounds **1a**, **3b**, **4b** and **5b**.

Further, oral administration of all synthetic compounds (**9d**, **10d**, **11d** and **11e**) and cleomiscosin A (**15**) at 50 mg/kg bodyweight exhibited potential anti-inflammatory effect when tested under two different in-vivo experiments i.e. LPS-induced endotoxemia and carragenan-induced paw edema models. Compound **10d** showed 66.41% inhibition of IL-1β, 62.56% inhibition of TNF-α and 43.15 % inhibition of IL-6 at 50 mg/kg body weight under LPS-stimulated mouse endotoxemia model. Also, compound **10d** was found to be most active showing inhibition effect at 50 mg, 30 mg and 10 mg/kg body weight as well, through oral administration. Besides, compound **10d** demonstrated inhibition of TNF-α (50.03%) and IL-1β (36.58%) expressions under carrageenan-induced inflammatory model and also effectively controlled the induced paw-edema for early two hours at 50 mg/kg body weight.

Further, compound **10d** was tested under crystal-induced renal nephropathy model. It exhibited inhibition of elevated levels of plasma blood urea nitrate (BUN) (49.95%) and IL-1β (37.5%)

and effectively controlled the induced renal inflammation as indicated by reduced RNA expression of renal inflammatory markers (IL-1β, IL-6 and TNF-α) and injury marker (KIM-1). Thus, compound **10d** also showed protection in renal histological damage induced by oxalate nephropathy.

Nevertheless, other compounds **9d**, **11d** and **11e** were also found to show significant (P<0.05) anti-inflammatory activity under mouse endotoxemia and carrageenan models. All the synthesized compounds were found to be more active than the natural coumarinolignan, cleomiscosin A (**15**). The structure-activity relationship of these set of molecules had also also been discussed. To the best of our knowledge the newly synthesized fused-cyclic coumarin-based lignans are structurally novel molecules discovered as pro-inflammatory cytokine inhibitors.

In another attempt of phase **III**, a glycoside derivative of cleomiscosin A (**15**) a natural coumarinolignan was designed. Synthesis, in-vitro assay and in-vivo studies of cleomiscosin A-9′-*O*-glycoside (**15g**) were carried out. The newly synthesized glycoside (**15g**) significantly inhibited (P<0.001 at 100 μM) LPS-induced IL-6 and IL-1β (IC_{50} values 7.94 and 45.76 μM, respectively) secretions. Under mouse endotoxemia model, cleomiscosin A glycoside (**15g**) showed 5-fold rise in TNF-α inhibition (52.03 % and 29.23 % at 50 and 25 mg/kg body weight, respectively) than its parent molecule, **15**. Further, docking studies on **15g** was performed over TNF- α, IL-1β and IL-6 proteins and was compared with **15** to understand the binding pattern and hydrophobic interactions. This is the first report of semi-synthesis and pro-inflammatory cytokine inhibition effect of a coumarinolignan glucoside.

In conclusion, all the chemical entities reported in the present work are novel small molecule inhibitors having molecular weight ranging between 300-550 daltons and possessing less cytotoxicity which can overcome the problems associated with macromolecules. Thus the compounds unveiled here are excellent therapeutic agents as they are blockers of multiple cytokines.

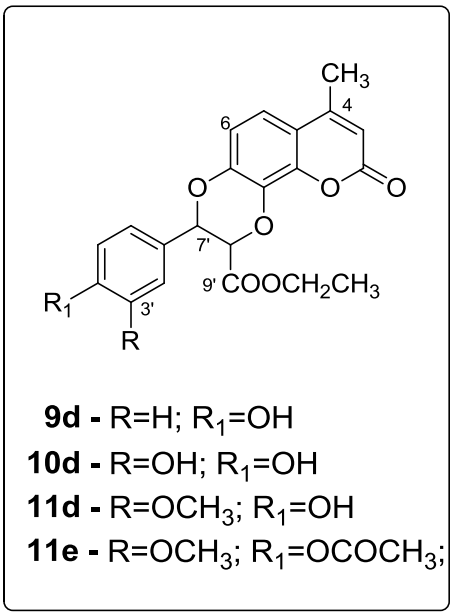

9d - R=H; R_1=OH
10d - R=OH; R_1=OH
11d - R=OCH_3; R_1=OH
11e - R=OCH_3; R_1=$OCOCH_3$;

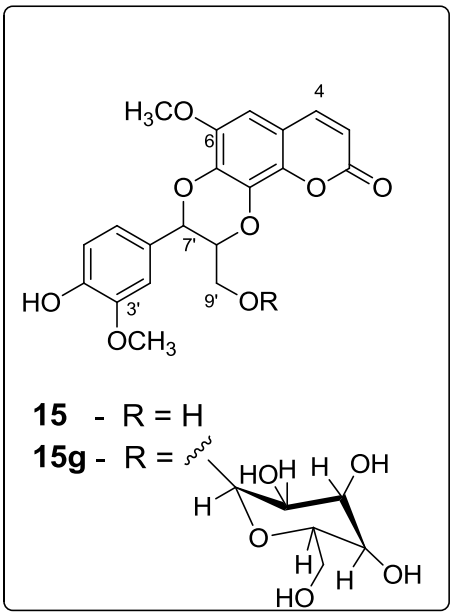

15 - R = H
15g - R =

TABLE OF CONTENTS

LIST OF TABLES

LIST OF FIGURES

LIST OF SCHEMES

ABBREVIATIONS

Ala	Alanine
APCI	Atmospheric Pressure Chemical Ionization
Arg	Arginine
Asn	Asparagine
Asp	Aspartic acid
BALB/c	Mouse strain
Cys	Cysteine
DCM	Dichloromethane
DMSO	Dimethyl Sulphoxide
DMSO-d6	Duteriorated Dimethyl Sulphoxide
ELISA	Enzyme-linked immune sorbent assay
ESI	Electro Spray Ionization
FT-IR	Fourier Transformer Infra Red
Gln	Glutamine
Glu	Glutamic acid
Gly	Glycine
GOLD	Genetic Optimization Ligand Docking
HETERO-COSY	Heteronuclear shift correlation
His	Histidine
HMBC	Heteronuclear Multiple-Bond Correlation
HPLC	High Performance Liquid Chromatography

IL-1β	Interleukin-1β
IL-6	Interleukin-6
Ile	Isoleucine
Leu	Leucine
LPS	LipoPolySaccharide
Lys	Lysine
Met	Methionine
min	Minute
mmol	millimole
MS	Mass Spectrum
MTT	[3-(4,5-dimethylthiazol-2-yl)-2,5-diphenyltetrazolium bromide]
NMR	Nuclear Magnetic Resonance
NO	Nitric Oxide
PDB	Protein Data Bank
Phe	Phenylalanine
ppm	Part Per Million
Pro	Proline
RCSB	Research Collaboratory for Structural Bioinformatics
SEM	Standard Error of Mean
Ser	Serine
Thr	Threonine
TLC	Thin Layer Chromatography
TMS	Tetramethylsilane
TNF-α	Tumor Necrosis Factor – α

Trp	Tryptophan
Tyr	Tyrosine
UV	Ultraviolet-Visible
Val	Valine
Ver	Version

SYMBOLS

°C	Degree Celsius
µg	Microgram
Å	Angstrom
C57BL/6J	Mouse strain
Cγ	Gamma carbon
h	Hour
$HClO_4 \cdot SiO_2$	Silica coated with perchloric acid
KDa	Kilodalton
MHz	Megahertz
nm	nanometer
ver	Version
δ	Chemical Shift
µl	Microlitre
µM	Micromolar

CHAPTER 1

INTRODUCTION

CHAPTER 1

INTRODUCTION

Up-regulation of specific pro-inflammatory cytokines has turned to be the key factor for the cause of most of the chronic inflammatory diseases. In acute and chronic condition cytokines exhibit signaling via complex and contradictory network of interactions. Since the sixty years span of first cytokine discover, more than 300 cytokines, chemokines, growth factors have been identified and studied for their specific role on human immune as well as organ system (Turner MD *et al*., 2014). Cytokines are found to be secreted by all type of nucleated cells, whereas hormones are produced by specific cells. They exhibit highly potent actions compared to hormones. Cytokines have been classified based on immune response, such as adaptive immunity, pro-inflammatory and anti-inflammatory cytokines. While, pro-inflammatory cytokines promote the inflammation, anti-inflammatory cytokines suppress the pro-inflammatory cytokines thereby reduce inflammation and promote wound healing (Dinarello CA., 2000). Up regulation of key cytokines IL-1β, IL-6 and TNF-α are detected in most of the chronic inflammatory diseases. These three cytokines play a key role in the spread and sustainment of inflammation. Additionally these cytokines lead to potent inflammation resulting in tissue damage and death (Zhang J-M and An J., 2007; Tsokos GC., 2011; Mclnnes LB and Schett G., 2011; Landskron G *et al*., 2014, Barnes PJ., 2018). Cytokines signal through oligomers of single-pass, type I transmembrane receptors, having distinct extracellular domains for ligand binding and intracellular domains that allow signal transduction (Turner MD *et al*., 2014).

TNF-α is a homo tetramer consisting of four chains (A, B, C and D) with sequence length 148 AA and its theoretical weight 16.41 KDa. IL-β is a monomer with sequence length 158 AA and its theoretical weight 17.81 KDa. IL-6 is homo dimer with sequence length 186 AA and its theoretical weight 21 to 28 KDa (data collected from RCSB PDB).

The existing steroid therapy for treating pain and inflammation often leads to organ toxicity via intracellular mechanism. Whereas biological anti-cytokines are found to be better than steroid drugs as they act via extracellular mechanism and they out-weigh the risk of organ damage. However, the biological anti-cytokines are highly challenging in their efficacy, safety and affordable cost. Also, at present no oral biological anti-cytokines are available commercially. Hence, development of small molecule inhibitors targeting the key cytokines, TNF-α, IL-6 and IL-1β may improve the current treatment of chronic inflammatory disease (Dinarello CA., 2010). Natural molecules such as flavonoids, polyphenolic compounds, coumarins, cinnamic derivatives, lignans have been reported for their anti-inflammatory property (Bisht K *et al*., 2010; Fylaktakidou KC *et al*., 2004; Katsori A-M and Hadjipavlou-Litina D., 2014; Grover J and Jachak SM., 2015; Zhou K *et al*., 2017; Godoy ME *et al*., 2000; Yuan G *et al*., 2006; Begum SA *et al*., 2010). However, most of the molecules are yet under clinical development for the treatment of chronic inflammatory disease. Among these, coumarins and phenylpropanoids were recognized to be interesting and hence the present study was carried out on these two groups of metabolites to develop oral anti-inflammatory molecule against chronic disease.

In the present research work, some phenyl propanoids and coumarin were synthesized and screened for their in-vitro pro-inflammatory cytokine inhibition activity. These moieties along with other compounds of similar derivatives were designed and docked against TNF-α, IL-1β and IL-6, and compared with standard drugs like prednisolone and diclofenac. Later fused

compounds of phenylpropanoids coupled with coumarins were designed and were similarly subjected for molecular docking. These novel molecules exhibited increased GOLDScore_fitness compared to the above set of molecules and this clearly indicated improved ligand affinity towards the target. Further, few representative feasible compounds having safe metabolism were synthesized and screened exclusively for their biological activity using in-vitro and in-vivo anti-inflammatory model. Also, attempts to make a glycoside derivative of cleomiscosin A as pro-inflammatory cytokine inhibitor are also discussed in this thesis.

CHAPTER 2

LITERATURE REVIEW

CHAPTER 2

LITERATURE REVIEW

2.1 Inflammation

Inflammation is a complex biological immune response caused due to injury. It involves cascade of molecular and cellular signals resulting in dilation of blood vessels, increased blood flow, increased vascular permeability, fluid exudation containing immunoglobulins (antibodies) and leukocytes (granulocytes, macrophages and lymphocytes). Among the leukocytes, long lived matured macrophages make the inflammation as chronic. These matured macrophages are formed from monocytes when it leaves the bloodstream and enters tissue. In turn macrophage release various chemical mediators IL-1, TNF-α and prostaglandins that bring about pro-inflammatory response. At later stages, B lymphocytes and T lymphocytes invade the affected tissues and destroy the cells (Nathan C and Ding A., 2010; Zhang H *et al*., 2008).

Finally, macrophages and other leukocytes release reactive oxygen species and protease causing the destruction of inflammation source. Often this damages the body's own tissue. Regeneration capacity of cells also play important role in the recovery of chronic inflammation, in which, neurons, cardiac cells, and skeletal muscle cells have little regenerative capacity. Inflammations to these cells are difficult to treat, but the skin cells proliferate faster thus making quicker wound healing (Zhang H *et al*., 2008).

Non-healing wound is the sign for chronic inflammation leaving the scientists a big challenge for treating the diseases like, rheumatoid arthritis, osteoarthritis, inflammatory bowel disease, chronic obstructive pulmonary disease and cancer (Drake VJ., 2007).

2.2 Inflammatory disease conditions

2.2.1 Vascular wall inflammatory and anti-inflammatory mechanisms

The inflammatory reaction involves the complex interactions between inflammatory cells (neutrophils, lymphocytes, and monocytes/macrophages) and vascular cells (endothelial cells and smooth muscle cells). It includes two groups of cytokines mediators functioning as pro-inflammatory signals (TNF, IL-1, IL-8, IFN-g, oncostatin M, IL-4, IL-13) and anti-inflammatory signals TGF-b, IL-10, IL-1ra, IL-13. Recently it has been revealed that, these pro-inflammatory cytokines play a vital role in causing vascular inflammation in several pathological conditions, including atherosclerosis, ischemia/reperfusion, hypertension, restenosis, angiogenesis, septic shock, and cerebral malaria (Tedgui A and Mallat Z., 2001).

2.2.2 Chronic Obstructive Pulmonary Disease (COPD)

COPD is caused due to chronic inflammation of the peripheral airways and lung parenchyma, followed by progressive narrowing of the airways and shortness of breath. This inflammation is resistant to treatment with corticosteroids and currently there are no safe and effective alternative anti-inflammatory treatments. Barriers to the development of anti-inflammatory treatments for COPD include poor understanding of the underlying inflammatory mechanisms and heterogeneity of disease, poor animal models, lack of biomarkers to predict therapeutic response, lack of a 'gold standard' for anti-inflammatory drugs and long duration of studies are needed to demonstrate clinical efficacy (Barnes PJ., 2013). The pro-inflammatory cytokines TNF-α, IL-6 and IL-1β are found to be present in the sputum, serum and bronchoalveolar lavage and these cytokines importantly act as the inflammation amplifier (Dentener MA., 2008; Dhimolea E., 2010; Strand V *et al*., 2012).

2.2.3 Alzheimer's disease and role of pro-inflammatory cytokines

Astrocytes are capable of producing a range of pro-inflammatory cytokines such as IL-1α, IL-1β, IL-6, and TNF-α, that have been found in the brain of Alzheimer's disease patients (Rubio-Perez JM and Morillas-Ruiz JM., 2012)

2.2.4 Neuroinflammation and the generation of neuropathic pain

Neuropathic pain is associated with excessive inflammation in both the peripheral and central nervous system which may contribute to the initiation and maintenance of persistent pain. Chemical mediators, such as cytokines, chemokines, and lipid mediators which are released during an inflammatory response cause sensitizing and stimulating nociceptors, their central synaptic targets or both (Ellis A and Bennett DLH., 2013). These changes can promote long-term maladaptive plasticity resulting in a persistent neuropathic pain. IL-1β, TNF-α and IL-6 are present in Schwann cells, mast cells, neutrophils, lymphocytes, macrophages, microglia, and astrocytes. Their action cause sensitizing nociceptors. TNF-α enhances excitatory currents, IL-6 reduces inhibitory currents, IL-1β enhances excitatory currents and reduces inhibitory currents. IL-1β directly sensitizes Transient Receptor Potential Vanilloid type 1 (TRPV1) receptors (Leung L and Cahill CM., 2010; Ren K and Torres R., 2009; Oka T *et al*., 1994).

2.2.5 Rheumatoid Arthritis (RA)

RA is an autoimmune disease which results in erosive joint destruction, progressive functional deterioration, systemic complications and high mortality (Scott DL *et al*., 2010). In addition, continuous use of biologics not only spurs an increase in the total medical cost but also may increase the risk of serious infections (Scott DL *et al*., 2012). The pathology in which T-cells become activated leading to stimulation of monocytes, macrophages, and synovial fibroblasts to produce inflammatory mediators. These mediators include TNF-α, IL-1, and IL-6 which cause

other cells to proliferate and release destructive matrix metalloproteinases, further promoting inflammation. These actions lead to the destruction of connective tissue and also drive receptor activator NF-kappaB ligand (RANKL) expression and osteoclast activation, the precursor to bone destruction (Choy EH and Panayi GS., 2001; Klareskog L *et al*., 2009; Lee DM and Weinblatt ME., 2001).

2.3 Anti-inflammatory drugs in clinical use

2.3.1 Non-Steroidal Anti-Inflammatory Drugs (NSAIDS)

a) Non-selective (Inhibit both COX-1 and COX-2) drugs – This include drugs like aspirin, ibuprofen and naproxen, which are safe for coronary artery disease. However they cause gastric irritation on prolonged use.

b) Selective COX-2 inhibitor - Drugs such as celecoxib, etoricoxib and lumiracoxib are in current use. Drugs, rofecoxib and valdecoxib have been withdrawn from market since 2004 due to adverse effects like heart attack and stroke. Also, these drugs cause cardiotoxicity, nephrotoxicity and are contraindicated in irritable bowel disorders (Chen YF *et al*., 2008).

Generally, NSAIDs should be used with caution in those with gastrointestinal, cardiovascular, or kidney problems. They appear to have no effect on people's long-term disease course and thus are no longer first line agents (Scarpignato C *et al*., 2015)

2.3.2 Disease-modifying antirheumatic drugs (DMARD)

Examples for DMARD include methotrexate, sulfasalazine, hydroxychloroquine, and leflunomide. Less frequently used medications include gold salts, azathioprine and cyclosporine which suppress the body's overactive immune and/or inflammatory systems. They take effect over weeks or months and are not designed to provide immediate relief of symptoms. The most

common side effects observed for these classes of molecules include liver damage, lung damage and low blood cell counts, fever, infections, and swollen lymph nodes (Kulkarni RG *et al*., 2006).

2.3.3 Biological agents

Biological agents are used if methotrexate and other conventional agents are not effective after a trial of three months. The adverse effects associated with TNF-α inhibitors are potentially serious. However, these risks are interpreted in the context of the potential benefits and of the adverse effects associated with conventional therapies for the treatment of immune-mediated diseases by physicians. The conventional therapies include drug treatments using glucocorticoids, methotrexate, cyclophosphamide, azathioprine, etc., (Belgi G and Friedmann PS., 2002).

The popular TNF-α blockers include infliximab and etanercept. Anakinra is a first-line interleukin 1 blocker. The monoclonal antibodies against B cells like rituximab and T cell costimulation blocker like abatacept are few of the well known therapies for auto-immune diseases (Beavers C and Adams A., 2010). Table 2.1 presents the information on the drugs used in various inflammatory disease conditions with their adverse reactions (Allosterix pharma 2011).

Table 2.1 Anti-inflammatory drugs in clinical use

Drug	Target	Rheumatoid arthritis	Psoriasis	Ankylosing Spondylitis	Crohn's disease	Ulcerative Colitis	Adverse events
NSAID	COX 1/COX 2	Pain relief	-	Pain relief	-	-	Cardiovascular risk
Methotrexate	T cells	First Line #1 effective Reverses disease, well tolerated	First Line #2 Effective	Second Line Pain relief, no DMARD	-	-	Liver damage: tolerated Works for 30-50% patients
Sulfasalazine	-	Used after MTX	-	Used after MTX no DMARD	effective	effective	GI events Allergy to sulphur
Arava leflunomide Sanofi	T cells	Used after MTX	-	-	-	-	Liver Toxicity
Enbrel etanercept Wyeth/ Amgen	TNF-α	#2 effective	#3 Effective	#2 effective, no DMARD	-	-	Cost, IV events antibodies
Remicade infliximab Schering-Plough	TNF-α	#3 effective	#1 Effective	#1 effective no DMARD	Used only if previous are not effective	Used only if previous are not effective	Cost, increase in TB/sepsis
Humira adalimumab.	TNF-α	Used only if previous are not effective	Used only if previous are not effective	#3 effective no DMARD	-	-	Upper respiratory TB
Orencia abatacept	T-cells	Used only if previous are not effective	-	-	-	-	Respiratory infections COPD
Other FDA approved drugs		Hydroxychloroquine Rituxan Celebrex	Cyclosporin with MTX, Raptiva	Physiotheray Kenalog Aristospan	Tysabri Cimzia	Colazad	-

- effectiveness rating from cross-analysis of randomized clinical trials (Allosterix pharma 2011).

2.4 Natural products as anti-inflammatory agents

Natural products play a significant role in the prevention and treatment of inflammatory conditions. There are different groups of natural products possessing good anti-inflammatory activity which include curcumin, parthenolide, cucurbitacins, 1,8-cineole, pseudopterosins, lyprinol, bromelain, flavonoids, saponins, marine sponge natural products and *Boswellia serrata* gum resin (Yuan G *et al*., 2006; Bisht K *et al*., 2010).

Curcumin is a polyphenol obtained from the rhizomes of *Curcuma longa.* The anti-inflammatory activity of curcumin is mainly due to the inhibition of arachidonic acid metabolism, cyclooxygenase, lipoxygenase, cytokines, interleukin and tumor necrosis factor and nuclear factor kappa B (Bisht K *et al*., 2010). Parthenolide, a sesquiterpene lactone found in *Tanacetum parthenium* possess anti-inflammatory action *via* inhibiting the gene-expression in inflammation such as nitric oxide (NO) synthase, intracellular adhesion molecule-1, and pro-inflammatory cytokines TNF-α, IL-1, IL-4, IL-8 and IL-12. In addition parthenolide also act as potent inhibitors of the pro-inflammatory transcription factor nuclear factor kappa B (Li-Weber M *et al*., 2002).

Cucurbitacins are the diverse triterpenes from cucurbitaceae, such as cucurbitacin B, D, E, I, dihydrocucurbitacin B and cucurbitacin R. They show anti-inflammatory activity *via* blocking nuclear factor kappa B activation (Kaushik U *et al*., 2015). 1,8-Cineole (eucalyptol), is a monoterpene oxide present in many essential oils from eucalyptus, sage, rosemary and Psidium reported to be useful in treating bronchitis, sinusitis and rheumatism. It has shown anti-inflammatory activity by inhibiting the production of TNF-α, IL-1, leukotriene B_4 and thromboxane B_2 (Yuan G *et al*., 2006)

Bromelain obtained from both the stem and fruit of the pineapple plant has been known to have anti-inflammatory effect by reducing oedema and pain. It also decreases the levels of PGE_2 and thromboxane A_2 (TXA_2) (Pavan R *et al*., 2012). Pseudopterosins, a diterpene glycosides mixture from *Pseudopterogorgia elisabethae* possess anti-inflammatory action through inhibiting the eicosanoid release from inflammatory cells (Correa H *et al*., 2009).

Flavonoids which are widely found in fruits, vegetables, grains, bark, roots, stems, flowers, tea, and wine have been proved to exert their anti-inflammatory effects *via* inhibition of COX and LOX activities, eicosanoid biosynthesis, and neutrophil degranulation. Several steroidal and triterpenoid saponins have shown anti-inflammatory activity (Yuan G *et al*., 2006). A recent study on non-conventional lignans like coumarinolignans, flavonolignans and stilbenolignans has revealed them as an interesting class of natural product found to have anti-inflammatory action and only fewer mechanistic studies have been carried out (Begum SA *et al*., 2010). In view of these, the focus of the present research turned towards coumarinolignans for developing newer anti-inflammatory drug.

2.4.1 Coumarinolignans: hope for anti-inflammatory drugs

Coumarinolignans are relatively newer group of plant-derived natural products, having two C_6C_3 units linked together but have additional structural features to place them also under the category of coumarins.

Literature search had revealed that coumarinolignans majorly cleomiscosins isolated from *Zanthoxylum avicennae, Hyoscyamus niger* had shown anti-inflammatory activities (Begum SA *et al*., 2010; Begum S *et al*., 2010) and fewer synthetic cleomiscosin A and its methyl ether analogs had shown significant inhibition of pro-inflammatory targets (TNF-α, IL-6 and IL-1β)

(Sharma S *et al*., 2010). Such biologically important anti-inflammatory coumarinolignans have been selected for the study to disocver safe and effective potent molecules.

2.5 Chemistry of coumarinolignans

Around 55 coumarinolignans has so far been isolated from various plant sources belonging to diverse families. The list of plants with the specific part and their families reported after 2008 are presented in Table 2.2. A review by Begum *et al*., had reported the data published before 2008 (Begum SA *et al*., 2010). The structures of all the natural coumarinolignans isolated and reported so far has been presented in Figures 2.1, 2.2 and 2.3.

Table 2.2 Sources of coumarinolignans

S. No.	Plant family	Plant species	Plant Part used for isolation (References)
1	Aceraceae	1a. *Acer saccharum* M.	Wood (Yoshikawa K *et al*., 2011)
		1b. *Acer mono* M.	Heartwood (Yim SH *et al*., 2015)
2	Annonaceae	2a. *Annona squamosa* L.	Air dried and pulverized seeds (Ranjan R and Sahai M., 2009)
3	Asteraceae	3a. *Chromolaena odorata* L.	Whole dried plants (Zhang ML *et al*., 2012)
4	Capparidaceae	4a. *Cleome viscose* L.	Seeds (Bawankule DU *et al*., 2008; Yadav NP *et al*., 2010; Tandon S *et al*., 2010)
5	Calycanthaceae	5a. C*himonanthus salicifolius* H.	Shade dried and powdered aerial parts (Li D *et al*., 2016; Wang KW *et al*., 2016)
		5b. *Chimonanthus nitens* Oliv.	Sun dried fine powder of roots, stems, leaves, branches and seeds (Tan T *et al*., 2017)
6	Chloranthaceae	6a. *Chloranthus japonicus* S.	Whole air-dried plants (Kuang HX *et al*., 2009)
7	Combretaceae	7a. *Terminalia tropophylla* H.	Dried roots (Cao S *et al*., 2010)
8	Compositae	8a. *Artemisia minor* J.	Powdered dry aerial parts (He ZZ *et al*., 2009)
		8b. *Xanthium sibiricum* P. (*Xanthium strumarium* L.)	Dried roots (Kan S *et al*., 2011)
9	Euphorbiaceae	9a. *Jatropha multifida*	Shade dried stem (Das B *et al*., 2008)
		9b. *Croton regelianus* var. *matosii* M.	Stems (Torres MCM *et al*., 2010)
		9c. *Euphorbia macrostegia* B.	Dried and crushed aerial parts (Demirkiran O *et al*., 2014)
		9d. *Euphorbia bupleuroides* D.	Powdered roots (Aichour S *et al*., 2014)
		9e. *Mallotus apelta* M.	Air dried and powdered roots (Xu JF *et al*., 2008)
		9f. *Sapium discolor*	Air-dried, powdered twigs and leaves (Liu H-B *et al*., 2016)
		9g. *Neoboutonia macrocalyx* Beng	Dried and powdered roots (Maffo T *et al*., 2018)
10	Malvaceae	10a. *Melochia umbellate* S.	Dried heartwood (Erwin *et al*., 2014)
		10b. *Kosteletzkya virginica* (L.) P.	Fresh tubers(Bai B *et al*., 2015)
		10c. *Durio zibethinus* M.	Cleaned, air-dried peels of durian (Feng J *et al*., 2016)
		10d. *Reevesia formosana*	Dried fruits (Hsiao P-Y *et al*., 2016)
		10e. *Abelmoschus sagittifolius*	Shade dried , coarse powdered stem tubers (Chen D-L *et al*., 2018)
11	Meliaceae	11a. *Aglaia odorata* L.	Air-dried, powdered twigs and leaves (Zhang H *et al*., 2012) Roots (Liu B and Xu YK., 2015)
		11b. *Turraeanthus mannii* B.	Dried and powdered root bark (Sielinou VT *et al*., 2012)

Table 2.2 Sources of coumarinolignans (Cont.)

S. No.	Plant family	Plant species	Plant Part used for isolation (References)
12	Oleaceae	12a. *Fraxinus rhynchophylla* D.	Stem barks (Ahn JH *et al*., 2012; Ahn JH *et al*., 2013)
13	Rubiaceae	13a. *Pentas schimperi* (Hook f.) V.	Dried and powdered stem bark (Donfack ARN *et al*., 2014) Air-dried and fine powdered roots (Dzoyem JP *et al*., 2016)
14	Rutaceae	14a. *Zanthoxylum avicennae* L.	Dried stem wood (Chen JJ *et al*., 2008)
		14b. *Melicope denhamii* S.	Air-dried leaves (Nakashima KI et al., 2012)
15	Sapindaceae	15a. *Eurycorymbus cavaleriei* L.	Air-dried pieces of the twigs (Cheng L *et al*., 2009)
		15b. *Pancovia Pedicellaris* R.	Air-dried and powdered stem bark (Soh RF *et al*., 2009)
		15c. *Allophylus longipes* R.	Air-dried, powdered stems (Xiang-Yun Z *et al*., 2012)
16	Simaroubaceae	16a. *Brucea javanica* M.	Dried Fruits (Yamada K *et al*., 2009) Seeds (Chen QJ *et al*., 2009) Dried ripe fruits (Zhao M *et al*., 2011) Powdered seeds (Yang J *et al*., 2014)
17	Solanaceae	17a. *Hyoscyamus niger* L.	Dried and coarsely powdered seeds (Begum S *et al*., 2010; Begum SA., 2010a; Begum S *et al*., 2006)
		17b. *Solanum indicum* L.	Air dried seeds (Yin HL *et al*., 2013)
18	Thymelaeaceae	18a. *Daphne mucronata* R.	Shade dried whole plant (Rasool MA *et al*., 2010; Ferheen S *et al*., 2014)
19	Tiliaceae	19a. *Christiana africana* DC.	Barks (Michalet S *et al*., 2008)
		19b. *Tilia taquetii* S.	Pulverized stems (Kang YM and Lee NH., 2011)
		19c. *Grewia optiva* D.	Stem bark (Uddin G *et al*., 2013)
20	Verbenaceae	20a. *Duranta repens* L.	Dried whole plant (Ahmad N *et al*., 2009)

Table 2.3 Coumarinolignans and their plant sources

Compound name (see Figure. 2.1 & 2.2)	Plant source(s) (see Table 2.2) (References)
Cleomiscosin A (**1**)	2a (Ranjan R and Sahai M., 2009) 3a (Zhang ML *et al*., 2012) 4a (Bawankule DU *et al*., 2008; Yadav NP *et al*., 2010; Tandon S *et al*., 2010) 5a (Li D *et al*., 2016; Wang KW *et al*., 2016); 5b (Tan T *et al*., 2017) 8a (He ZZ *et al*., 2009); 8b (Kan S *et al*., 2011) 9a (Das B *et al*., 2008); 9b (Torres MCM *et al*., 2010); 9e (Xu JF *et al*., 2008); 9f (Liu H-B *et al*., 2016) 10a (Erwin *et al*., 2014); 10b (Bai B *et al*., 2015); 10c (Feng J *et al*., 2016); 10e (Chen D-L *et al*., 2018) 11a (Zhang H *et al*., 2012); 11b (Sielinou VT *et al*., 2012) 12a (Ahn JH *et al*., 2012) 13a (Dzoyem JP *et al*., 2016; Donfack ARN *et al*., 2014) 15a (Cheng L *et al*., 2009); 15c (Xiang-Yun Z *et al*., 2012) 16a [Yang J et al., 2014; Yamada K *et al*., 2009; Zhao M *et al*., 2011) 17a [Begum SA., 2010a; Begum S *et al*., 2006) 19a (Michalet S *et al*., 2008); 19b (Kang YM and Lee NH., 2011) 20a (Ahmad N *et al*., 2009)
Cleomiscosin A methyl ether (**17**)	17a (Begum SA., 2010a)
Cleomiscosin B (**2**)	2a (Ranjan R and Sahai M., 2009) 4a (Bawankule DU *et al*., 2008; Yadav NP *et al*., 2010; Tandon S *et al*., 2010) 5a (Wang KW *et al*., 2016) 8a (He ZZ *et al*., 2009) 9e (Xu JF *et al*., 2008) 10b (Bai B *et al*., 2015); 10c (Feng J *et al*., 2016); 10d (Hsiao P-Y *et al*., 2016) 11a (Liu B and Xu YK., 2015) 12a (Ahn JH *et al*., 2012) 16a [18, Zhao M *et al*., 2011) 17a (Begum SA., 2010a; Begum S *et al*., 2006) 19b (Kang YM and Lee NH., 2011)
Cleomiscosin B methyl ether (**19**)	17a (Begum SA., 2010a)

Table 2.3 Coumarinolignans and their plant sources (Cont.)

Compound name (see Figure. 2.1 & 2.2)	Plant source(s) (see Table 2.2) (References)
Cleomiscosin C (**3**)	1a (Yoshikawa K *et al*., 2011); 1b (Yim SH *et al*., 2015) 2a (Ranjan R and Sahai M., 2009) 4a (Bawankule DU *et al*., 2008; Yadav NP *et al*., 2010; Tandon S *et al*., 2010) 5a (Li D *et al*., 2016; Wang KW *et al*., 2016); 5b (Tan T *et al*., 2017) 9d (Aichour S *et al*., 2014); 9g (Maffo T *et al*., 2018) 10b (Bai B *et al*., 2015) 12a [Ahn JH *et al*., 2012; Ahn JH *et al*., 2013) 15a (Cheng L *et al*., 2009) 16a (Zhao M *et al*., 2011)
Cleomiscosin D (**5**)	1a (Yoshikawa K *et al*., 2011); 1b (Yim SH *et al*., 2015) 3a (Zhang ML *et al*., 2012) 10b (Bai B *et al*., 2015);10d (Hsiao P-Y *et al*., 2016) 14a (Chen JJ *et al*., 2008)
Cleomiscosin E (**25**)	16a (Yang J *et al*., 2014)
Daphnecin (**21**)	18a (Rasool MA *et al*., 2010)
5′-Demethylaquillochin (**11**)	1a (Yoshikawa K *et al*., 2011) 9e (Xu JF *et al*., 2008) 15a (Cheng L *et al*., 2009)
8-*epi*-cleomiscosin A (**15**)	15b (Soh RF *et al*., 2009)
Grewialin (**24**)	19c (Uddin G *et al*., 2013)
Hyosgerin (**20**) (cleomiscosin B-9′-acetate)	17a (Begum SA., 2010a; Begum S *et al*., 2006)
Indicumine A (**33**)	17b (Yin HL *et al*., 2013)
Indicumine B (**34**)	17b (Yin HL *et al*., 2013)
Indicumine C (**35**)	17b (Yin HL *et al*., 2013)
Indicumine D (**36**)	17b (Yin HL *et al*., 2013)
Jatrocin A (**29**)	10c (Feng J *et al*., 2016)
Jatrocin B (**12**)	8b (Kan S *et al*., 2011) 10b (Bai B *et al*., 2015) 15a (Cheng L *et al*., 2009)

Table 2.3 Coumarinolignans and their plant sources (Cont.)

Compound name (see Figure. 2.1 & 2.2)	Plant source(s) (see Table 2.2) (References)
Malloapelins A (**30**)	9e (Xu JF *et al*., 2008)
Malloapelins B (**31**)	9e (Xu JF *et al*., 2008)
Malloapelins C (**32**)	9e (Xu JF *et al*., 2008)
Melicodin C (**23**)	14b (Nakashima KI *et al.*, 2012)
5′-methoxy-7′-*epi*-jatrorin A (**26**)	10c (Feng J *et al*., 2016)
Moluccanin (**14**)	15a (Cheng L *et al*., 2009)
Mucronin A (**37**)	18a (Ferheen S *et al*., 2014)
Mucronin B (**38**)	18a (Ferheen S *et al*., 2014)
4′-*O*-Cinnamoyl cleomiscosin A (**16**)	7a (Cao S *et al*., 2010)
4′-*O*-Methoxyljatrocin B (**13**)	15a (Cheng L *et al*., 2009)
(7′*S*,8′*S*)-4′-*O*-methylcleomiscosin D (**4**)	14a (Chen JJ *et al*., 2008)
Propacin (**27**)	10c (Feng J *et al*., 2016)
Propacin isomer (**28**)	10c (Feng J *et al*., 2016)
8-(7′,8′,9′-propanetriol-4′-methoxy-3′-*O*-phenylpropanoid)-7-hydroxy-6-methoxycoumarin (**22**)	11a (Zhang H *et al*., 2012)
Repenin A (**7**)	20a (Ahmad N *et al*., 2009)
Repenin B (**8**)	20a (Ahmad N *et al*., 2009)
Repenin C (**9**)	20a (Ahmad N *et al*., 2009)
Repenin D (**10**)	20a (Ahmad N *et al*., 2009)
Venkatasin (**18**) (Cleomiscosin A-9′-acetate, Durantin A)	17a (Begum SA., 2010a; Begum S *et al*., 2006) 20a (Ahmad N *et al*., 2009)
Yinxiancaoside C (**6**) (Coumarinolignan glucoside - cleomiscosin C-4-*O*- -D-glucopyranoside)	6a (Kuang HX *et al*., 2009)

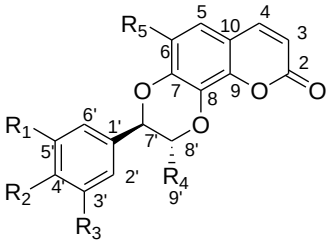

1 R_1 - H, R_2 - OH, R_3 - OCH_3, R_4 - CH_2OH, R_5 - OCH_3

3 R_1 - OCH_3, R_2 - OH, R_3 - OCH_3, R_4 - CH_2OH, R_5 -OCH_3

6 R_1 - OCH_3, R_2 - 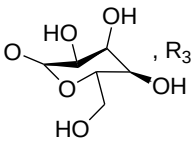 , R_3 - OCH_3, R_4 - CH_2OH, R_5 -OCH_3

7 R_1 - H, R_2 - OH, R_3 - OCH_3, R_4 - 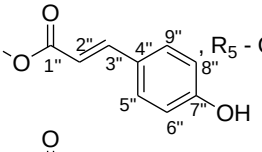 , R_5 - OCH_3

8 R_1 - H, R_2 - OH, R_3 - OCH_3, R_4 - 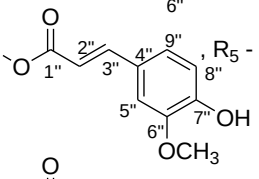 , R_5 - OCH_3

9 R_1 - H, R_2 - OH, R_3 - OCH_3, R_4 - 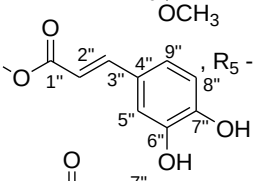 , R_5 - OCH_3

10 R_1 - OCH_3, R_2 - OH, R_3 - OCH_3, R_4 - 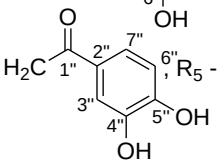 , R_5 - OCH_3

11 R_1 - OCH_3, R_2 - OH, R_3 - OH, R_4 - CH_2OH, R_5 - OCH_3

12 R_1 - OCH_3, R_2 - OH, R_3 - OCH_3, R_4 - CH_3, R_5 - OCH_3

13 R_1 - OCH_3, R_2 - OCH_3, R_3 - OCH_3, R_4 - CH_3, R_5 - OCH_3

16 R_1 - H, R_2 - 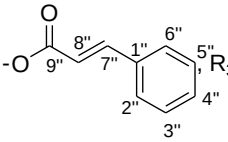 , R_3 - OCH_3, R_4 - CH_2OH, R_5 - OCH_3

17 R_1 - H, R_2 - OCH_3, R_3 - OCH_3, R_4 - CH_2OH, R_5 - OCH_3

18 R_1 - H, R_2 - OH, R_3 - OCH_3, R_4 - CH_2OAc, R_5 - OCH_3

25 R_1 - H, R_2 - OCH_3, R_3 - OH, R_4 - CH_2OH, R_5 - OCH_3

27 R_1 - H, R_2 - OH, R_3 - OCH_3, R_4 - CH_3, R_5 - OCH_3

29 R_1 - H, R_2 - OH, R_3 - OCH_3, R_4 - CH_3, R_5 - OH

30 R_1 - OH, R_2 - OH, R_3 - OCH_3, R_4 - CH_2OH, R_5 - OH

Figure 2.1 Structure formulas of coumarinolignans

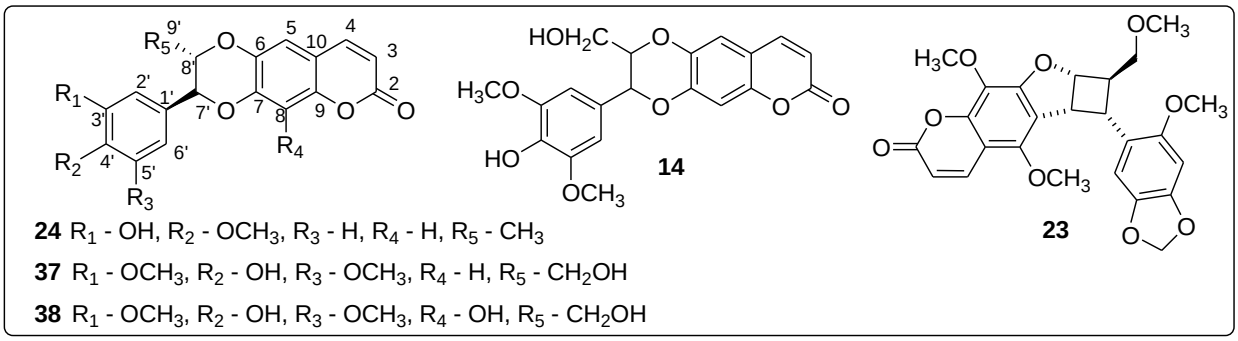

24 R_1 - OH, R_2 - OCH_3, R_3 - H, R_4 - H, R_5 - CH_3

37 R_1 - OCH_3, R_2 - OH, R_3 - OCH_3, R_4 - H, R_5 - CH_2OH

38 R_1 - OCH_3, R_2 - OH, R_3 - OCH_3, R_4 - OH, R_5 - CH_2OH

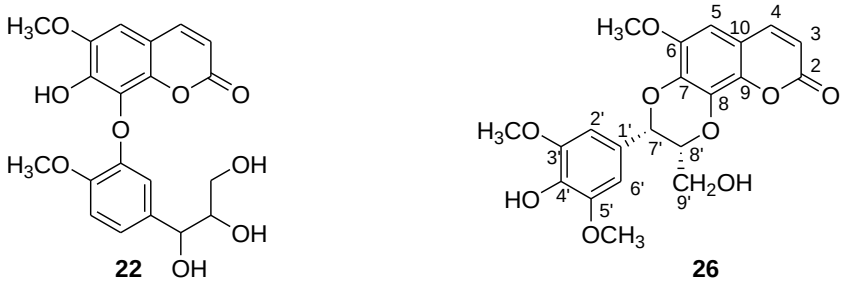

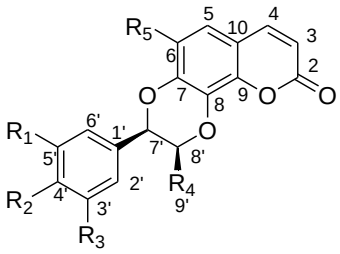

15 R_1 - H, R_2 - OH, R_3 - OCH_3, R_4 - CH_2OH, R_5 - OCH_3

33 R_1 - H, R_2 - OH, R_3 - OCH_3, R_4 - 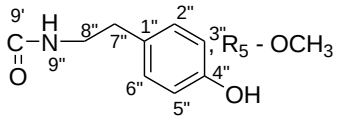 , R_5 - OCH_3

34 R_1 - H, R_2 - OH, R_3 - OCH_3, R_4 - 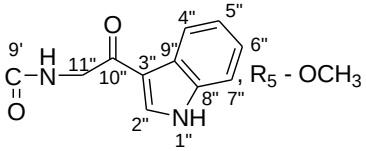 , R_5 - OCH_3

35 R_1 - H, R_2 - OH, R_3 - OCH_3, R_4 - COOH, R_5 - OCH_3

36 R_1 - H, R_2 - OH, R_3 - OCH_3, R_4 - $COOCH_2CH_3$, R_5 - OCH_3

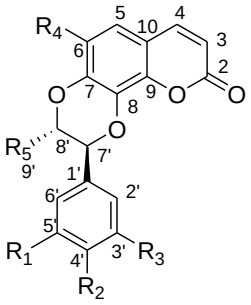

2 R_1 - H, R_2 - OH, R_3 - OCH_3, R_4 - OCH_3, R_5 - CH_2OH

4 R_1 - OCH_3, R_2 - OCH_3, R_3 - OCH_3, R_4 - OCH_3, R_5 - CH_2OH

5 R_1 - OCH_3, R_2 - OH, R_3 - OCH_3, R_4 - OCH_3, R_5 - CH_2OH

19 R_1 - H, R_2 - OCH_3, R_3 - OCH_3, R_4 - OCH_3, R_5 - CH_2OH

20 R_1 - H, R_2 - OH, R_3 - OCH_3, R_4 - OCH_3, R_5 - CH_2OAc

21 R_1 - OCH_3, R_2 - OH, R_3 - OCH_3, R_4 - OH, R_5 - CH_2OH

28 R_1 - H, R_2 - OH, R_3 - OCH_3, R_4 - OCH_3,R_5 - CH_3

31 R_1 - OH, R_2 - OH, R_3 - OCH_3, R_4 - OH, R_5 - CH_2OH

32 R_1 - OH, R_2 - OH, R_3 - OCH_3, R_4 - OCH_3, R_5 - CH_2OH

Figure 2.2 Structure formulas of some more coumarinolignans

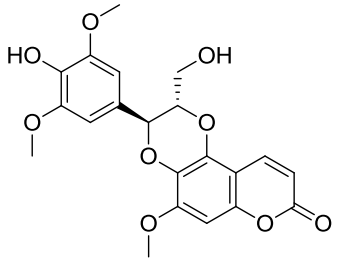

Aleuritin (**39**)

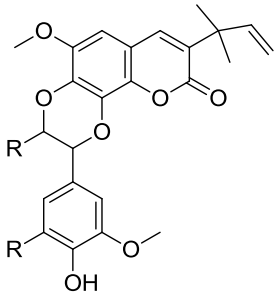

Antidesmanin A (**40**)- (R=OCH_3, R_1=CH3)
Antidesmanin C (**41**)- (R=H, R_1=$C(CH_3)_2CH=CH_2$)

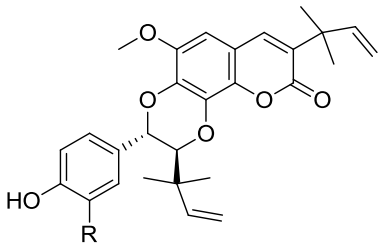

Antidesmanin B (**42**) - (R=OCH_3)
Antidesmanin D (**43**)- (R=OH)

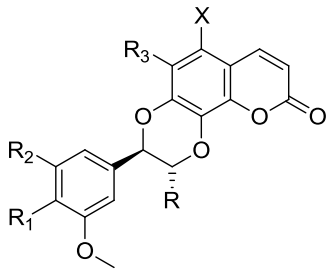

5-Chloropropacin (**44**)- (R=CH_3, R_1=OH,R_2=H, R_3=OCH_3, X=Cl)
Daphneticin (**45**)- (R=CH_2OH, R_1=H,R_2=OCH_3, R_3=OCH_3, X=H)
Durantin B(**46**) - (R=CH_2OAc, R_1=OCH_3, R_2=H, R_3=OCH_3, X=H)
Durantin C (**47**)- (R=CH_2OAc, R_1=OH, R_2=OCH_3, R_3=OCH_3, X=H)
Jatrorin A (**48**) - (R=CH_2OH, R_1=OH, R_2=H, R_3=OH, X=H)
Jatrorin B (**49**) - (R=CH_2OH, R_1=OCH_3, R_2=H, R_3=OH, X=H)
5-Methoxypropacin (**50**)- (R=CH_3, R_1=OH, R_2=H, R_3=OCH_3, X=OCH_3)

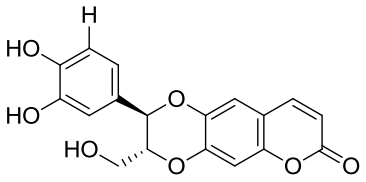

Maoyancaosu (**55**)

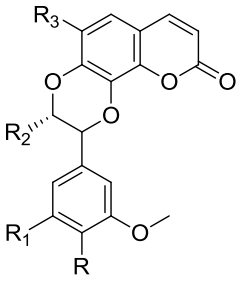

Hemidesmin 1 (**51**) - (R=OCH_3, R_1=OCH_3, R_2=CH_2OH, R_3=OH)
Hemidesmin 2 (**52**) - (R=H, R_1=OH, R_2=CH_2OH, R_3=OCH_3)

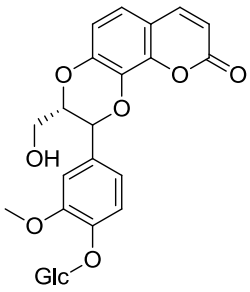

Daphneticin glucoside (**53**)

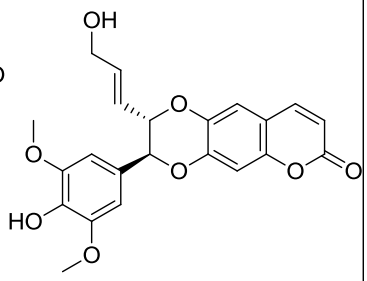

Hemidesminin (**54**)

Figure 2.3 Structure formulas of some more reported coumarinolignans

2.6 Pharmacological effects of coumarinolignans

Coumarinolignans have exhibited many interesting pharmacological activities. Most of the reported studies had explored anti-inflammatory, cytotoxic, anti-oxidant and hepatoprotective activity.

2.6.1 Anti-inflammatory effect of coumarinolignans

Literature review has disclosed anti-inflammatory effects of coumarinolignans. The first natural coumarinolignan, cleomiscosins A (**1**) along with B (**2**) and C (**3**) had shown synergistic effect in the inhibition of proinflammatory cytokines like tumor necrosis factor-alpha (TNF-α) and interleukin-6 (IL-6) in a dose dependent manner. This combination also reduced NO production and increased anti-inflammatory cytokines IL-4 significantly when compared to peritoneal macrophages stimulated with only lipopolysaccharide (LPS) treatment (Bawankule DU *et al*., 2008). The methanolic extract of *H. niger* containing both cleomiscosins A (**1**) and -B (**2**) individually as well as in methylated form and acetylated form had shown anti-inflammatory, analgesic and moderate antipyretic effect under in-vivo animal models. Among the regioisomers, cleomiscosins A (**1**), but not B (**2**) reduced wet and dry weight of cotton pellet granuloma in mice models. The principle compound responsible for the activity had been identified to be cleomiscosin A (**1**) (Begum S *et al*., 2010).

Cleomiscosin E (**25**), was found to possess improved inhibition of LPS induced NO production in RAW 264.7 macrophages compared to cleomiscosin A (**1**) (Yang J *et al*., 2014). Another study also proved the moderate inhibition effect of cleomiscosin A (Dzoyem JP *et al*., 2016). Both cleomiscosins E (**25**) and A (**1**) are structural isomers that differ in the positions of

hydroxyl and methoxyl groups in the phenyl propanoid unit. The targets are so precise that such minor change in the structure leads to variation in the inhibition potential.

Compared to cleomiscosins A (**1**), B (**2**) significantly reduced LPS induced NO production with IC_{50} value of 3.56±0.49 μM, which was significantly less than the standard drug indomethacin (IC_{50} 47.40±4.50 μM). However, propacin (**27**) and its regioisomer (**28**), prepared by replacing –CH_2OH group with –CH_3 group in cleomiscosins A (**1**) and B (**2**), respectively exhibited loss of activity. This claims the requirement of primary alcohol group for NO reduction. In the same study, jatrocin A (**29**) which differed from cleomiscsoin A with the substituents at C-6 (hydroxyl group) and C-8′ (methyl group) positions had been observed to possess moderate (IC_{50} value 21.70±2.35 μM) inhibitory effect (Feng J *et al*., 2016). However, according to Bai *et al*., coumarinolignans, jatrocin B (**12**), cleomiscosins A (**1**), B (**2**), C (**3**) and D (**5**) displayed no effect on NO production (IC_{50} > 100 μM) (Bai B *et al*., 2015). This ambiguity need to be resolved as the method followed by both the groups is same i.e. Griess reaction. Novel 5′-methoxy-7′-*epi*-jatrorin A (**26**) also exhibited weak inhibitory effect (Feng J *et al*., 2016). Further, by analyzing the structure activity relationship of these compounds, it can be corroborated that the inhibitory effect increases if there is a presence of aromatic moiety close to C-8 position as found in cleomiscosin B (**2**).

Cleomiscosin D (**5**) as an anti-inflammatory moiety was found to be most effective in the suppression of formyl-L-methionyl-L-leucyl-L-phenylalanine/cytochalasin B (FMLP/CB) induced superoxide radical anion (O_2●-) generation from human neutrophils showing IC_{50} of 13.08 μM and its analogue (7′*S*, 8′*S*)-4′-*O*-methylcleomiscosin D (**4**) also exhibited potent anti-inflammatory activity with IC_{50} value of 14.72 μM (Chen JJ *et al*., 2008).

2.6.2 Cytotoxic effect of coumarinolignans

In order to explore the anti-cancer potentiality of coumarinolignans, scientists have screened the cytotoxicity of natural coumarinolignans against a series of cancer cell lines. Cleomiscosins A (**1**), B (**2**), C (**3**) and D (**5**), jatrocin B (**12**), 5′-demethyl aquillochin (**11**), 4-O-methoxyjatrocin B (**13**), moluccanin (**14**), yinxiancaoside C (**6**) and melicodin C (**23**) are the coumarinolignans so far screened for cytotoxic effect. Cleomsicosin B (**2**) had been found to be toxic to human hepatocarcinoma SMMC-7721 (IC_{50} 4.16 μM), human lung cancer A-549 (IC_{50} 3.46 μM), breast cancer MCF-7 cells (IC_{50} 1.69 μM) and colon cancer SW-480 (IC_{50} 13.30 μM) cell lines, the effect was found to be better than cisplatin. Cleomiscosin B (**2**) was also found to be toxic against HL-60 with IC_{50} value of 3.56 μM (Liu B and Xu YK., 2015).

Cleomiscosin A (**1**), was found to be moderately cytotoxic against human liver cancer cell lines HepG2 (IC_{50} value 23.32±0.18 μM) and HeLa cells (IC_{50} value 31.82±1.12 μM) (He ZZ *et al*., 2009; Chen D-L *et al*., 2010). However, it was reported to be inactive against P-388 murine leukemia cells (Erwin *et al*., 2014), BGC 823 human cancer cell line (Donfack ARN *et al*., 2014) and *Artemia salina* (Sielinou VT *et al*., 2012). Further, cleomiscosins A (**1**) and D (**5**) had shown no cytotoxicity against human tumor cell lines (HeLa, HOC-21, T-98, U251-SP, MCF-7, QG-56, PC-6, HLE, MM1-CB, and HMV-1) (Zhang ML *et al*., 2012). Also, no antiproliferative activity on A2780 ovarian cancer cell line (Cao S *et al*., 2010) was shown by 4′-*O*-cinnamoyl cleomiscosin A (**16**).

Cleomiscosin C-4-*O*-*β*-D-glucopyranoside, trivially named as yinxiancaoside C (**6**), had shown marginal cytotoxic activities against human hepatoma (Hepg-2), ovarian carcinoma (OV420), and breast cancer (MCF-7) cells (Kuang HX *et al*., 2009).

Coumarinolignans, cleomiscosins A (**1**), -C (**3**), 5′-demethylaquillochin (**11**), jatrocin B (**12**), 4-*O*-methoxyljatrocin B (**13**) and moluccanin (**14**) had been screened for the induction of NAD(P)H:quinine oxidoreductase to determine the chemopreventive property. 5′-demethylaquillochin (**11**) and its isomer obtained from the dichloromethane extract of *E. cavaleriei* expressed the potential chemopreventive property. 5′-Demethylaquillochin (**11**) was seen to possess most potential ability to induce oxidoreductase. All the coumarinolignoids cleomiscosins A (**1**), C (**3**), 5′-demethylaquillochin (**11**), jatrocin B (**12**), 4-*O*-methoxyljatrocin B (**13**) except moluccanin (**14**) exhibited strong activity. Cleomiscosins A (**1**), C (**3**) and 5′-demethylaquillochin (**11**) had also shown high cell viability (Cheng L *et al*., 2009).

A significant antitumor activity against human colon cancer cells DLD-1 had been exhibited by melicodin C (**23**) at higher concentration via apoptosis mechanism (Nakashima KI *et al.*, 2012).

Attempts to improve the solubility by complexing *β*-cyclodextrin with cleomicosins C (**3**) and its positional isomer D (**5**) had been also found in the literature. Cleomiscosin D - cyclodextrin complex was found to be active in a dose dependent manner against human colon cancer cells (Yim SH *et al*., 2015). Jatrocin B (**12**), cleomiscosins A (**1**), B (**2**), C (**3**) and D (**5**) had been found to be negative against human colorectal adenocarcinoma (LOVO) and human acute promyelocytic leukemia (HL-60) (Bai B *et al*., 2015).

2.6.3 Anti-oxidant and hepatoprotective effect of coumarinolignans

A hepatoprotective formulation, cliv-92 had been patented by Yadav *et al*. It included a mixture of cleomiscosins A (**1**), -B (**2**) and -C (**3**) (ratio 21:25:4) which exhibited hepatoprotective effect against CCl_4 induced toxicity. Malloapelins A (**30**), B (**31**) and C (**32**) have shown inhibitory activity at 10^{-4} M concentration against D-galactosamine-induced *in vitro* hepatotoxicity model

using WB-F344 cells without any cytotoxic effects. Malloapelin C (**32**) had exhibited promising activity on comparison with positive control bicyclol and silybin (Xu JF *et al*., 2008).

Indicumines A (**33**) and B (**34**) had been screened for antihepatitis B virus (HBV) assay using human hepatoblastoma cell lines (HepG2.2.15 cell). At no cytotoxic concentration of both, indicumine A (**33**) had exhibited moderate activities on HBsAg and HBeAg, whereas indicumine B (**34**) exhibited weak anti-HBV activities on HBsAg (Yin HL *et al*., 2013).

Cleomiscosins C (**3**) and D (**5**) were found to be positional isomers and they had exhibited the significant anti-oxidant property. Modifcation of 8-*O*-7' position phenyl ring group of cleomiscosin D (**5**) to 8-*O*-8' position $–CH_2OH$ group of cleomiscosin C (**3**) slightly decreased the activity and further replacement of methoxy group with hydroxy at position C-5' of demethylaquillochin (**11**) had exhibited loss in activity (Yoshikawa K *et al*., 2011).

The unusual group of coumarinolignans, repenins A-D (**7-10**) and durantin A (**18**) had shown potent antioxidant activity against 2,2-diphenyl-1-picrylhydrazyl (DPPH) radicals (Ahmad N *et al*., 2009). The activity of cleomiscosins B (**2**) was found to be better active than A (**1**). Inclusion of $-OCH_3$ group at C-5 position in both cleomiscosins A and B would yield respectively, cleomiscosins C and D, which were found to be moderately active (Bai B *et al*., 2015). Cleomiscosin A (**1**) was found to be devoid of anti-oxidant activity as proved by DPPH and PMS/NADH-NBT methods for the measurement of anti-oxidant activity. Similarly, jatrocin A (**6**) and cleomiscosin B (**2**) did not exhibit anti-oxidant effect by DPPH assay (Feng J *et al*., 2016). Hence, it can be clinched that antioxidant effect of coumarinolignans are not promising.

2.6.4 Miscellaneous effect

Antimicrobial screening reports on coumarinolignans are not favourable. Cleomiscosin A (**1**) had not shown any antifungal (*Candida albicans*, *Mucor miehei*), antibacterial (*Staphylococcus aureus*, *Bacillus subtilis*, *Escherichia coli*) and phycotoxicity properties against green micro-algae (*Chlorella vulgaris*, *Chlorella sorokiniana*, and *Scenedesmus subspicatus*) (Sielinou VT *et al*., 2012). When tested by agar plate diffusion test cleomiscosin (regioisomer undefined by author) had demonstrated moderate tyrosinase inhibitory activity (Demirkiran O *et al*., 2014) . Cleomiscosins A (**1**), B (**2**) and C (**3**) had exhibited weak inhibitory activity on porcine pancreatic lipase *in vitro* model (Ahn JH *et al*., 2012). Cleomiscosin A (**1**) had displayed moderate anti-babesial activity against dog parasite *Babesia gibsoni* (Yamada K *et al*., 2009). Cleomiscosin B (**2**) had shown very low inhibitory activity against tobacco mosaic virus (Chen QJ *et al*., 2009). Mucronins A (**37**) and B (**38**) have shown significant inhibition against *Mycobacterium tuberculosis* with MIC value of 62.5 µg/ml and 60.5 µg/ml, respectively (Ferheen S *et al*., 2014).

2.7 Synthesis of coumarinolignans and their derivatives

Kuboki *et al*. had synthesized cleomiscosin C (**3**) from a phenol precursor following a seventeen step process (Kuboki A *et al*., 2008a and 2008b).

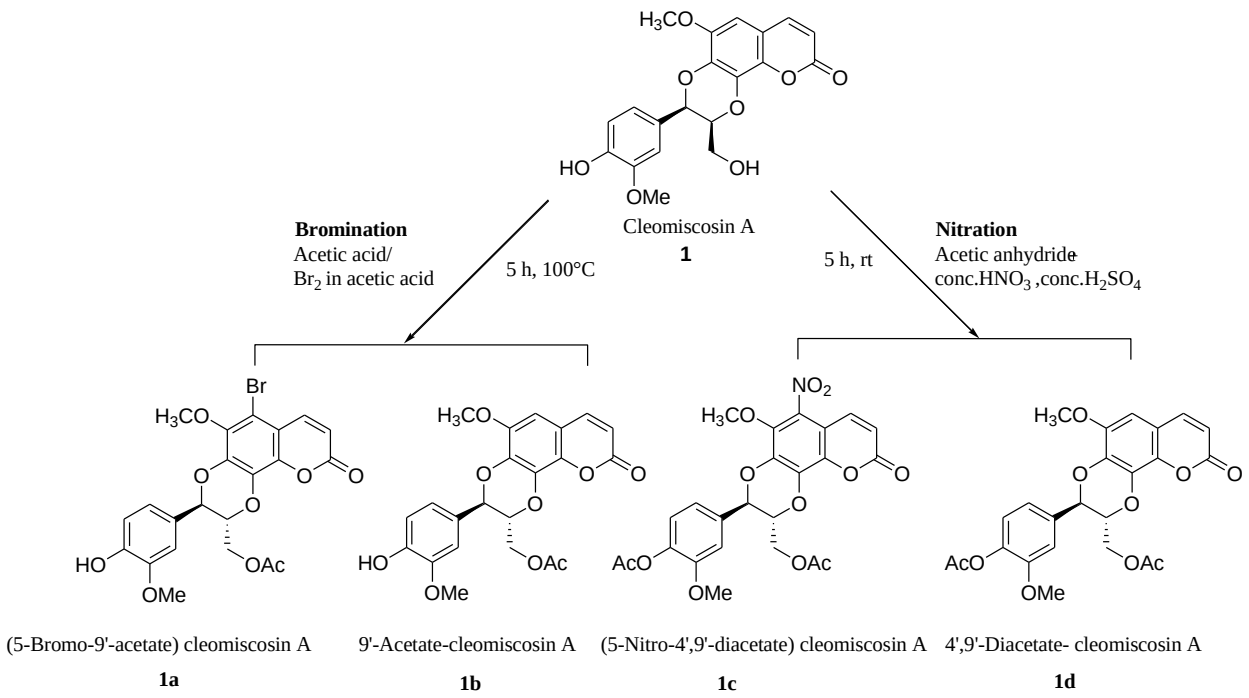

Scheme 2.1 Synthesis of Cleomiscosin A derivatives

Sharma *et al*., had synthesized four cleomiscosin A derivatives (**1a**-**1d**) via bromination and nitration reaction following Scheme 2.1. In bromination, cleomiscosin A (**1**) and bromine in acetic acid were refluxed at 100 °C for 5 h to yield a mixture of (5-bromo-9′-acetate) cleomiscosin A (**1a**) and cleomiscosin A 9′-acetate (**1b**). In nitration, cleomiscosin A (**1**) was mixed with acetic anhydride, conc. HNO_3, conc. H_2SO_4 and kept at room temperature for 5 h to yield a mixture of (5-nitro-4′,9′-diacetate) cleomiscosin A (**1c**) and 4′,9′-diacetate-cleomiscosin A (**1d**) (Sharma S *et al*., 2010).

Further semi-synthesis of cleomiscosin A methyl ether derivatives (**17a**-**17d**) as per Scheme 2.2 had also been reported by Sharma et al. Nitration was done by mixing cleomiscosin A methyl ether (**17**) with conc. HNO_3 at 0 °C to -5 °C and kept for 2 h to yield mixture of 5,6′,9′-trinitro-cleomiscosin A methyl ether (**17b**) and 5,6′-dinitro-cleomiscosin A methyl ether (**17c**). In chlorination, cleomiscosin A methyl ether (**17**) was refluxed with N-chlorosuccinimide in $CHCl_3$

at 65 °C for 2 h to yield 5-chloro-cleomiscosin A methyl ether (**17d**). Similarly bromination using N-bromosuccinimide yielded 5-bromo-cleomiscosin A methyl ether (**17a**) (Sharma S *et al*., 2010).

Further, Sharma *et al*., had reported synthesis of six cleomiscosin A methyl ether derivatives (**17e**-**17j**) via halogenation and esterification reaction following Scheme 2.2. In halogenation, BF_3-Etherate and respective N-halosuccinimide were added to cleomiscosin A methyl ether (**17**) and stirred at room temperature. Corresponding five halogenated products were obtained, which included a mixture of trichloro (**17f**) and dichloro (**17g**) derivatives via chlorination, a mixture of triiodo (**17i**) and diiodo (**17j**) derivatives via iodination and tetrabromo (**17h**) derivative via bromination. Further cleomiscosin A methyl ether (**17**) was subjected for esterification under reflux at 100°C using K_2CO_3, dimethyl carbonate and DMF to yield methyl ester product (**17e**). However, the above reaction was not proceeding when cleomiscosin A (**1**) was used as a starting material (Sharma S *et al*., 2012).

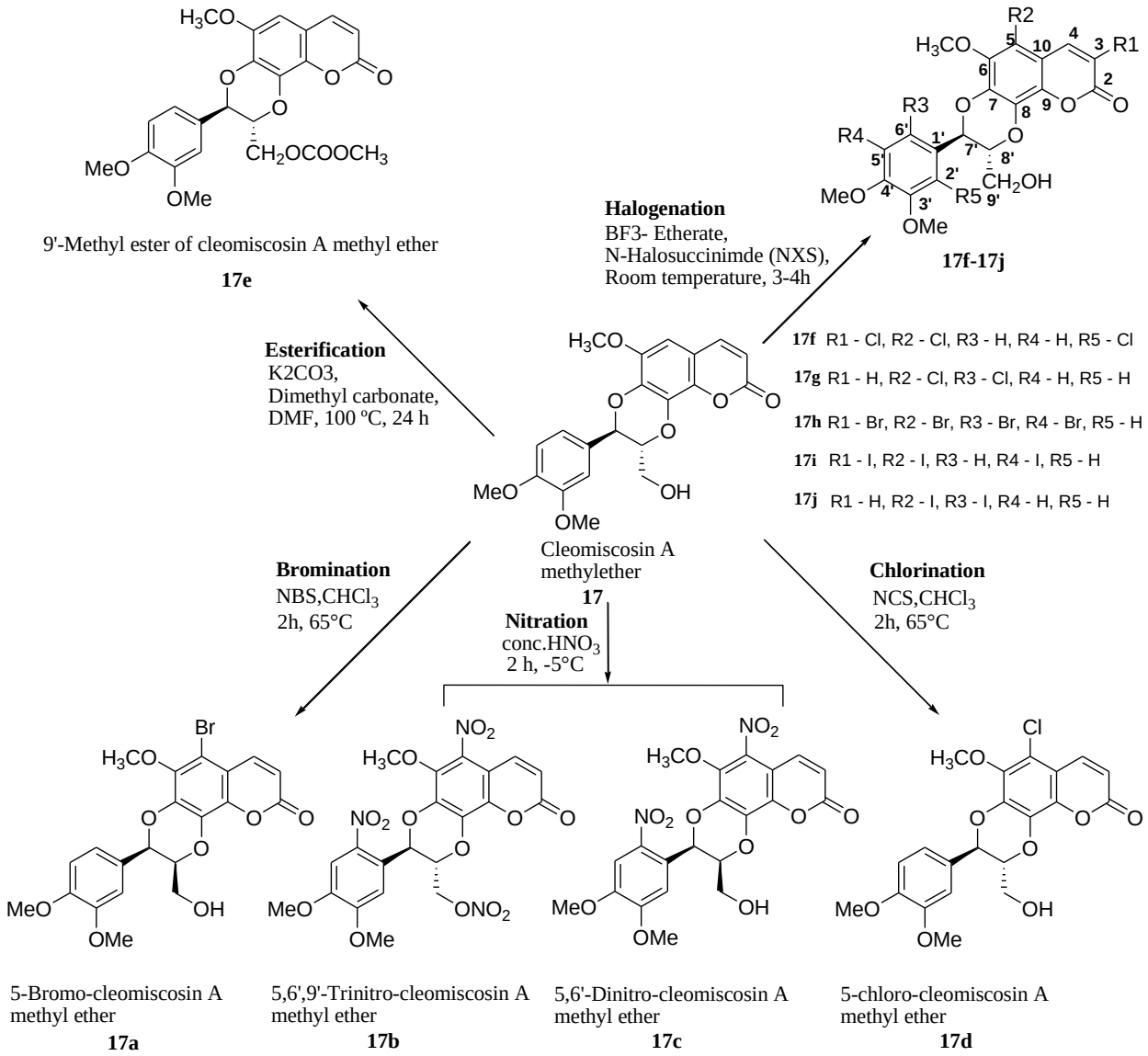

Scheme 2.2 Synthesis of cleomiscosin A methyl ether (17) derivatives

2.7.1 Anti-inflammatory activity of synthetic derivatives

Sharma *et al*. had screened the synthetic derivatives of cleomiscosin A for in-vitro anti-inflammatory activity using LPS induced macrophages cell line. Compounds, (5-bromo-9'-acetate) cleomiscosin A (**1a**), 5-bromo-cleomiscosin A methyl ether (**17a**) and 5-chloro-cleomiscosin A methyl ether (**17d**) had shown significant inhibition of pro-inflammatory targets IL1β, IL-6 and TNF-α mediators for chronic inflammation (Sharma S *et al*., 2010). Further,

trichloro (**17f**), tetrabromo (**17h**), diiodo (**17j**) and methyl ester (**17e**) derivatives of cleomiscosin A methyl ether had also shown the significant inhibition of all above pro-inflammatory targets. Trichloro (**17f**) and methyl ester (**17e**) derivatives at 10 µg/ml concentration had inhibited ($P < 0.05$) the production of TNF-α, IL-1β and IL-6. Dichloro (**17g**) and tetrabromo (**17h**) derivatives at concentration of 10 and 1 µg/ml had inhibited TNF-α production. Trichloro (**17f**), tetrabromo (**17h**), triiodo (**17i**) and methyl ester (**17e**) derivatives at concentration level of 1 and 10 µg/ml had inhibited IL-1β production (Sharma S *et al*., 2012).

2.8 Gaps in existing Research

Currently available anti-inflammatory drugs for managing painful chronic arthritis have been observed to lack long term safety (Table 2.1). The drawbacks with the existing anticytokines or NSAIDS involved severe side effects, poor bioavailability for oral administration and high cost. Hence, there is a need for safe and effective small molecules for managing chronic inflammatory pain. Structurally modified natural molecules like coumarinolignans can overcome the currently available unsafe molecules for inhibition of key targets like TNF-α, IL-6 and IL-1β.

CHAPTER 3

OBJECTIVES AND PLAN OF WORK

CHAPTER 3

OBJECTIVES AND PLAN OF WORK

3.1 Objectives

Inflammation is the basic cause for the most of the chronic diseases namely autoimmune disorder (rheumatoid arthritis, systemic lupus erythematosus, alzheimer's disease), cancer, myocardial damage, asthma, chronic obstructive pulmonary disease, renal injury, arthrosclerosis, and ulcerative colitis and neurogenerative disorders. In inflammation, the up-regulated pro-inflammatory cytokines play a vital role in the sustainment and spread of inflammation from one inflamed cell to the other healthy cell. This will result in the development of chronic inflammation from the acute inflammatory conditions (Zhang J-M and An J., 2007; Tsokos GC., 2011; Mclnnes LB and Schett G., 2011; Landskron G *et al*., 2014, Barnes PJ., 2018). The key cytokines involved in the inflammatory pathways are identified as IL-1β, IL-6, and TNF-α. Although several biological macromolecular inhibitors targeting these cytokines are available, their severe toxic effects and cost involvement in managing chronic condition are high (Dinarello CA., 2010). Hence there is a need for the discovery of potentially active small molecular inhibitors involving simple method of preparation. In view of this, the following objectives were set to explore novel pro-inflammatory cytokine inhibitors.

I. Synthesis and in-vitro biological evaluations on methyl coumarin and phenyl propanoid derivatives followed by molecular docking studies towards developing novel coumarin-based pro-inflammatory cytokines inhibitors.

II. Synthesis of coumarin-based lignans followed by in-vitro and in-vivo pharmacological evaluations towards developing pro-inflammatory cytokines inhibitors

III. Synthesis, in-vitro, in-vivo and docking studies on glucoside of cleomiscosin A, a natural coumarinolignan

3.2 Plan of work

The plan of work for this project was drafted as follows:

I. Synthesis and in-vitro biological evaluations on methyl coumarin and phenyl propanoid derivatives followed by molecular docking studies towards developing novel coumarin-based pro-inflammatory cytokines inhibitors.

   A. Synthesis and characterization of 7,8-dihydroxy-4-methyl coumarin and phenyl propanoid derivatives.

   B. In-vitro screening of synthesized coumarin and phenyl propanoid derivatives by cell based protein inhibition assay using ELISA kits.

   C. Designing of structural analogues of coumarin and phenyl propanoid derivatives and molecular docking studies onto TNF-α, IL-6 and IL-1β proteins.

   D. Designing of fused-cyclic coumarin-based lignans using previously docked coumarins and phenyl propanoids.

   E. Molecular docking studies on coupled products on fused-cyclic coumarin-based lignans over TNF-α, IL-6 and IL-1β proteins.

II. Synthesis of coumarin-based lignans followed by in-vitro and in-vivo pharmacological evaluations towards developing pro-inflammatory cytokines inhibitors.

A. Synthesis of feasible hit molecules of coumarin-based lignans and their characterization

B. Isolation of natural coumarinolignan, cleomiscosin A from *Cleome viscosa*

C. In-vitro screening of synthesized coumarin-based lignans and cleomiscosin A by protein inhibition assay using ELISA.

D. Nitric oxide reduction effect and cytotoxicity of coumarin-based lignans and cleomiscosin A.

E. In-vivo pharmacological evaluation of synthesized coumarin-based lignans and cleomiscosin A for pro-inflammatory cytokines inhibitory effect under mouse endotoxemia model.

F. In-vivo pharmacological evaluation of synthesized coumarin-based lignans and cleomiscosin A for anti-inflammatory effect through carrageenan-induced paw edema model.

G. In-vivo pharmacological evaluation of potentially active coumarin-based lignan compound under crystal-induced renal nephropathy.

III. Synthesis, in-vitro, in-vivo and docking studies on glucoside of cleomiscosin A, a natural coumarinolignan

A. Synthesis and characterization of cleomiscosin A glucoside

B. In-vitro (ELISA protein estimation) studies on cleomiscosin A and cleomiscosin A glucoside

C. In-vivo (mouse endotoxemia model) study on cleomiscosin A and its glucoside for pro-inflammatory cytokines inhibitory effect

D. Molecular docking studies on cleomiscosin A and its glucoside over TNF-α, IL-6 and IL-1β proteins.

CHAPTER 4

MATERIALS AND METHODS

CHAPTER 4

MATERIALS AND METHODS

4.1 General

Analytical reagent grade chemicals, solvents and reagents were used. HPLC grade solvents (Merck) were used for HPLC purity analysis of compounds. Synthesis was done by using available laboratory grade reagents and analytical grade solvents. The solvents and reagents were purified and dried according to the procedure given in Vogel's text book of practical organic chemistry. Thin layer chromatography (TLC) was performed to monitor the reactions and to determine the purity of the products. Further the compounds were purified by recrystallisation using appropriate solvents. Column chromatography was done to separate the pure product from the by-product using specific solvents in fixed ratios. For conventional synthesis, hot plate with magnetic stirrer and water bath were used. Instruments, Multi detection reader (Spectramax M4, California, USA), IR (Jasco FT/IR-4200, Maryland, US), MS (LC-MS-2020, Shimadzu, Japan), HPLC (Shimadzu UFLC, Japan), YMC flash chromatography and plethysmometer (Ugo basile 7140). ^{1}H-NMR, ^{13}C-NMR and HMBC spectra were recorded on JNM-AL 300 , JEOL (Japan) spectrometer using DMSO-*d6*, $CDCl_3$ and CD_3OD as solvent and TMS as internal standard. MTT (3-(4,5-dimethylthiazol-2-yl)-2,5-diphenyltetrazolium bromide) was purchased from Himedia Laboratories Pvt. Ltd., Mumbai, India. Mouse macrophages cell line RAW 264.7 was obtained from the Cell Bank of National Center for Cell Sciences, Pune (Maharashtra, India). Silica gel (#230-400 and 100-200), silica gel for TLC (G and GF254), dimethyl sulfoxide (DMSO) were procured from Merck Specialties Private Limited, India. Concentrated suphuric

acid and absolute ethanol (S. D. Fine-chem Ltd. Mumbai, India), chemicals and solvents for synthesis (Sigma- Aldrich; Alfa Aesar; Merck Millipore), prednisolone (Sigma-Aldrich, MO, USA) and lipopolysaccharide (*E. coli* serotype 0111:B4, Sigma-Aldrich, MO, USA), TRI Reagent (Sigma-Aldrich, MO, USA) were used. ELISA kits for TNF-α, IL-6 and IL-1β were purchased from eBiosciences Inc. (San Diego, USA). All reagents used were of analytical grade. Synthesized compounds and standard prednisolone (**17**) were dissolved in DMSO and added directly to the culture media before the addition of LPS. The final concentration of DMSO was never allowed to exceed 0.1%.

4.2 Molecular docking studies

Molecular docking studies were carried using software GOLD 5.2. Proteins were downloaded from protein data bank (PDB) available at RCSB. Further all the proteins were processed using protein preparation wizard tools of SYBYL X ver. 2.1.1. Training set ligands were prepared using Accelrys – Discovery Studio ver. 2.5.

4.2.1 Protein preparation

The 3D structural coordinates of TNF-α (extracellular domain), IL-6-α (extracellular domain) and IL-1β proteins were retrieved from RCSB PDB (https://www.rcsb.org/) with assigned PDB IDs viz. 2AZ5, 1N26 and 3O4O, respectively. The crystal structures of the above proteins were prepared for docking using protein preparation module of SYBYL X ver. 2.1.1. The protein preparation steps involved the addition of protons, removal of water molecules, fixing of side chains and protein backbone φ, ψ and ω angles. The protonation states of the acidic residues, such as Asp and Glu were set at normal physiological pH of 7.4. The amide group orientations in

Gln and Asn and the tautomeric states of Histidine residues were fixed for optimal hydrogen bond interactions with the neighbouring residues. Gasteiger Huckel charges were applied on protein residues, followed by energy minimization using MMF94S forcefield. The optimized protein structures were used for docking experiments.

4.2.2 Ligand preparation

The 2D structures of the ligands (Table 5.1.3 and 5.1.6) were obtained from ChemDraw ver. 8.0. These ligand structures were further prepared for docking using the *Prepare Ligands* module of Biovia Discovery Studio ver. 3.5 using default settings.

4.2.3 Protein-ligand docking

For docking experiments involving TNF-α as target protein (PDB ID: 2AZ5), the co-crystallized ligand [6,7-dimethyl-3-[(methyl{2-[methyl({1-[3-(trifluoromethyl)phenyl]-1h-indol-3-yl}methyl)amino]ethyl}amino)methyl]- 4h-chromen-4-one; IC_{50} = 22 μM] present on the interface region of B, C and D chains was extracted and the same was assigned as the centroid. From the centroid, amino acid residues covering within a radius of 6 Å were defined as active site residues for the purpose of docking, which included Leu55B, Leu157B, Leu57C-Gln61C, Tyr119C-Gly122C, Tyr151C, Leu57D, Tyr59D-Gln61D, Tyr119D-Gly121D, Tyr151D and Ile155D.

In case of IL-6-α (PDB ID: 1N26), the Cγ atom of the Phe103 residue with x, y, z coordinate values of 16.471, 48.983, 82.154 respectively was assigned as the centroid; and the binding site radius was set to 12 Å as described in the previous literature (Sharma S *et al*., 2012). Thus, active

site residues covered within 12 Å radius included the Ser101A, Ser224A, Lys105A, Glu114A, Asp198, Val112A, Phe103 and Gln196 residues.

For IL-1β (PDB ID: 3O4O), the backbone carbonyl oxygen atom of Lys26 was defined as the centroid with x, y, z coordinate values of -5.0840, 7.195, 4.932 respectively; and the radius was set to 10 Å from the centroid. The binding site region included the residues viz. Asp10B, Arg13B, Lys26B, Ile15B, Ile25B, Pro28B, Phe30B and Phe107B which were considered based on the previously reported literature (Sharma S *et al*., 2012).

For each ligand, 10 docked solutions were generated with their corresponding GOLD fitness scores. The selection of best ligand pose was done based on their interactions with amino acid residues of the target protein showing least clashes and having highest fitness score. Higher the GOLDScore_fitness of the ligand pose, better is the activity because it is calculated based on the negative sum of the component energy terms. The optimized fitness function was used for the prediction of well-fitted ligand binding position that has the least energy with average GOLDScore_fitness.

The prepared ligands were docked to the TNF-α, IL-6 and IL-1β (domain) proteins using GOLD 5.2. software enabling them to undergo flexible docking process and commenced with default parameters.

4.3 Synthetic procedures, purification and characterization of compounds

4.3.1 Preparation of $HClO_4$–SiO_2 catalyst

$HClO_4$–SiO_2 catalyst was prepared by adding perchloric acid 70% aqueous solution (12.5 mmol) to silica gel (23.75 g, 230–400 mesh) suspension in diethyl ether. This mixture was kept under vacuum for 72 h at 100°C to yield $HClO_4$–SiO_2 (Chakraborti AK and Gulhane R., 2003; Maheswara M *et al*., 2006).

4.3.2 Preparation of 7, 8-dihydroxy-4-methyl-2H-chromen-2-one (1a)

Pyrogallol (1 mmol), ethyl acetoacetate (1.1 mmol) and $HClO_4 \cdot SiO_2$ (50 mg) were mixed and stirred at 130 °C in a pre-heated oil bath for 90 mins. The reaction was monitored through TLC. After the completion of reaction, the reaction mixture was filtered and the residue was washed with ethyl acetate. The combined ethyl acetate layer was evaporated to get a solid residue. Further column purification was done using DCM and methanol to get pure yellow color compound (Chakraborti AK and Gulhane R., 2003; Maheswara M *et al*., 2006)

7,8-Dihydroxy-4-methyl-2H-chromen-2-one (**1a**): Yellow amorphous powder, yield: 94%; m. p.: 241-242 °C; IR (FT/IR, KBr cm^{-1}): 3416, 3233, 3080, 1648, 1609, 1513, 1457, 1300, 1026; APCI-MS (*m/z*): calcd $[M]^+$ 192.04, found $[M-1]^+$ 191.1000; $[M+1]^+$ 192.9500

4.3.3 Preparation of cinnamic esters

One gm of cinnamic acid derivative was weighed and dissolved in 10 ml of absolute ethanol. To this cautiously, 1ml of concentrated sulphuric acid was added along sides. The reaction generally proceeds for 12 h and it was monitored through TLC. After the completion of reaction, excess

ethanol was evaporated under reduced pressure and extracted using ethyl acetate. The extract was then washed with sodium bicarbonate to remove acid impurities. Further the product was purified through column chromatography using hexane and ethyl acetate as mobile phase.

(*E*)-ethyl 3-(4-hydroxyphenyl)acrylate (**3b**): White amorphous powder, yield: 92%; mp: 73-74 °C; IR (FT/IR, KBr cm^{-1}): 3290, 2984, 1682, 1633, 1604, 1583, 1515, 1439, 1371, 1034, 977, 830; APCI-MS (*m/z*): calcd $[M]^+$ 192.07, found $[M-1]^+$ 191.2; $[M+1]^+$ 193.00

(*E*)-ethyl 3-(3,4-dihydroxyphenyl)acrylate (**4b**): Brown amorphous powder, yield: 95%; mp: 149-150 °C; IR (FT/IR, KBr cm^{-1}): 3455, 2983, 1669, 1605, 1522, 1443, 1371, 1282, 1187, 1137, 1043, 984, 870; APCI-MS (*m/z*): calcd $[M]^+$ 208.07356, found $[M-1]^+$ 207.0000; $[M]^+$ 208.2500

(*E*)-ethyl 3-(4-hydroxy-3-methoxyphenyl)acrylate (**5b**): Pale yellow crystal, yield: 96%; mp: 64-65 °C; IR (FT/IR, KBr cm^{-1}): 3421, 2979, 1702, 1633, 1592, 1516, 1430, 1372, 1269, 1180, 1034, 978, 846; APCI-MS (*m/z*): calcd $[M]^+$ 222.08921, found $[M-1]^+$ 221.0; $[M-2]^+$ 222.0

4.3.4 Preparation of diphenyl selenoxide oxidative coupling catalyst

Diphenyl selenide (10 mmol) was dissolved in 20 ml of (1/1) (v/v) of methanol/DCM at 0 ºC. N-chlorosuccinimide (10.5 mmol) was added to the above solution and stirred for 30 mins. Then the reaction mixture was diluted with 20 ml of DCM and 30 ml of 10% sodium hydroxide was added. The organic phase was separated, dried over sodium sulphate and concentrated to obtain diphenyl selenoxide as pink solid. Further diphenyl selenoxide was recrystallized using 4:1 of hexane: DCM (Michael RD., 1980).

4.3.5 Preparation of fused-cyclic coumarin-based lignans

7, 8-dihydroxy-4-methyl-2H-chromen-2-one (**1a**) (1.9228 mmol) and diphenyl selenoxide (3.2561 mmol) were dissolved in a mixture of methanol (15 ml) and benzene (15 ml) solvent. The solution was stirred at room temperature for 15 mins to obtain a homogenized solution. Corresponding cinnamic ester derivative (**3b/4b/5b**) (2.6656 mmol) was dissolved in 5 ml of methanol and drop wise it was added to the above homogenized solution. This solution was kept for stirring at room temperature. The completion of reaction was monitored through TLC. Once when the reaction was completed, the solvent was evaporated, 15 ml of ice water was added and then extracted with ethyl acetate. The combined ethyl acetate layer was dried using sodium suphate, evaporated and dried. The product obtained was purified by column chromatography using hexane: ethyl acetate solvent system. Pure compound of single isomer was obtained using silica gel column chromatography followed by flash chromatographic purification. The column eluates obtained using hexane:ethyl acetate (65:35) solvent system was subjected for flash chromatography [Conditions: Mobile phase: hexane (A) and ethyl acetate (B); Flash silica (40-60 µ); Flow rate – 5 ml/min; Detection wavelength – 274 nm; Binary gradient 0 % B - 25 min; 10 % B - 30 min; 15 % B - 25 min; 20 % B - 30 min; 25 % B - 30 min; 30 % B - 30 min; 35 % B - 30 min; 40 % B - 25 min; 100 % B - 20 min] to get pure crystals of respective compounds (**9d**/**10d**/**11d**). (Tanaka H *et al*., 1988).

Ethyl 3,9-dihydro-3-(4-hydroxyphenyl)-7-methyl-9-oxo-2H-[1,4]dioxino[2,3-h]chromene-2-carboxylate (**9d**): Pale brown amorphous solid; yield: 3.19%; APCI-MS (*m/z*): calcd $[M]^+$ 382.105, found $[M-1]^+$ 381.2; $[M+1]^+$ 383.0

Ethyl 3,9-dihydro-3-(3,4-dihydroxyphenyl)-7-methyl-9-oxo-2H-[1,4]dioxino[2,3-h]chromene-2-carboxylate (**10d**): Colourless crystals; yield: 10.87%; ^{1}H-NMR (400 MHz, DMSO-d_6): δ 7.17 (1H, d, 9 Hz, 5-H), 6.92 (1H, d, 8.7 Hz, 6-H), 6.88-6.78 (3H, m, 2′-, 5′-, 6′-H), 6.19 (1H, d, 1.5 Hz, 3-H), 5.20 (1H, d, 5.7 Hz, 7′-H), 4.80 (1H, d, 6.0 Hz, 8′-H), 4.14 (2H, q, 9′-O$\underline{CH_2}$ CH_3), 2.42 (3H, d, 0.9 Hz, 4-CH_3), 1.13 (3H, t, 9′-OCH_2 $\underline{CH_3}$); ESI-MS (*m/z*): calcd $[M]^+$ 398.100, found $[M-1]^+$ 397.15; $[M+1]^+$ 399.10.

Ethyl-3,9-dihydro-3-(4-hydroxy-3-methoxyphenyl)-7-methyl-9-oxo-2H-[1,4]dioxino[2,3-h]chromene-2-carboxylate (**11d**): Pale yellow amorphous powder, yield: 12.53%; ^{1}H-NMR (300 MHz, $CDCl_3$:CD_3OD [1:10]): δ 7.18 (1H, d, 8.7 Hz, 5-H), 6.95 (1H, d, 9 Hz, 6-H), 6.93-6.89 (3H, m, 2′-, 5′-, 6′-H), 6.20 (1H, d, 6.3 Hz, 7′-H), 6.20 (1H, d, 1.2 Hz, 3-H), 5.23 (1H, d, 6.3 Hz, 8′-H), 4.21 (2H, q, 9′-O$\underline{CH_2}CH_3$), 3.89 (3H, s, 3′-OCH_3), 2.43 (3H, d, 1.2 Hz, 4- CH_3), 1.12 (3H, t, 9′-$OCH_2\underline{CH_3}$); ^{13}C-NMR (75.5 MHz, $CDCl_3$:CD_3OD [1:10]): δ 166.8 (9′-C), 160.8 (2-C), 153.3 (4-C), 147.2 (9-C), 146.8 (3′-C), 145.7 (4′-C), 143.0 (7-C), 130.1 (8-C), 125.7 (1′-C), 120.5 (6′-C), 116.7 (5-C), 113.3 (10-C), 112.3 (2′-C), 114.8 (5′-C), 114.7 (3-C), 109.8 (6-C), 76.3 (8′-C), 76.1 (7′-C), 61.9 (9′-O$\underline{C}H_2CH_3$), 55.8 (3′-OCH_3), 18.7 (4-CH_3), 13.7 (9′-$OCH_2\underline{C}H_3$); APCI-MS (*m/z*): calcd $[M]^+$ 412.1158, found $[M-1]^+$ 411.20; $[M+1]^+$ 413.10

4.3.6 Preparation of acetylated compound (11e)

Compound **11d** was treated with acetic anhydride and pyridine, and stirred for 12 h under room temperature. The reaction mixture was extracted with dichloromethane and then washed with distilled water and then dried by passing through sodium sulphate bed. The dichloromethane layer was evaporated under reduced pressure to obtain ethyl 3-(4-acetoxy-3-methoxyphenyl)-3,9-dihydro-7-methyl-9-oxo-2H-[1,4]dioxino[2,3-]chromene-2-carboxylate (**11e**).

Ethyl 3-(4-acetoxy-3-methoxyphenyl)-3, 9-dihydro-7-methyl-9-oxo-2H-[1,4]dioxino[2,3-]chromene-2-carboxylate (**11e**): White amorphous solid; yield: 90%; ^{1}H-NMR (300 MHz, $CDCl_3$:CD_3OD [1:10]): δ 7.16 (1H, d, 8.5 Hz, 5-H), 7.05 (1H, d, 8.5 Hz, 6-H), 6.99 (2H, dd, 9.5 Hz, 2′, 6′-H), 6.93 (1H, d, 8.5 Hz, 5′-H), 6.19 (1H, d, 0.5 Hz, 3-H), 5.33 (1H, d, 6.0 Hz, 7′-H), 4.82 (1H, d, 5.5 Hz, 8′-H), 4.14 (2H, q, 9′-O$\underline{CH_2}CH_3$), 3.83 (3H, s, 3′-OCH_3), 2.41 (3H, d, 1.0 Hz, 4-CH_3), 2.32 (3H, s, 4′-OCO$\underline{CH_3}$), 1.13 (3H, t, 9′-$OCH_2\underline{CH_3}$); ^{13}C-NMR (75.5 MHz, $CDCl_3$:CD_3OD [1:10]): δ 168.7 (4′-O$\underline{C}OCH_3$), 166.7 (9′-C), 160.2 (2-C), 152.6 (4-C), 151.4 (4′-C), 145.3 (9-C), 143.2 (7-C), 140.5 (3′-C), 133.3 (6′-C), 130.2 (8-C), 123.2 (1′-C), 119.5 (5′-C), 116.8 (5-C), 114.3 (3-C), 113.1 (10-C), 112.7 (2′-C), 111.1 (6-C), 75.9 (8′-C), 75.8 (7′-C), 62.1 (9′-O$\underline{C}H_2CH_3$), 56.0 (3′-OCH_3), 20.1 (4′-OCO$\underline{C}H_3$), 18.9 (4-CH_3), 13.8 (9′-$OCH_2\underline{C}H_3$); APCI-MS (*m/z*): calcd $[M]^+$ 454.12638, found $[M+1]^+$ 455.0; $[M+2]^+$ 456.0

4.4 Isolation of cleomiscosin A (15)

Around 5 kg of powdered *Cleome viscosa* seeds were defatted using petroleum ether and then subjected for hot extraction using methanol (45–50 °C; 3 h; thrice). The methanolic extract was then concentrated and kept aside for 24 h. The yellow colored solid precipitate formed was filtered and then washed using cold methanol to yield cleomiscosin A. It was recovered as amorphous solid (5.2 g) whose identity was established by co-TLC studies with authentic sample, comparison of ^{1}H-NMR data with reported values (Begum S *et al*., 2010) and through APCI-MS analysis.

Cleomiscosin A (**15**): Yellow amorphous powder; APCI-MS: m/z: $[M–H]^+$ - calcd for $C_{20}H_{17}O_8$, 385.1002; found, 385.15; $[M+H]^+$ - calcd for $C_{20}H_{19}O_8$, 387.1002; found, 387.10.

4.5 Preparation of cleomiscosin-A-9′-O-glucoside (15g)

A mixture of cleomiscosin A (200 mg, 0.518 mmol), absolute pyridine (20 mL), and dry chloroform (10 mL) was treated dropwise with a solution of acetobromo-α-D-glucose (213 mg, 0.518 mmol) in chloroform (15 mL) and stirred at room temperature for 24 h under nitrogen atmosphere. Then the reaction mass was diluted with chloroform (100 mL) and water (50 mL) to isolate the precipitate ($C_5H_5N{\cdot}HBr$). The organic layer was treated with $NaHCO_3$ and water until neutral, following which the organic layer was washed with 1N HCl, water and brine. The collected organic layer was then dried with sodium sulphate, filtered and concentrated to get a crude product of cleomiscosin A glycoside (50 mg), which was purified through preparative TLC using DCM and methanol (7:3) solvent system. The structure of purified **15g** was elucidated based on proton NMR and APCI-MS analyses (Kren V *et al*., 1997).

Cleomiscosin-A-9 ′-O-glucoside (**15g**): White color amorphous solid; ^{1}H-NMR (400 MHz, DMSO-d_6): δ 9.21 (1H, s, 4′-OH), 7.97 (1H, d, J=12.8 Hz, 4-H), 7.03 (1H, s, 5-H), 6.92 (1H, narrow d, 2′-H), 6.87 (1H, m, 6′-H), 6.81 (1H, d, J=10.8 Hz, 5′-H), 6.34 (1H, d, J=12.8 Hz, 3-H), 4.99 (1H, d, J=10.8 Hz, 7′-H), 4.90 (1H, narrow d, 1′′-H), 4.76 (br s, Glu-OH), 4.62 (br s, Glu-OH), 4.43 (br s, Glu-OH), 4.34 (m, Glu-OH), 4.34 (1H, m, 8′-H), 3.78 (s, 3H,−OCH_3), 3.77 (s, 3H, −OCH_3), 3.68-3.52 (2H, m, 9′-H2), 3.44-3.38 (2H, m, 6′′-H_2), 3.11-2.99 (4H, m, 2′′-,3′′-, 4′′-, 5′′-H). APCI-MS: (m/z: $[M]^+$ - calcd for $C_{26}H_{27}O_{13}$, 548.15299; found, 548.1500; $[M+Na]^+$ - calcd for $C_{26}H27O_{13}Na$,; found, 571.14279; found, 571.1000.

4.6 Biological activity

4.6.1 In-vitro screening procedures

4.6.1.1 In-vitro screening of compounds using LPS and crystal induced model

In-vitro assays were carried out in order to determine the anti-inflammatory efficacy of the test compounds (**1a**, **3b**, **4b** and **5b**) in LPS-stimulated mouse macrophage RAW 264.7 cell lines against pro-inflammatory cytokines using ELISA.

4.6.1.2 Bioassay for TNF-α and IL-6

RAW 264.7 cell lines were pre-treated with four different concentrations of compounds i.e. 100 μM, 30 μM, 10 μM and 3 μM for 1 h, followed by stimulation of the cells using 1 μg/ml of LPS. The supernatant was collected after 6 h of stimulation for TNF-α and IL-6 estimations using ELISA kit. ELISA assay was performed as per the manufacturer's instruction (Zhang X *et a*l., 2008)

4.6.1.3 Bioassay for IL-1β

IL-1β estimations were carried out by pre-treating RAW 264.7 cell lines for 1 h with different concentrations of compounds (100 μM, 30 μM, 10 μM and 3 μM), followed by induction using 1 μg/ml of LPS and 250μg/ml oxalate crystals. Levels of IL-1β was then determined in the collected supernatant using ELISA kit (Ouyang X *et a*l., 2013; Mulay SR *et a*l., 2013).

4.6.1.4 Determination of NO production

The compounds were tested for their ability to inhibit NO production. For this RAW 264.7 cells were cultured in a 96 well plate and treated with compounds for 6 h followed by induction with LPS for 24 h. Around 100 µl of supernatant was collected and then mixed with 100 µl of Griess reagent (1% sulfanilamide and 0.1% naphthylethylenediamine dihydrochloride in 2.5% phosphoric acid) and kept for incubation at room temperature for 10 min. Then the absorbance was measured at 540 nm in a multiplate reader (Sun J *et a*l., 2003).

4.6.1.5 Cytotoxicity assay

MTT assay or cell viability assay was carried out to determine the toxicity of the compounds on RAW 264.7 cell lines. RAW 264.7 cells were seeded and cultured in a 96 well plate. Cells were treated with compounds after adherence. After 24 h of treatment, 50 µL of MTT reagent (5 mg/ml dissolved in phosphate buffer saline) was added into each well and incubated at 37 ^{0}C for 3 h. Then the whole media was removed and 100 µL of DMSO was added into each well to dissolve the formed crystal. Absorbance was measured at 570 nm in multiplate reader (van Meerloo J *et a*l., 2011; Mosmann T., 1983).

4.6.2 In-vivo anti-inflammatory studies

All in-vivo studies were performed as per standard guidelines following standard protocols. The study protocols were reviewed by Institutional Animal Ethical Committee and was granted approval with approval nos. BITS-Hyd/IAEC/2017/09 and BITS-Hyd/IAEC/2017/23.

4.6.2.1 In-vivo screening of the compounds by mouse endotoxemia model

Anti-inflammatory efficacy of the compounds was tested using mouse endotoxemia model. In this model, animals were divided into eight different groups each containing six animals.

Group 1: Normal control group

Group 2: LPS control group

Group 3: Standard (Prednisolone) control group

Group 4: Compound **9d** treated group

Group 5: Compound **10d** treated group

Group 6: Compound **11d** treated group

Group 7: Compound **11e** treated group

Group 8: Compound **15** treated group

Animals were pretreated with the compounds at a dose of 50 mg/kg. Compounds were prepared as suspension in a vehicle consisting of 0.5% methylcellulose and 0.025% Tween 20 and administered through oral route using a gavage at dose volume of 10 ml/kg. After one hour of drug treatment, LPS was injected by intraperitoneal route at a dose of 0.3 mL/kg (Dose volume 1

mL/kg in sterile saline). Blood was withdrawn through retro orbital route at different time points (1 h and 6 h after LPS administration). ELISA studies were carried out on isolated plasma to estimate the levels of cytokines TNF-α, IL-1β and IL-6 using commercially available kits. ELISA assays were carried out as per the manufacturer's instruction (Howard M *et al*., 1993; Wang H *et al*., 1999; Choi Y *et al*., 2008).

4.6.2.2 In-vivo screening of the compounds by carrageenan-induced mouse paw edema model

In this model animals were classified into eight different groups, each having six animals:

Group 1: Normal control group

Group 2: Carrageenan control group

Group 3: Standard (Prednisolone) control group

Group 4: Compound **9d** treated group

Group 5: Compound **10d** treated group

Group 6: Compound **11d** treated group

Group 7: Compound **11e** treated group

Group 8: Compound **15** treated group

25 μL of carrageenan (1% w/v solution in 0.9% sterile saline) was injected into the paw of the BALB/c mouse to test the efficacy of the test compounds in local inflammation. Test compounds (Dose 50 mg/kg) were administered by oral route 1 h prior to carrageenan injection using

gavage. Then carrageenan was injected in sub-plantar region of left hind paw subcutaneously. Paw volume was measured on hourly basis using plethysmometer till 4 h of carrageenan administration. Animals were sacrificed after fourth paw volume reading. Paws were collected, and snap frozen for cytokine estimations using ELISA kits (Morris CJ., 2003).

4.6.2.3 In-vivo testing of compound 10d in a mouse model of oxalate nephropathy

Anti-inflammatory efficacy of the compounds was tested using oxalate model of renal nephropathy. Briefly, in oxalate nephropathy model, study was carried out in three different groups of C57/BL6 mice (Male, 6-8wks old). Each group contained six animals.

Group 1: Normal control group

Group 2: Oxalate control group

Group 3: Compound **10d** treated group

Mice were fasted overnight and were then administered with the test compound at a dose of 50 mg/kg after 12 h of fasting. Compound was prepared as suspension in a vehicle consisting of 0.5% methylcellulose and 0.025% Tween 20 and administered through oral route using a gavage at dose volume of 10 mL/kg. After one hour of drug administration, sodium oxalate solution was injected at a dose of 100mg/kg body weight by intra-peritoneal route. Immediately after the injection of sodium oxalate the mice were fed with normal diet and water premixed with 3% w/v of sodium oxalate. After 24 h of injection of sodium oxalate, the mice were sacrificed to harvest the blood samples and kidney tissue samples.

The renal damage caused by the oxalate nephropathy was evaluated by determining the BUN (Blood-Urea-nitrogen) levels in plasma (renal function parameter), expression of KIM-1 (kidney injury molecule-1, a renal injury marker) and expression of IL-1β, IL-6 and TNF-α (inflammatory markers) in the renal tissue.

Also, histological analysis of renal tissue by H&E staining was performed. Histological scoring was done by quantifying tubular injury by semi-quantitative scoring method and scores were given on a scale of 0-5 (0 for nil damage and 5 for severe damage) based on renal damage such as tubular dilation, tubular necrosis and casts. ELISA studies were carried out on isolated plasma to estimate the levels of IL-1β using commercial kits (Mulay SR *et al*., 2013).

4.7 Statistical Analysis

All results were expressed as mean ± SEM for each group. Statistical differences between the groups were determined by one way ANOVA followed by multiple comparisons with *Graph pad prism 6.0* statistical software. The level of statistical significance was set at $P < 0.05$.

CHAPTER 5

RESULTS AND DISCUSSION

CHAPTER 5 RESULTS AND DISCUSSION

5.1 Synthesis and in-vitro biological evaluations on methyl coumarin and phenyl propanoid derivatives followed by molecular docking studies towards developing novel coumarin based pro-inflammatory cytokines inhibitors

5.1.1 Introduction

Controlling the inflammation with considerable efficacy is a challenge, as several factors play a role in inflammation. Pro-inflammatory cytokines like TNF-α, IL-6 and IL-1β are the major players involved in the development of inflammation and neuropathic pain leading to chronic inflammatory and autoimmune diseases. Pro-inflammatory cytokine antagonists could be a non-opioid therapeutic approach for the treatment of pathological pain and inflammation due to nerve injury (Zhang J-M and An J., 2007) as they act on both immune cells and cancer cells (Taniguchi K and Karin M., 2018). Further, the development of inflammatory diseases involves participation of multiple cytokines, so blocking one particular cytokine provides only partial protection. Hence there is a need to develop inhibitors having pan-cytokine inhibition effect. Discovery and development of such inhibitors could be achieved through research on structurally diverse natural molecules with the help of molecular modeling and docking studies.

5.1.2 Coumarin and phenyl propanoid derivatives as anti-inflammatory test compounds

Several small natural molecules have been reported in the literature for their efficacy against inflammation, which can further be repurposed as lead molecules for developing anti-cytokine drugs (Arulselvan P *et al*., 2016). While searching the literature, coumarins and cinnamic acid derivatives were identified as potential target molecules based on their effect to control inflammation and cytokine expression.

Coumarins are the benzopyrone-group of bioactive plant secondary metabolites known to diminish tissue oedema and inflammation, and inhibit prostaglandin biosynthesis (Fylaktakidou KC *et al*., 2004). Also, several coumarin derivatives, especially those having the substitution at the C-4 position had been reported to be active against pro-inflammatory cytokines (Katsori A-M and Hadjipavlou-Litina D., 2014). Coumarin derivatives with substitution at C-5 are relatively unexplored (Grover J and Jachak SM., 2015) and hence 5-methyl and 4-methyl substituted coumarin derivatives were included as the initial lead compounds in the present study. Haggar *et al*., had proved the efficacy of certain coumarin derivatives under carrageenan-induced edema and against cyclooxygenase enzymes (El-Haggar R and Al-Wabli RI., 2015). Cheng JF *et al*., had elaborated structure-activity relationship of coumarin derivatives as inhibitors of TNF-α by synthesizing an array of C-3 and C-4 modified coumarins of dimethyl-carbamic acid 3-benzyl-4-methyl-2-oxo-2H-chromen-7-yl ester, which had exhibited an IC_{50} value of 1.8 μM (Cheng J-F *et al*., 2004). In the literature, C-4 methyl coumarin derivatives with C-7 and C-8 hetero atoms or C-7 and C-8 fused heterocycles had been reported to attenuate the chronic inflammation and tissue damage associated with collagen induced arthritis (Fylaktakidou KC *et al*., 2004). Thus, 7,8-dihydroxy-4-methyl cinnamic acid (**1a**) was selected for the study and synthesized.

Another set of interesting natural molecules evaluated in the present study was cinnamic acid derivatives, which belong to phenylpropanoid (C_6C_3) group of compounds. They had been reported to possess various pharmacological actions such as anti-inflammatory, anti-microbial, anti-cancer, anti-human immunodeficiency virus, and anti-parasitic (Zhou K *et al*., 2014). Cinnamate esters of menthol and puligol had been reported to display potential anti-inflammatory activity (Godoy ME *et al*., 2000).

In case of cinnamic acid derivatives, esters of bioactive *p*-coumaric acid, caffeic acid and ferulic acid were chosen for the study, as ester derivatives are good pro-drugs, releasing acid

derivatives in the physiological system to impart intended biological activities. The acid group can have good ionic interactions with the targeted cytokines to inhibit and control their over-expressions during chronic inflammation. Also, *p*-coumaric acid, caffeic acid and ferulic acid had been reported to inhibit LPS-induced TNF-α and IL-6 secretions and also control production of nitric oxide (NO) (Lampiasi N and Montana G., 2016; Patel NK and Bhutani KK., 2014). Generally, ethyl ester groups are excellent prodrugs undergoing metabolism by esterases in the body and forming non-toxic by-products like ethanol (Testa B., 2006). Hence, compounds ethyl-*p*-coumarate (**3b**), ethyl caffeate (**4b**) and ethyl ferulate (**5b**) were synthesised.

5.1.3 Synthesis and characterization of 7,8-dihydroxy-4-methyl coumarin (1a)

7,8-Dihydroxy-4-methyl coumarin (**1a**) was prepared by reacting pyrogallol and ethyl acetoacetate in the presence of $HClO_4.SiO_2$ at 130 °C (Scheme 5.1) (Chakraborti AK and Gulhane R., 2003; Maheswara M *et al*., 2006). The product was purified through column chromatography and homogeneity was confirmed through TLC studies. 7,8-Dihydroxy-4-methyl-2H-chromen-2-one (**1a**) was obtained as yellow amorphous powder showing melting point of 241-242 °C. The IR spectrum of **1a** (Figure 5.1.1) displayed absorption bands due to hydroxyl and benzochromone groups confirming the formation of hydroxyl coumarin nucleus. Further, the product **1a** was confirmed from its APCI-MS spectrum (Figure 5.1.2) which showed $[M-H]^+$ peak at m/z 191.100 and $[M+1]^+$ 192.9500.

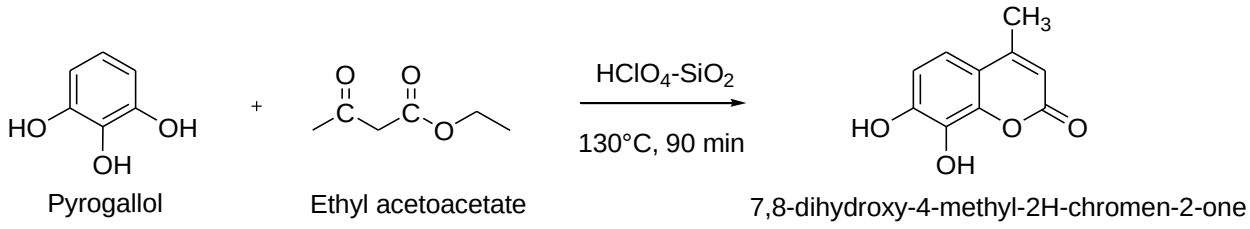

Scheme 5.1 Preparation of 7,8-Dihydroxy-4-methyl coumarin (1a)

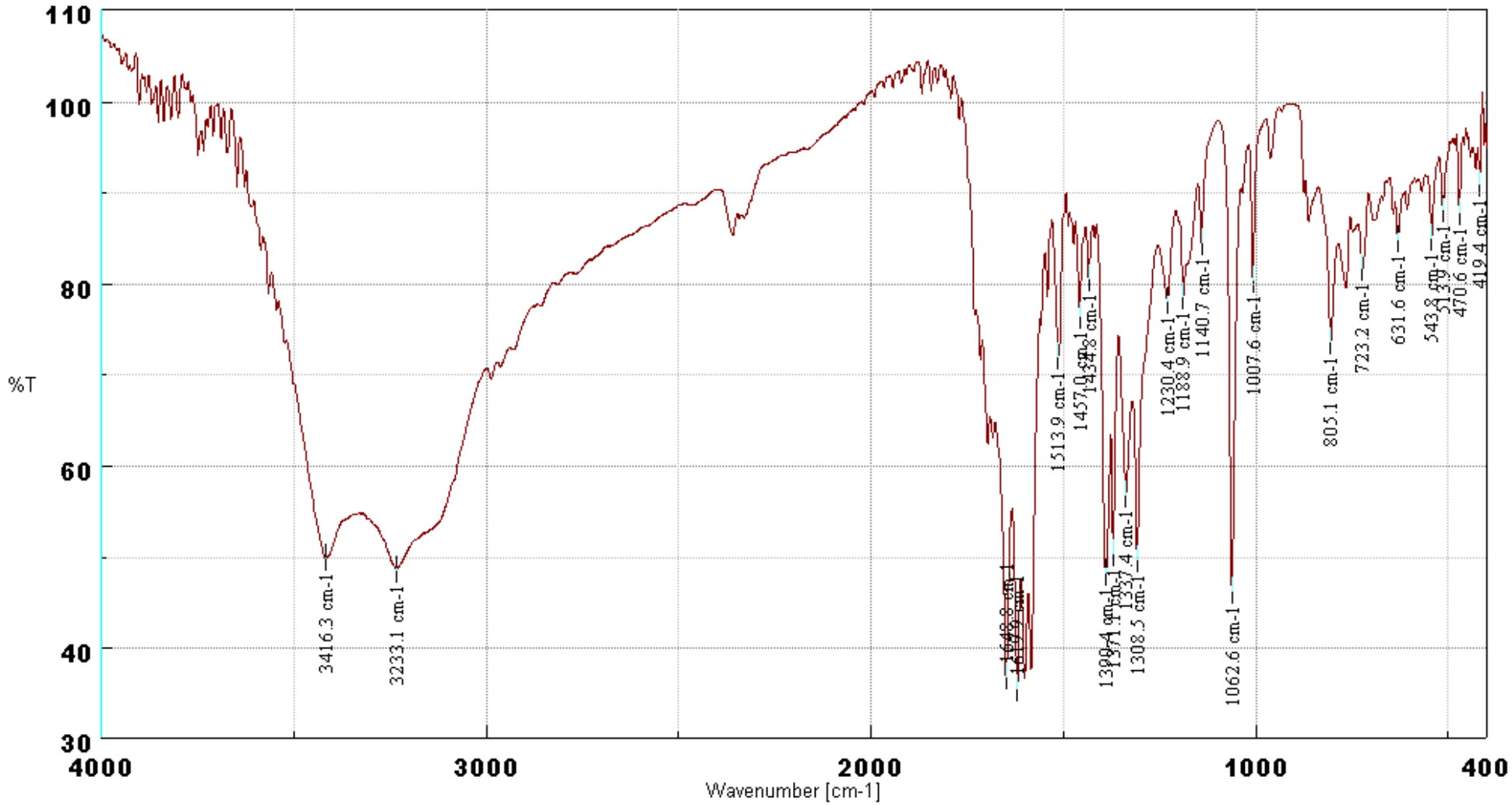

Figure 5.1.1 IR spectrum of 7,8-Dihydroxy-4-methyl coumarin (1a)

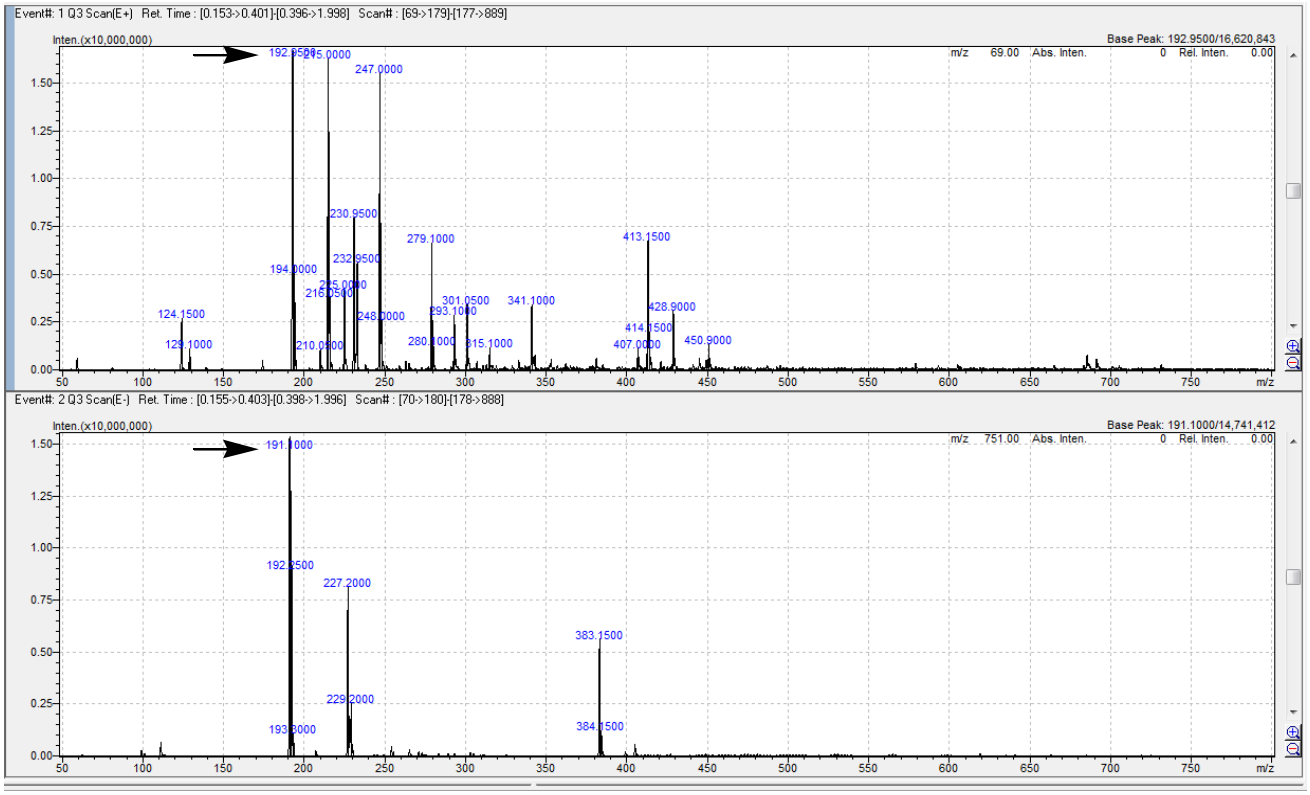

Figure 5.1.2 APCI mass spectrum of 7,8-dihydroxy-4-methyl coumarin (1a)

5.1.4 Synthesis and characterization of cinnamic acid ester derivatives (3b, 4b and 5b)

Compounds **3b**, **4b** and **5b** were prepared by reaction between the corresponding cinnamic acid derivatives (*p*-coumaric acid **3**, caffeic acid **4** and ferulic acid **5**), ethanol and conc. H_2SO_4 (Scheme 5.2). The products were purified through column chromatography and confirmed through IR spectroscopy and ESI-MS analysis.

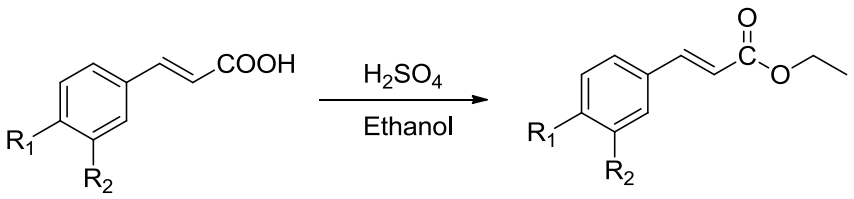

Cinnamic acid derivatives

***p*-Coumaric acid (3)** - R_1 -OH, R_2 -H

Caffeic acid (4) - R_1 -OH, R_2 -OH

Ferulic acid (5)- R_1 -OH, R_2 -OCH_3

Cinnamic ester derivatives

Ethyl-*p*-coumarate (3b) - R_1 -OH, R_2 -H

Ethyl caffeate (4b) - R_1 -OH, R_2 -OH

Ethyl ferulate (5b)- R_1 -OH, R_2 -OCH_3

Scheme 5.2 Preparation of cinnamic acid ester derivatives

(*E*)-ethyl 3-(4-hydroxyphenyl)acrylate (**3b**) was obtained as white amorphous powder showing melting point of 73-74 °C. Comparision of IR spectra of *p*-coumaric acid (**3**) (Figure 5.1.3a) and its ester derivative (**3b**) (Figure 5.1.3b) corroborated the product formation. Further, the APCI-MS (Figure 5.1.4) showed $[M-1]^+$ at m/z 191.2 and $[M+1]^+$ at m/z 193.00 ascertaining the product **3b**.

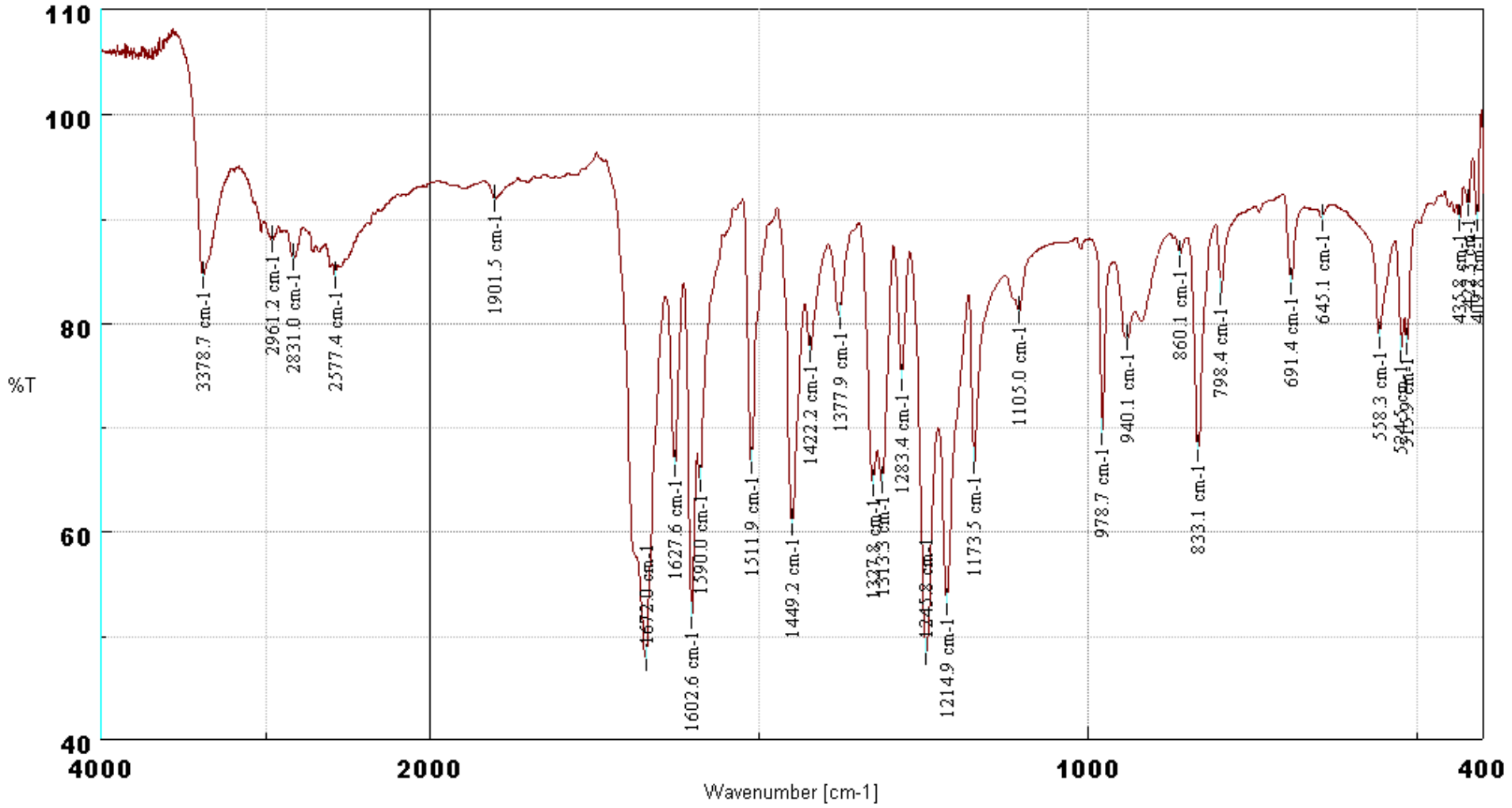

Figure 5.1.3a IR spectrum of *p*-coumaric acid (3)

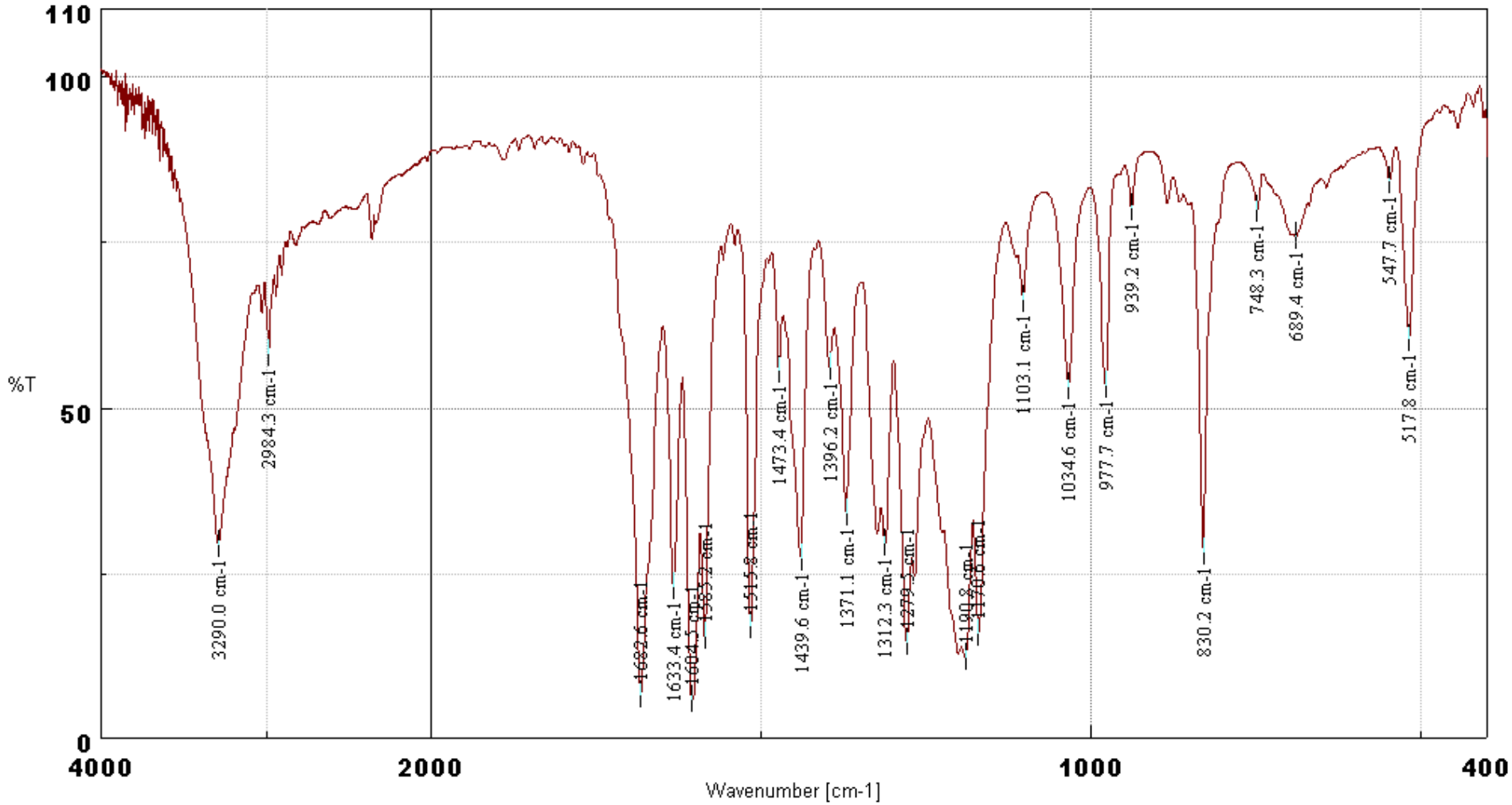

Figure 5.1.3b IR spectrum of ethyl *p*-coumarate (3b)

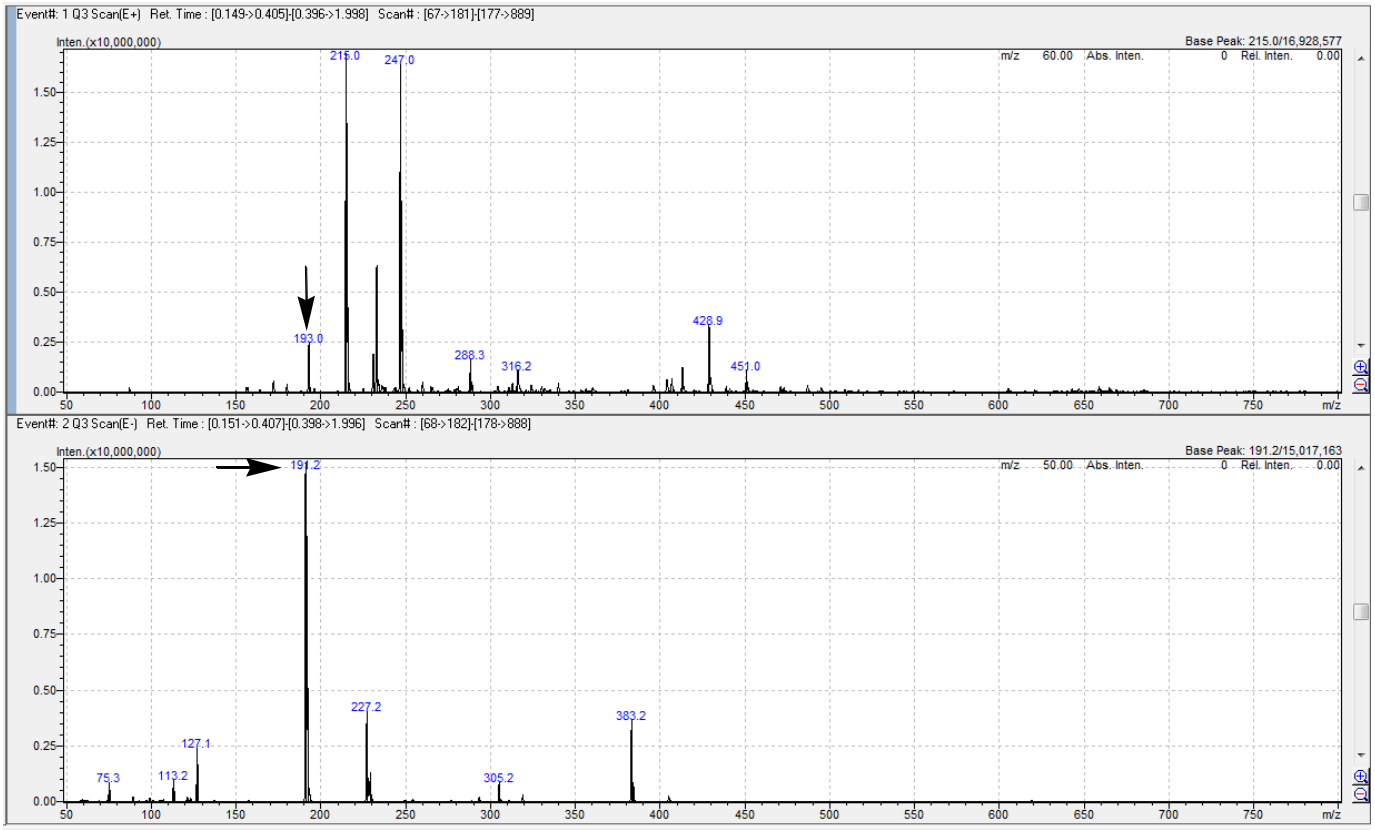

Figure 5.1.4 APCI mass spectrum of ethyl *p*-coumarate (3b)

(*E*)-ethyl 3-(3,4-dihydroxyphenyl)acrylate (**4b**) was synthesized as brown amorphous powder showing melting point of 149-150 °C. The disappearance of absorption bands due to acid –OH and –C=O groups and appearance of aliphatic C-H stretching bands in the IR spectrum (Figure 5.1.5a and 5.1.5b) of **4b** confirmed the product formation. Further, the APCI-MS (Figure 5.1.6) showed $[M-1]^+$ at m/z 207.0000 and $[M]^+$ at m/z 208.2500 ascertaining the product **4b**.

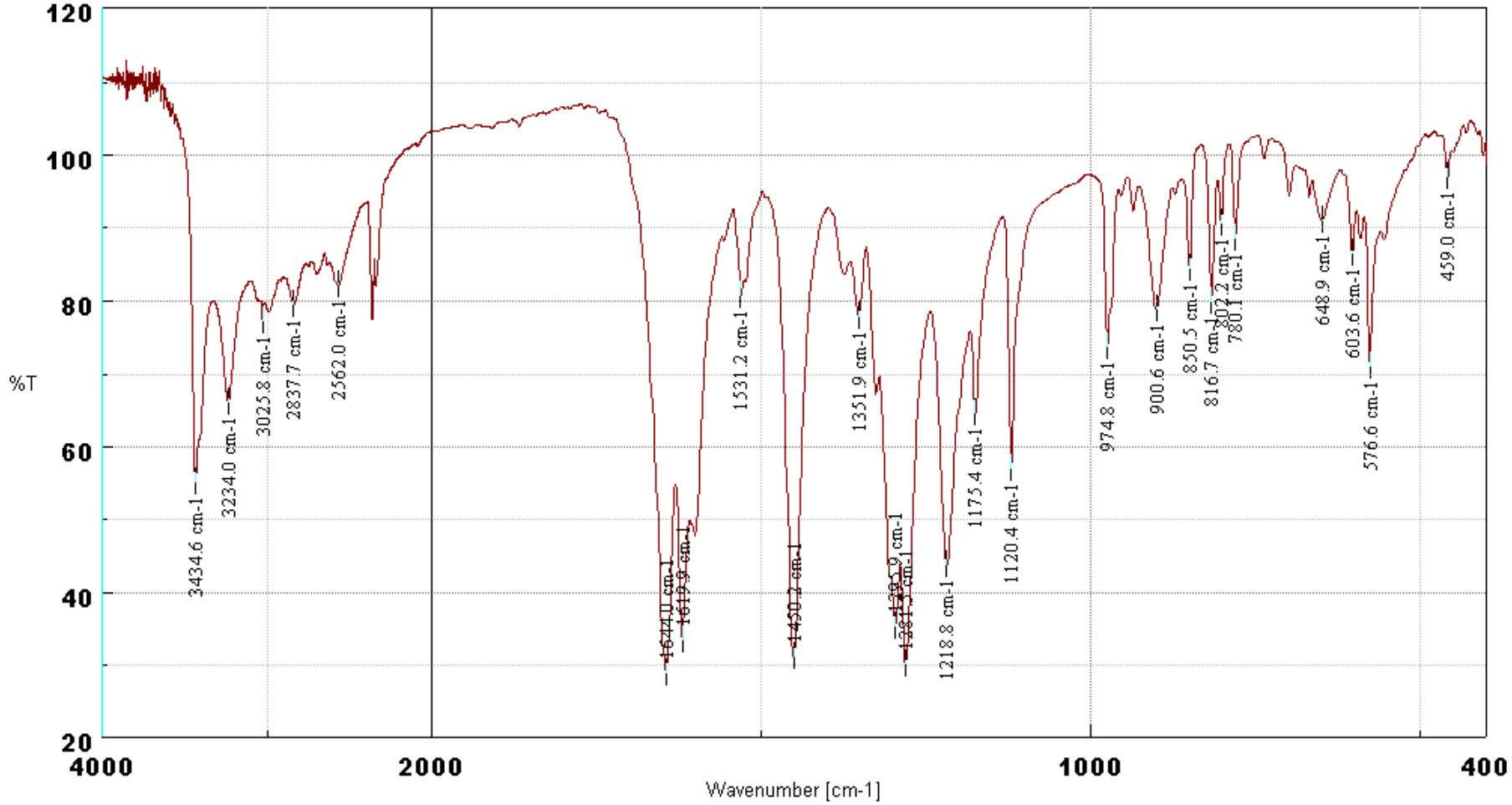

Figure 5.1.5a IR spectrum of caffeic acid (4)

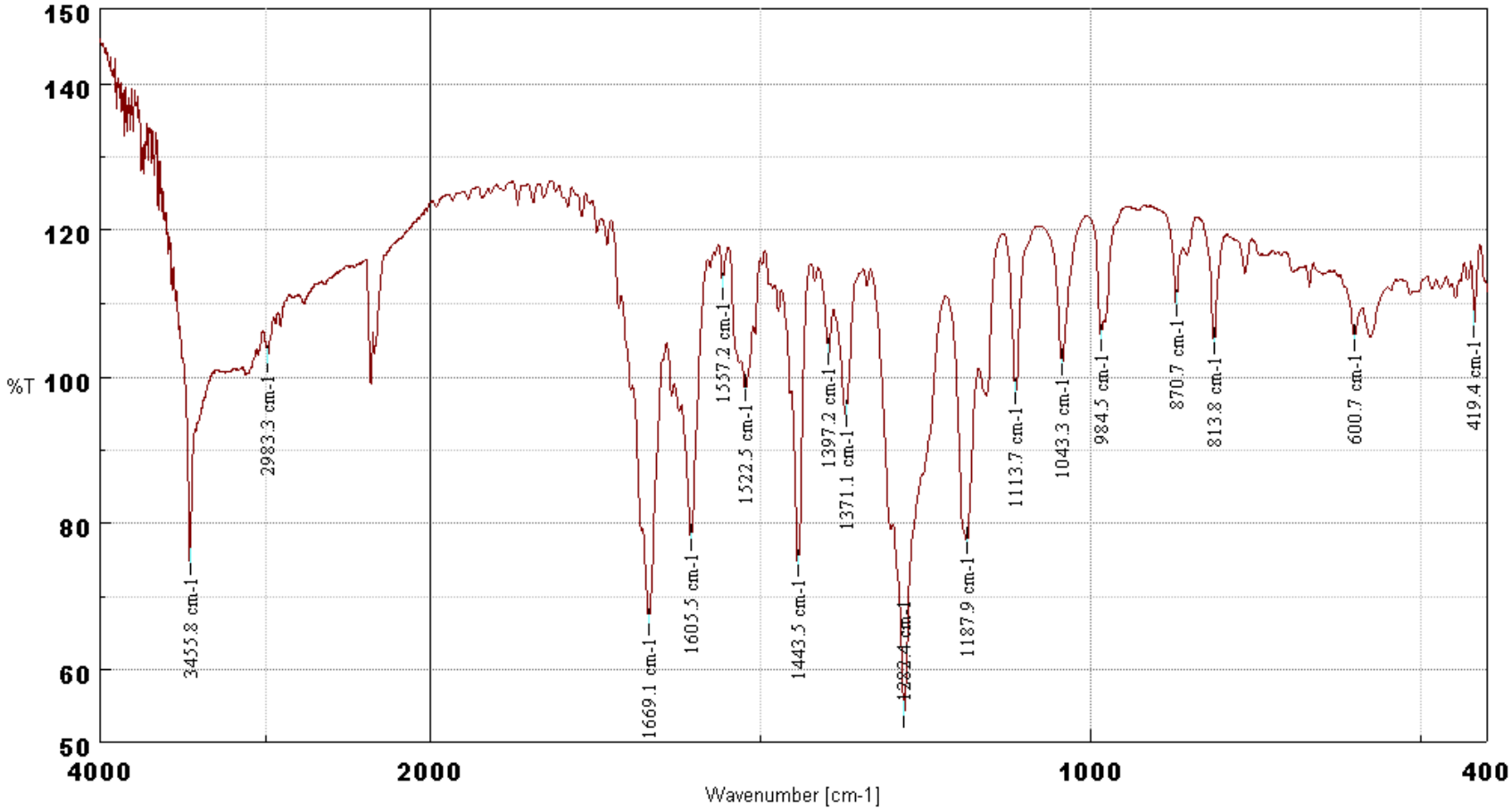

Figure 5.1.5b IR spectrum of ethyl caffeate (4b)

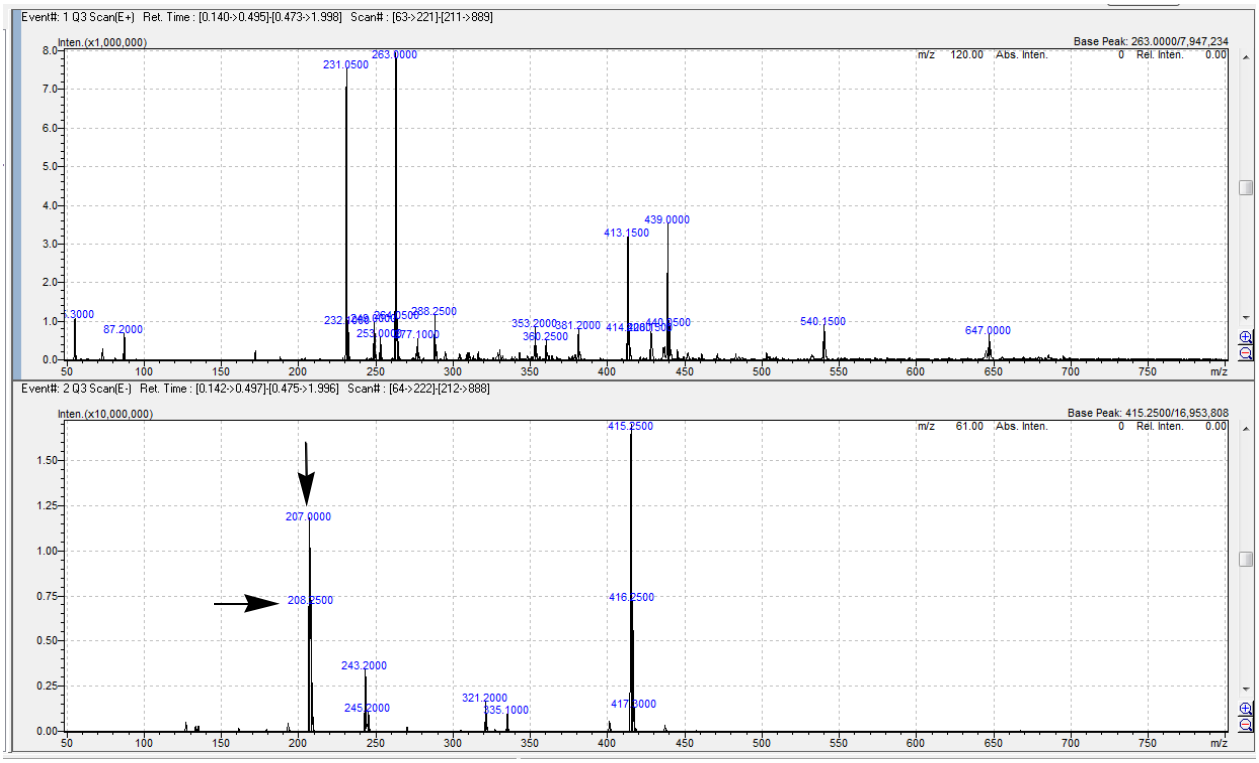

Figure 5.1.6 APCI mass spectrum of ethyl caffeate (4b)

(*E*)-ethyl 3-(4-hydroxy-3-methoxyphenyl)acrylate (**5b**) was recovered as pale yellow crystal showing melting point of 64-65 °C. On comparing the IR spectrum of ferulic acid (**5**) (Figure 5.1.7a) with that of ethyl ferulate (**5b**) (Figure 5.1.7b), the disappearance of absorption bands due to acid –OH and –C=O groups and appearance of aliphatic C-H stretching bands were observed, which confirmed the product formation. Also, the the APCI-MS (Figure 5.1.8) showed $[M-1]^+$ at m/z 221.0 and $[M-2]^+$ at m/z 220.0 ascertaining the product **5b**.

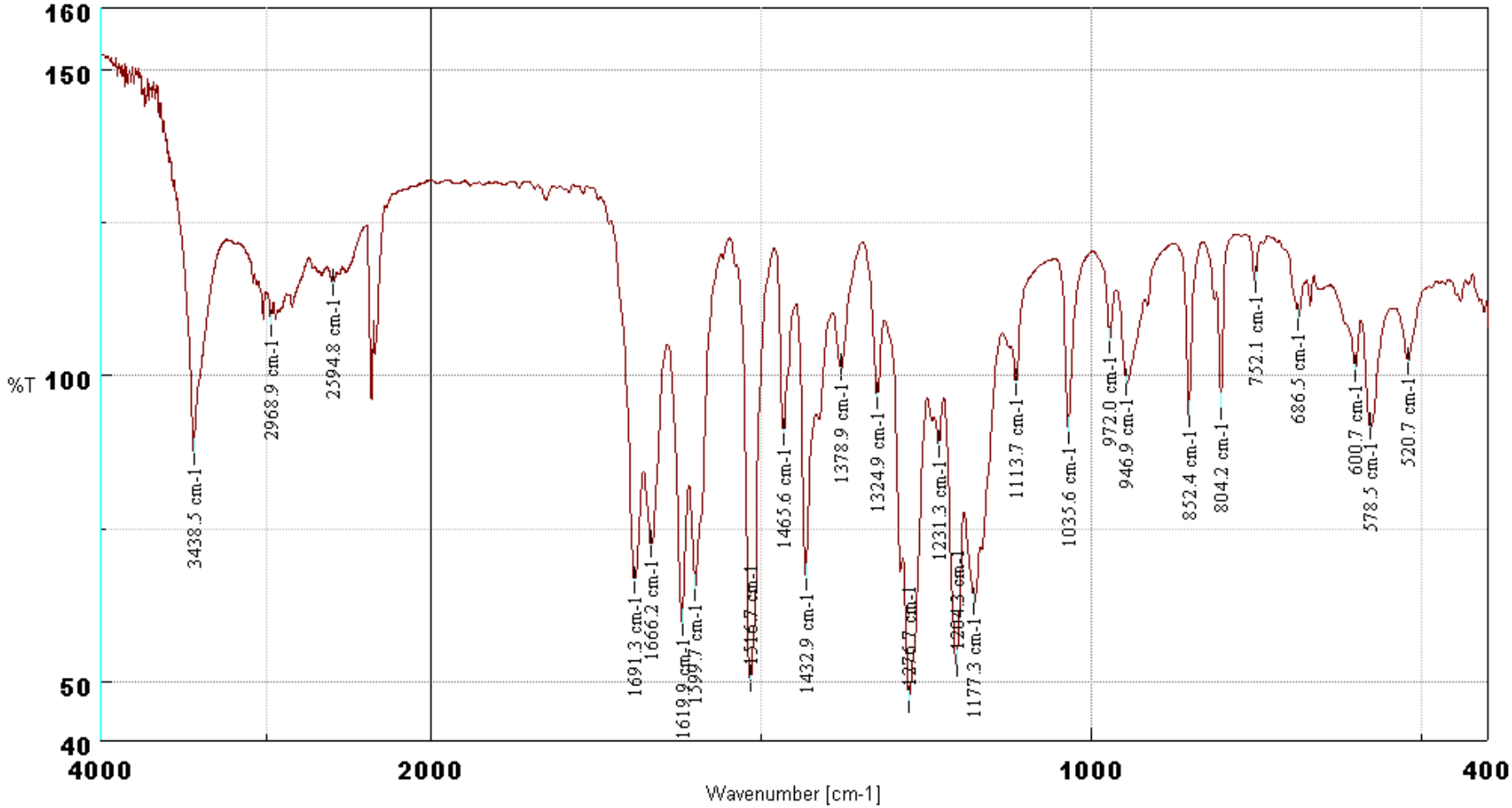

Figure 5.1.7a IR spectrum of ferulic acid (5)

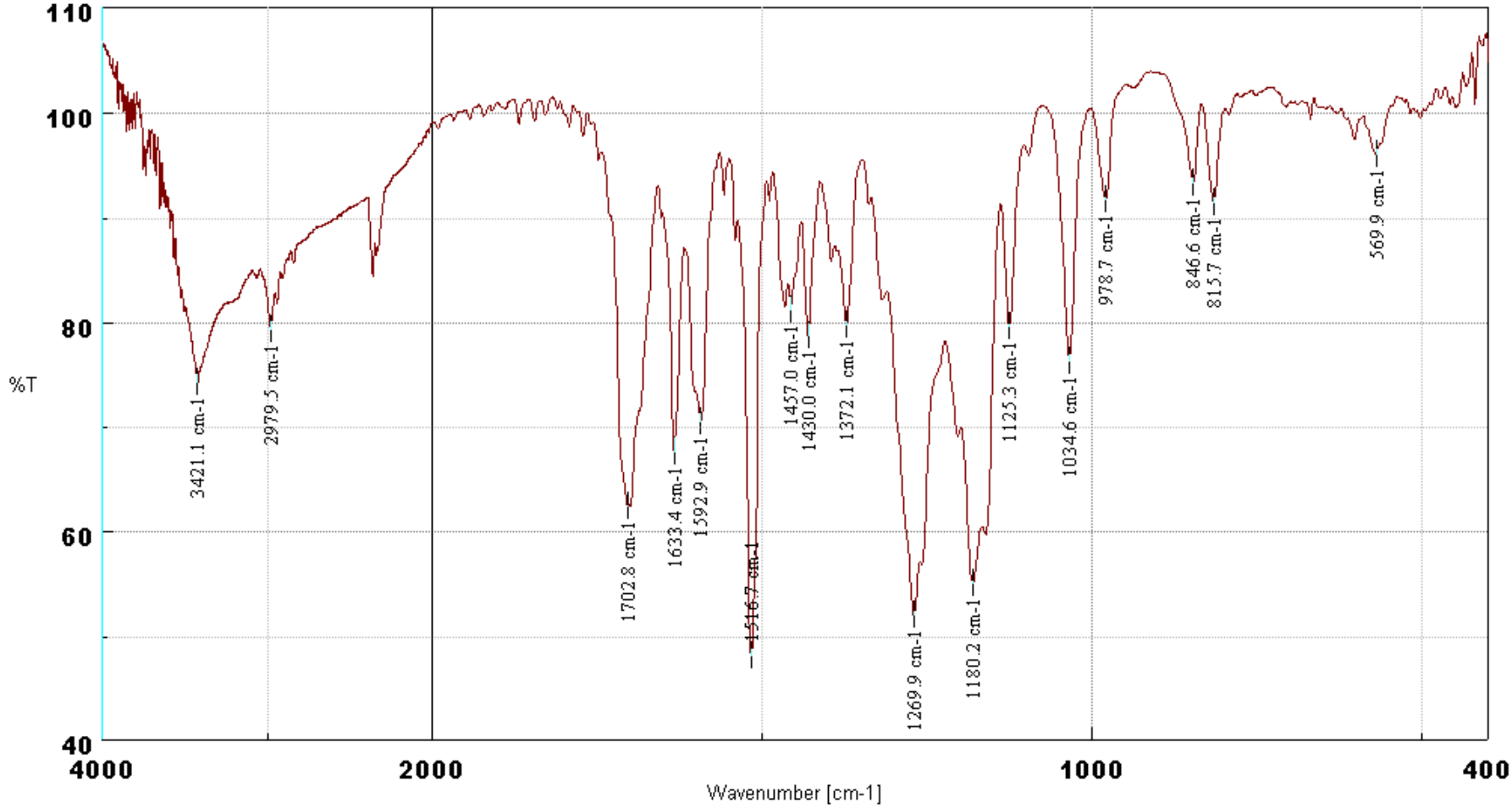

Figure 5.1.7b IR spectrum of ethyl ferulate (5b)

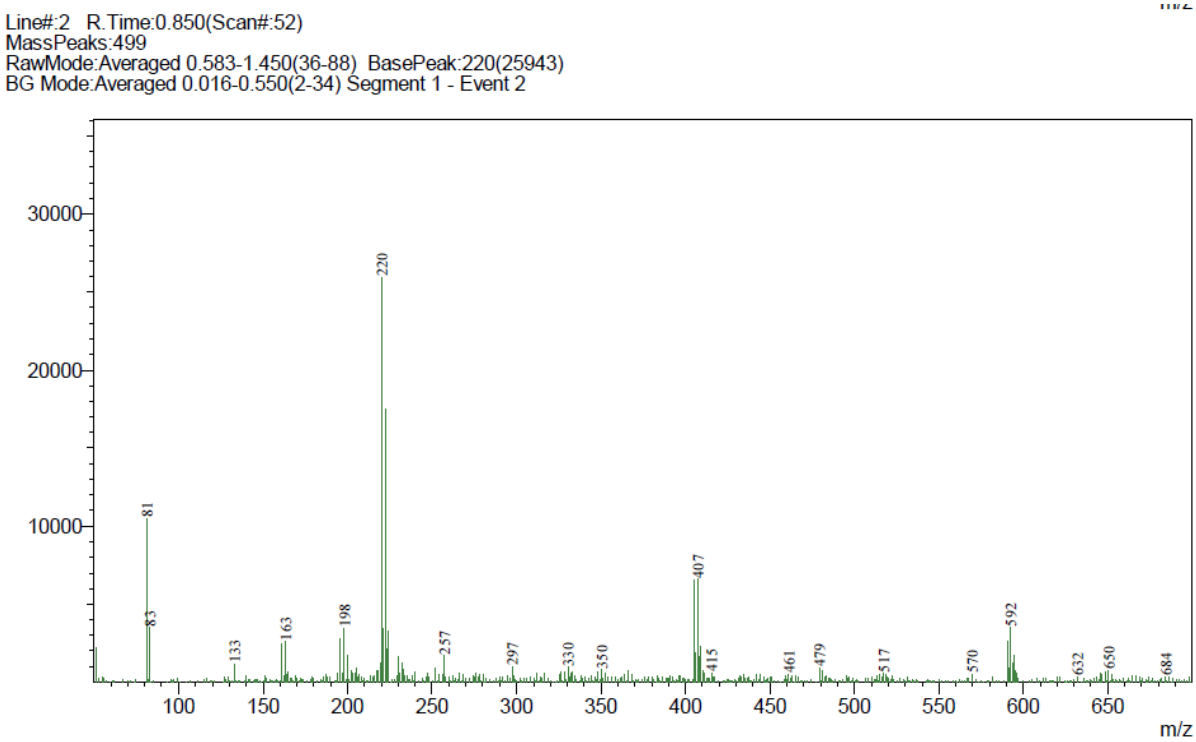

Figure 5.1.8 APCI mass spectrum of ethyl ferulate (5b)

5.1.5 In-vitro studies on synthesized coumarin (1a) and phenyl propanoid derivatives (3b, 4b and 5b)

5.1.5.1 In-vitro protein inhibition assay of compounds1a, 3b, 4b and 5b using ELISA

The compounds **1a**, **3b**, **4b** and **5b** were tested for their effect on production of TNF-α, IL-1β and IL-6 in the culture supernatant of LPS-induced RAW 264.7 cells using ELISA assay kit. Comparison of the TNF-α inhibition effect of the synthesized compounds revealed ethyl ferulate (**5b**) to be significantly active with IC_{50} value of 7.12 µM, followed by ethyl caffeate (**4b**, IC_{50} 16.68 µM/mL), dihydroxy methyl coumarin (**1a**, IC_{50} 62.36 µM) and ethyl-*p*-coumarate (**3b**, IC_{50} 74.07 µM). Further, **4b** and **5b** were found to significantly inhibit IL-1β with IC_{50} values of 32.51 and 47.84 µM, respectively. The other two compounds **3b** and **1a** showed inhibition of IL-1β with IC_{50} values of 62.19 and 113.72 µM, respectively. In inhibiting IL-6, compound **3b** demonstrated more potency (29.39 µM) compared to **4b** (33.39 µM), **1a** (41.22 µM) and **5b** (68.03 µM). The study elaborated a dose dependent effect by all

compounds in inhibiting the cytokines (Figure 5.1.9-5.1.11 and Table 5.1.1). Prednisolone (**17**), a corticosteroid used in the treatment of a wide range of inflammatory and autoimmune diseases was used as a reference standard (10 μM), which showed percentage inhibition of 50.32%, 69.79% and 94.59% against TNF-α, IL-1β and IL-6, respectively (Table 5.1.1). Thus, the in-vitro bioassay results disclosed the effectiveness of tested coumarin and phenyl propanoid derivatives to downregulate the pro-inflammatory cytokines, which are overexpressed in ischemic injury, autoimmune diseases, pain and other chronic inflammatory diseases (Iwalewa EO *et al*., 2007).

Table 5.1.1 Percentage inhibition of compounds 1a, 3b, 4b and 5b against TNF-α, IL-6 and IL-1β under in-vitro protein inhibition assay by ELISA

Compounds	**Concentration μM**	**Percentage Inhibition**		
		TNF-α	**IL-6**	**IL-1β**
Standard [Prednisolone]	10	50.32	94.59	69.79
1a	100	50.31	68.77	57.30
	30	48.94	43.14	16.37
	10	47.30	18.45	2.09
	3	42.72	8.90	0
3b	100	50.54	80.41	61.11
	30	46.85	52.80	35.25
	10	43.64	15.38	12.49
	3	36.89	2.29	0
4b	100	64.70	84.81	75.64
	30	48.94	36.28	49.12
	10	45.86	14.52	17.85
	3	41.59	6.78	4.92
5b	100	62.54	65.17	66.49
	30	55.25	25.57	40.71
	10	50.85	13.94	13.62
	3	47.05	5.50	0

Table 5.1.2 IC_{50} value of compounds 1a, 3b, 4b and 5b against TNF-α, IL-6 and IL-1β under in-vitro protein inhibition assay by ELISA

Compounds	IC_{50} values (μM)		
	TNF-α	IL-1β	IL-6
1a	62.36	113.72	41.22
3b	74.07	62.19	29.39
4b	16.68	32.51	33.39
5b	7.12	47.84	68.03

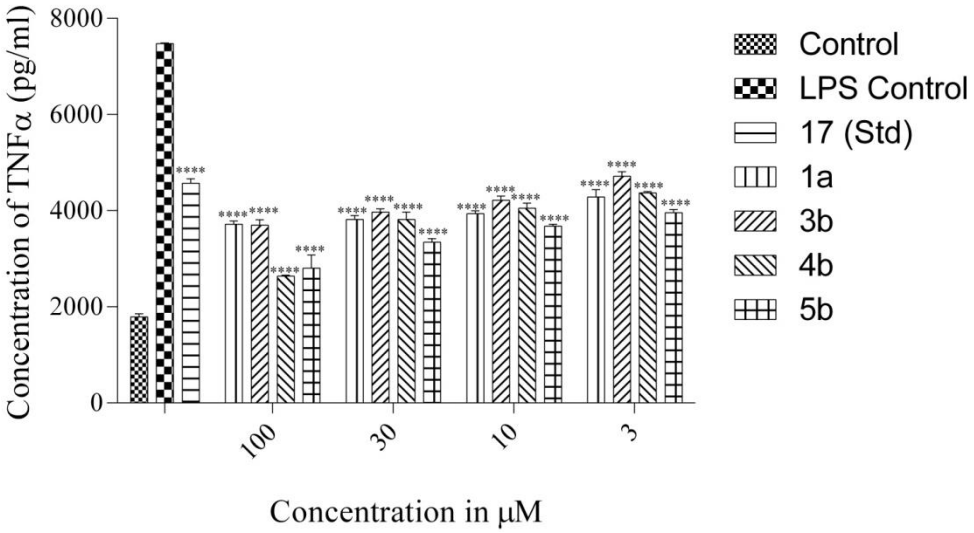

Figure 5.1.9 In-vitro TNF-α inhibitory effect of synthesized coumarin (1a) and phenyl propanoid derivatives (3b, 4b and 5b) on LPS induced RAW 264.7 cells using ELISA. Cells were pretreated with the indicated concentrations of compound **1a**, **3b**, **4b**, **5b** and standard prednisolone (**17**) (10 μM) for 1 h and then incubated with LPS (1 μg/mL) for 6 h. TNF-α concentration was determined by ELISA kit. The values are presented as mean ± SEM from triplicate. ****$P < 0.0001$ vs LPS control.

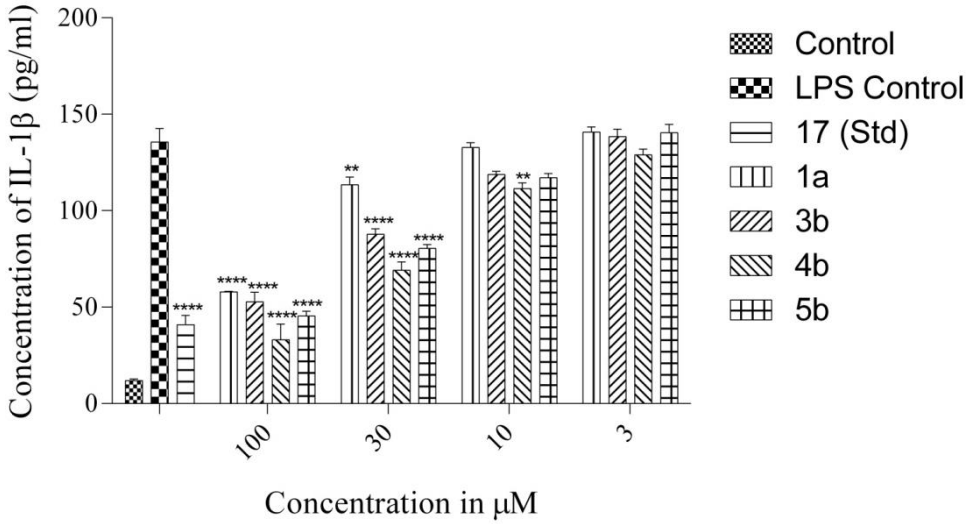

Figure 5.1.10 In-vitro IL-1β inhibitory effect of synthesized coumarin (1a) and phenyl propanoid derivatives (3b, 4b and 5b) on LPS induced RAW 264.7 cells using ELISA. Cells were pretreated with the indicated concentration of the compounds as well as with the standard prednisolone (**17**) (10μM) 1 h before the incubation with LPS (1 μg/mL) and oxalate crystals (250μg/ml). After 6 h of incubation supernatant was collected and subjected to ELISA assay for IL-1β estimations. The values are presented as mean ± SEM from triplicate. ****$P < 0.0001$ vs LPS control, **$P < 0.01$ vs LPS control.

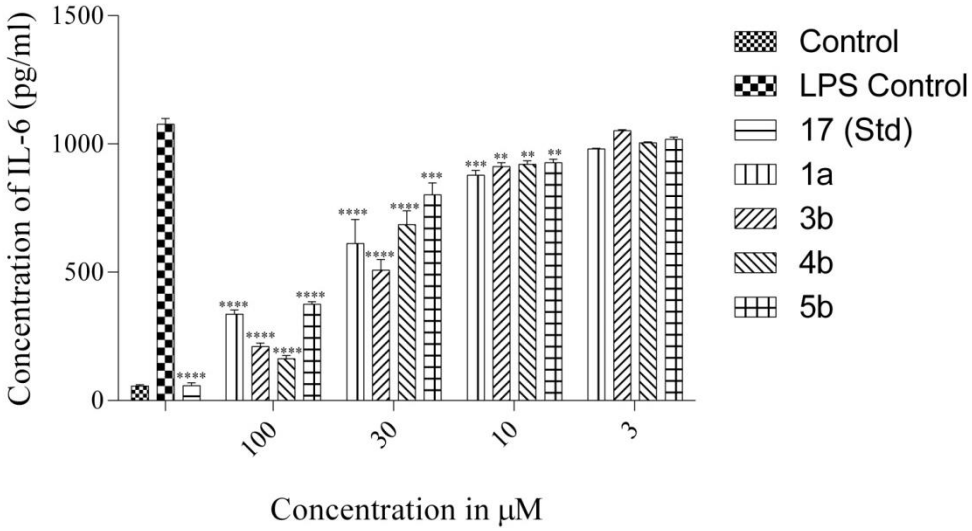

Figure 5.1.11 In-vitro IL-6 inhibitory effect of synthesized coumarin (1a) and phenyl propanoid derivatives (3b, 4b and 5b) on LPS induced RAW 264.7 cells using ELISA. Cells were treated with the indicated concentrations of compounds and standard prednisolone (**17**) (10μM) for 1 h and then incubated with LPS (1 μg/mL) for 6 h. Supernatant collected after incubation was used for estimating IL-6 levels using ELISA. The values are presented as mean ± SEM from triplicate. ****$P < 0.0001$ vs LPS control, ***$P < 0.001$ vs LPS control, **$P < 0.01$ vs LPS control.

5.1.5.2 Inhibition of Nitric oxide (NO) production by synthesized compounds

Overexpression of pro-inflammatory cytokines upregulate genes that produce NF-κB, NADPH oxidase, phospholipase A_2, cyclo-oxygenase-1 and -2, 5-lipoxygenase, myeloperoxidase, inducible nitric oxide synthase, increasing oxygen consumption and producing many oxygen-free radicals that can finally lead to certain degenerative diseases (Iwalewa EO *et al*., 2007). Nitric oxide (NO) is a reactive species that participates in normal physiological processes such as vasodilation and neurotransmission; however, its overexpression might result in disease like asthma, cardio-vascular disorders and organ transplant rejection (Coleman JW., 2002). Hence, the in-vitro study on the compounds was extended to measure the percentage NO production using Griess method.

Dihydroxy methyl coumarin (**1a**) exhibited significant control over the production of LPS-induced NO level showing IC_{50} value of 25.4 μM. The phenyl propanoids were also found to reduce the NO production under LPS induction with IC_{50} values of 33.22 μM (**4b**), 47.74 μM (**3b**) and 50.27 μM (**5b**) (Figure 5.1.12). Such inhibition effect over the production of NO level added support to the pro-inflammatory cytokine inhibitory effect of the compounds. No basal NO production was found when the cells were incubated with compounds but without LPS.

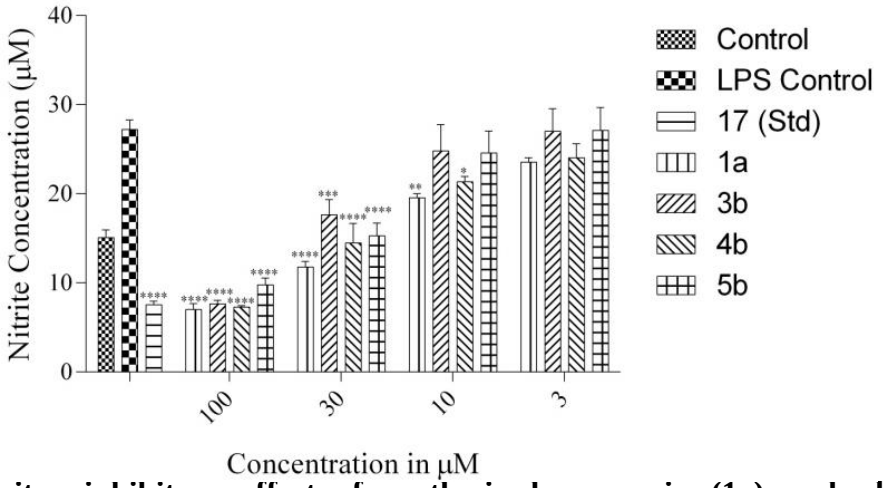

Figure 5.1.12 In-vitro inhibitory effect of synthesized coumarin (1a) and phenyl propanoid derivatives (3b, 4b and 5b) on LPS induced NO production RAW 264.7 cells. Cells were treated with the indicated concentration of compounds and standard prednisolone (**17**) (10 μM) for 1 h and then incubated with LPS (1 μg/mL) for 16 h. Supernatant collected was used for NO estimations using Griess method. The values are presented as mean ± SEM from triplicate. ****$P < 0.0001$vs LPS control, *** $P < 0.001$ vs LPS control, ** $P < 0.01$ vs LPS control, * $P < 0.05$ vs LPS control.

5.1.5.3 Cytotoxicity (MTT) assay of synthesized compounds

The cytotoxicity of synthesized compounds against LPS-stimulated RAW 264.7 macrophages was studied. Viability of the cells treated with various concentrations of compounds **1a**, **3b**, **4b** and **5b** for 1 h followed by the addition of LPS and incubation for 24 h was determined by MTT assay. No cytotoxicity was observed against the cells by the compounds. The IC_{50} values were found to be 423.79 (**1a**), 354.68 (**3b**), 333.82 (**5b**) and 252.78 (**4b**) μM (Figure 5.1.13). These results verified that the inhibition effect was through controlling the LPS-elevated cytokines levels but not through cell toxicity.

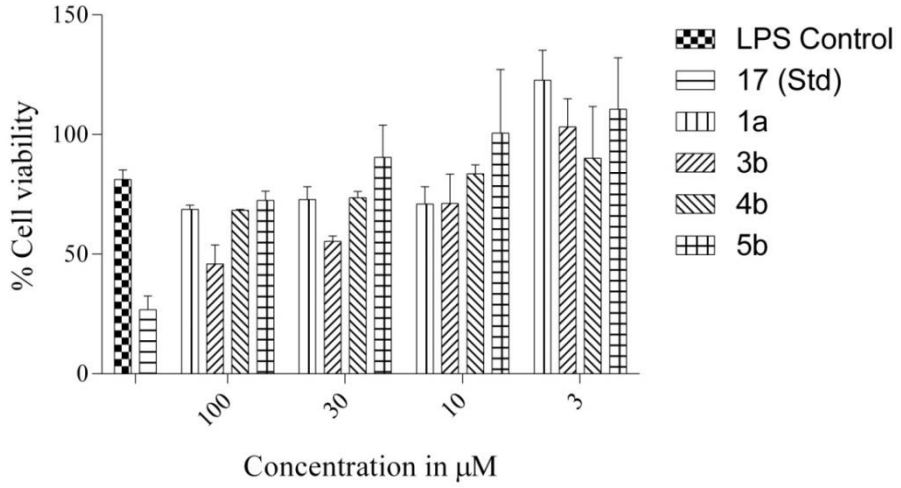

Figure 5.1.13 Cytotoxicity (MTT) effect of synthesized coumarin (1a) and phenyl propanoid derivatives (3b, 4b and 5b). Figure shows the effect of treatment of cells with the indicated concentration of compounds for 24 h. The viability assay was carried out using MTT reagent. The values are presented as mean ± SEM from triplicate.

The various bioassays revealed coumarin and phenyl propanoid derivatives as potential compounds acting against pro-inflammatory cytokines. In order to understand the putative binding efficacy of **1a**, **3b**, **4b** and **5b** into the inflammatory proteins, TNF-α, IL-6 and IL-1β, docking study was performed. Additionally, some simple structural analogues of these tested compounds were designed and docked to identify more potential compounds.

5.1.6 Molecular docking studies on coumarin and phenyl propanoid derivatives

Twenty cinnamic acid derivatives (**2-7c**) and two coumarin derivatives (**1a** and **1b**) were designed as test compounds (Table 5.1.3) and docked against the key pro-inflammatory cytokines using Genetic Optimization Ligand Docking-GOLD 5.2 molecular docking mechanism. The interactions between the active site of targeted proteins (TNF-α, IL-1β, and IL-6) and ligands were studied. Crystal co-ordinates for Human TNF-α were taken from protein data bank (PDB ID: 2AZ5). Protein was prepared for docking using protein preparation wizard of SYBYL X ver 2.1.1. The 2D structures of the test ligands and standard

drugs (prednisolone and diclofenac sodium) were obtained from Chemdraw ver. 8.0. These ligand structures were further prepared for docking using the *Prepare Ligands* module of Accelrys Discovery Studio ver. 2.5. The prepared ligands were docked to the TNF-α, IL-6 and IL-1β (domain) proteins using GOLD 5.2. software enabling them to undergo flexible docking process and commenced with default parameters.

In case of TNF-α, the co-crystallised ligand [6,7-dimethyl-3-[(methyl{2-[methyl({1-[3-(trifluoromethyl)phenyl]-1h-indol-3-yl}methyl)amino]ethyl}amino)methyl]- 4h-chromen-4-one; PDB ID -2AZ5 having IC_{50} = 22 µM] present on the interface region of B, C and D chains was extracted and assigned as the binding site centre. From the binding centre, amino acid residues covering a radius of 6 Å were defined as active site residues for the purpose of docking, which included, Leu55B, Leu157B, Leu57C- Gln61C, Tyr119C-Gly122C, Tyr151C, Leu57D, Tyr59D- Gln61D, Tyr119D-Gly121D, Tyr151D and Ile155D.

In case of IL-6 (PDB ID: 1N26), Cγ atom of Phe-103 with coordinates x=16.471, y=48.983 and z= 82.154 was assigned as binding site centre, and the radius was set to 12 Å based on the previous reports (Sharma S *et al*., 2012). Thus, the active site residues covered within the 12 Å radius included Ser-101A, Ser-224A, Lys-105A, Glu-114A, Asp-198, Val-112A, Phe-103 and Gln-196.

For IL-1β (PDB ID: 3O4O), the backbone carbonyl oxygen atom of Lys-26 was defined as the binding site centre with coordinates, x=-5.0840, y=7.195 and z= 4.932 and the radius was set to 10 Å. The binding site region included residues Asp-10B, Arg-13B, Lys-26B, Ile-15B, Ile-25B, Pro-28B, Phe-30B and Phe-107B based on reported literature (Sharma S *et al*., 2012).

For each ligand, 10 different poses were generated with their corresponding GOLDScore_fitness. The selection of best ligand pose was done based on their best

interaction towards aminoacid residues showing no short contacts and having highest fitness score. Higher the GOLD fitness score of the ligand pose, better will be the activity because it was calculated based on the negative of the sum of the component energy terms. The optimized fitness function was used for the prediction of well fitted ligand binding position that has the least energy with average GOLDScore_fitness. The interactions between the active site of targeted proteins and test/standard ligands were studied.

Table 5.1.3 Structures of coumarin and phenyl propanoid ligands

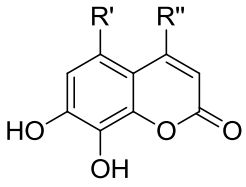

1a - R'-H; R"-CH_3

1b - R'-CH_3; R"-H

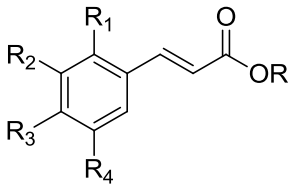

3-7c

S. No	Compound code	R	R_1	R_2	R_3	R_4
1	**2**	H	H	H	H	H
2	**2a**	C_2H_5	H	H	H	H
3	**3**	H	H	H	OH	H
4	**3a**	H	H	H	OAc	H
5	**3b**	C_2H_5	H	H	OH	H
6	**3c**	C_2H_5	H	H	OAc	H
7	**4**	H	H	H	OH	OH
8	**4a**	H	H	H	OAc	OAc
9	**4b**	C_2H_5	H	H	OH	OH
10	**4c**	C_2H_5	H	H	OAc	OAc
11	**5**	H	H	H	OH	OCH_3
12	**5a**	H	H	H	OAc	OCH_3
13	**5b**	C_2H_5	H	H	OH	OCH_3
14	**5c**	C_2H_5	H	H	OAc	OCH_3
15	**6**	H	H	H	C_6H_5	H
16	**6a**	C_2H_5	H	H	C_6H_5	H
17	**7**	H	NO_2	H	H	H
18	**7a**	C_2H_5	NO_2	H	H	H
19	**7b**	H	H	NO_2	H	H
20	**7c**	C_2H_5	H	NO_2	H	H

5.1.6.1 Docking interactions of coumarin and phenyl propanoid derivatives into TNF-α protein

Reference anti-inflammatory drugs such as, diclofenac sodium (**16**) (GOLDScore_fitness of 47.87) and prednisolone (**17**) (GOLDScore_fitness of 47.9332) individually showed some common interesting hydrophobic interaction pattern with TNF-α residues such as Leu-344, Tyr-346, Tyr-406, Leu-407, Gly-408, Gly-409, Leu-492, Tyr-494, Ser-495, Tyr-554, Leu-555 and Gly-556 (Figure 5.1.14). While cinnamates (**2**–**7c**) were observed to interact with most of the common TNF-α hydrophobic residue of standard drugs, coumarins (**1a** and **1b**) exhibited only a few common interactions (Figure 5.1.14).

In case of coumarin derivatives, dihydroxy-4-methyl coumarin (**1a**) (GOLDScore_fitness, 39.6371) was found to possess relatively high GOLDScore_fitness as compared to dihydroxy-5-methyl coumarin (**1b**) (GOLDScore_fitness, 36.7150). In case of phenylpropanoid moieties, most of them showed high GOLDScore_fitness ranging from 33 to 50 when compared to the coumarin derivatives (Table 5.1.4). The top three highest fitness scores of 52.35, 48.44 and 47.59 were exhibited by compounds **4c**, **5c** and **6a**, respectively.

Table 5.1.4 GOLD fitness score of coumarins, phenyl propanoids and standards ligands

S. No.	Code	GOLDScore_fitness			S.No.	Code	GOLDScore_fitness		
		TNF-α	IL-1β	IL-6			TNF-α	IL-1β	IL-6
1	**1a**	39.6371	36.0630	33.2572	13	**5**	38.3304	40.4810	C
2	**1b**	36.7150	37.6342	32.7255	14	**5a**	42.0710	C	36.6038
3	**2**	33.0836	35.4120	C	15	**5b**	41.8482	41.6374	32.0876
4	**2a**	35.5602	37.1717	C	16	**5c**	48.4354	43.9733	29.9335
5	**3**	33.9676	37.3230	36.8807	17	**6**	44.1037	42.4658	C
6	**3a**	39.2807	40.4697	39.6625	18	**6a**	47.5894	43.1172	C
7	**3b**	36.2836	39.1552	28.3808	19	**7**	35.6355	39.6456	32.5114
8	**3c**	42.9940	42.0356	30.7187	20	**7a**	39.3024	37.9971	25.6510
9	**4**	34.1892	39.4171	33.4072	21	**7b**	35.1135	39.8929	32.9254
10	**4a**	45.7224	47.5829	35.7948	22	**7c**	38.0254	38.9802	28.1634
11	**4b**	37.7156	40.5260	32.3594	23	**16**	47.8740	49.5659	31.22
12	**4c**	52.3522	47.3047	36.5551	24	**17**	47.9332	44.8907	28.54

C - Clashes

Table 5.1.5 Docking interactions of diclofenac sodium (16), prednisolone (17), coumarin (1a) and phenyl propanoids (3b, 4b, 5b)

Code	Protein	Hydrophobic residues	Hydrogen bond atoms*	Diclofenac and prednisolone common interaction residues
16	TNF-α	Leu344, Tyr346, Tyr406, Leu407, Gly408, Gly409, Leu492, Tyr494, Ser495, Gln496, Tyr554, Leu555, Gly556	**Tyr586:HH-O4 (1.87428)**	Leu344, Tyr346, Tyr406, Leu407, Gly408, Gly409, Leu492, Tyr494, Ser495, Tyr554, Leu555, Gly556
17	TNF-α	Leu344, Tyr346, Ser347, Tyr406, Leu407, Gly408, Gly409, Tyr438, Ile442, Leu492, Tyr494, Ser495, Tyr554, Leu555, Gly556, Tyr586	**Tyr586:HH-O1** Gln496:OE1-H54	Leu344, Tyr346, Tyr406, Leu407, Gly408, Gly409, Leu492, Tyr494, Ser495, Tyr554, Leu555, Gly556
1a	TNF-α	Leu381, Tyr406, Leu407, Gly408, Tyr494, Ser495, Gln496, Tyr554, Leu555, Gly556, Tyr586	-	Tyr406, Leu407, Gly408, Tyr494, Ser495, Tyr554, Leu555, Gly556
3b	TNF-α	Leu344, Tyr346, Tyr406, Leu407, Gly408, Gly409, Leu492, Tyr494, Gln496, Tyr554, Tyr586, Ile590	-	Leu344, Tyr346, Tyr406, Leu407, Gly408, Gly409, Leu492, Tyr494, Tyr554
4b	TNF-α	Leu344, Tyr346, Ser347, Gln348, Tyr406, Leu407, Gly408, Gly409, Tyr438, Leu492, Tyr494, Gln496, Tyr554, Leu555, Gly556, Tyr586	H26-Ser495:O (1.57369)	Leu344, Tyr346, Tyr406, Leu407, Gly408, Gly409, Leu492, Tyr494, Tyr554, Leu555, Gly556
5b	TNF-α	Leu344, Tyr346, Ser347, Gln348, Tyr406, Leu407, Gly408, Gly409, Tyr438, Leu492, Tyr494, Ser495, Gln496, Tyr554, Leu555, Gly556, Tyr586, Ile590	-	Leu344, Tyr346, Tyr406, Leu407, Gly408, Gly409, Leu492, Tyr494, Ser495, Tyr554, Leu555, Gly556
16	IL1-β	Arg10 (π-cation), Ile12, Ile22, Lys23, Cys24, Pro25, Leu26, Phe27 (π-π stacking)	Arg10:HE-O3 (2.03036); Arg10:HH21-O4 (2.01886)	Ile12, Ile22
17	IL1-β	Ile12, Gln13, Val14, Glu18, Pro19, Ala20, Ile22, Met119, Asn139, Tyr143, Arg204	Phe15:HN-O5 (2.04942); H53- Arg21:O (2.09613)	Ile12, Ile22
3b	IL1-β	Asp7, Arg10, Ile12, Ile22, Lys23, Cys24, Pro25, Leu26, Phe27, Lys32, Phe104 (π-π stacking)	-	Ile12, Ile22
4b	IL1-β	Arg10 (π- π stacking), Lys23, Cys24, Pro25, Phe27, Phe30, Lys32	**Arg10:HE-O8 (2.10488);** **Arg10:HH21-O7 (1.7956);** Leu26:HN-O13 (2.4121)	
5b	IL1-β	Asp7, Arg10 (π- π stacking), Ile12, Lys23, Cys24, Pro25, Leu26, Phe104	**Arg10:HE-O8 (2.14282)**	Ile12
16	IL-6	Ser101, Cys102, Phe103, Lys105 (π-cation), Pro197, Asp198, Pro199, Glu286	Lys105:HZ3-O4 (1.93898); H29-Gln196:OE1 (1.79201)	Ser101, Cys102, Phe103, Pro199, Glu286
17	IL-6	Ser101, Cys102, Phe103, Lys105, Gln196, Pro199, Glu286	Gln187:HE22-O5 (2.05477); H54-Asp198:OD1 (2.07084)	Ser101, Cys102, Phe103, Pro199, Glu286
3b	IL6	Phe103, Gln196, Asp198, Pro199, Ser285	**Lys105:HZ3-O11 (1.65758);** H26-Pro197:O (1.71226); Glu286:HN-O7 (2.08552)	Phe103
4b	IL6	Ser101, Phe103, Lys105 (π-cation), Glu114, Lys154, Ser224	**Lys105:HZ3-O12 (1.52133)** **H26-Asp198:OD2 (1.977)**	Ser101, Phe103
5b	IL6	Ser101, Phe103, Lys105 (π-cation), Glu114, Lys154, Ser224	**Lys105:HZ3-O12 (1.51785)** **H30-Asp198:OD2 (2.08162)**	Ser101, Phe103

* Donor atom-Acceptor atom (Hydrogen bond length [Å])

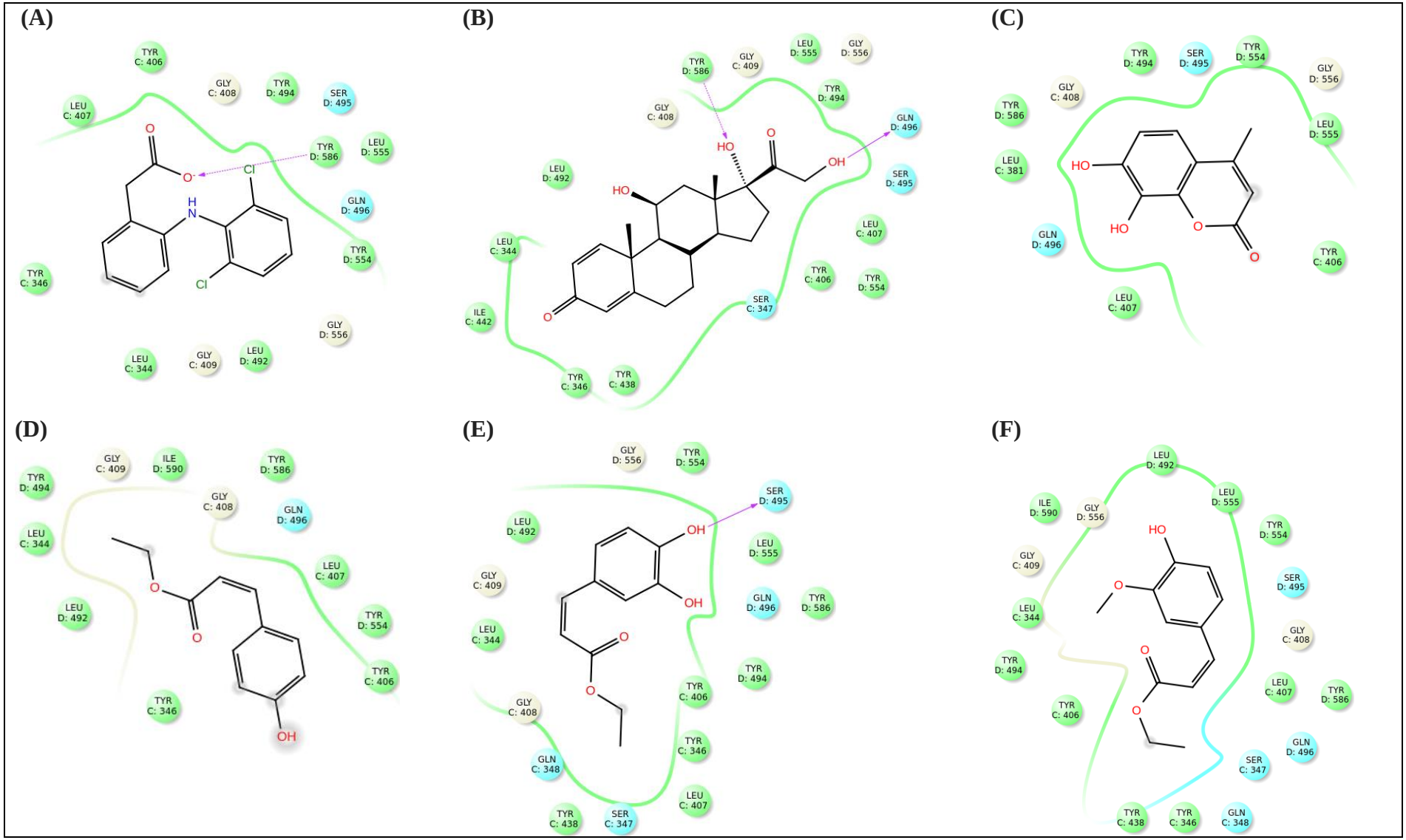

Figure 5.1.14 2D TNF-α docking interaction map displaying binding and interactions of standards [16 (A), 17 (B)], coumarin [1a (C)], phenyl propanoids [3b (D), 4b (E) and 5b (F)]

5.1.6.2 Docking interactions of methyl coumarin and phenyl propanoid derivatives into IL-1β protein

Docking with IL-1β as the target protein revealed diclofenac (**16**) and prednisolone (**17**) to exhibit similar hydrophobic interactions with Ile12 and Ile22 residues with the fitness scores of 49.56 and 44.89, respectively (Figure 5.1.15). Similar interactions had also been observed in phenylpropanoids. Comparative analysis of docking poses of ethyl-*p*-coumarate (**3b**) (GOLDScore_fitness, 39.15), ethyl caffeate (**4b**) (GOLDScore_fitness, 40.52) and ethyl ferulate (**5b**) (GOLDScore_fitness, 41.63) with that of the standard drugs revealed similar interactions as that of diclofenac reference ligand (Asp7, Arg10, Lys23, Cys24, Pro25, Leu26, Phe27 and Phe104), but not of prednisolone (Table 5.1.3-5.1.5 and Figure 5.1.15). Further, a majority of the phenylpropanoid compounds exhibited high fitness scores (**4a**, GOLDScore_fitness, 47.58; **4c**, GOLDScore_fitness, 47.30; **5c**, GOLDScore_fitness, 43.97) as compared to coumarin derivatives but were found to be slightly lesser than the reference ligands. Dihydroxy methyl coumarin derivatives **1a** and **1b** exhibited fitness scores of 36.0630 and 37.6342 (GOLDScore_fitness), respectively (Table 5.1.4).

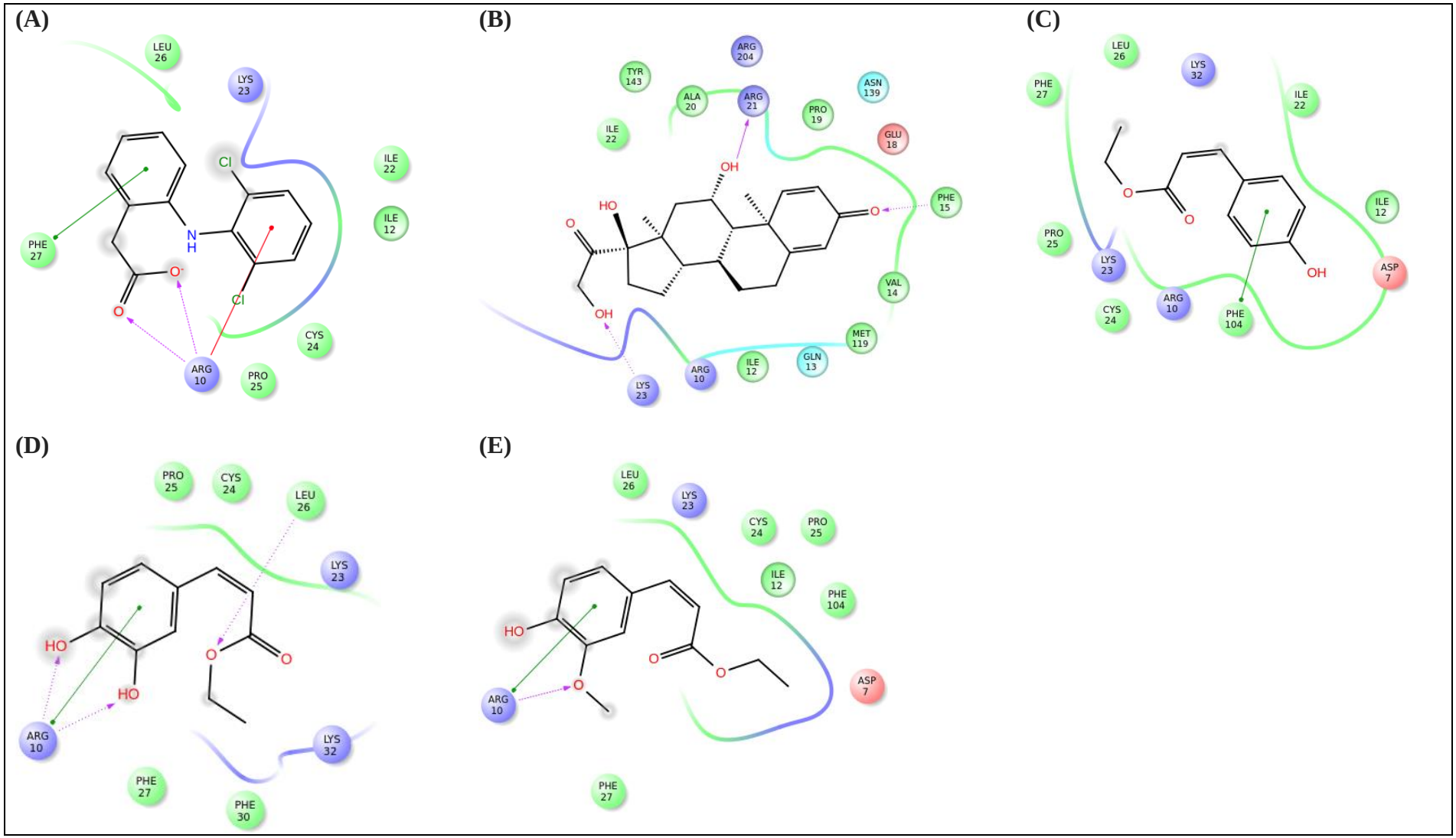

Figure 5.1.15 2D IL-1β docking interaction map displaying binding and interactions of standards [16 (A), 17 (B)], phenyl propanoids [3b (C), 4b (D) and 5b (E)]

5.1.6.3 Docking interactions of methyl coumarin and phenyl propanoid derivatives into IL-6 protein

Docking of reference ligands *viz*., diclofenac sodium (**16**) (GOLDScore_fitness 31.22) and prednisolone (**17**) (GOLDScore_fitness 28.54) with IL-6 revealed that they share common hydrophobic residues for interaction, which are identified as Ser101, Cys102, Phe103, Pro199 and Glu 286 (Figure 5.1.16). Among the coumarins, **1a** with GOLDScore_fitness of 33.25 exhibited slightly higher score than **1b** (GOLDScore_fitness, 32.72) (Table 5.1.4).

Interestingly, docking of cinnamates with IL-6 revealed few compounds *viz*., **3a**, **4c** and **5a** having GOLDScore_fitness 39.66, 36.55 and 36.60, respectively higher than the reference ligands (Table 5.1.4). Upon comparing the 3D docked poses of ethyl-*p*-coumarate (**3b**), ethyl caffeate (**4b**) and ethyl ferulate (**5b**) with that of the reference ligands (**16** and **17**), Phe103 was found as common interaction residue (Figure 5.1.16). Compounds **4b** and **5b** were exhibiting an additional common interaction with Ser101 similar to that of the reference ligands (Table 5.1.5 and Figure 5.1.16).

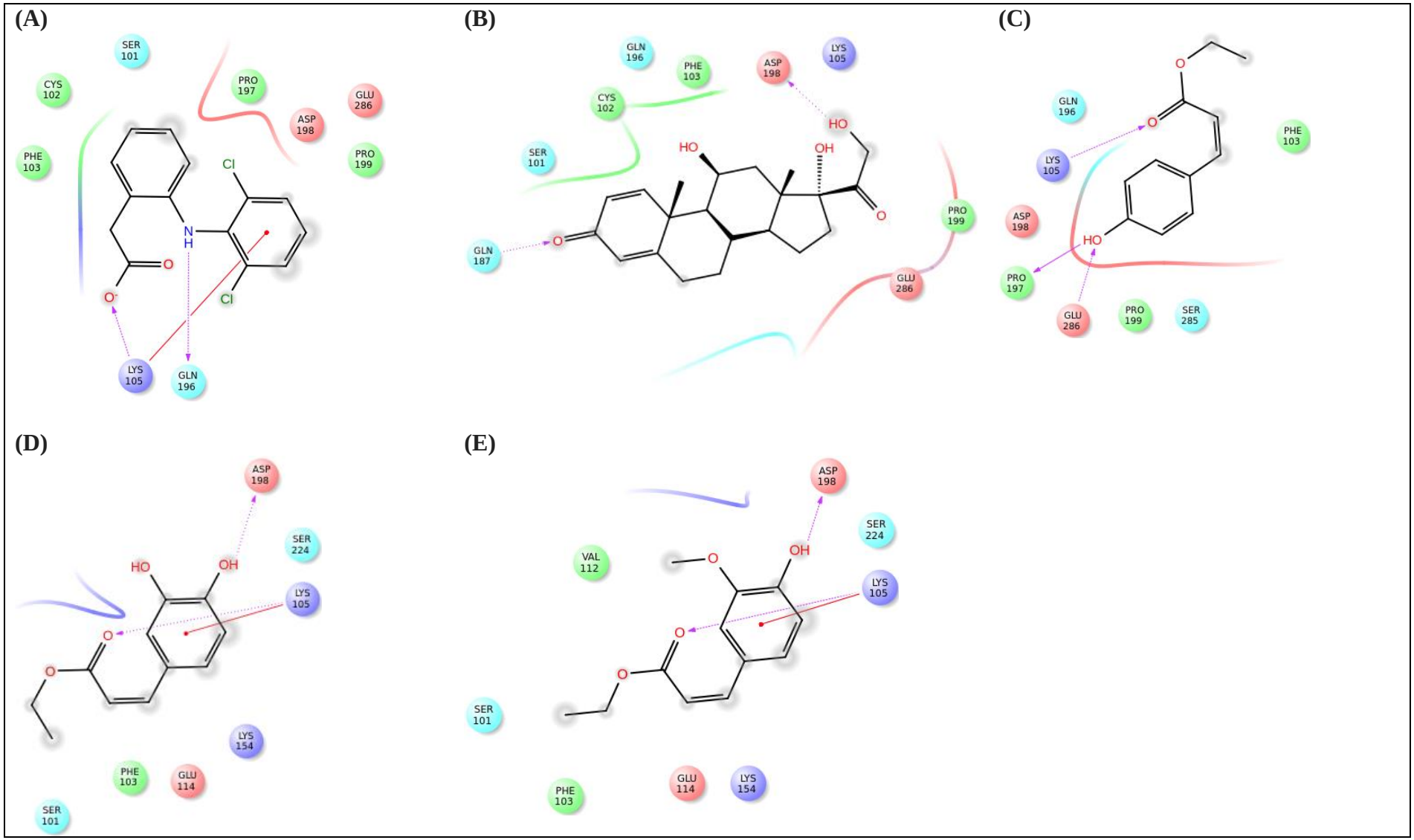

Figure 5.1.16 2D IL-6 docking interaction map displaying binding and interactions of standards [16 (A), 17 (B)], phenyl propanoids [3b (C), 4b (D) and 5b (E)]

5.1.6.4 Outcome of in-vitro and docking studies on coumarin and cinnamic acid derivatives

On perceiving the proinflammatory cytokine inhibitory effect demonstrated by the coumarin and cinnamates under in-vitro ELISA protein assay and on witnessing the docking interactions between the active sites of targeted proteins and designed ligands, an idea of making novel inhibitors by fusing the various coumarins (**1a** and **1b**) and cinnamic acid derivatives (**2-7c**) had emerged. This fusion might yield inhibitors having a synergistic effect. Hence molecular docking studies were performed on the new set of fused-cyclic compounds with an intention to understand their fitness and binding interactions with the TNF-α, IL-6 and IL-1β proteins. Such coupling resulted in creating cyclic molecules which mimicked a group of natural secondary metabolites called, coumarinolignans. These coumarinolignans belong to natural nonconventional lignans which are formed by the oxidative coupling of dihydroxy coumarins and phenylpropane derivatives possessing 1,4-dioxane bridge (Begum SA *et al*., 2010). Although these coumarinolignans exist as linearly/angularly fused compounds and as positional isomers, our docking study was restricted to one type of regioisomer having an angularly fused structure. Around sixty novel fused-cyclic coumarin-based lignans molecules were designed (Table 5.1.6) and studied using the same drug design software. The results were compared with cleomiscosin A (**15**), diclofenac sodium (**16**) and prednisolone (**17**). Cleomiscosin A was selected as a reference compound as it was the first natural coumarinolignan reported to possess anti-inflammatory activity (Begum S *et al*., 2010)

5.1.7 Molecular docking studies of fused-cyclic coumarin-based lignans

5.1.7.1 Molecular docking studies of fused-cyclic coumarin-based lignans into TNF-α protein

Initially, a comparative analysis of GoldScore_fitness of the selected reference compounds was done. The fitness score of cleomiscosin A (**15**) was observed to be higher (GoldScore_fitness, 57.57) than that of the reference drugs namely, diclofenac (**16**) (GoldScore_fitness, 47.87) and prednisolone (**17**) (GoldScore_fitness, 47.93) (Table 5.1.7). All the three reference compounds displayed interactions with most of the hydrophobic residues found on the active site residues of the TNF-α protein. Those residues were Leu344, Tyr346, Tyr406, Leu407, Gly408, Gly409, Leu492, Tyr494, Ser495, Tyr554, Leu555, and Gly556. Cleomiscosin A (**15**) and diclofenac sodium (**16**) were found to form hydrogen bond interaction with Tyr586 residue which was not observed in case of prednisolone (**17**). Further, in the case of cleomiscosin A (**15**), an exclusive π-π stacking interaction between the aromatic rings of Tyr346 and coumarin was observed which was not found in case of the other two reference drugs. Such π-π stacking interaction and hydrogen bond interaction could be a reason for the higher GoldScore_fitness (GoldScore_fitness, 57.57) of cleomiscosin A (**15**) (Figure 5.1.17, Table 5.1.7 and 5.1.8).

Table 5.1.6 Structures of fused-cyclic coumarin-based lignans designed for docking study

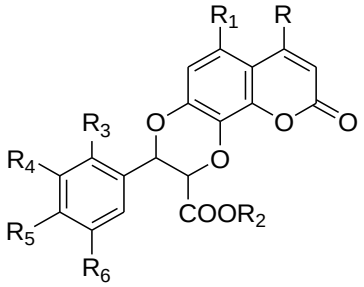

S.No	Code	R	R_1	R_2	R_3	R_4	R_5	R_6	S.No	Code	R	R_1	R_2	R_3	R_4	R_5	R_6
1	**8**	CH_3	H	H	H	H	H	H	31	**11**	CH_3	H	H	H	H	OH	OCH_3
2	**8a**	CH_3	H	CH_3	H	H	H	H	32	**11a**	CH_3	H	H	H	H	OAc	OCH_3
3	**8b**	CH_3	H	C_2H_5	H	H	H	H	33	**11b**	CH_3	H	CH_3	H	H	OH	OCH_3
4	**8c**	H	CH_3	H	H	H	H	H	34	**11c**	CH_3	H	CH_3	H	H	OAc	OCH_3
5	**8d**	H	CH_3	CH_3	H	H	H	H	35	**11d**	CH_3	H	C_2H_5	H	H	OH	OCH_3
6	**8e**	H	CH_3	C_2H_5	H	H	H	H	36	**11e**	CH_3	H	C_2H_5	H	H	OAc	OCH_3
7	**9**	CH_3	H	H	H	H	OH	H	37	**11f**	H	CH_3	H	H	H	OH	OCH_3
8	**9a**	CH_3	H	H	H	H	OAc	H	38	**11g**	H	CH_3	H	H	H	OAc	OCH_3
9	**9b**	CH_3	H	CH_3	H	H	OH	H	39	**11h**	H	CH_3	CH_3	H	H	OH	OCH_3
10	**9c**	CH_3	H	CH_3	H	H	OAc	H	40	**11i**	H	CH_3	CH_3	H	H	OAc	OCH_3
11	**9d**	CH_3	H	C_2H_5	H	H	OH	H	41	**11j**	H	CH_3	C_2H_5	H	H	OH	OCH_3
12	**9e**	CH_3	H	C_2H_5	H	H	OAc	H	42	**11k**	H	CH_3	C_2H_5	H	H	OAc	OCH_3
13	**9f**	H	CH_3	H	H	H	OH	H	43	**12**	CH_3	H	H	H	H	C_6H_5	H
14	**9g**	H	CH_3	H	H	H	OAc	H	44	**12a**	CH_3	H	CH_3	H	H	C_6H_5	H
15	**9h**	H	CH_3	CH_3	H	H	OH	H	45	**12b**	CH_3	H	C_2H_5	H	H	C_6H_5	H
16	**9i**	H	CH_3	CH_3	H	H	OAc	H	46	**12c**	H	CH_3	H	H	H	C_6H_5	H
17	**9j**	H	CH_3	C_2H_5	H	H	OH	H	47	**12d**	H	CH_3	CH_3	H	H	C_6H_5	H
18	**9k**	H	CH_3	C_2H_5	H	H	OAc	H	48	**12e**	H	CH_3	C_2H_5	H	H	C_6H_5	H
19	**10**	CH_3	H	H	H	H	OH	OH	49	**13**	CH_3	H	H	NO_2	H	H	H
20	**10a**	CH_3	H	H	H	H	OAc	OAc	50	**13a**	CH_3	H	H	H	NO_2	H	H
21	**10b**	CH_3	H	CH_3	H	H	OH	OH	51	**13b**	CH_3	H	CH_3	NO_2	H	H	H
22	**10c**	CH_3	H	CH_3	H	H	OAc	OAc	52	**13d**	CH_3	H	CH_3	H	NO_2	H	H
23	**10d**	CH_3	H	C_2H_5	H	H	OH	OH	53	**13c**	CH_3	H	C_2H_5	NO_2	H	H	H
24	**10e**	CH_3	H	C_2H_5	H	H	OAc	OAc	54	**13e**	CH_3	H	C_2H_5	H	NO_2	H	H
25	**10f**	H	CH_3	H	H	H	OH	OH	55	**13f**	H	CH_3	H	NO_2	H	H	H
26	**10g**	H	CH_3	H	H	H	OAc	OAc	56	**13g**	H	CH_3	H	H	NO_2	H	H
27	**10h**	H	CH_3	CH_3	H	H	OH	OH	57	**13h**	H	CH_3	CH_3	NO_2	H	H	H
28	**10i**	H	CH_3	CH_3	H	H	OAc	OAc	58	**13i**	H	CH_3	CH_3	H	NO_2	H	H
29	**10j**	H	CH_3	C_2H_5	H	H	OH	OH	59	**13j**	H	CH_3	C_2H_5	NO_2	H	H	H
30	**10k**	H	CH_3	C_2H_5	H	H	OAc	OAc	60	**13k**	H	CH_3	C_2H_5	H	NO_2	H	H

Table 5.1.7 GoldScore_fitness of fused-cyclic coumarin-based lignans, fraxetin (14), cleomiscosin A (15) and standards (16, 17)

S. No.	Code	GOLD fitness score			S.No.	Code	GOLD fitness score		
		TNF-α	IL-1β	IL-6			TNF-α	IL-1β	IL-6
1	**8**	46.6835	46.5559	32.8437	34	**11c**	52.6564	51.1333	36.8913
2	**8a**	51.4547	48.1702	33.2933	35	**11d**	56.1472	53.2784	48.0317
3	**8b**	53.6472	50.9737	35.4272	36	**11e**	52.1771	58.1060	40.8652
4	**8c**	48.4196	49.0282	36.6735	37	**11f**	53.2147	43.5003	43.6014
5	**8d**	49.2526	49.8731	32.0130	38	**11g**	55.5148	52.1821	42.1018
6	**8e**	47.1398	45.1339	37.3528	39	**11h**	50.1984	50.0924	40.1319
7	**9**	49.8308	46.0206	39.4931	40	**11i**	53.9055	50.0165	38.7230
8	**9a**	53.9619	54.5236	41.5125	41	**11j**	56.3945	49.8465	43.9686
9	**9b**	47.0372	47.5044	38.7284	42	**11k**	58.8847	58.3145	36.5802
10	**9c**	51.9952	53.6919	40.5444	43	**12**	57.7514	53.9526	39.3797
11	**9d**	59.4029	51.7056	38.9855	44	**12a**	51.8688	55.4296	39.4247
12	**9e**	57.6349	57.9566	39.5485	45	**12b**	56.5652	58.3562	41.3329
13	**9f**	51.7274	50.2477	41.5324	46	**12c**	56.2755	49.1496	43.8684
14	**9g**	49.4624	50.6667	42.5869	47	**12d**	56.6258	62.4274	41.4689
15	**9h**	53.1731	52.0776	35.5819	48	**12e**	58.0009	60.5262	40.8035
16	**9i**	45.3250	51.8900	42.5262	49	**13**	47.6642	49.5333	38.5448
17	**9j**	46.8089	53.2484	35.3333	50	**13a**	48.9603	46.5412	41.5983
18	**9k**	56.8943	57.4901	40.3730	51	**13b**	50.2107	52.9579	35.3154
19	**10**	52.0526	57.9928	44.0145	52	**13d**	51.8740	52.4619	34.9193
20	**10a**	56.7857	53.0583	47.1820	53	**13c**	50.5442	48.6569	39.8088
21	**10b**	56.0628	54.7027	39.5441	54	**13e**	53.3481	51.5739	39.6346
22	**10c**	61.1623	52.7946	42.6145	55	**13f**	48.4341	45.1603	37.5192
23	**10d**	59.9119	52.6486	44.1542	56	**13g**	47.4747	46.7880	40.7927
24	**10e**	62.3072	61.0903	44.7179	57	**13h**	46.9380	48.0753	37.4956
25	**10f**	51.1031	50.5193	41.7252	58	**13i**	52.2485	47.7728	36.6347
26	**10g**	60.4847	51.6898	47.0590	59	**13j**	55.4013	45.5244	40.3923
27	**10h**	50.5115	51.8350	40.4457	60	**13k**	57.9702	51.8253	42.0117
28	**10i**	60.1746	61.5607	42.3399	61	**14**	41.3391	39.2916	31.6331
29	**10j**	51.6454	49.3056	38.8646	62	**15**	57.5719	53.8236	50.9474
30	**10k**	55.7624	60.0575	36.0019	63	**15g**	61.4666	58.2413	44.8447
31	**11**	53.6585	51.1453	44.5141	64	**16**	47.8740	49.5659	31.22
32	**11a**	54.6883	51.9669	39.3284	65	**17**	47.9332	44.8907	28.54
33	**11b**	52.5530	52.0693	44.0750					

Table 5.1.8 Docking interactions of cleomiscosin A (15) and fused-cyclic coumarin-based lignans (9d, 10d, 11d)

Code	Protein	Hydrophobic residues	Hydrogen bond atoms *	Diclofenac and prednisolone common interacting residues
15	TNF-α	His302, Leu344, Ile345, Tyr346 (π-π stacking), Ser347, Gln348, Tyr406, Leu407, Gly408, Gly409, Tyr438, Ile442, Leu492, Tyr494, Gln496, Tyr554	**Tyr586:HH-O7 (2.44841)**	Leu344, Tyr346, Tyr406, Leu407, Gly408, Gly409, Leu492, Tyr494, Gln496, Tyr554
9d	TNF-α	His302, Leu344, Ile345, Tyr346 (π-π stacking), Ser347, Gln348, Tyr406, Leu407, Gly408, Gly409, Tyr438, Ile442, Leu492, Tyr494, Ser495, Gln496, Tyr554, Leu555, Tyr586, Ile590	-	Leu344, Tyr346, Tyr406, Leu407, Gly408, Gly409, Tyr494, Ser495, Tyr554, Leu555
10d	TNF-α	His302, Leu344, Ile345, Tyr346 (π-π stacking), Ser347, Gln348, Tyr406, Leu407, Gly408, Gly409, Tyr438, Ile442, Leu492, Tyr494, Ser495, Gln496, Tyr554, Leu555, Tyr586, Ile590		Leu344, Tyr346, Tyr406, Leu407, Gly408, Gly409, Tyr494, Ser495, Tyr554, Leu555
11d	TNF-α	His302, Leu344, Ile345, , Tyr346 (π-π stacking), Ser347, Tyr406, Leu407, Gly408, Gly409, Tyr438, Ile442, Leu492, Tyr494, Ser495, Gln496, Tyr554, Leu555, Gly556, Ile590	**Tyr586:HH-O7 (2.01659)**	Leu344, Tyr346, Tyr406, Leu407, Gly408, Gly409, Leu492, Tyr494, Tyr554, Leu555, Gly556
15	IL1-β	Asp7, Gln11, Ile12, Gln13, Val14, Phe15, Ala20, Arg21, Ile22, Lys23, Pro25, Leu26, Phe27, Phe104, Met119, Tyr143	**Arg10:HH22-O25 (1.75577**)	Ile12, Ile22
9d	IL1-β	Asp7, Arg10 (π-cation), Gln11, Ile12, Arg21, Ile22, Lys23, Cys24, Pro25, Leu26, Phe27(π-π stacking), Phe30, Phe104, Pro105	**Arg10:HE-O19 (2.34974)**	Ile12, Ile22
10d	IL1-β	Asp7, Arg10 (π-cation), Gln11, Ile12, Arg21, Ile22, Lys23, Cys24, Pro25, Leu26, Phe27, Phe104, Asn139	**Arg10:HE-O20 (1.8631)**	Ile12, Ile22
11d	IL1-β	Asp7, Arg10 (π-cation), Gln11, Ile12, Val14, Arg21, Ile22, Lys23, Pro25, Leu26, Phe27, Phe104, Asn139, Tyr143, Arg204	-	Ile12, Ile22
15	IL-6	Phe103, Lys105 (π-cation), Arg104, Asn110, Val111, Val112, Glu114, Ser149, Ser152, Ser156, Gln158, Asp198, Ser224	**Lys105:HN-O8 (2.05837)**; Lys154:HZ2-O23 (2.19787)	Phe103
9d	IL-6	Phe103 (π-π stacking), Arg104, Lys105 (π-cation), Ser106, Asn110, Val112, Glu114, Lys157, Gln158, Asp198, His223, Ser224	**Lys105:HN-O23(1.93778)**; Ser109:HG-O23 (1.83984)	Phe103
10d	IL-6	Phe103, Arg104, Ser106, Asn110, Val112, Lys154, Gln158, Asp198, His223, Ser224	**Lys105:HN-O24 (2.1858)**; Ser109:HG-O24 (1.57551); H46-Glu114:OE2 (2.00086)	Phe103
11d	IL-6	Phe103 (π-π stacking), Arg104, Ser106, Asn110, Val111, Val112, Glu114, Ser149, Ser152, Ser156, Asp198, His223, Ser224	**Lys105:HZ2-O26(1.87906)**; Ser109:HG-O8 (1.50264); Lys154:HZ2-O24 (2.36267)	Phe103

* Donor atom-Acceptor atom (Hydrogen bond length [Å])

Majority of the designed novel ligands exhibited high GOLDScore_fitness values (GOLDScore_fitness ranging from 45.32 to 62.30) when compared to coumarins, phenylpropanoids, reference drugs and cloemiscosin A (**15**) (Table 5.1.4 and 5.1.7). The molecular bulkiness of the test compounds had improved their ligand fitness within the binding sites and favoured the moieties for hydrophobic interactions with more TNF-α residue. Also, these fused cyclic compounds were found to show all the common hydrophobic interactions that were found in diclofenac (**16**), prednisolone (**17**) and cleomiscosin A (**15**). Further, on examining the ligand-TNF-α docking interaction map of some representative compounds, it was found that compounds **9d** (GOLDScore_fitness, 59.4029), **10d** (GOLDScore_fitness, 59.9119), **11d** (GOLDScore_fitness, 56.1472) were having an additional π-π interaction with Tyr346 similar to that of natural cleomiscosin A (**15**) (Figure 5.1.17, Table 5.1.7 and 5.1.8). All these interactions have collectively made the fused-cyclic coumarin-based lignans to show high GOLDScore_fitness values (Table 5.1.7 and 5.1.8).

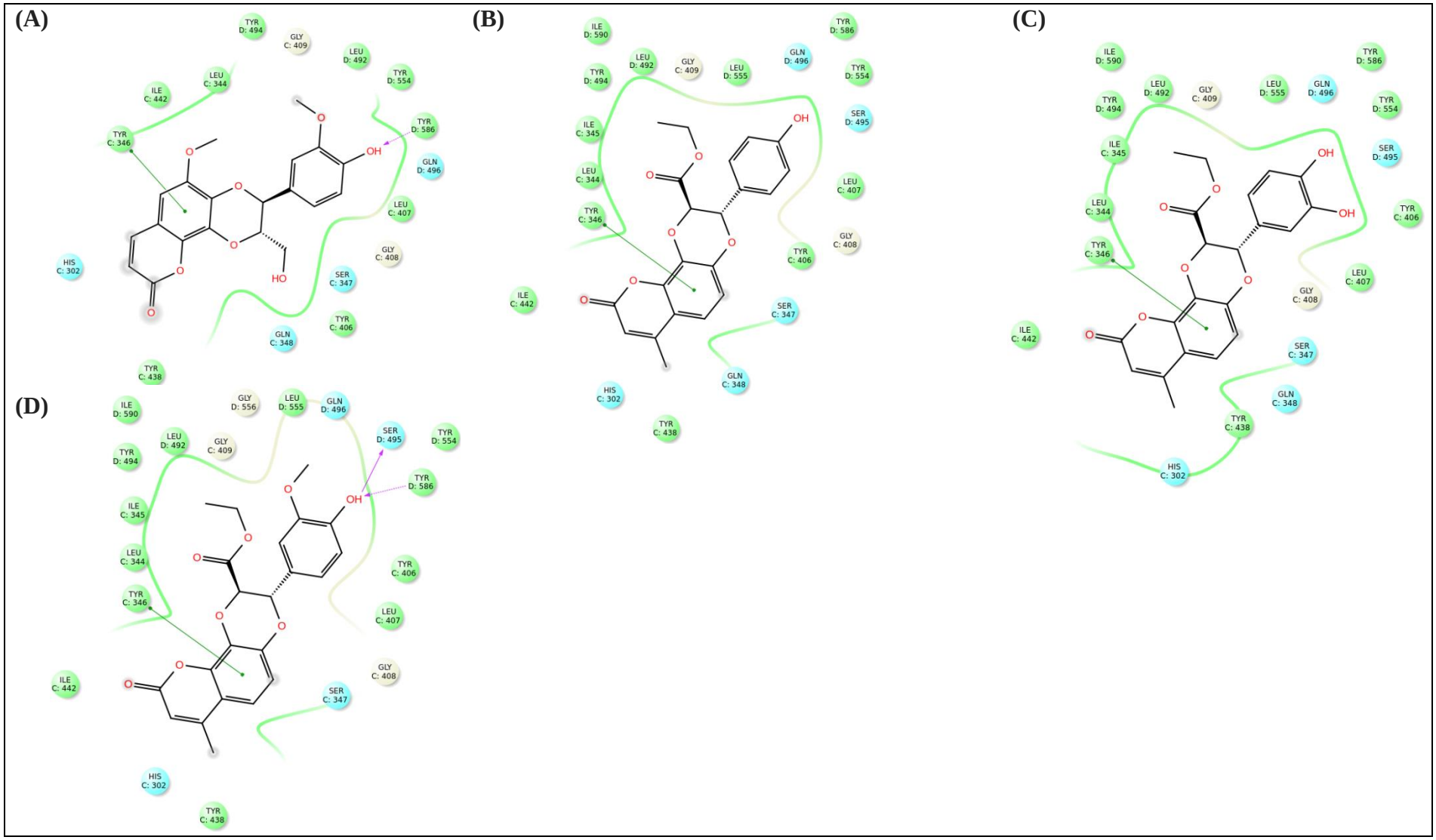

Figure 5.1.17 2D TNF-α docking interaction map displaying the binding and interactions of 15 (A), fused-cyclic coumarin-based lignans [9d (B), 10d (C) and 11d (D)]

5.1.7.2 Molecular docking studies of fused coumarin-based lignans into IL-1β protein

Amongst the reference compounds, cleomiscosin A (**15**) was found to display highest GOLDScore_fitness of 53.82 (Table 5.1.7). The ligand-IL-1β docking interaction map revealed a common hydrophobic interaction with Ile12 and Ile22 residues by all fused coumarin-based lignans and the reference compounds. Further, cleomiscosin A (**15**) formed the interactions with the residues which were observed with prednisolone (Gln13, Val14, Ala20, Met119, Tyr143) and diclofenac (Lys23, Pro25, Leu26, Phe27, HB with Arg10). Apart from these, cleomiscosin A (**15**) formed additional hydrophobic interactions with IL-1β residues such as Asp7, Gln11and Phe104 (Figure 5.1.15 and 5.1.18; Table 5.1.4 and 5.1.7).

In terms of GOLDScore_fitness, most of the fused-cyclic compounds (**8** – **13k**) were found to show higher scores as compared to the reference drugs (Table 5.1.7). Further, the compounds *viz*., **9d** (GOLDScore_fitness, 51.7056), **10d** (GOLDScore_fitness, 52.6486) and **11d** (GOLDScore_fitness, 53.2784) upon docking had equally interacted with prednisolone-interacting IL-1β residues (Val14, Asn139 and Tyr143), diclofenac-interacting IL-1β residues (Arg10, Lys23, Pro25, Leu26, Phe27) and cleomiscosin A-interacting IL-1β residues (Asp7, Gln11, Arg21 and Phe104) (Figure 5.1.15 and 5.1.18; Table 5.1.6 and 5.1.7). The common interacting hydrophobic residues found between **9d**, **10d**, **11d**, **15** and the reference ligands were Ile12 and Ile22. These features have collectively made most of the compounds to show better fitness score than the reference compounds.

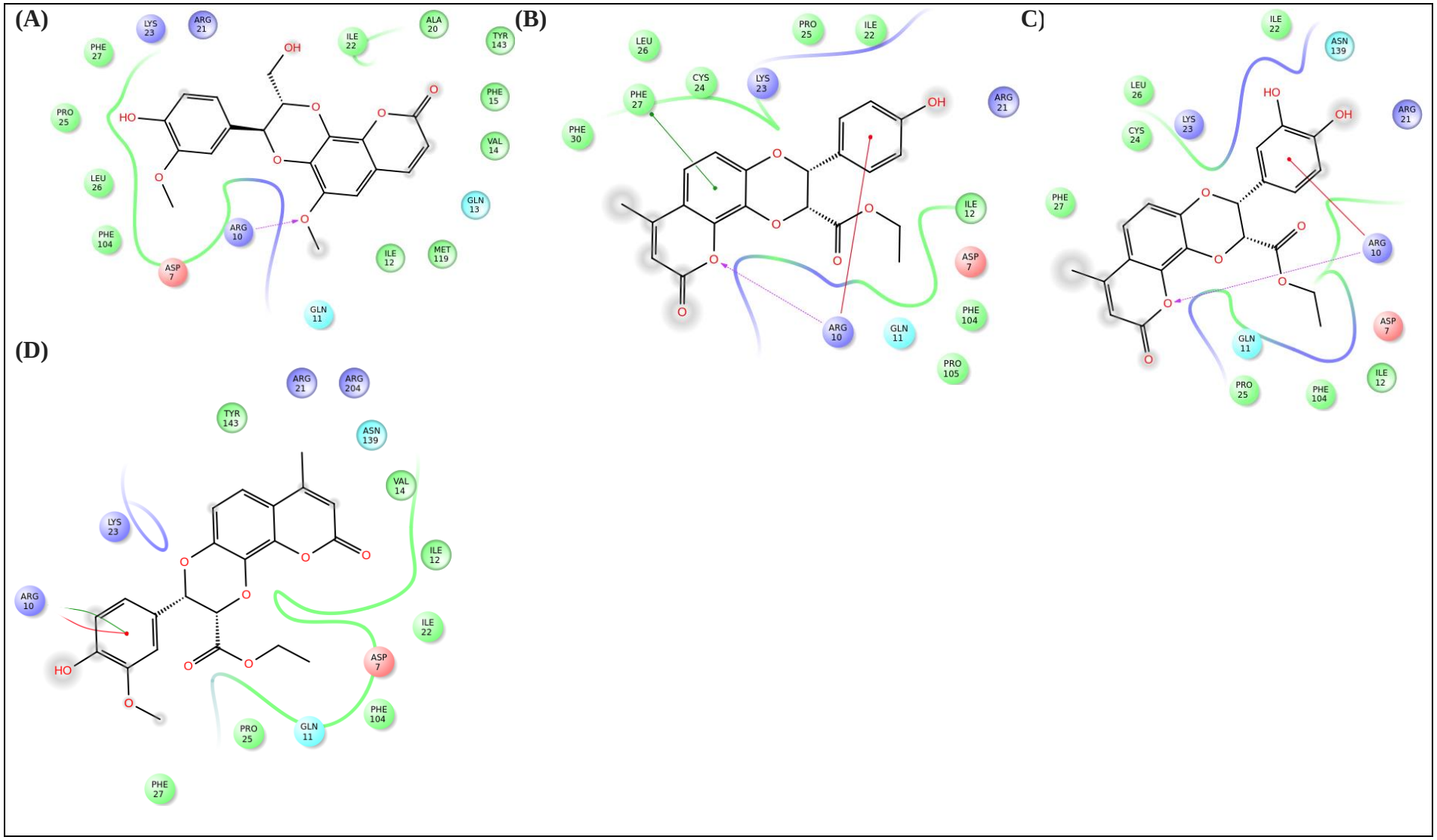

Figure 5.1.18 2D IL-1β docking interaction map displaying the binding and interactions of 15 (A), fused-cyclic coumarin-based lignans [9d (B), 10d (C) and 11d (D)]

5.1.7.3 Molecular docking studies of fused-cyclic coumarin-based lignans into IL-6 protein

In case of docking with IL-6 protein, cleomiscosin A (**15**) showed a strikingly higher GOLDScore_fitness value of 50.9474 compared to the reference compounds, diclofenac (**16**) (GOLDScore_fitness, 31.22) and prednisolone (**17**) (GOLDScore_fitness, 28.54) (Table 5.1.7). On examining the ligand-IL-6 binding interaction map, the hydrophobic residues found in diclofenac (**16**) and prednisolone (**17**) were observed to be relatively lesser than cleomiscosin A (**15**). The residues observed during the interaction of cleomiscosin A with IL-6 were found to be Phe103, Arg104, Asn110, Val111, Val112, Glu114, Ser149, Ser152, Ser156, Gln158, Asp198 and Ser224. However, only one common interaction residue (Phe103) was observed among all three (**15**, **16** and **17**). Additionally, cleomiscosin A (**15**) exhibited four hydrogen bond interactions, i.e. two with lysine residues (Lys105 similar to diclofenac (**16**), Lys154) and other two with serine residues (Ser106 and Ser109) (Table 5.1.5 and 5.1.8). These exclusive interactions could be the reason behind the higher GOLDScore_fitness of cleomiscosin A (**15**) (Table 5.1.7 and 5.1.8).

Docking analysis of fused-cyclic compounds (**8**-**13k**) has indicated that they interacted with most of the hydrophobic residues which are similar as in case of cleomiscosin A (**15**) i.e. Phe103, Arg104, Asn110, Val111, Val112, Glu114, Ser149, Ser152, Ser156, Asp198, and Ser224 (Figure 5.1.19). The unique hydrophobic interaction residues found among the newly designed compounds were Ser106, Glu114 and His223. This made the fused cyclic compounds to actively bind and gain fitness scores higher than the reference drugs (**16** and **17**) and cleomiscosin A (**15**) (Table 5.1.7).

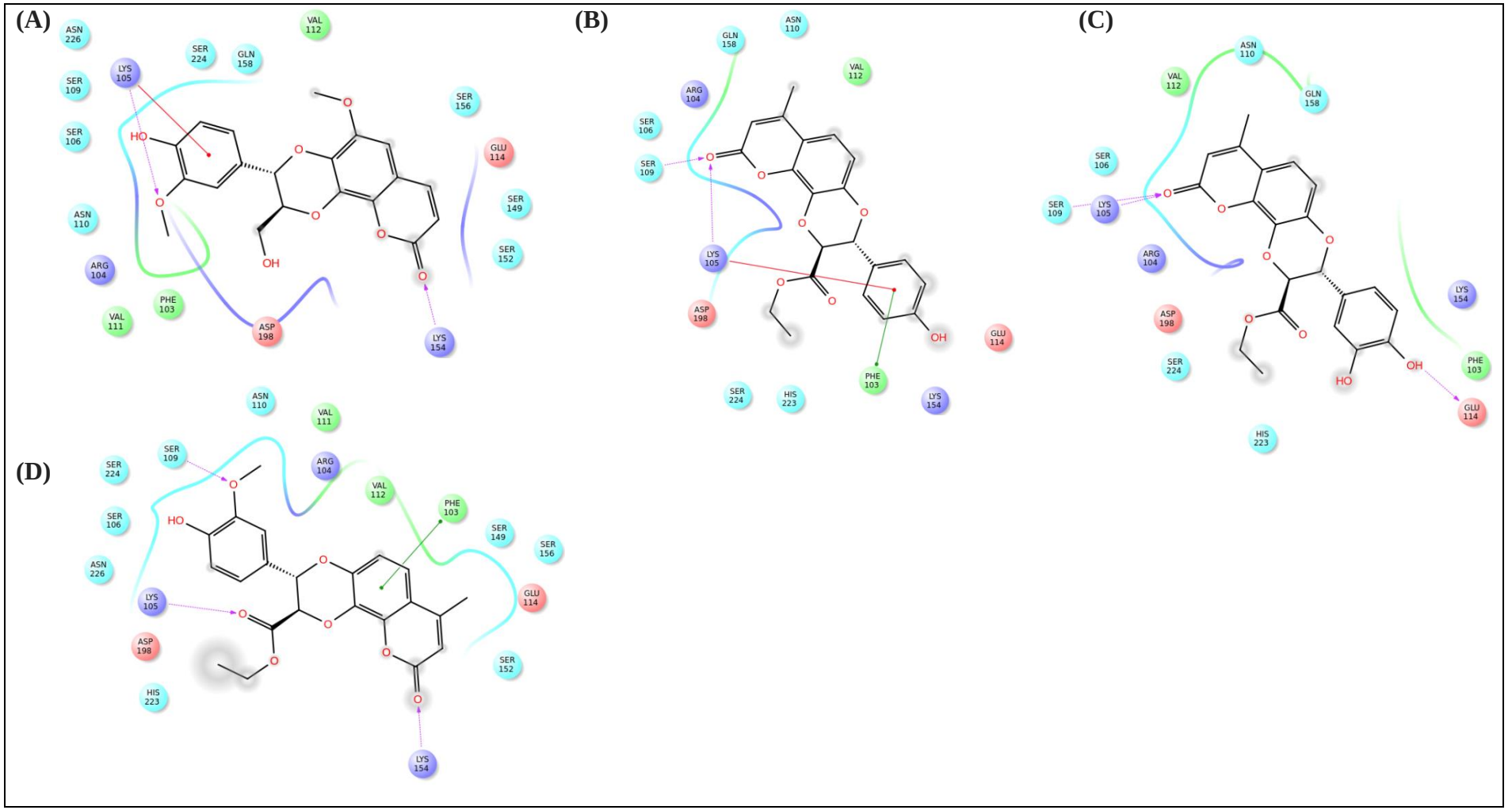

Figure 5.1.19 2D IL-6 docking interaction map displaying the binding and interactions of 15 (A), fused-cyclic coumarin-based lignans [9d (B), 10d (C) and 11d (D)]

5.1.7.4 Outcome of docking studies on fused-cyclic coumarin-based lignans

The study demonstrated significant TNF-α, IL-1β, and IL-6 protein inhibition effect of 7,8-dihydroxy-4-methyl coumarin (**1a**) and ethyl cinnamate derivatives (**3b**, **4b** and **5b**) through LPS induced cell model using ELISA. This was continued with docking studies directly targeting TNF-α, IL-1β, and IL-6 proteins by designing some simple ligands (**1**-**7c**) to identify potentially active inhibitors using GOLD ver. 5.2 docking protocol. Cinnamic acid derivatives displayed better interactions and fitness scores than the coumarins and the results were comparable to that of diclofenac and prednisolone. The continued work on ligand-based docking on fused-cyclic coumarin and cinnamate based compounds (**8**-**13**k) evidenced higher GOLD fitness scores, active site interactions, distinctive π-π interactions when compared to the natural coumarinolignan, cleomiscosin A (**15**) and clinically used acute and chronic anti-inflammatory drugs like diclofenac (**16**) and prednisolone (**17**). The active site residues (Leu-Gly-Gly) identified in the PDB reported co-crystal ligand over a β strand of the TNF-α subunit C was observed in the designed fused coumarin-based lignans compounds and standard drugs as well, which unambiguously confirmed the inhibition effect and possible emergence of newly designed molecules as the anti-inflammatory agents.

A structure-based study on the discovery of quinuclidine (IC_{50}-5μM) and indoloquinozolidine (IC_{50}-10μM) derivatives as TNF-α inhibitors had also revealed the contact of hydrophobic ring system with a β strand (Leu-Gly-Gly) of TNF-α subunit A (Chan DS-H *et al*., 2010). This active site interaction which is important for the binding and inhibition effect further authenticated the effect of these compounds. Also, the fitness scores were found to be doubled in some fused-cyclic coumarin-based lignans molecules when compared to the tested individual coumarins and

cinnamates, which corroborated the synergistic effect (virtual) of newly designed lignin compounds.

Overall analysis of docking results revealed, compounds **10c**, **10d**, **10e**, **10i**, **11d**, **11e**, **15** to be highly active and were identified as small molecule potent inhibitors active against multiple cytokines. Moreover, it was observed that fused-cyclic coumarin-based lignans made by coupling 7,8-dihydroxy-4-methyl coumarin with phenylpropanoids possessing acid ester (ethyl) and two acetyl substituents consistently demonstrated excellent score, selectivity and binding mode towards all the proteins. Noticeably, cleomiscosin A (**15**) stood alike in terms of binding mode into the binding sites of all three proteins compared to diclofenac (**16**) and prednisolone (**17**).

All these results yielded a positive indication to work further on this group of fused-cyclic coumarin-based lignans to develop anti-inflammatory drugs.

5.2 Synthesis of coumarin-based lignans followed by in-vitro and in-vivo pharmacological evaluations towards developing pro-inflammatory cytokines inhibitors

5.2.1 Introduction

Based on the results of molecular docking studies on coumarins, phenyl propanoids and their fused-cyclic coumarin-based lignans, attempts were taken to synthesis and develop the fused cyclic compounds as pro-inflammatory cytokines inhibitors. As a first step, some representative compounds were selected based on their overall GOLDScore_fitness and interaction efficacy into the inflammatory proteins. Compounds **9d**, **10d**, **11d** and **11e** which scored well and could conveniently be synthesized using the earlier studied **1a**, **3b**, **4b** and **5b** were selected for the further study.

5.2.2 Preparation of diphenyl selenoxide

Diphenyl selenoxide was used as a catalyst for the oxidative coupling reaction between the dihydroxy methyl coumarin and phenyl propanoid (cinnamate) derivatives. Diphenyl selenoxide rapidly oxidises the hydroxyl groups of 7,8-dihydroxy-4-methyl coumarin (**1a**) to generate corresponding ortho-quinones, in which the oxygen atom at C-8 position was immediately attacked by the double bond of cinnamate derivatives to form coumarinolignans (Tanaka H *et al*., 1988). It was prepared by dissolving diphenyl selenide in methanol/DCM and adding with N-chlorosuccinimide under stirring. The product was then purified and recrystallized using hexane and DCM mixture (Michael RD., 1980) (Scheme 5.3).

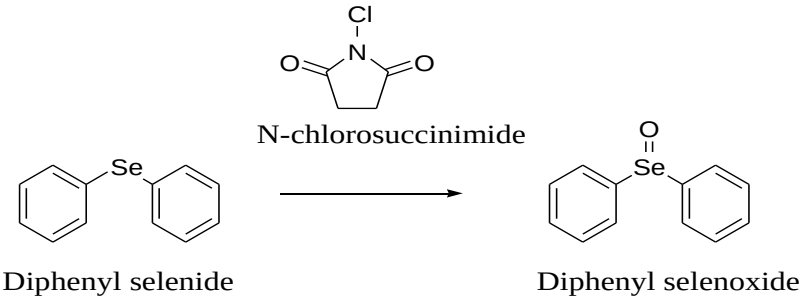

Scheme 5.3 Preparation of diphenyl selenoxide

5.2.3 Synthesis of coumarin-based lignans 9d, 10d and 11d

7, 8-dihydroxy-4-methyl-2H-chromen-2-one (**1a**) and diphenyl selenoxide were dissolved in a mixture of methanol and benzene and stirred at room temperature for 15 min. This mixture was added drop-wise with corresponding cinnamic ester derivative (**3b**/**4b**/**5b**) dissolved in methanol. This solution was stirred at room temperature and completion of the reaction was monitored through TLC (Scheme 5.4). The product obtained was purified by chromatography using hexane: ethyl acetate solvent system. Pure compound of single isomer was obtained using silica gel column chromatography followed by flash chromatographic purification. The column eluates obtained using hexane:ethyl acetate (65:35) solvent system was subjected for flash chromatography [Conditions: MP: hexane (A) and ethyl acetate (B); Flash silica (40-60 µ); Flow rate – 5 ml/min; Detection wavelength – 274 nm; Binary gradient 0% B - 25 min; 10% B - 30 min; 15% B - 25 min; 20% B - 30 min; 25% B - 30 min; 30% B - 30 min; 35% B - 30 min; 40% B - 25 min; 100% B - 20 min] to get pure crystals of respective compounds (**9d**/**10d**/**11d**).

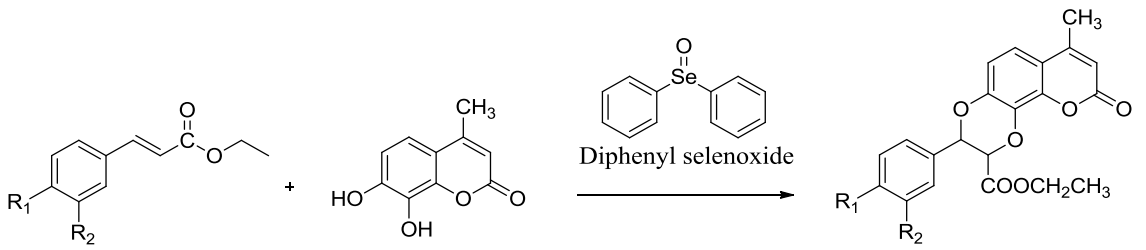

3b - R_1 -OH, R_2 -H
4b - R_1 -OH, R_2 -OH
5b - R_1 -OH, R_2 -OCH_3

1a

9d - R_1 -OH, R_2 -H
10d - R_1 -OH, R_2 -OH
11d - R_1 -OH, R_2 -OCH_3

Scheme 5.4 Preparation of fused-cyclic coumarin-based lignans

5.2.4 Characterisation of oxidative coupled product 11d

Ethyl-3,9-dihydro-3-(4-hydroxy-3-methoxyphenyl)-7-methyl-9-oxo-2H-[1,4]dioxino[2,3-h]chromene-2-carboxylate (**11d**) was prepared as white crystals by oxidative coupling of 7,8-dihydroxy-4-methyl coumarin (**1a**) with ethyl ferulate (**5b**) in the presence of diphenyl selenoxide as oxidative agent. The singularity of **11d** was ascertained by performing RP- LC-PDA-ESI-MS (Rt 8.08 min) ESI interface; Mass scan range 50-1000 *m/z*; method run time 16.02 min stationary phase (Zodiac column C18, 150 mm x 4.6 mm, 5 µm), mobile phase (aqueous phase-pump A - formic acid (0.1% in milli-Q water-pH – 2.97) and organic phase-pump-B - HPLC MeOH) Initial pump B conc - 20%, flow rate 1 ml/min, binary gradient method details [(0- 3.0 min (20% B); 3.01-6.00 (50% to 80% B); 6.01-12.01 (80% B); 12.02-14.01 (80% B to 20% B); 14.02-16.01 (20% B) and 16.02 (stop)] (Figure 5.2.1).

The melting point of **11d** was found to be 139-141 °C. The product formation was confirmed through the Electro Spray Ionisation mass spectral ESI-MS analysis which showed $[M-1]^+$ 411.20; $[M+1]^+$ 413.10 [calc. 412.1158] (Figure 5.2.2). The molecular formula was determined to be $C_{22}H_{20}O_8$ through APCI-MS analysis and ^1H – and ^{13}C – NMR analysis. The UV spectrum of **11d** displayed absorption bands at λ_{max} 194, 229, 259 and 312 nm, which were characteristic of coumarinolignans (Figure 5.2.3) (Begum SA *et al*., 2010). The

300 MHz proton NMR and 75 MHz carbon NMR spectra were measured by dissolving **11d** in a mixture of $CDCl_3$-CD_3OD (10:1) (Figure 5.2.4 and 5.2.5).

The proton NMR spectrum (Figure 5.2.4) revealed various signals ascertaining the formation of oxidative coupled product **11d** by coupling 7,8-dihydroxy-4-methyl coumarin (**1a**) and ethyl ferulate (**5b**). The spectrum displayed signals at δ 6.20 (s), 7.18 (d, *J*=8.7 Hz) and 6.95 (d, *J*=9 Hz) ppm for protons at C-3, C-5 and C-6 of coumarin nucleus, respectively. The signals due to the protons of ethyl ferulate [1.12 (t, -COO-$CH_2C\underline{\mathbf{H}}_3$), 3.89 (s, Ar-OMe), 4.21 (q, -COO-$C\underline{\mathbf{H}}_2CH_3$) and 6.89-6.94 (m, 3xAr-H) ppm were found in the spectrum. Additionally, the spectrum exhibited two mutually coupled doublets at 5.23 and 6.20 ppm (*J* = 6.3 Hz), which corroborated the oxidative coupling and product formation (**11d**). The proton and carbon NMR data with probable position assignments are presented in Table 5.2.1.

Through this coupling reaction, a mixture of regio- and stereo-isomers (A-D)were expected to be formed and hence **11d**, a purified single isomer could have one of the four possible structures (**A**-**B**) as given in scheme 5.5. Therefore, for the identification of exact isomeric structure of **11d**, a thorough structure elucidation was required.

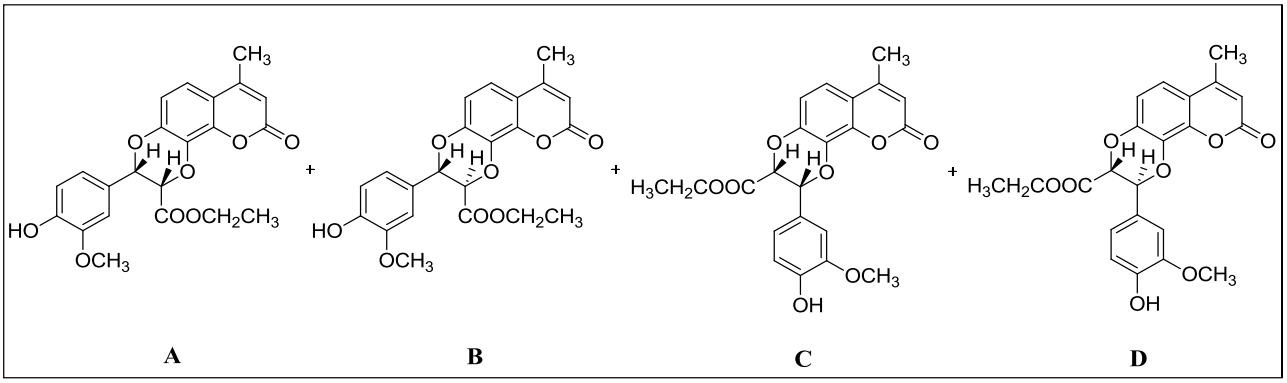

Scheme 5.5 Possible isomeric structures of compound **11d**

Oxidative coupling reaction using diphenyl selenoxide had been reported to be highly regio-selective and stereo-selective in synthesizing natural coumarinolignans (Tanaka H *et al*., 1988). Attempts to synthesize cleomiscosin acetate and daphneticin acetate by Tanaka et al., had resulted in the formation of A as major product along with other isomers as minor products (Scheme 5.5) (Begum SA *et al*., 2010). In order to identify the exact stereomeric structure of **11d**, its acetate derivative (**11e**) was synthesized and analyzed spectroscopically.

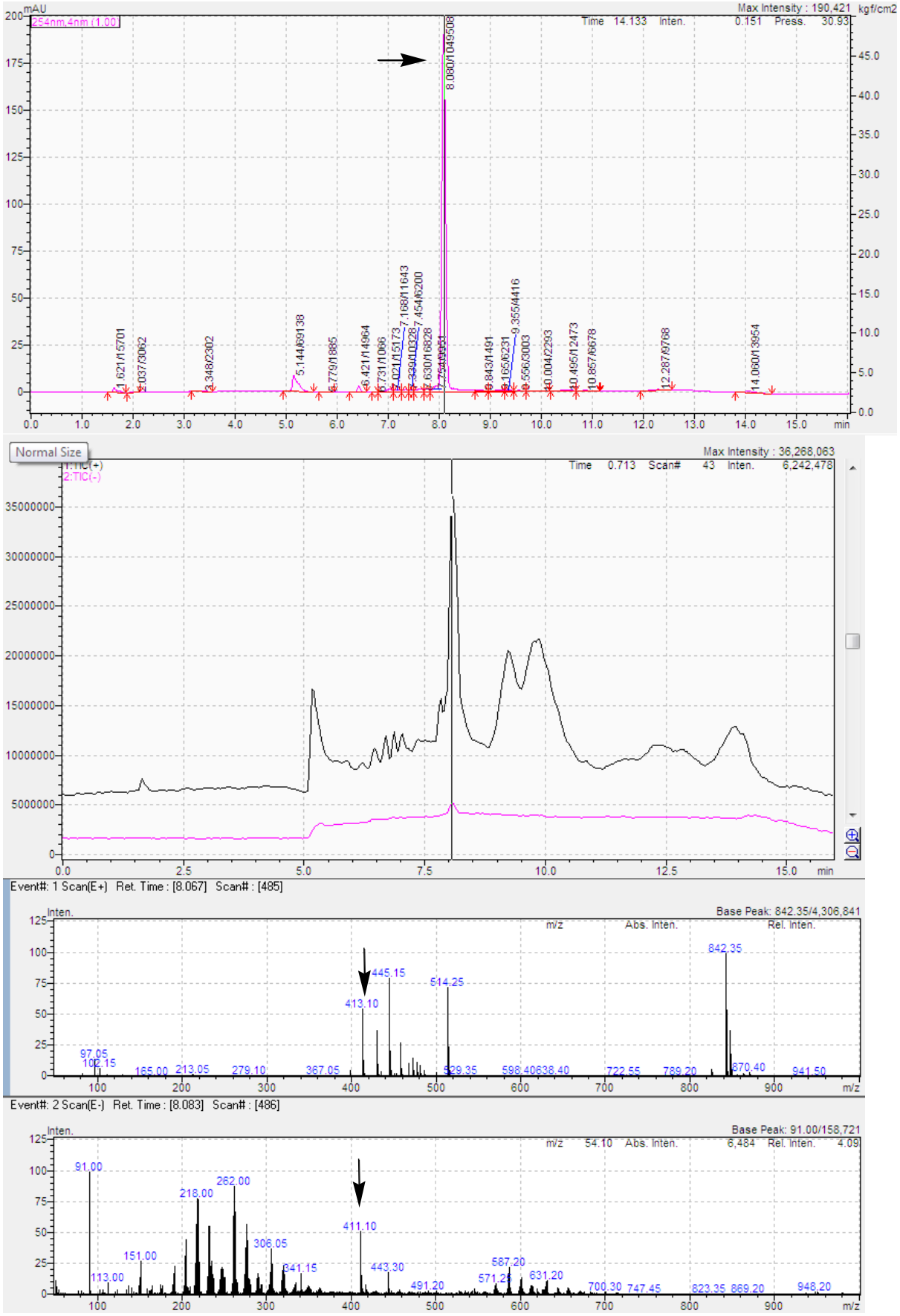

Figure 5.2.1 LCMS PDA chromatogram at 254 nm, mass chromatogram and ESI-mass spectrum of 11d

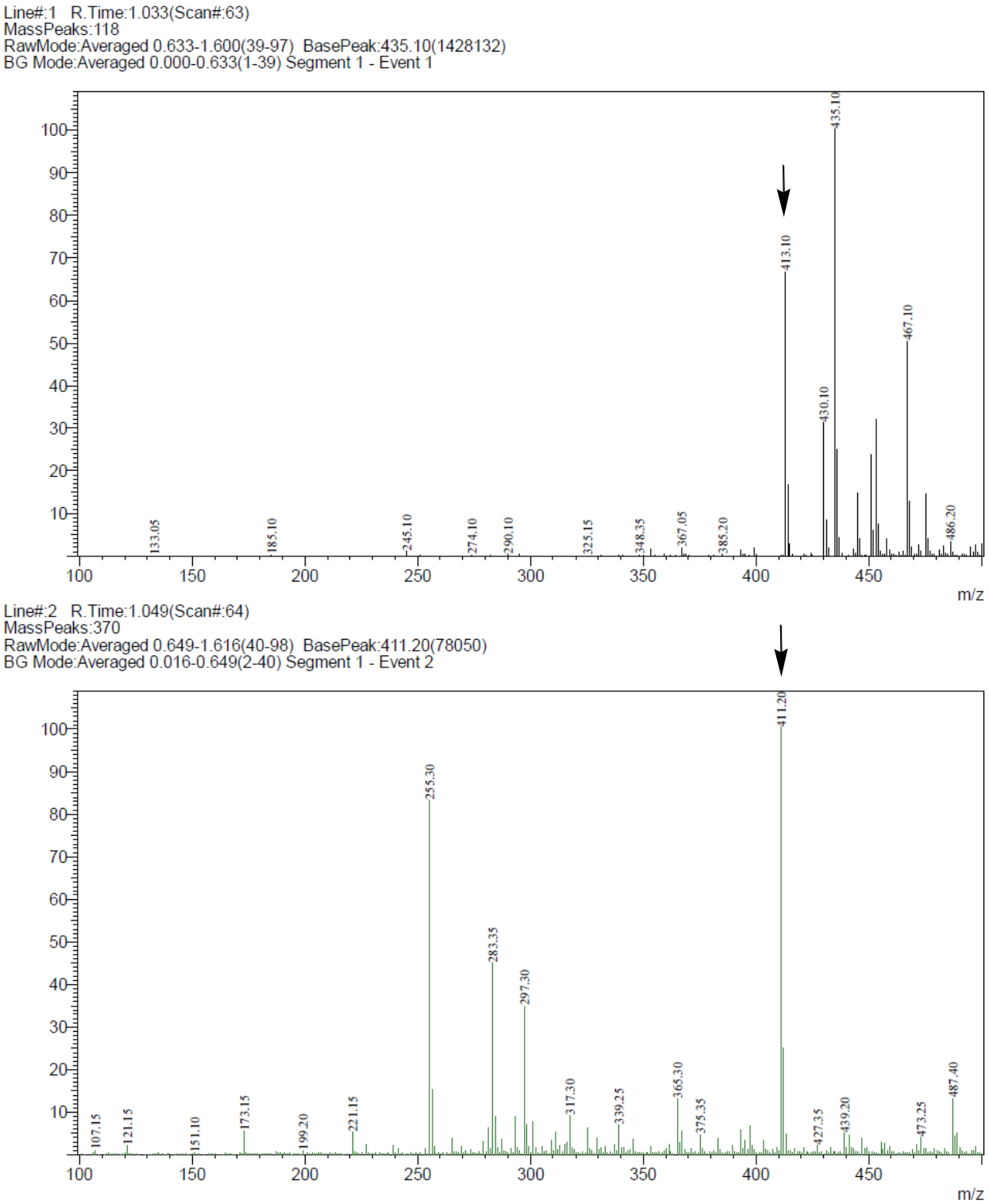

Figure 5.2.2 APCI mass spectrum of compound 11d

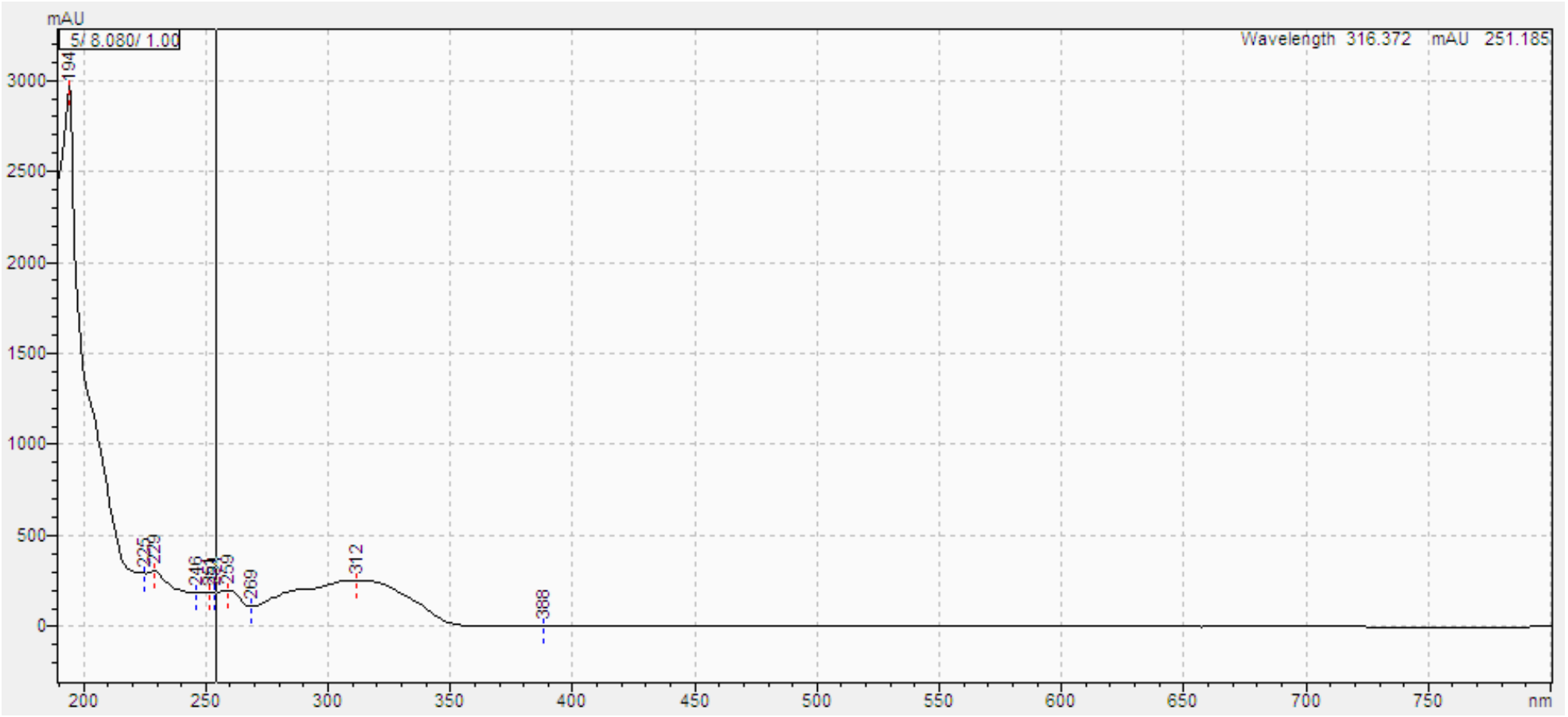

Figure 5.2.3 UV chromatogram of compound 11d

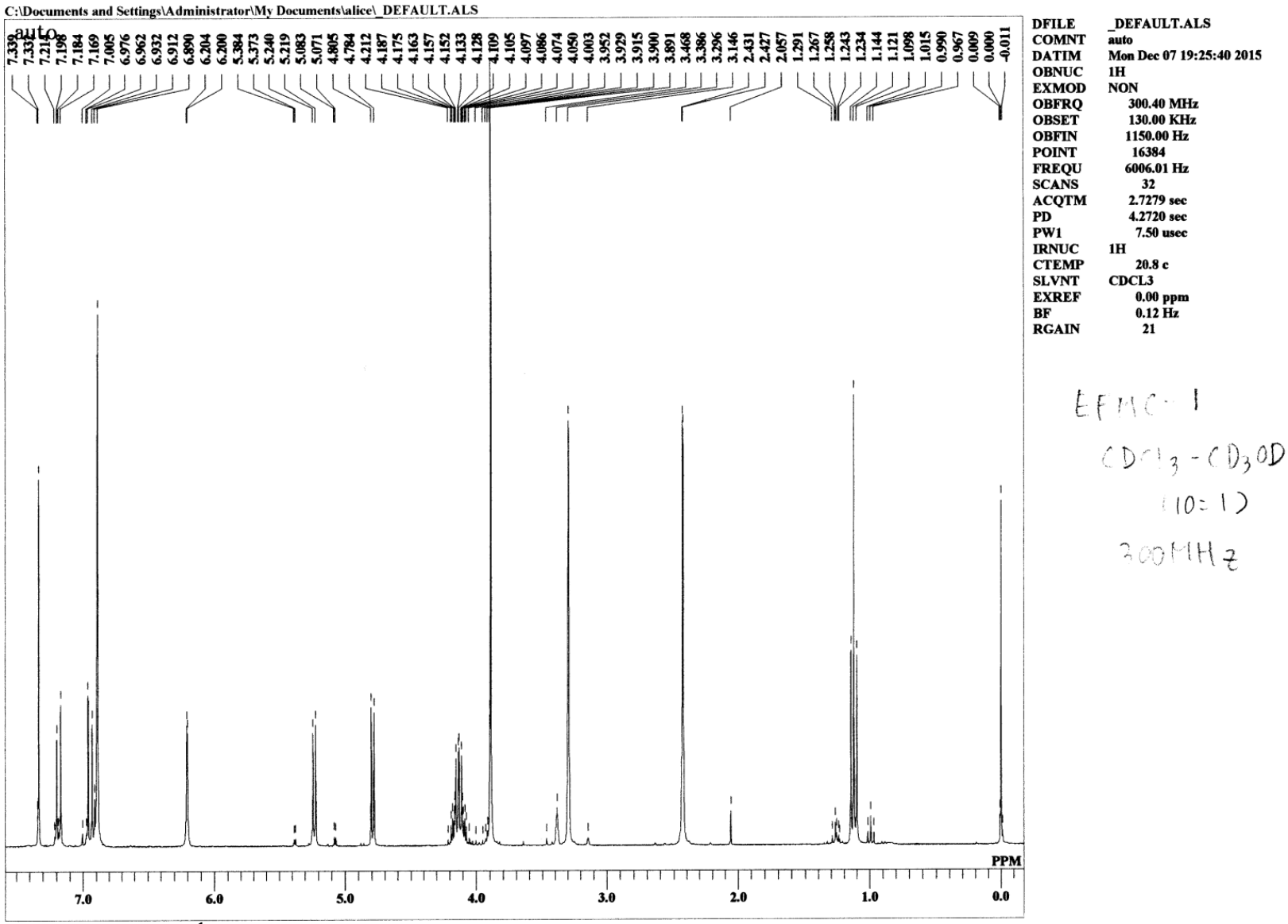

Figure 5.2.4 The 300 MHz ^{1}H NMR spectrum of compound 11d

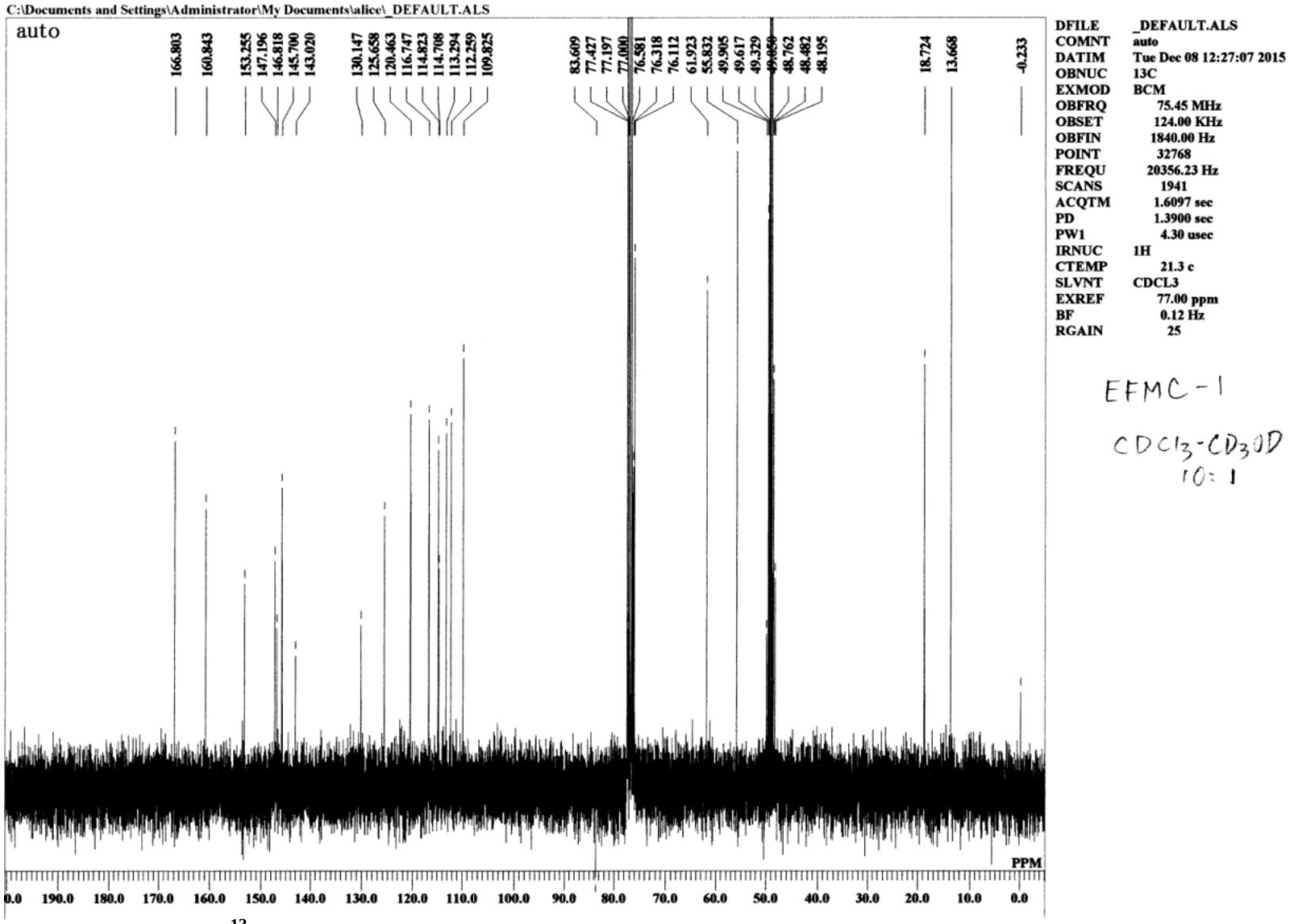

Figure 5.2.5 The 300 MHz ^{13}C NMR spectrum of compound 11d

Table 5.2.1 ^{1}H and ^{13}C NMR spectroscopic data (δ/ppm) ^{1}H and ^{13}C NMR spectroscopic data (δ/ppm) of compound 11d measured in a 1:10 mixture of $CDCl_3$ and CD_3OD

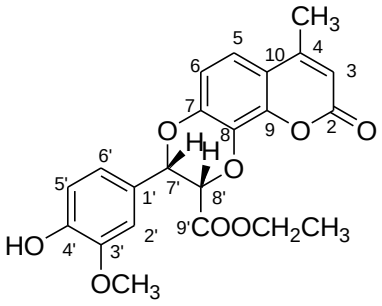

11d

Positions	**δ_C in ppm**	**δ_H in ppm**
2	160.8	-
3	114.7	6.20 (1H, d, 1.2 Hz)
4	153.3	-
5	116.7	7.18 (1H, d, 8.7 Hz)
6	109.8	6.95 (1H, d, 9 Hz)
7	143.0	-
8	130.1	-
9	147.2	-
10	113.3	-
1′	125.7	-
2′	112.3	6.93-6.89 (m)
3′	146.8	-
4′	145.7	-
5′	114.8	6.93-6.89 (m)
6′	120.5	6.93-6.89 (m)
7′	76.1	6.20 (1H, d, 6.3 Hz)
8′	76.3	5.23 (1H, d, 6.3 Hz)
9′	166.8	-
C-9′-O$\underline{CH_2}CH_3$	61.9	4.21 (2H, q)
C-9′-O$CH_2\underline{CH_3}$	13.7	1.12 (3H, t)
C-4-$\underline{\ }CH_3$	18.7	2.43 (3H, d, 1.2 Hz)
C-3′-OCH_3	55.8	3.89 (3H, s)

5.2.5 Synthesis and characterisation of compound 11e

Compound **11d** was acetylated by treating with acetic anhydride and pyridine, and stirred for 12 h under room temperature. The reaction mixture was extracted with dichloromethane and was then washed with distilled water and dried by passing through sodium sulphate bed. The dichloromethane layer was evaporated under reduced pressure to obtain compound **11e** (Scheme 5.6).

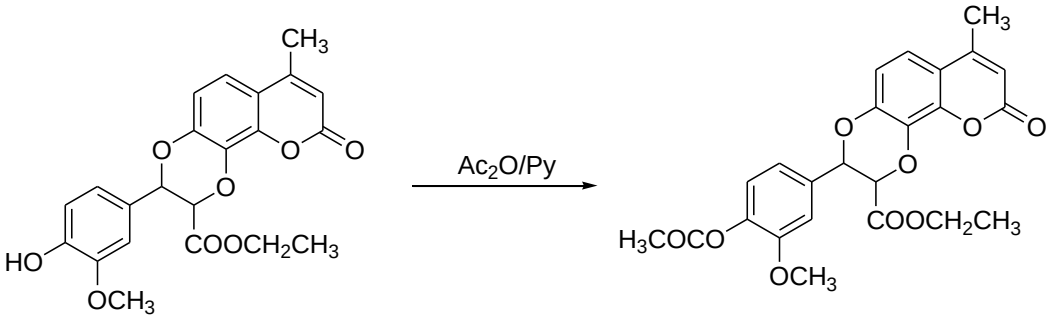

11d **11e**

Scheme 5.6 Preparation of compound 11e

Compound **11e** was obtained as white amorphous solid showing $[M+H]^+$ at *m/z* 455 under APCI-MS analysis (Figure 5.2.6). The NMR spectra of **11e** showed clearly discerned signals for acetate protons at δ_H 2.32 (s, -COC**H**$_3$) ppm and carbons at δ_C 20.1 and 168.7 (-**C**O**C**H$_3$) ppm (Figure 5.2.7 and 5.2.8). Further, the assignment of signals to corresponding protons as presented in Table 5.2.2, was verified by interpreting HMBC spectrum (Figure 5.2.9). The identification of exact isomeric structure out of the form possible structures of A-D was done with the help of HMBC. The key correlation between the different carbons and protons of **11e** are explained in (Figure 5.2.10). In the HMBC spectrum, the oxymethine proton at δ 4.82 ppm showed a weak but distinct three bond correlation with C-8 (δ 130.2 ppm). This unambiguously stated that the purified product must have the isomeric structure **A** as drawn in Scheme 5.7.

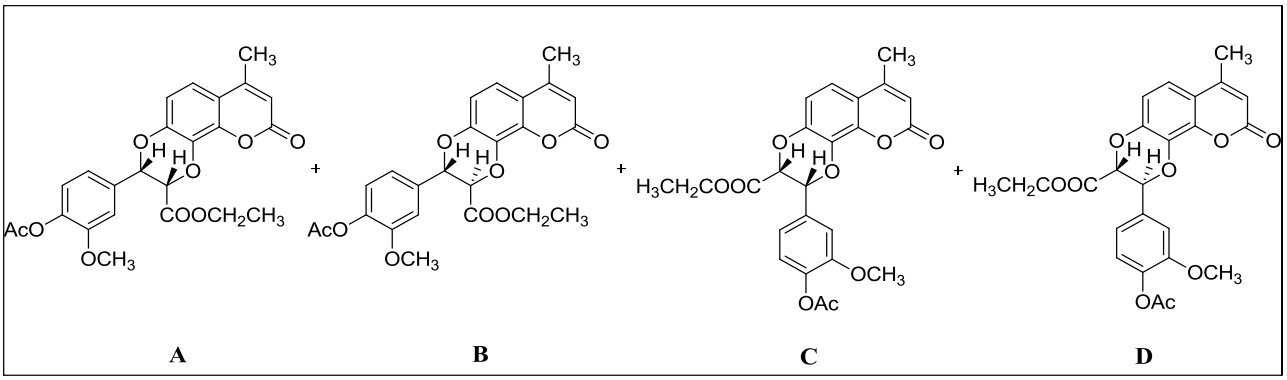

Scheme 5.7 Possible isomeric structures of 11e

Further, 1D Nuclear Overhauser Effect (NOE) difference analysis of **11e** was carried out to understand the relationship between the oxy methine protons at C-7′ and C-8′. The *cis*-relationship between the protons 7′-H and 8′-H was confirmed by observing the mutual intensification of peaks when signals at δ 5.33 and 4.82 ppm were irradiated separately (Figure 5.2.11). Thus **11d** and **11e** were corroborated to possess the structures as the given in scheme 5 and 7 as structure type A.

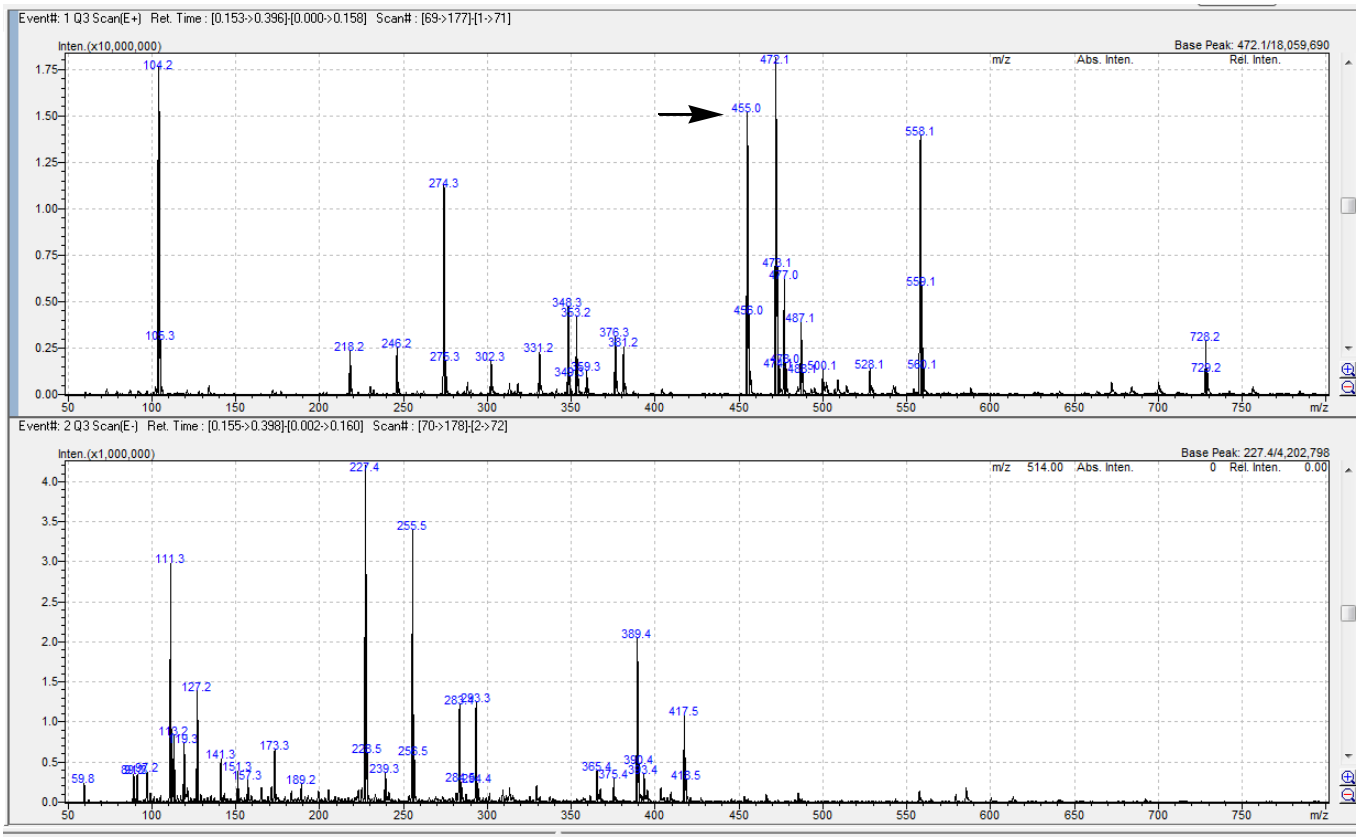

Figure 5.2.6 APCI Mass spectrum of compound 11e

Table 5.2.2 ^{1}H and ^{13}C NMR spectroscopic data (δ/ppm) of compound 11e measured in a 1:10 mixture of $CDCl_3$ and CD_3OD

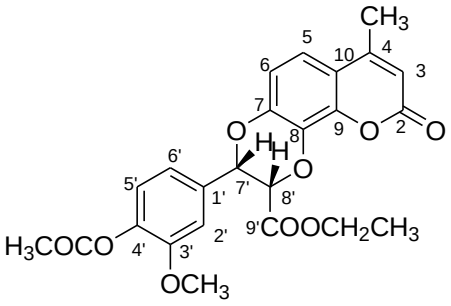

11e

Positions	**δ_C in ppm**	**δ_H in ppm**
2	160.2	-
3	114.9	6.19 (1H, d, 0.5 Hz)
4	152.6	-
5	116.8	7.16 (1H, d, 8.5 Hz)
6	111.1	7.05 (1H, d, 8.5 Hz)
7	143.2	-
8	130.2	-
9	145.3	-
10	113.1	-
1′	123.2	-
2′	112.7	6.99 (1H, dd, 9.5 Hz)
3′	140.5	-
4′	151.4	-
5′	119.5	6.93 (1H, d, 8.5 Hz)
6′	133.3	6.99 (1H, dd, 9.5 Hz)
7′	75.8	5.33 (1H, d, 6.0 Hz)
8′	75.9	4.82 (1H, d, 5.5 Hz)
9′	166.7	-
C-9′-O$\underline{CH_2}CH_3$	62.1	4.14 (2H, q)
C-9′-O$CH_2\underline{CH_3}$	13.8	1.13 (3H, t)
C-4-CH_3	18.9	2.41 (3H, d, 1.0 Hz)
C-3′-OCH_3	56.0	3.83 (3H, s)
C-4′-O$\underline{C}OCH_3$	168.7	-
C-4′- OCO$\underline{CH_3}$	20.1	2.32 (3H, s)

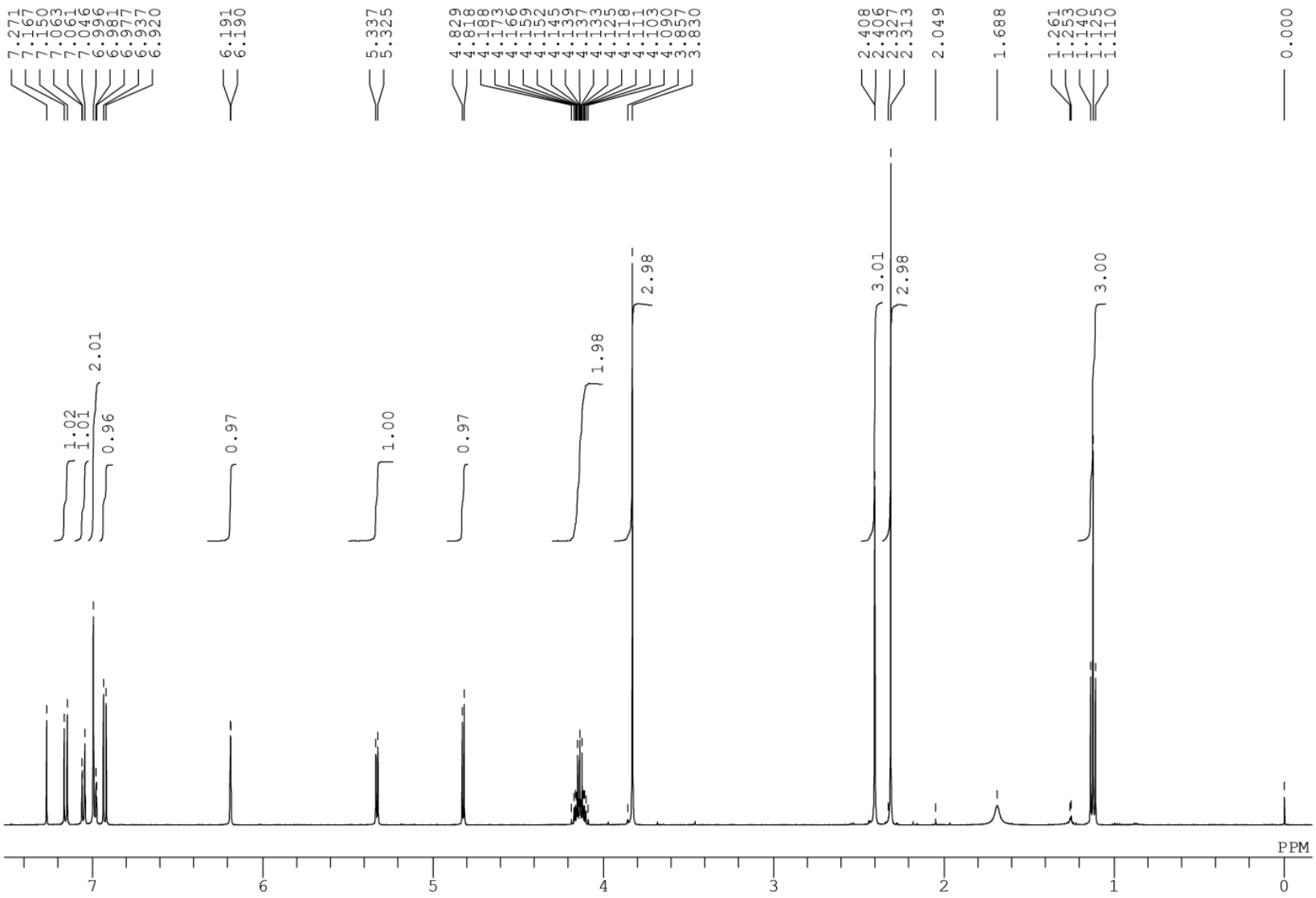

Figure 5.2.7 The 300 MHz ^{1}H NMR spectrum of compound 11e

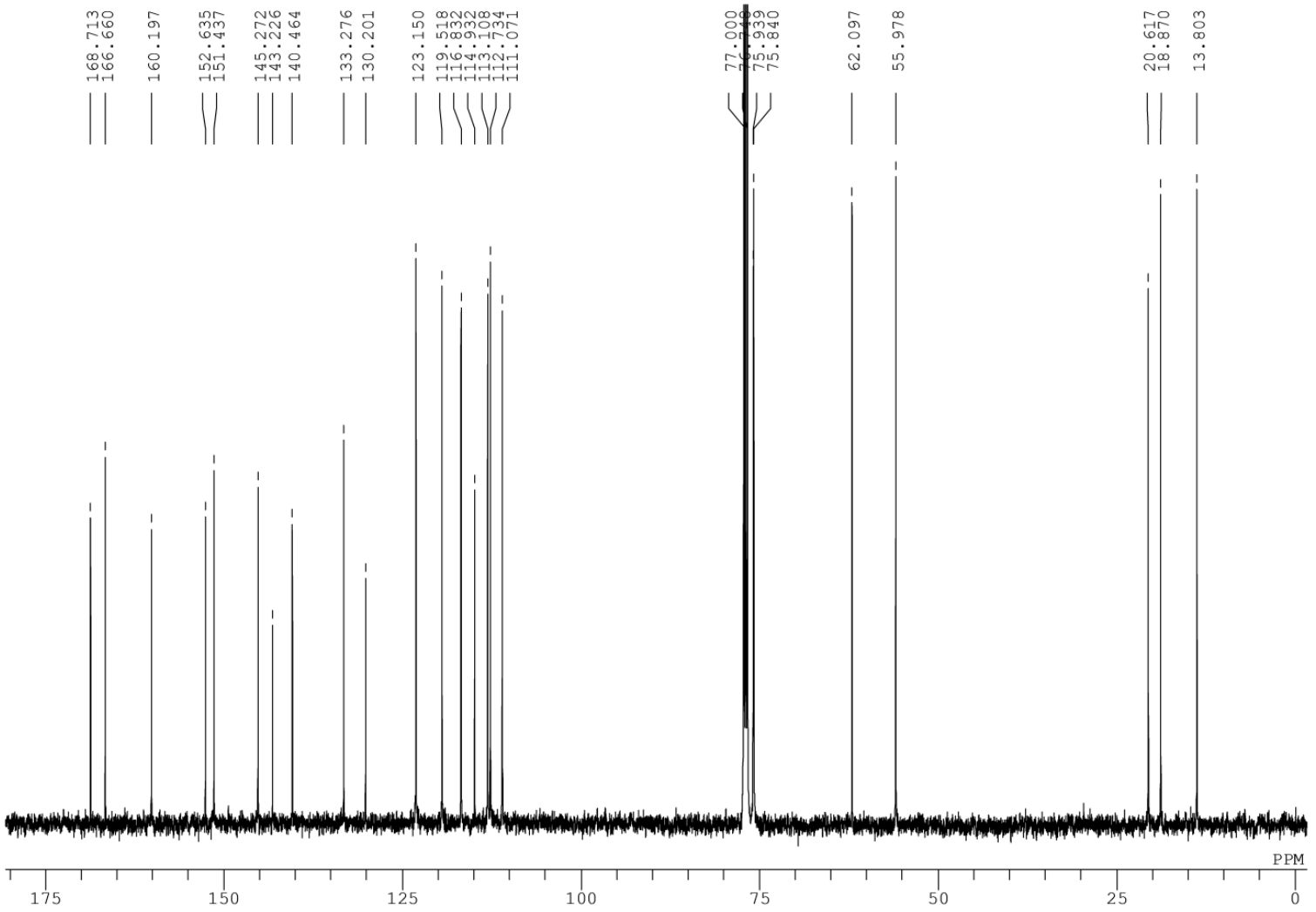

Figure 5.2.8 The 300 MHz ^{13}C NMR spectrum of compound 11e

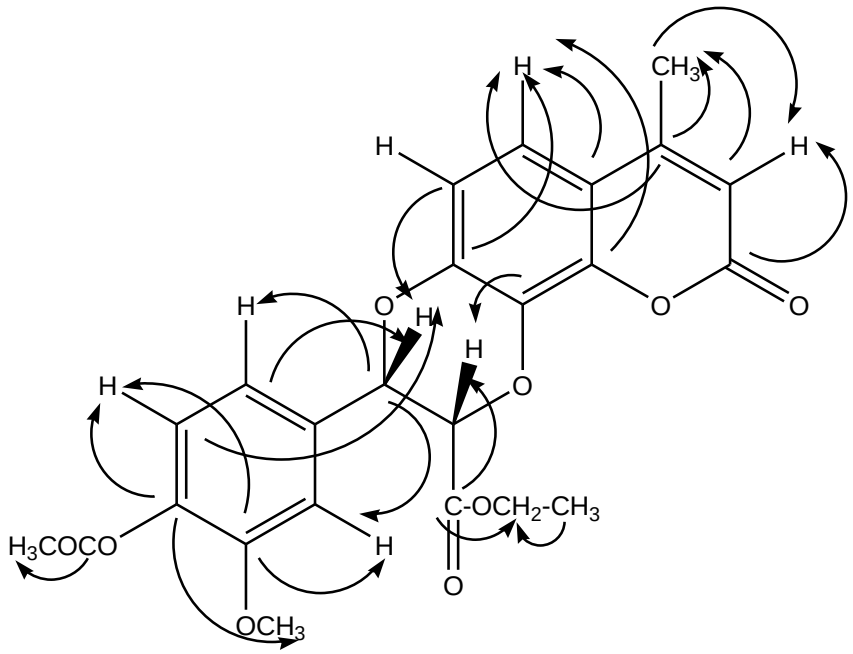

Figure 5.2.9 Key correlations (C→H) observed in the HMBC spectrum of 11e

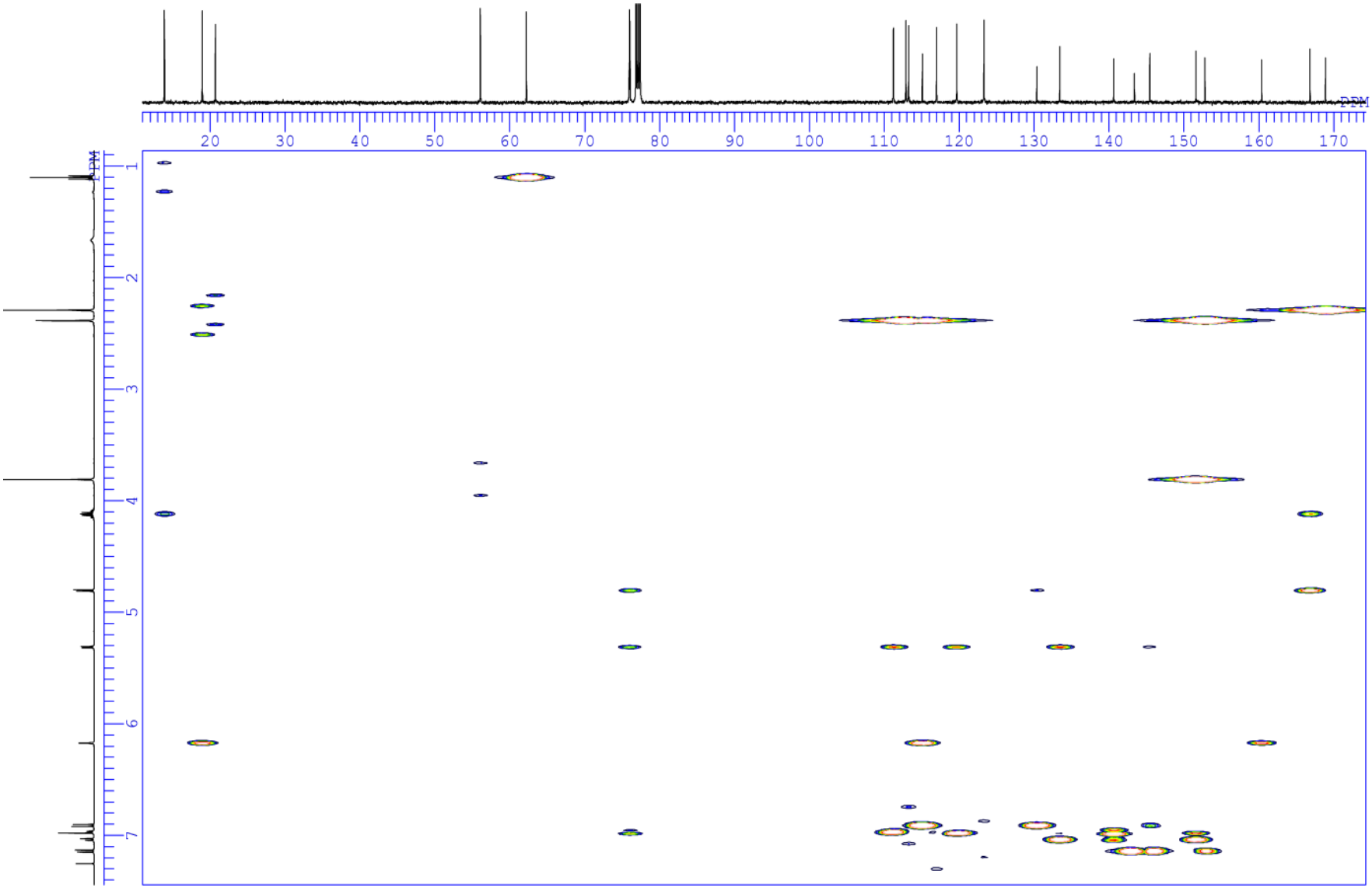

Figure 5.2.10 HMBC spectrum of compound 11e

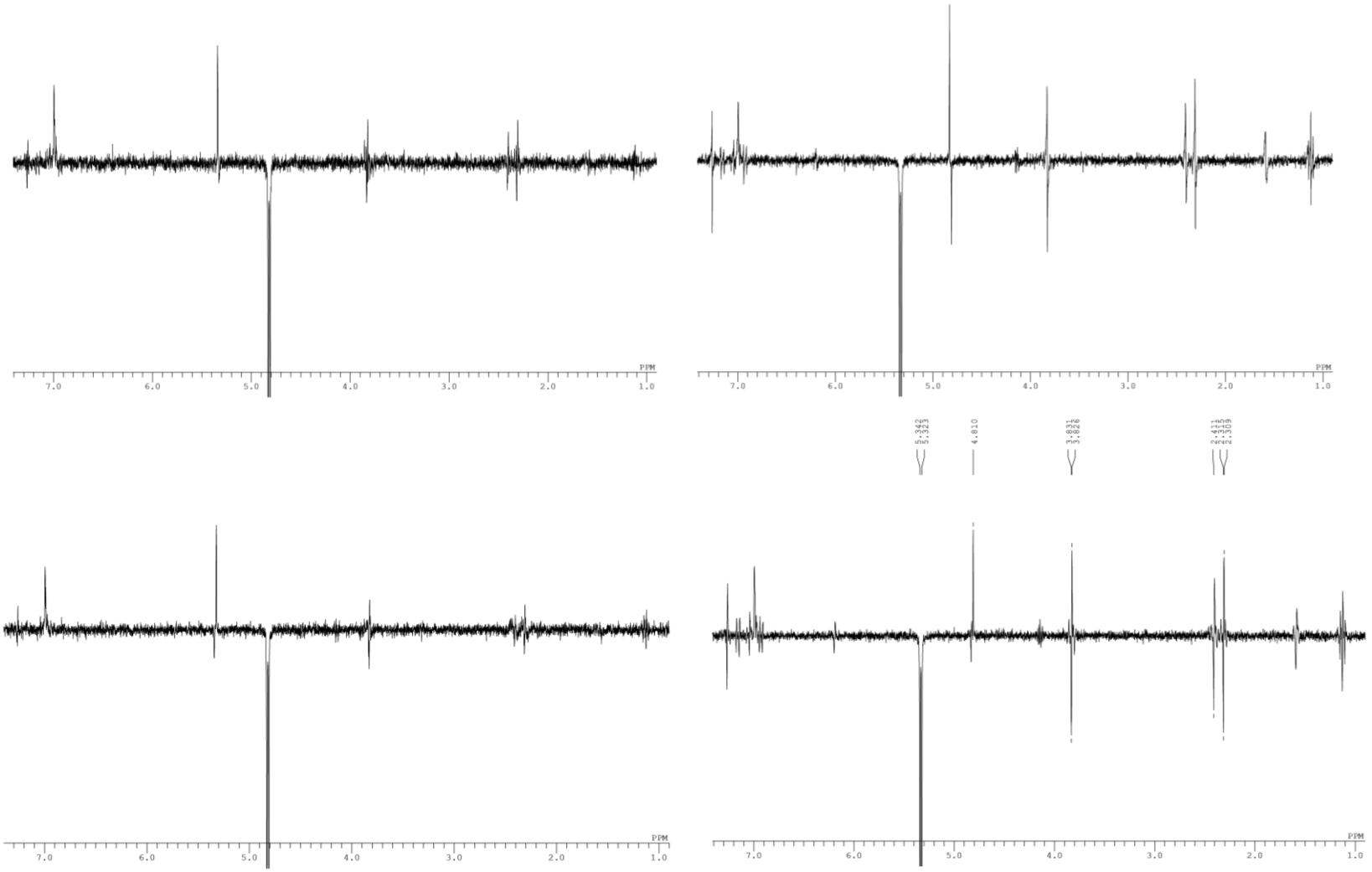

Figure 5.2.11 NOE difference spectrum of compound 11e

5.2.6 Characterization of compound 10d

Ethyl 3,9-dihydro-3-(3,4-dihydroxyphenyl)-7-methyl-9-oxo-2H-[1,4]dioxino[2,3-h]chromene-2-carboxylate (**10d**) having molecular formula $C_{21}H_{18}H_8$, was obtained as colourless crystals. The purity and product identity of **10d** was analysed by LC-PDA-ESI-MS; Mass scan range 50-1000 *m/z* ; method run time 16.02 min; stationary phase (Zodiac column C18, 150 mm x 4.6 mm, 5 µm), mobile phase: (pump A - formic acid (0.1% in milli-Q water-pH – 2.97) and pump B - MeOH); Initial pump B conc - 20%, flow rate 1 ml/min; binary gradient method details [(0- 3.0 min (20% B); 3.01-6.00 (50% to 80% B); 6.01-12.01 (80% B); 12.02-14.01 (80% B to 20% B); 14.02-16.01 (20% B) and 16.02 (stop)]. It was found to be a homogenous compound from the appearance of single peak at 7.6 min Rt in the PDA chromatogram (Figure 5.2.14). Further, the identity of **10d** as coumarinolignan was established based on UV spectrum (Figure 5.2.13) and ESI-mass spectrum (Figure 5.2.12). The APCI-MS of **10d** clearly showed peaks due to $[M-1]^+$ at *m/z* 397.15 and $[M+1]^+$ at *m/z* 399.10 [calc. 398.100] (figure 5.2.11) satisfying the revealed molecular formula. Further, the complete structure was elucidated using 300 MHz proton NMR analysis (Figure 5.2.15). The various proton signals along with their splitting pattern and coupling constant values are presented in Table 5.2.3. The positions assignment of signals and structure elucidation were finally arrived by comparing the spectrum with that of **11d** and **11e**.

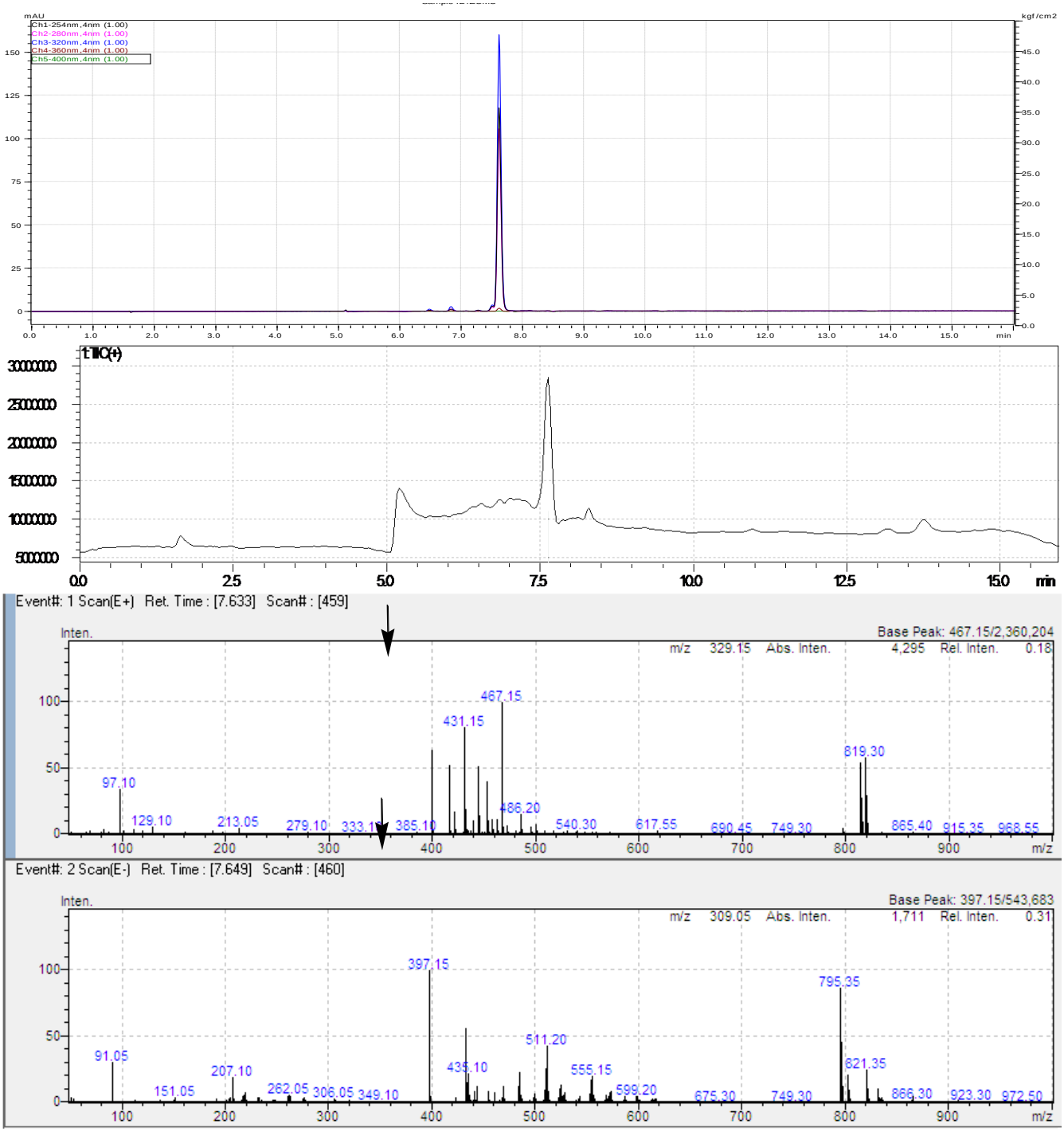

Figure 5.2.12 LCMS PDA chromatogram overlay at 254, 280, 320, 360 and 400 nm, ESI-mass chromatogram and mass spectrum of compound 10d.

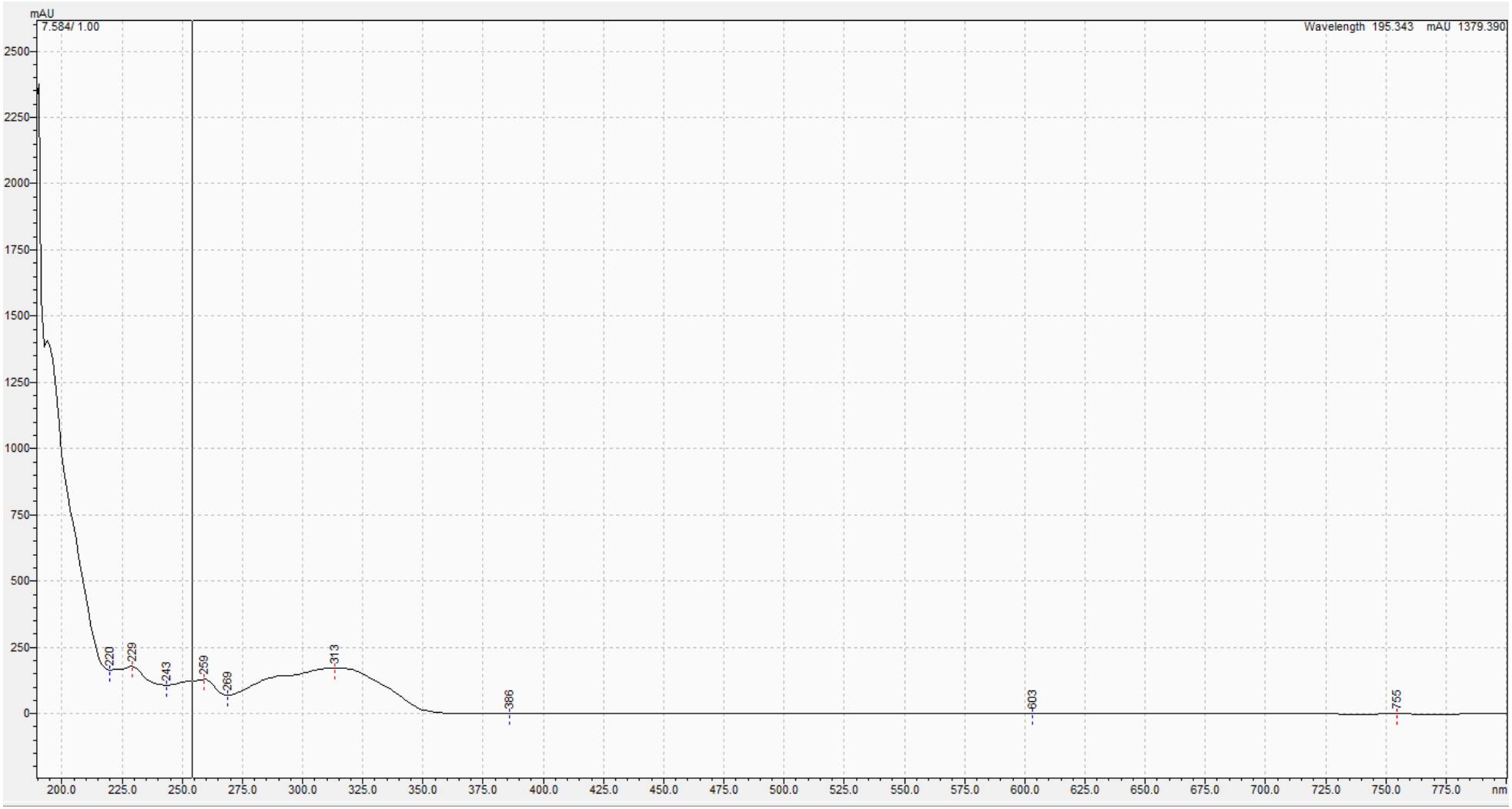

Figure 5.2.13 UV chromatogram of compound 10d

Line#:1 R.Time:1.067(Scan#:65)
MassPeaks:373
RawMode:Averaged 0.700-1.533(43-93) BasePeak:157.05(666191)
BG Mode:Averaged 0.000-0.667(1-41) Segment 1 - Event 1

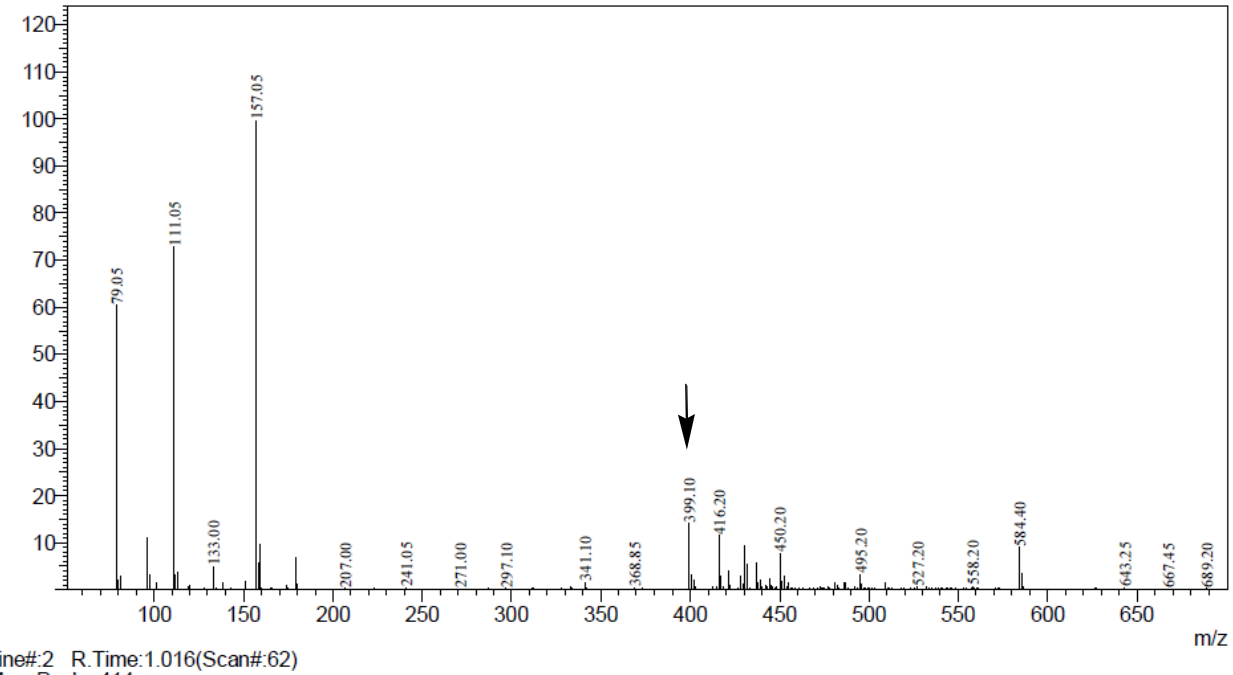

Line#:2 R.Time:1.016(Scan#:62)
MassPeaks:414
RawMode:Averaged 0.716-1.550(44-94) BasePeak:467.20(54739)
BG Mode:Averaged 0.016-0.683(2-42) Segment 1 - Event 2

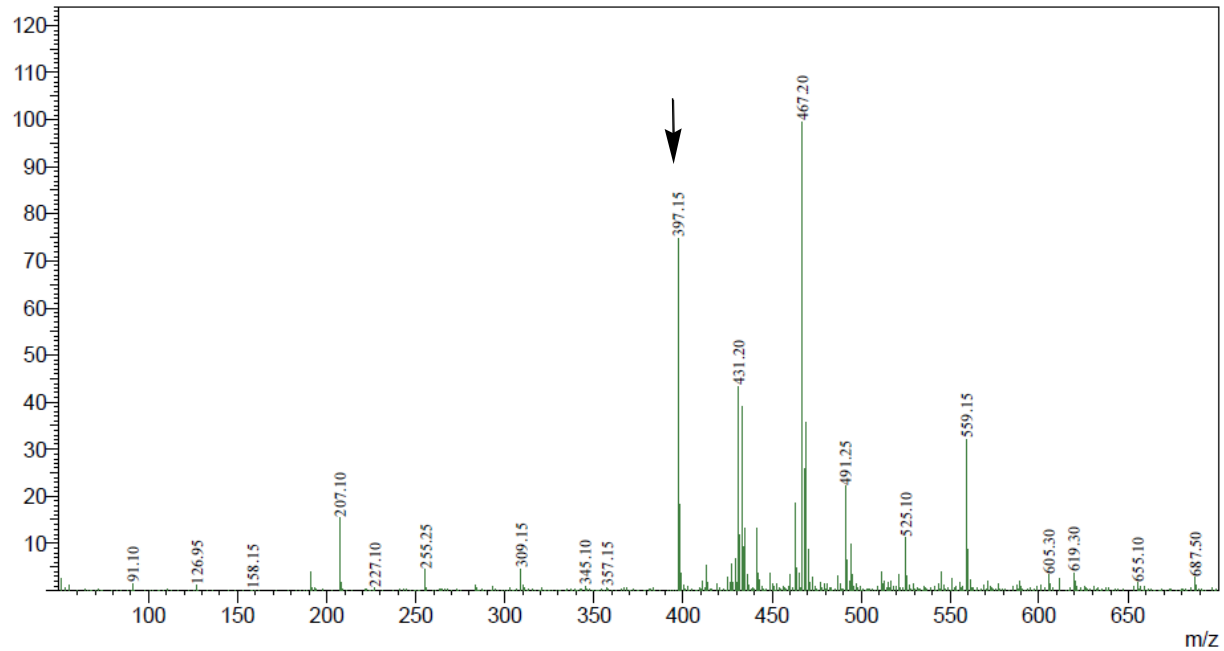

Figure 5.2.14 APCI mass spectrum of compound 10d

Table 5.2.3 ^{1}H spectroscopic data (δ/ppm) of compound 10d measured in a 1:10 mixture of $CDCl_3$ and CD_3OD

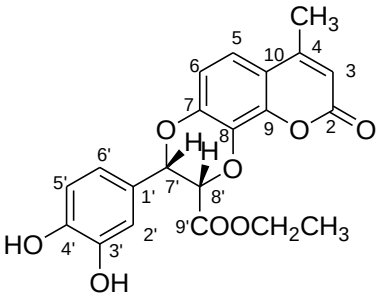

10d

Positions	***δ*** $_{H}$ **in ppm**
2	-
3	6.19 (1H, d, 1.5 Hz)
4	-
5	7.17 (1H, d, 9 Hz)
6	6.92 (1H, d, 8.7 Hz)
7	-
8	-
9	-
10	-
1′	-
2′	6.88-6.78 (m)
3′	-
4′	-
5′	6.88-6.78 (m)
6′	6.88-6.78 (m)
7′	5.20 (1H, d, 5.7 Hz)
8′	4.80 (1H, d, 6.0 Hz)
9′	-
C-9′-O$\underline{CH_2}$ CH_3	4.14 (2H, q)
C-9′-OCH_2 $\underline{CH_3}$	1.13 (3H, t)
C-4-$\underline{\ }CH_3$	2.42 (3H, d, 0.9 Hz)

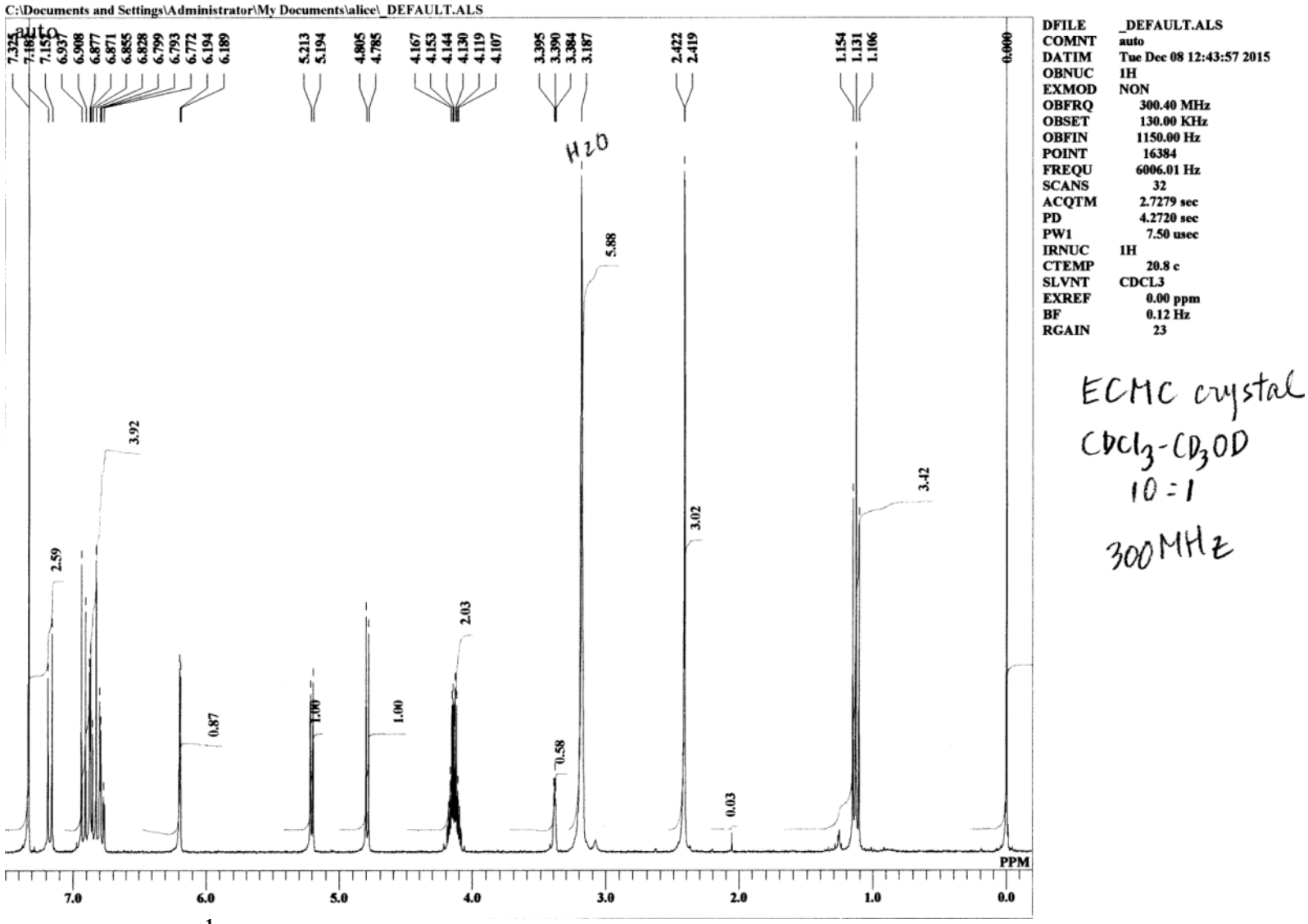

Figure 5.2.15 The 300 MHz ^{1}H NMR spectrum of compound 10d

5.2.7 Characterization of compound 9d

Ethyl 3,9-dihydro-3-(4-hydroxyphenyl)-7-methyl-9-oxo-2H-[1,4]dioxino[2,3-h]chromene-2-carboxylate (**9d**) was obtained as pale brown amorphous solid. The product singularity was assessed by TLC studies using various solvent systems. The product formation was confirmed from the mass spectral analysis. APCI-MS analysis of **9d** showed $[M-1]^+$ at *m/z* 381.2 and $[M+1]^+$ at *m/z* 383.0 [calc. 382.105] (Figure 5.2.16).

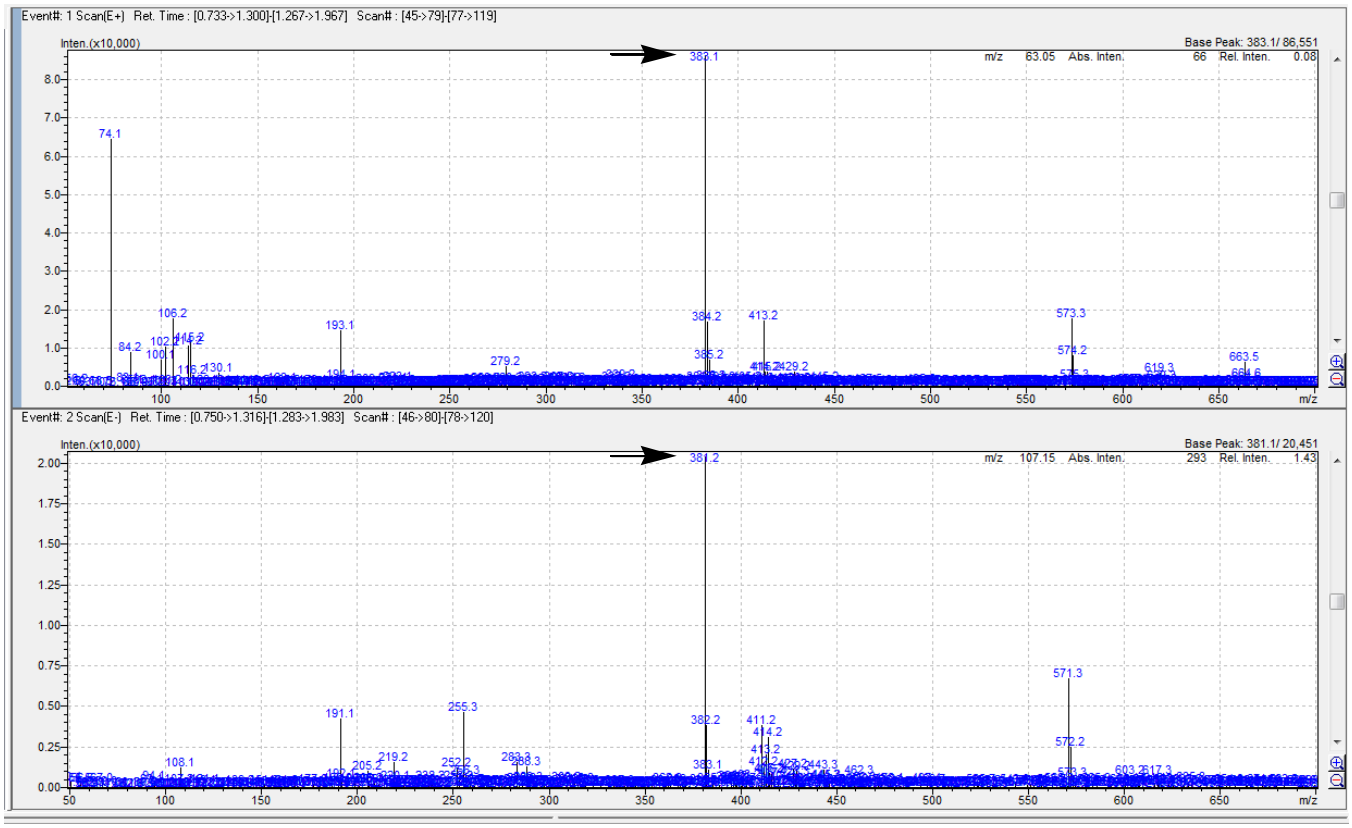

Figure 5.2.16 APCI mass spectrum of compound 9d

5.2.8 Isolation and characterization of cleomiscosin A (15)

The reference compound clemiscosin A (**15**) used under the molecular docking studies was isolated and tested for pro-inflammatory inhibition effect. Also, in order to validate the docking results and compare the inhibition effect of new molecules, these attempts were taken.

Around 5 Kg of powdered *Cleome viscosa* seeds (Family: Capparidaceae) were defatted using petroleum ether and then subjected for hot extraction using methanol. The methanolic extract was concentrated and kept aside for one day. The yellow colored solid precipitate formed was filtered and washed using cold methanol to yield cleomiscosin A (**15**) (Scheme 5.8).

Cleomiscosin A (**15**) was recovered as yellow amorphous solid whose identity was established by co-TLC studies with authentic sample, comparison of ^{1}H NMR data with reported values (Figure 5.2.16) (Begum SA et al., 2010) and through APCI-MS analysis which displayed $[M–H]^{+}$ at m/z 385.15 and $[M+H]^{+}$ at *m/z* 387.10 (Figure 5.2.17). Further, the purity of the isolated cleomiscosin A (15) was ascertained by HPLC analysis with PDA detection (Figure 5.2.18)

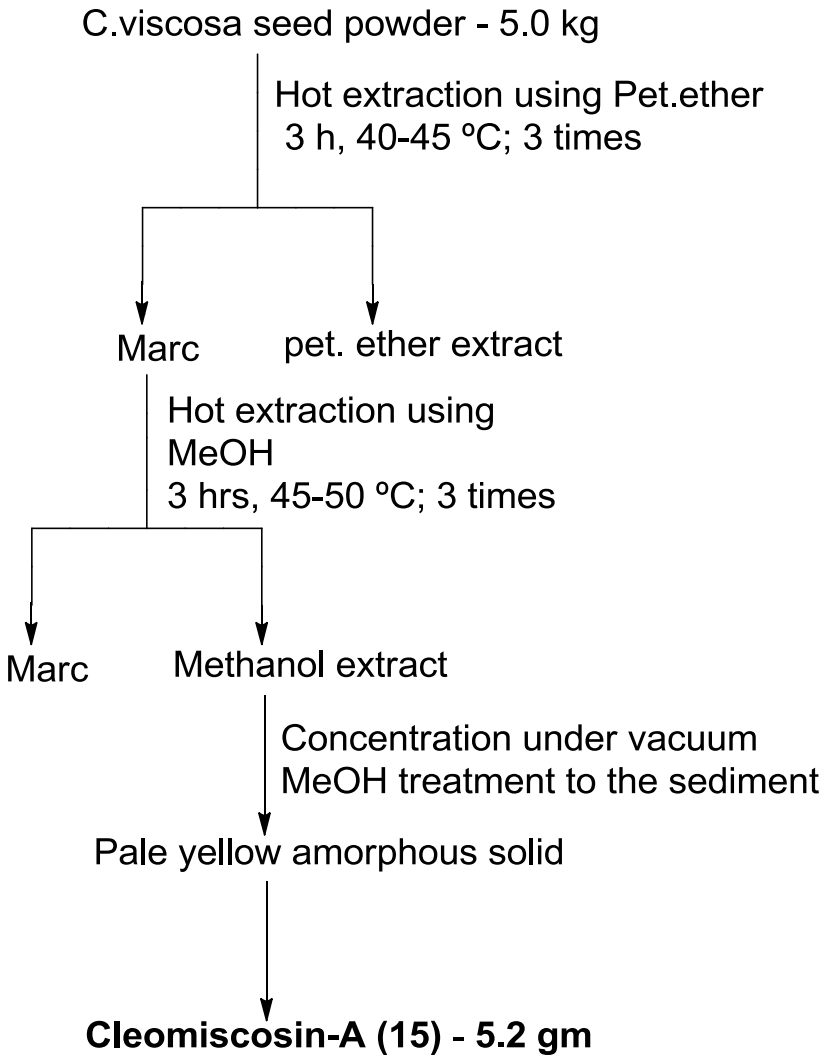

Scheme 5.8 Isolation of cleomiscosin A (15)

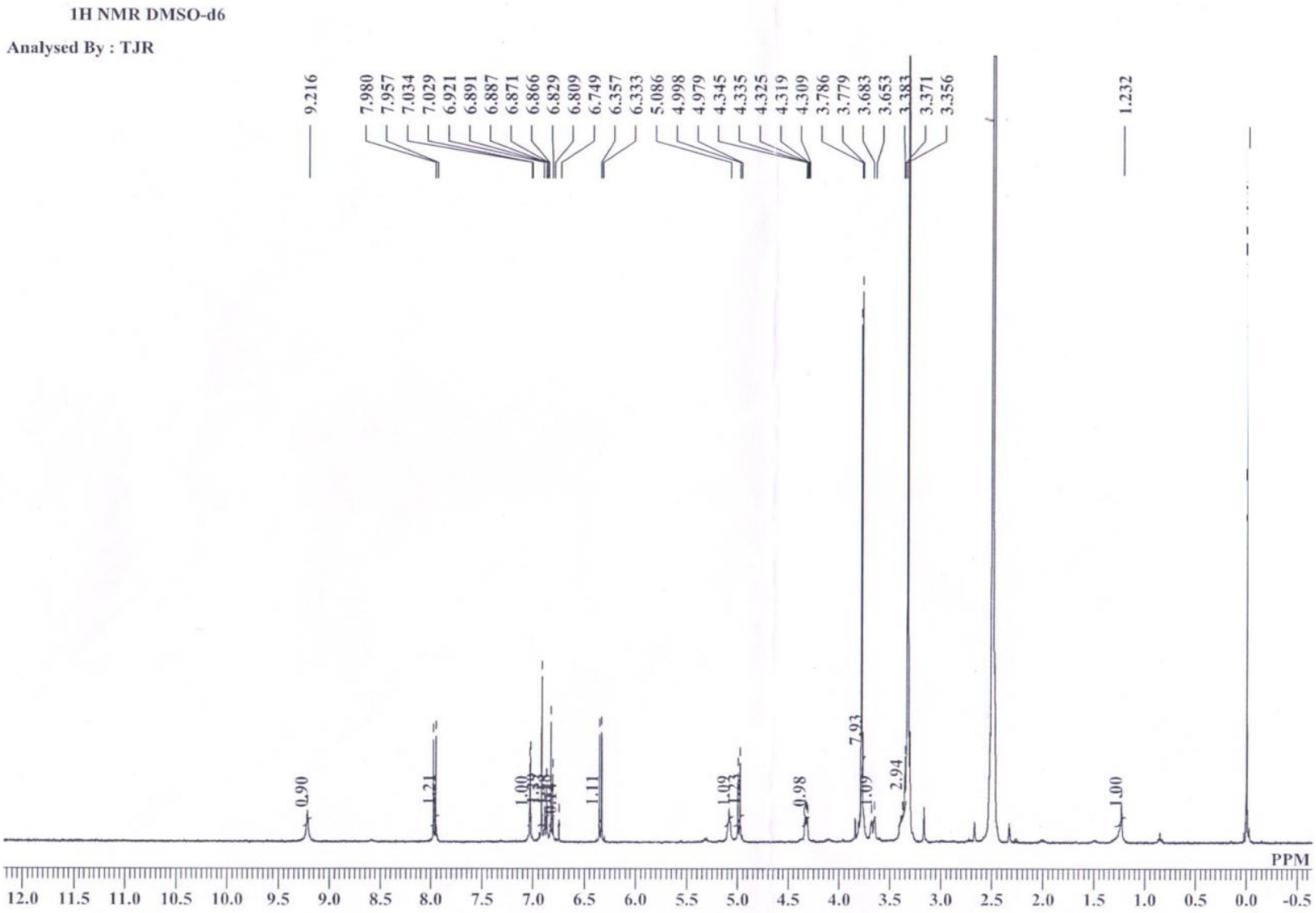

Figure 5.2.17 ^{1}H NMR spectrum of cleomiscosin A (15)

Figure 5.2.18 APCI mass spectrum of cleomiscosin A (15)

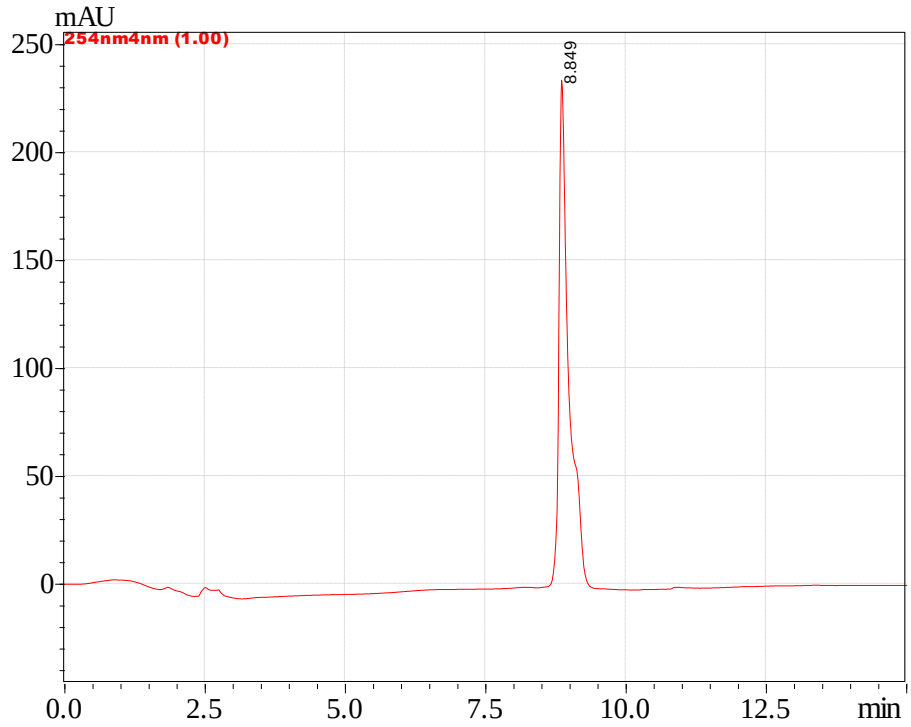

Figure 5.2.19 HPLC chromatogram of cleomiscosin A (15)

5.2.9 In-vitro testing of compounds 9d, 10d, 11d and 11e under LPS-induced and oxalate crystal-induced protein inhibition assay

In-vitro assay using ELISA kits to determine the inhibition effect of test compounds (**9d**, **10d**, **11d**, and **11e**) against pro-inflammatory cytokines was performed. LPS-induced model in mouse macrophage RAW 264.7 cell lines was followed and the results were compared with that of the standard drug prednisolone and natural coumarinolignan, cleomiscosin A (**15**). LPS used in the assay, triggers the secretion of pro-inflammatory cytokines such as TNF-α, IL-1β and IL-6.

5.2.9.1 Effect on the production of TNF-α, IL-6 and IL-1β

RAW 264.7 cell lines were pre-treated with four different concentrations of compounds 100 μM, 30 μM, 10 μM and 3 μM. Then the cells were stimulated with 1 μg/ml LPS. Supernatant was collected after 6 h of stimulation. The TNF-α and IL-6 estimations were done using ELISA kit as per the manufacturer's instruction.

IL-1β estimations were carried out by treating RAW 264.7 cell lines with different concentrations of compounds and stimulating the cells with 1 μg/ml LPS, followed by 100μg/ml oxalate crystals stimulation. Level of IL-1β was then determined in the supernatant using ELISA kit.

Results displayed significant inhibition effect against TNF-α and IL-6 ($P < 0.0001$vs LPS control) (Table 5.2.4 and 5.2.5). The compound **10d**, exhibited IC_{50} values of 8.5 μM, 22.48 μM, 47.57 μM against TNF-α, IL-6 and IL-1β, respectively. Another compound **11e** showed IC_{50} values of 18.37 μM, 13.29 μM and 17.94 μM against TNF-α, IL-6 and IL-1β, respectively. Compound **11d**, exhibited IC_{50} values of 23.63 μM, 18.79 μM and 23.81 μM against TNF-α, IL-6 and IL-1β, respectively. Compound **9d**, exhibited IC_{50} values of 36.31 μM, 16.04 μM and 29.99 μM against TNF-α, IL-6 and IL-1β, respectively. The natural compound cleomiscosin A **(15)** showed IC_{50} values of 39.89 μM, 12.67 μM and 57.7 μM against TNF-α, IL-6 and IL-1β, respectively (Table 5.2.5). The fused cyclic synthetic coumarinolignan compounds were found to be potentially active than the natural coumarinolignan (Table 5.2.5; Figures 5.2.20, 5.2.21 and 5.2.22). The standard drug, prednisolone (**17**) showed 50.32 %, 94.59 % and 69.79% inhibition of TNF-α, IL-6 and IL-1β, respectively.

Table 5.2.4 In-vitro percentage inhibition TNF-α, IL-6 and IL-1β by compounds 9d, 10d, 11d, 11e and cleomiscosin A (15) as determined by ELISA assay

Compounds	Concentration µM	Percentage Inhibition		
		TNF-α	IL-6	IL-1 β
Standard [Prednisolone (17)]	10	50.32	94.59	69.79
9d	100	68.20	73.47	95.81
	30	46.78	50.22	92.26
	10	25.42	29.99	21.69
	3	9.39	2.33	0.06
10d	100	57.57	64.45	101.22
	30	54.27	44.03	47.18
	10	50.66	14.8	20.33
	3	46.56	8.60	2.64
11d	100	56.48	79.82	99.83
	30	49.16	57.62	50.00
	10	47.12	30.73	32.31
	3	43.58	4.33	ND*
11e	100	56.72	79.99	100.49
	30	51.14	61.95	95.81
	10	47.41	46.34	33.77
	3	43.93	9.19	2.64
15	100	64.48	96.49	60.86
	30	48.68	88.56	38.77
	10	23.35	37.82	14.13
	3	6.71	10.58	ND*

ND* Not detectable

Table 5.2.5 IC_{50} values of compounds 9d, 10d, 11d, 11e and cleomiscosin A (15) to inhibit TNF-α, IL-6 and IL-1β as determined by ELISA assay

Compounds	IC_{50} values (µM)		
	TNF-α	IL-1β	IL-6
9d	36.31	29.99	16.04
10d	8.5	47.57	22.48
11d	23.63	23.81	18.79
11e	18.37	17.94	13.29
15	39.89	57.7	12.67

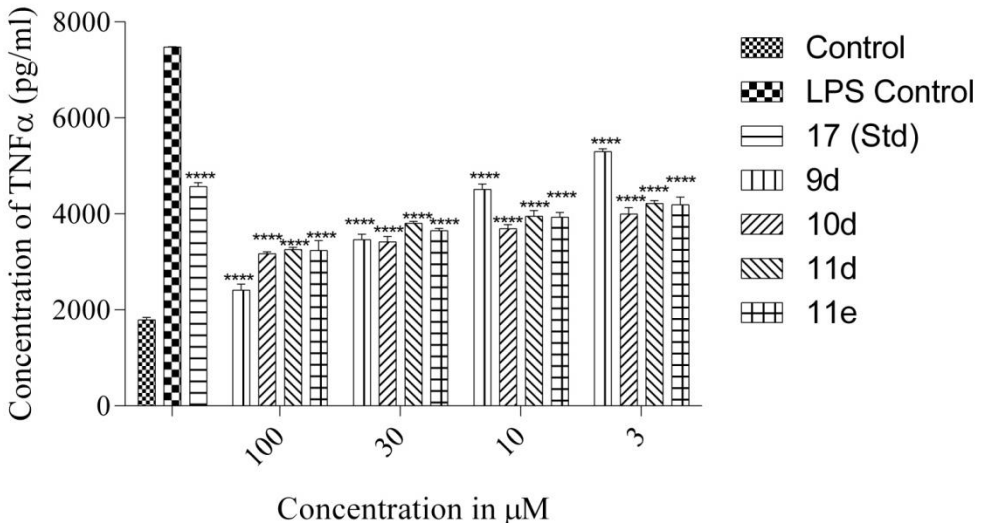

Figure 5.2.20 In-vitro TNF-α inhibitory effect of compounds 9d, 10d, 11d, 11e and cleomiscosin A (15) on LPS-induced RAW 264.7 cells. Cells were pretreated with the indicated concentrations of compound **9d**, **10d**, **11d**, **11e** and standard prednisolone (**17**) (10 μM) for 1 h and then incubated with LPS (1 μg/mL) for 6 h. TNF-α concentration was determined by ELISA kit. The values are presented as mean ± SEM from triplicate. ****$P < 0.0001$ vs LPS control

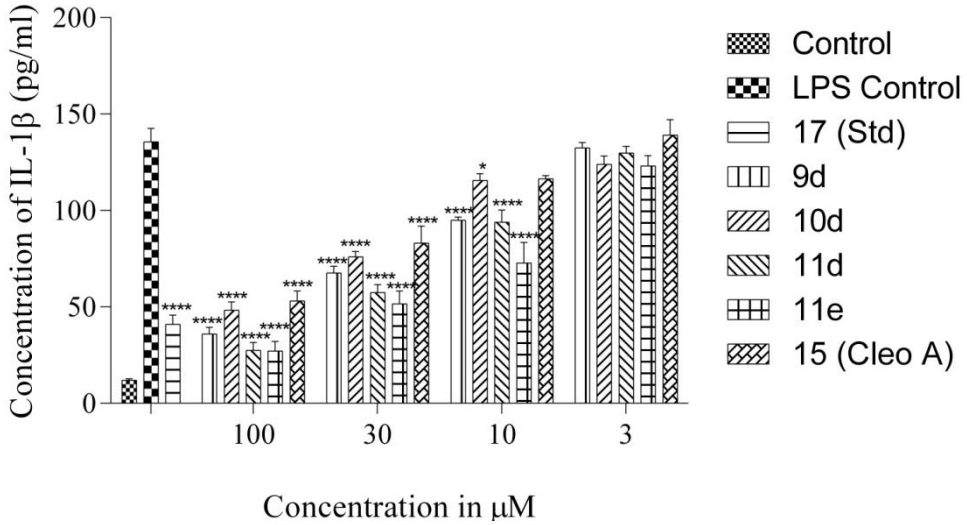

Figure 5.2.21 In-vitro IL-1β inhibitory effect of compounds 9d, 10d, 11d, 11e and cleomiscosin A (15) on LPS-induced RAW 264.7 cells. Cells were pretreated with the indicated concentration of the compounds as well as with the standard prednisolone (**17**) (10μM) 1 h before the incubation with LPS (1 μg/mL) and oxalate crystals (250μg/ml). After 6 h of incubation supernatant was collected and subjected to ELISA assay for IL-1β estimations. The values are presented as mean ± SEM from triplicate. ****$P < 0.0001$ vs LPS control, *$P < 0.05$ vs LPS control.

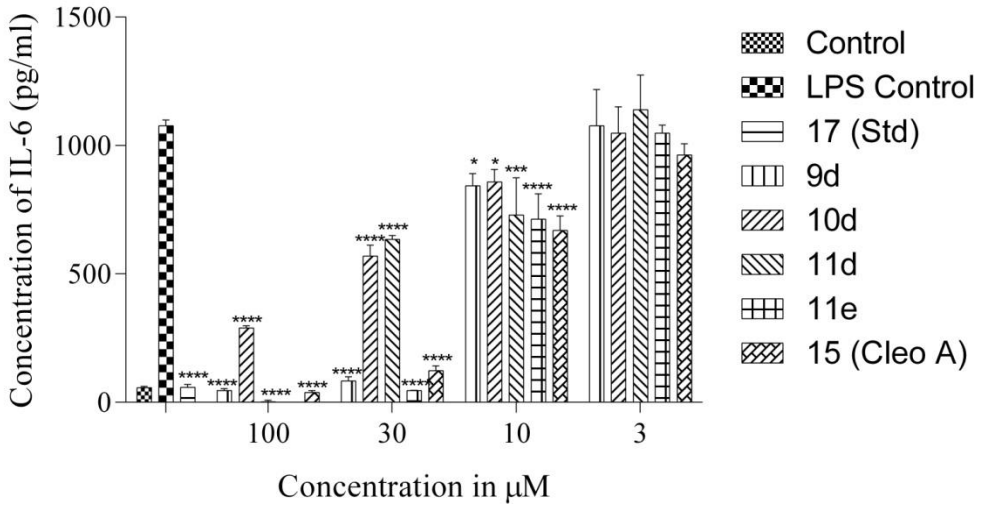

Figure 5.2.22 In-vitro IL-6 inhibitory effect of compounds 9d, 10d, 11d, 11e and cleomiscosin A (15) on LPS-induced RAW 264.7 cells. Cells were treated with the indicated concentrations of compounds and standard prednisolone (**17**) (10μM) for 1 h and then incubated with LPS (1 μg/mL) for 6 h. Supernatant collected after incubation was used for estimating IL-6 levels using ELISA. The values are presented as mean ± SEM from triplicate. ****$P < 0.0001$ vs LPS control, *$P < 0.05$ vs LPS control

5.2.9.2 Effect on Nitric oxide (NO) production

Compounds **9d**, **10d**, **11d**, **11e** and **15** were tested for their ability to inhibit NO production. For this RAW 264.7 cells were cultured in a 96 well plate and treatment with compound was given for 6 hours followed by induction with LPS for 24 h. The cell supernatant was collected, mixed with Griess reagent and kept for incubation at room temperature for 10 minutes. Absorbance was measured at 540 nm in a multiplate reader.

All the tested compounds were found to be significantly active (****$P < 0.0001$ vs LPS control, ** $P < 0.01$vs LPS control at 100μM concentration). Compounds **10d**, **9d**, **11e and 11d** demonstrated 64.9%, 56.33%, 48.54% and 33.6% inhibition of NO secretion at 100 μM concentrations. Cleomiscosin A (**15**) exhibited 56.53% inhibition on LPS-induced NO production (Figure 5.2.23).

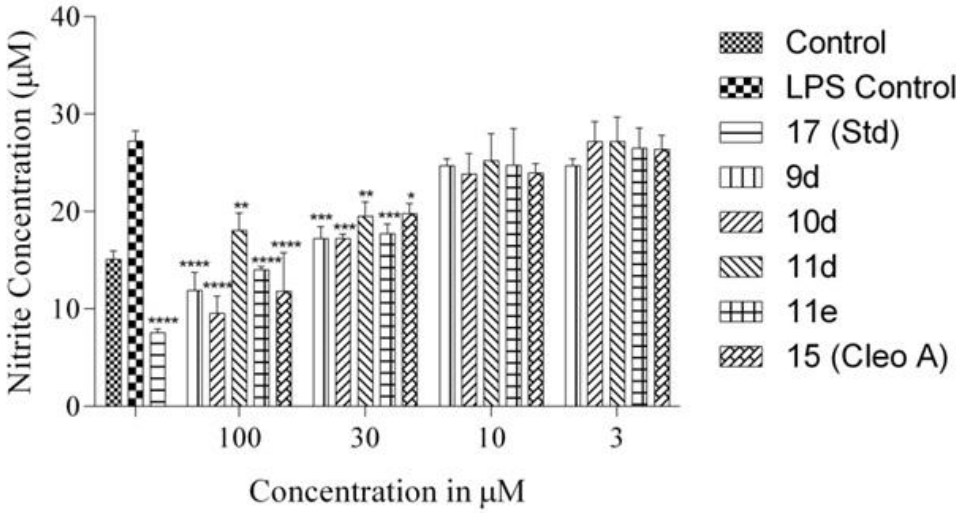

Figure 5.2.23 In-vitro NO production of compounds 9d, 10d, 11d, 11e and cleomiscosin A (15) on LPS-induced RAW 264.7 cells. Cells were treated with the indicated concentration of compounds and standard prednisolone (**17**) (10 μM) for 1 h and then incubated with LPS (1 μg/mL) for 16 h. Supernatant collected was used for NO estimations using Griess method. The values are presented as mean ± SEM from triplicate. ****P < 0.0001vs LPS control, *** P < 0.001 vs LPS control, ** P < 0.01 vs LPS control, * P < 0.05 vs LPS control.

5.2.9.3 Cytotoxicity

MTT assay was also carried out to determine the cytotoxicity of the compounds on RAW 264.7 cell lines. All the tested compounds (**9d**, **10d**, **11d, 11e** and **15**) were found to be non-toxic showing IC_{50}>150 μM against the macrophages (264.7 cells). The cell viability observed during the assay has been presented in Figure 5.2.24

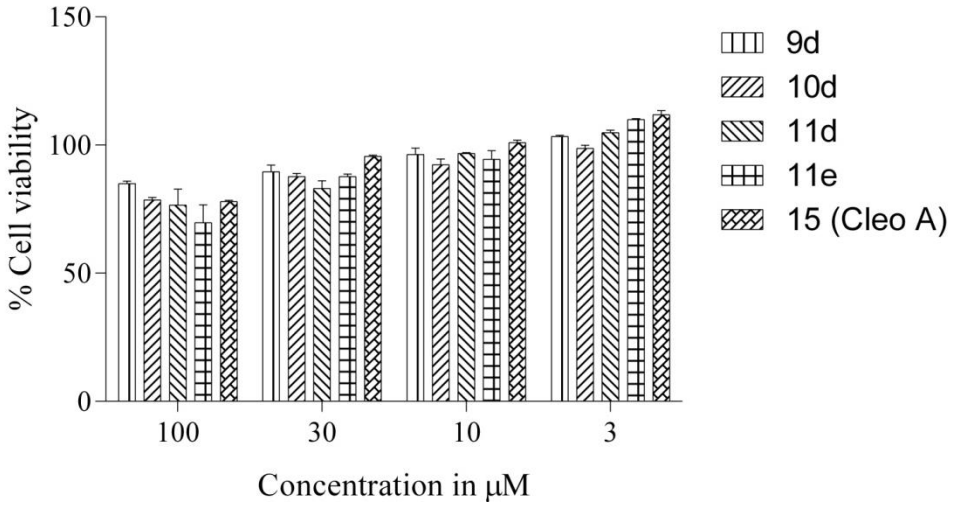

Figure 5.2.24 Effect of compounds 9d, 10d, 11d, 11e and 15 on % cell viability at 24 h. Figure shows the effect of treatment of cells with the indicated concentration of compounds for 24 h. The viability assay was carried out using MTT reagent. The values are presented as mean ± SEM from triplicate.

5.2.10 Anti-inflammatory effect of the synthesized compounds using mouse endotoxemia model

Results of in-vitro assays indicated the potentiality of the coumarin-based lignan compounds to control the LPS-induced expression of cytokines TNF-α, IL-6 and IL-1β. In order to evaluate the anti-inflammatory efficacy of the synthesized compounds **9d**, **10d**, **11d** and **11e** under in-vivo system, various inflammatory animal models were used. The study protocols were prepared as per standard guidelines and were approved by Institutional Animal Ethical Committee [IAEC approval number: BITS-Hyd/IAEC/2017/09 and BITS-Hyd/IAEC/2017/23].

All the synthesized compounds along with the natural compound cleomiscosin A (**15**) and standard drug, prednisolone (**17**) were tested using mouse endotoxemia model. Animals were classified into eight different groups, which included Group 1 - normal control; Group 2 - LPS

control; Group 3 - Standard (Prednisolone) control; Group 4 - Compound **9d** treated; Group 5 - Compound **10d** treated; Group 6 - Compound **11d** treated; Group 7 - Compound **11e** treated; Group 8 - Compound **15** treated.

Briefly, in endotoxemia model, animals (n=6) were pretreated with the compounds with a random single dose of 50 mg/kg body weight. Compounds were prepared as suspension in a vehicle consisting of 0.5% methylcellulose and 0.025% Tween 20 and administered through oral route using a gavage at a dose volume of 10 mL/kg. After one hour of drug treatment LPS was injected by intraperitoneal route at a dose of 0.3 mL/kg (Dose volume 1 mL/kg in sterile saline). Blood was withdrawn through retro orbital route at different time points (1 hour and 6 hours after LPS administration). ELISA studies were carried out to estimate the levels of cytokines TNF-α, IL-1β and IL-6 on isolated plasma using commercial kits and the results are presented in Table 5.2.6 and 5.2.7 The results are expressed as mean ± SEM between control and treated animals using one way analysis of variance (ANOVA), followed by multiple comparison of the mean of each column with the mean of LPS control column using graph pad prism software.

All the tested compounds were found to be significantly reducing the expression of pro-inflammatory cytokines at a dose of 50 mg/kg (****P<0.0001 vs LPS control, ***P<0.001vs LPS control, **P<0.01vs LPS control). The compound **10d** was very effective in controlling the expression of IL-1β showing 67.95 and 66.41% inhibition in lavage and plasma, respectively as shown in Figure 5.2.25 and Table 5.2.6. Compound **10d** exhibited 62.56 % inhibition of TNF-α production figure (Figure 5.2.25 and Table 5.2.6) and 43.15 % of IL-6 in plasma (Table 5.2.6). Compound **11e** displayed 62.76% inhibition of IL-1β as shown in figure (Figure 5.2.26), 55.29 % of IL-6 as shown in figure (Figure 5.2.27 and Table 5.2.6) and 41.31% of TNF-α as presented in figure (Figure 5.2.25 and Table 5.2.6). Other compounds which were revealed active under in-

vitro assay were also found to be effective under this model. Compounds **9d** and **11d**, respectively exhibited 57.54% and 51.48% inhibition of IL-1β as displayed in figure (Figure 5.2.26 and Table 5.2.6), 51.62% and 33.75% of TNF-α as shown in figure (Figure 5.2.25 and Table 5.2.6) and 27.88% and 46.23% of IL-6 as presented in figure (Figure 5.2.27 and Table 5.2.6). Interestingly, all the synthesized compounds of fused-cyclic coumarin-based lignans exhibited more than 50% inhibition of secretion of IL-1β in both plasma and lavage. The tested synthetic compounds significantly reduced expression of IL-1β in peritoneal lavage also. There was 63.57% reduction of LPS-induced IL-1β in peritoneal lavage by compound **9d**, 67.95% reduction by **10d**, 50.80% reduction by compound **11d** and 57.31% reduction by compound **11e** (Table 5.2.6).

Table 5.2.6 In-vivo TNF-α, IL-1β and IL-6 percentage inhibition of compounds 9d, 10d, 11d, 11e and 15 under mouse endotoxemia model

Compounds	Percentage Inhibition			
	TNF-α	IL-1β		IL-6
		Plasma	Lavage	
17	89.53	62.22	68.56	65.53
9d	51.62	57.54	63.57	27.88
10d	62.56	66.41	67.95	43.15
11d	33.75	51.48	50.80	46.23
11e	41.31	62.76	57.31	55.29
15	15.70	41.08	55.40	28.35

Interestingly all the synthesized molecules were more active than the natural compound **15**, which demonstrated 41.08 %, 28.35 % and 15.7 % inhibition of IL-1β, IL-6 and TNF-α, respectively in plasma (Table 5.2.6). Similar to the synthetic molecules, natural cleomiscosin A was more effective against IL-1β. As IL-1β plays a major role in various inflammations especially in renal injury, these compounds might effectively control renal nephropathy.

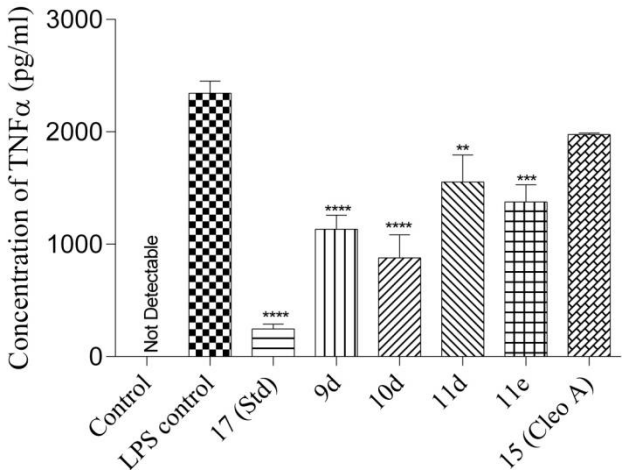

Figure 5.2.25 TNF-α inhibitory effect of compounds 9d, 10d, 11d, 11e and 15 in LPS-induced mouse endotoxemia model. Figure shows the inhibitory effect of compounds 9d, 10d, 11d, 11e and 15 at 50mg/kg dose on TNF-α secretions induced by LPS in mice (The values are presented as mean ±SEM (n=6). ****P<0.0001 vs LPS control, ***P<0.001vs LPS control, **P<0.01 vs LPS control)

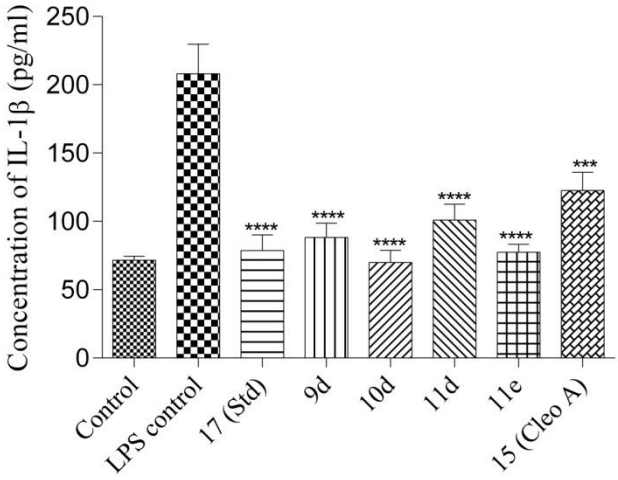

Figure 5.2.26 IL-1β inhibitory effect of compounds 9d, 10d, 11d, 11e and 15 on LPS-induced mouse endotoxemia model. Figure shows the inhibitory effect of compounds 9d, 10d, 11d, 11e and 15 at 50mg/kg dose on IL-1β secretions induced by LPS in mice (The values are presented as mean ±SEM (n=6). ****P<0.0001 vs LPS control, ***P<0.001 vs LPS control)

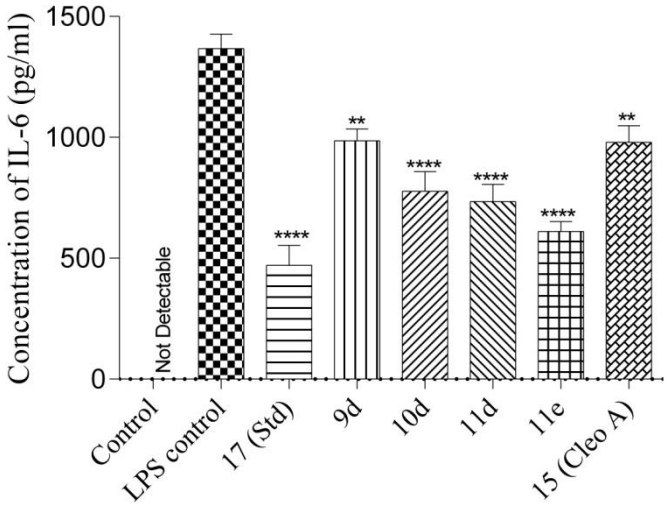

Figure 5.2.27 IL-6 inhibitory effect of compounds 9d, 10d, 11d, 11e and 15 on LPS-induced mouse endotoxemia model. Figure shows inhibitory effect of compounds 9d, 10d, 11d, 11e and 15 at 50mg/kg dose on IL-6 secretions induced by LPS in mice (The values are presented as mean ±SEM (n=6). ****P<0.0001 vs LPS control, **P<0.01 vs LPS control)

5.2.10.1 Dose dependent study on compound 10d

Further, the compound **10d**, which was found to exhibit highly significant activity against all the tested cytokines was subjected for a dose dependent study following same protocol. Animals were classified into six different groups, which included Group 1 - Normal control, Group 2 - LPS control, Group 3 - Standard (Prednisolone) control; Group 4 - Compound **10d**-50mg/kg treated; Group 5 - Compound **10d**-30mg/kg treated; Group 6 - Compound **10d**-10mg/kg treated.

It demonstrated inhibitory activity at 10 mg/kg (33.94% - IL-1β, 19.2% - TNF-α) and 30 mg/kg (48.38% - IL-1β, 33.36% - TNF-α, 19.01%-IL- 6) body weight as well (Figure 5.2.28-5.2.30 and Table 5.2.7). However, the inhibition effect was found to be lesser than the clinically used drug prednisolone.

Table 5.2.7 Dose dependent effect on percentage inhibition of compound 10d against TNF-α, IL-1β and IL-6 under mouse endotoxemia model

Dose of compound 10d	Percentage Inhibition			
	TNF-α	IL-1β		IL-6
		Plasma	Lavage	
10 mg/kg	19.20	24.42	33.94	0.28
30 mg/kg	33.36	41.00	48.38	19.01
50 mg/kg	59.70	65.11	71.05	47.02

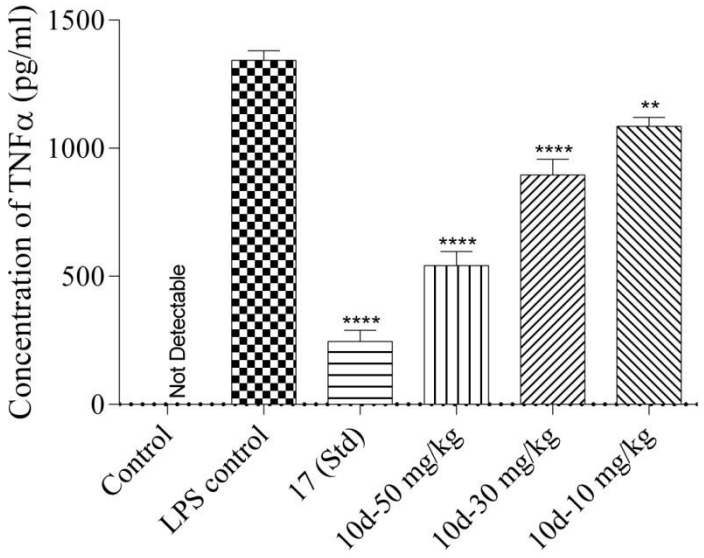

Figure 5.2.28 Dose dependent TNF-α inhibition effect of compound 10d on LPS-induced mouse endotoxemia model. Figure shows inhibition effect of compound 10d at indicated doses on TNF-α secretions under LPS-induction (The values are presented as mean ±SEM (n=6). ****P<0.0001vs LPS control, **P<0.01 vs LPS control)

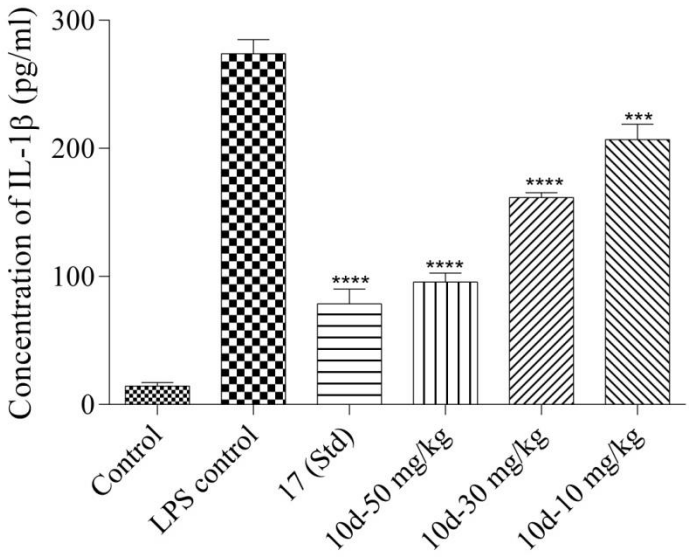

Figure 5.2.29 Dose dependent IL-1β inhibition effect of compound 10d on LPS-induced mouse endotoxemia model. Inhibition effect of compound 10d at indicated doses on IL-1β secretions under LPS-induced endotoxemia model (The values are presented as mean ±SEM (n=6). ****P<0.000 1vs LPS control, ***P<0.001 vs LPS control)

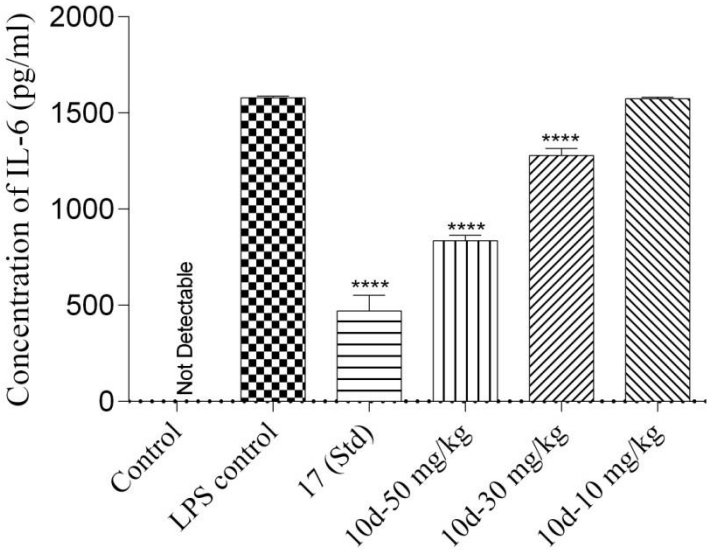

Figure 5.2.30 Dose dependent IL-6 inhibition effect of compound 10d on LPS-induced mouse endotoxemia model. Figure shows dose dependent inhibition effect of compound 10d at indicated doses on IL-6 secretions under LPS-induced endotoxemia model (The values are presented as mean ±SEM (n=6) ****P<0.0001 vs LPS control).

5.2.11 Anti-inflammatory activity of the synthesized compounds by carrageenan-induced mouse paw edema model

In this model 25 μL of carrageenan (1% w/v solution in 0.9% sterile saline) was injected in the paw of the BALB/c mouse to test the efficacy of the newly synthesized compounds in local inflammation. Animals were classified into eight different groups, which include Group 1 - Normal control; Group 2 - Carrageenan control, Group 3 - Standard (Prednisolone) control; Group 4 - Compound **9d** treated; Group 5 - Compound **10d** treated; Group 6 - Compound **11d** treated; Group 7 - Compound **11e** treated; Group 8 - Compound **15** treated.

Test compounds (**9d**, **10d**, **11d**, **11e** and **15** at dose 50 mg/kg) were administered 1 h prior to carrageenan injection using oral gavage. Then carrageenan was injected in plantar region of left hind paw subcutaneously. Paw volume was measured on hourly basis using plethysmometer till 4 h of carrageenan administration. Animals were sacrificed after fourth paw volume reading. Paws were collected, and snap frozen for cytokine estimations using ELISA kits.

5.2.11.1 Inhibition effect of compounds on expression of pro-inflammatory cytokines

All the tested compounds at 50 mg/kg weight were found to be effectively reducing the expression of pro-inflammatory cytokines in inflamed-paw homogenates. Compound **11e** displayed 54.90 % of TNF-α as shown in Figure 5.2.31 and 48.46% inhibition of IL-1β as given in Figure 5.2.32. The compound **10d**, showed 50.03% inhibition of TNF-α as shown in Figure 5.2.31 and 36.58% inhibition of IL-1β in inflamed-paw homogenate as presented in Figure 5.2.32. Other compounds revealed under in-vitro assay were also found to be effective under this model. Compounds **9d** and **11d**, respectively exhibited remarkable inhibition of 88.63% and 45.18% of TNF-α as shown in Figure 5.2.31, and 43.42% and 43.84% inhibition of IL-1β in inflamed-paw homogenate as presented in Figure 5.2.32.

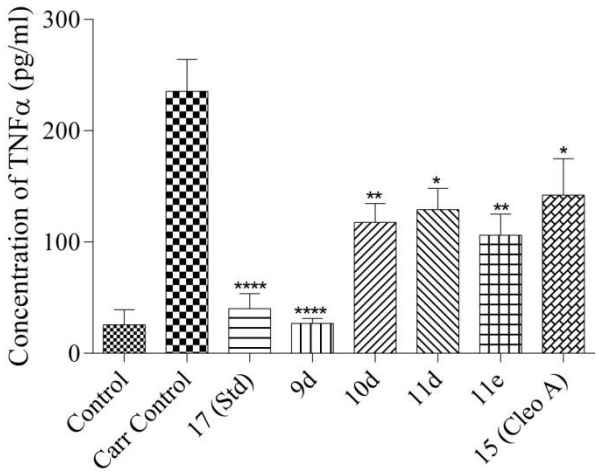

Figure 5.2.31 TNF-α inhibitory effect of compounds 9d, 10d, 11d and 11e and cleomiscosin A (15) on carrageenan-induced mouse paw edema model. Figure shows inhibition effect of compounds at 50mg/kg dose on TNF-α secretions under carrageenan induction (The values are presented as mean ±SEM (n=6). ****P<0.0001 vs carrageenan control, **P < 0.01 vs carrageenan control, *P < 0.05 vs carrageenan control)

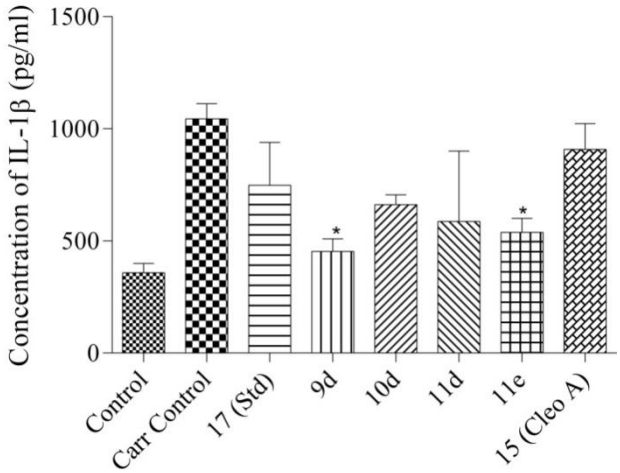

Figure 5.2.32 IL-1β inhibitory effect of compounds 9d, 10d, 11d and 11e and cleomiscosin A (15) on carrageenan-induced mouse paw edema model. Figure shows inhibition effect of compounds at 50mg/kg dose on IL-1β secretions under carrageenan induction model. (The values are presented as mean ±SEM (n=6). *P < 0.05vs carrageenan control)

5.2.11.2 Acute anti-inflammatory effect on mouse paw edema

The compounds (50 mg/kg) were also found to be effectively reducing the paw volume during different time points when measured using digital plethysmometer. Compound **10d** controlled the induced edema for the early 2 hours effectively. In the other case, animals injected with compound **11e**, were found to be effective after one hour of induction and the effect was sustaining for another two hours as shown in the Figure 5.2.33. All the newly synthesized compounds were found to be acting better than the natural coumarinolignan, **15**, which exhibited no effect on reducing the paw volume.

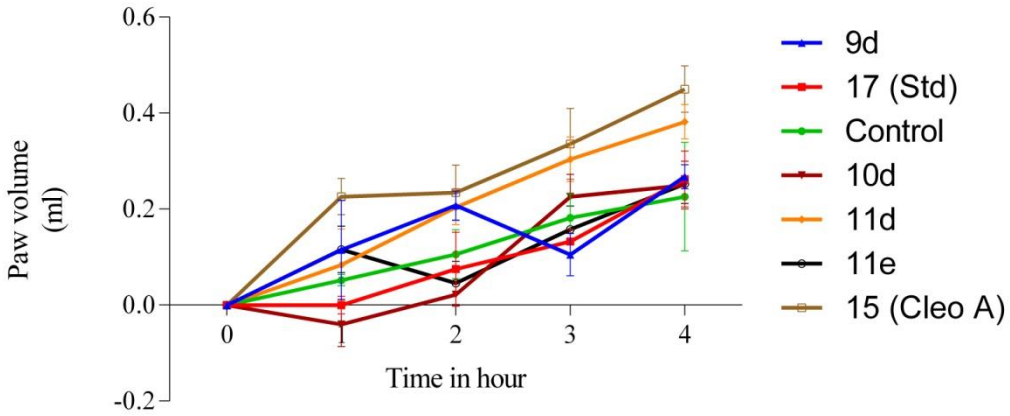

Figure 5.2.33 Paw volume difference study of compounds 9d, 10d, 11d and 11e and cleomiscosin A (15) on carrageenan-induced mouse paw edema model. Figure demonstrates the effect of compounds at 50mg/kg dose on paw volume under carrageenan induction (The values are presented as mean ±SEM (n=6))

5.2.12 Anti-inflammatory activity of compound 10d in a mouse model of oxalate nephropathy

Testing of anti-inflammatory efficacy of the synthesized compounds using mouse model of oxalate nephropathy was planned as they were potentially inhibiting secretions of IL-β compared to other cytokines TNF-α and IL-6 under endotoxemia model and LPS + crystal-induced in-vitro assays. Compound **10d** was selected as representative molecule to test the effect on renal inflammation. Study was carried out in three different groups, which included Group 1 - Normal control; Group 2 - Oxalate control; Group 3 - Compound **10d** treated.

Briefly, in oxalate nephropathy model, C57/BL6 mice (Male, 6-8wks old) were fasted overnight. The mice were administered with compound **10d** at dose of 50 mg/kg after 12 h fasting. The compound was prepared as suspension in a vehicle consisting of 0.5% methylcellulose and 0.025% Tween 20 and administered through oral route using a gavage at dose volume of 10 ml/kg. After one hour of drug treatment, sodium oxalate solution was injected at a dose of 100mg/kg body weight by intra-peritoneal route. Immediately after the injection of sodium oxalate the mice were fed with normal diet and water premixed with 3% w/v of sodium oxalate. After 24 h of injection of sodium oxalate the mice were sacrificed to harvest the blood samples and kidney tissue samples. The renal damage caused by the oxalate nephropathy was evaluated by determining the BUN (Blood-Urea-Nitrogen) levels in plasma (renal function parameter), expression of KIM-1 (kidney injury molecule-1, a renal injury marker) and expression of IL-1β, IL-6 and TNF-α (inflammatory markers) in the renal tissue and histological analysis of renal tissue by H&E staining. ELISA studies were carried out on isolated plasma to estimate the levels of IL-1β using commercial kits.

5.2.12.1 Estimation of blood urea nitrate

Compound **10d** significantly reduced the elevated levels of blood urea nitrate (BUN) at a dose of 50 mg/kg as shown in Figure 5.2.34 (****P<0.0001vs oxalate control), indicating the protection of renal function against the damage induced by oxalate nephropathy. The compound **10d** showed 49.95 % inhibition of elevated plasma BUN compared to oxalate nephropathy control group as shown in Figure 5.2.34, 37.5 % inhibition of plasma IL-1β as shown in Figure 5.2.35.

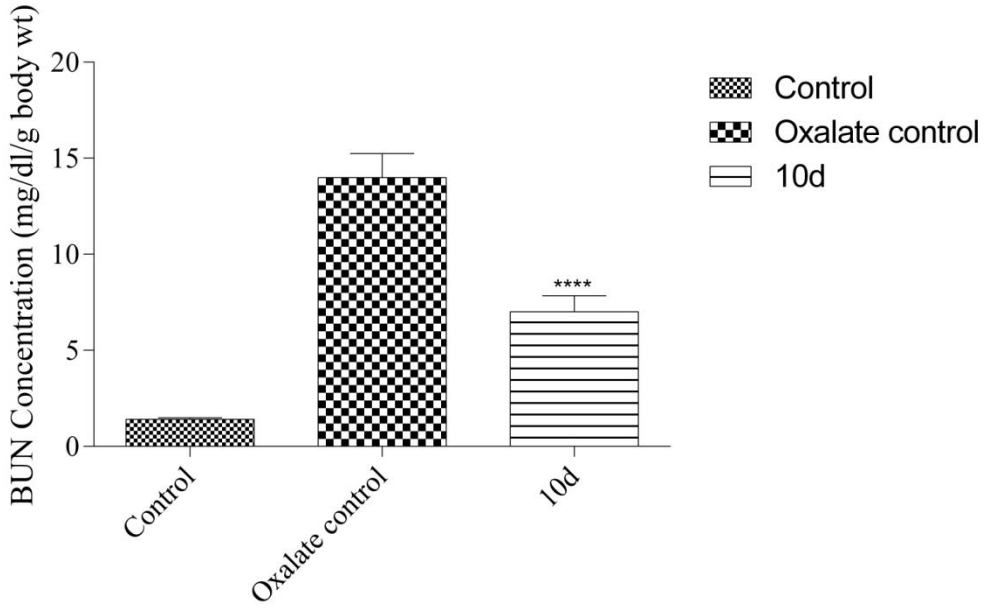

Figure 5.2.34 Plasma BUN inhibition effect of compound 10d on oxalate crystal induced renal nephropathy model. Figure demonstrates the inhibition effect of compound 10d at the dose of 50 mg/kg on plasma BUN levels induced by oxalate crystals. (The values are presented as mean ±SEM (n=6). ****P < 0.0001 vs oxalate control)

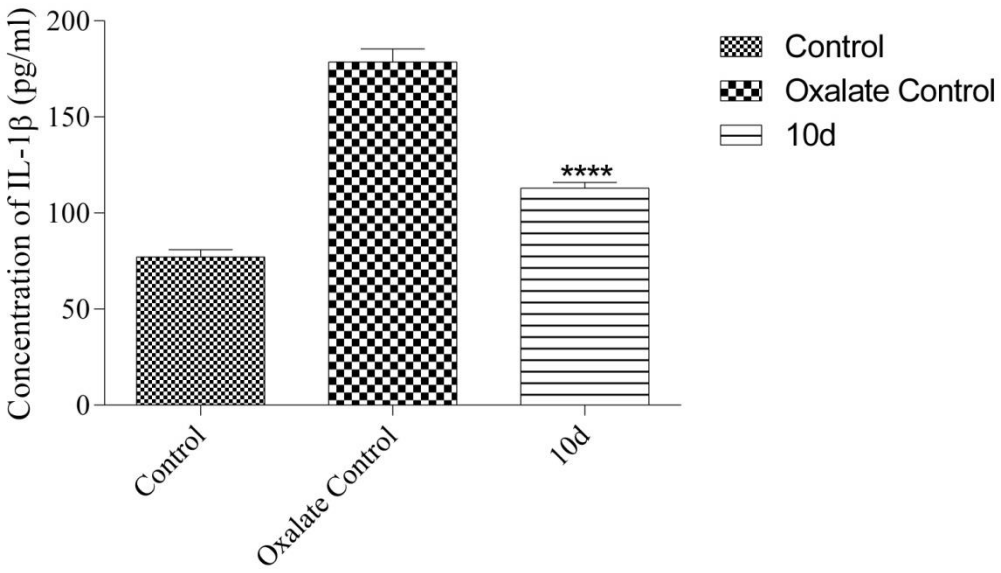

Figure 5.2.35 Inhibition of plasma IL-1β levels by compound 10d on oxalate crystal induced renal nephropathy model. Figure demonstrates the inhibitory effect of compound 10d at the dose of 50 mg/kg on plasma IL-1β levels induced by oxalate crystals (The values are presented as mean ±SEM (n=6). ****$P < 0.0001$vs oxalate control).

5.2.12.2 RT-PCR analysis of pro-inflammatory and renal injury markers

Further, compound **10d** attenuated renal injury as displayed by the reduction in the renal RNA expression of IL-1β, IL-6, TNF-α (pro-inflammatory markers) and KIM-1 (renal injury markers) as shown in Figure 5.2.36.

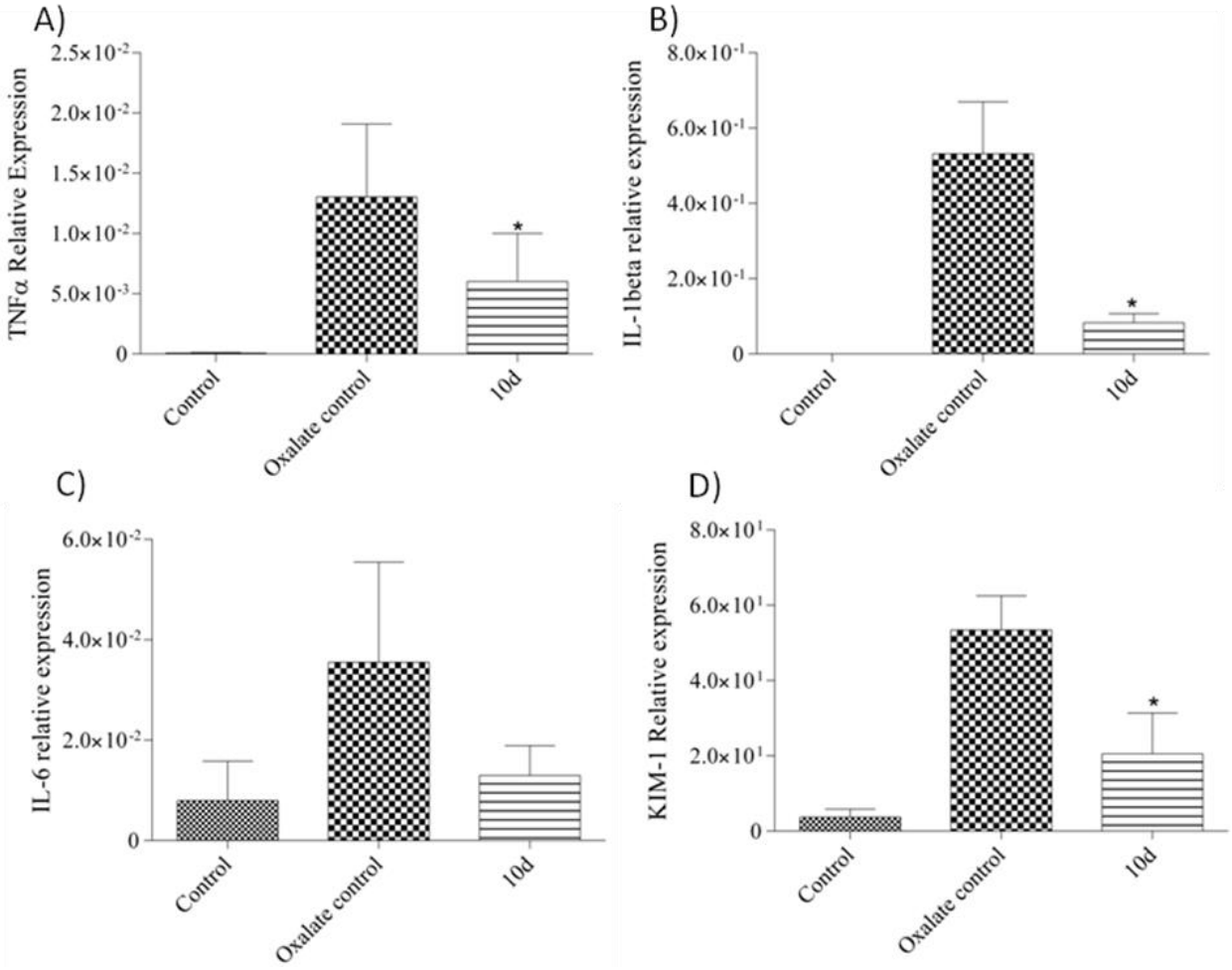

Figure 5.2.36 Inhibition effect of compound 10d on renal RNA expression of TNF-α, IL-1β, IL-6 (pro-inflammatory markers) and KIM-1 (renal injury markers) under oxalate crystal induced renal nephropathy model using RTPCR. Figure demonstrates the inhibitory effect of compound 10d at the dose of 50 mg/kg on renal RNA expression of TNF-α, IL-1β, IL-6 (pro-inflammatory markers) and KIM-1 (renal injury markers) induced by oxalate crystals in renal nephropathy model done using real time RTPCR. (The values are presented as mean ±SEM (n=6). *$P < 0.05$ vs oxalate control).

5.2.12.3 Histological analysis

Histological analysis of kidney tissue was performed by H&E staining. Compound **10d** exhibited protection of renal tissue as determined by keen observation of the slides. Tubular injury index was quantified using semiquantitative scoring method. Scores were given based on tubular dilation (thick arrows), tubular necrosis (thin arrows) and cast (star).The treatment with this compound significantly reduced tubular injury index as shown in the Figure 5.2.37.

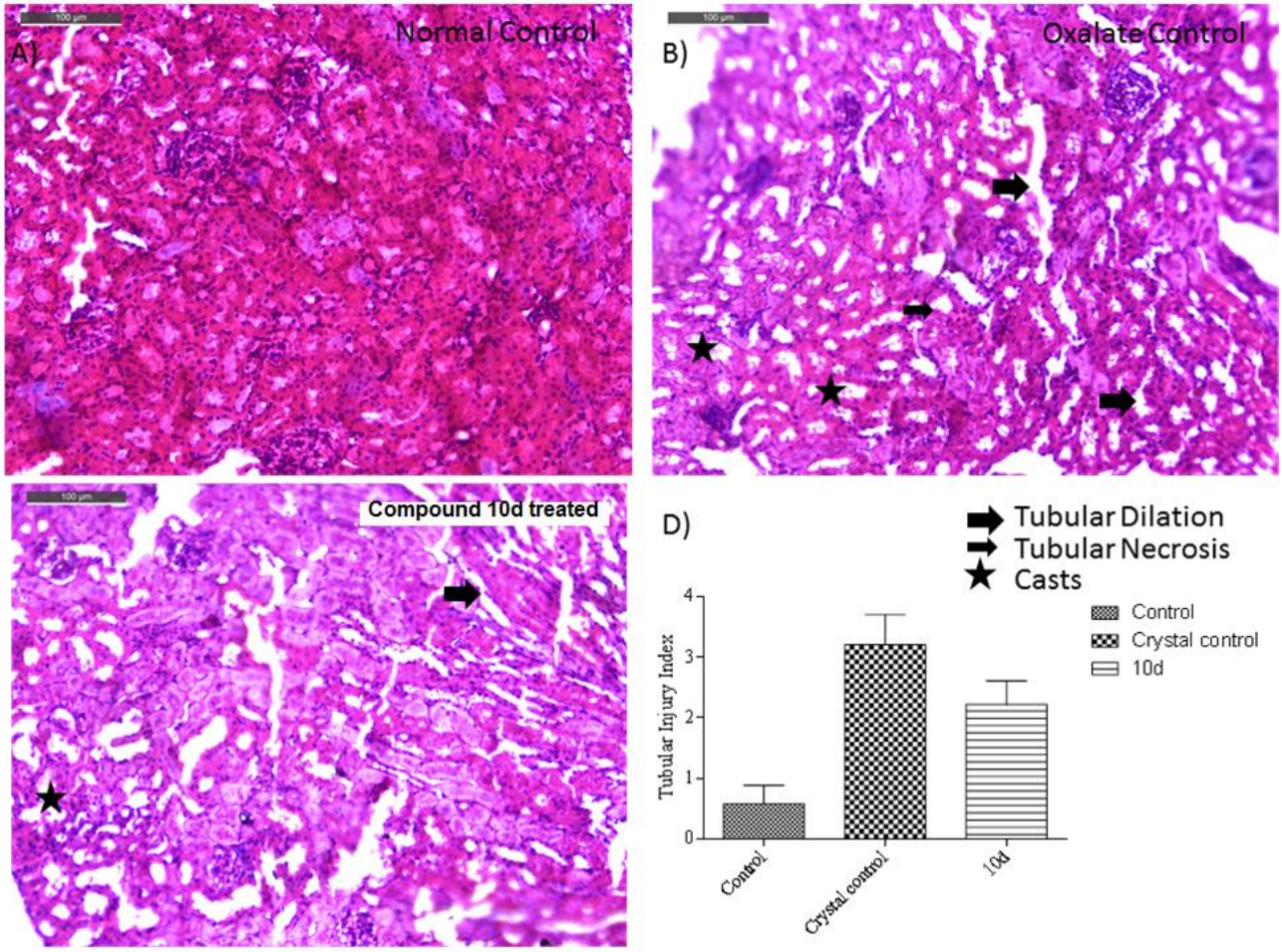

Figure 5.2.37 Renal protective effect of compound 10d on calcium oxalate induced renal nephropathy model via histology study. Figure illustrates effect at the dose of 50 mg/kg on histology of renal tissue in calcium oxalate. Representative photomicrograph of renal histological sections (H & E) at 40x from (A) control group (B) oxalate crystal control group (C) compound 10d treated group (D) indicates Tubular injury index which was quantified by semi-quantitative scoring (Tubular dilation, Tubular necrosis and tubular casts).

5.2.13 Comparative analysis of cytokine inhibition effect of methyl coumarin and phenyl propanoid derivatives versus fused-cyclic coumarin-based lignans

The in-vitro inhibition effect of fused-cyclic coumarin-based lignans (**9d**, **10d**, **11d** and **11e)** were compared with that of 7,8-dihydroxy-4-methyl coumarin (**1a**) and phenyl propanoids (**3b**, **4b**, and **5b**) in order to see if any synergistic effect was observed. Overall, the newly synthesized coupled products (**9d**, **10d** and **11d**) demonstrated higher cytokine-suppression effect than the individual compounds **1a**, **3b**, **4b** and **5b**. The IC_{50} values of all the compounds are presented in Table 5.2.8, for comparative understanding of activity.

Table 5.2.8 Comparative analysis of IC_{50} values of phenylpropanoids and coumarin (1a, 3b, 4b, 5b) v_s fused lignan compounds (9d, 10d, 11d and 11e) on cytokine inhibition

Compounds	IC_{50} values (μM)		
	TNF-α	IL-1β	IL-6
1a	62.36	113.72	41.22
3b	74.07	62.19	29.39
9d (1a+3b)	**36.31**	**29.99**	**16.04**
4b	16.68	32.51	33.39
10d (1a+4b)	**8.5**	47.57	**22.48**
5b	7.12	47.84	68.03
11d (1a+5b)	23.63	**23.81**	**18.79**
11e	18.37	**17.94**	**13.29**
15	39.89	57.7	12.67

In controlling LPS-induced TNF-α expression, the coupled product **10d** was excellently effective with IC_{50} value of 8.5 μM, than the coupling reactants **1a** and **4b** which showed IC_{50} values of 62.36 and 16.68 μM. Similarly, while the fused product **9d** exhibited IC_{50} value of 36.31 μM, the reactants **1a** and **3b** showed IC_{50} values of 62.36 and 74.04 μM. In the third case, the lignan **11d** displayed IC_{50} value of 23.63 μM and the reactants **5b** and **1a** showed IC_{50} values of 7.12 and

62.36 µM, respectively. Compound **11e** (IC_{50} value 18.37 µM), an acetate derivative of **11d** was found to be more active than **11d**. Among all the tested compounds, ethyl ferulate (**5b**) was found to be most active (IC_{50} value 7.12 µM) against TNF-α (Table 5.2.8).

In controlling LPS-induced IL-1β expression, the coupled product **9d** was significantly effective with IC_{50} value of 29.99 µM, than the coupling reactants **1a** and **3b** which showed IC_{50} values of 113.72 and 62.19 µM. Similarly, while the fused product **11d** exhibited IC_{50} value of 23.81 µM, the reactants **1a** and **5b** showed IC_{50} values of 113.72 and 47.84 µM. In the third case, the lignan **10d** displayed IC_{50} value of 47.57 µM and the reactants **4b** and **1a** showed IC_{50} values of 32.51 and 113.72 µM, respectively. Among all the tested compounds, the acetate derivative (**11e**) of **11d** was found to be most active with IC_{50} value 17.94 µM against IL-1β (Table 5.2.8).

In controlling LPS-induced IL-6 expression, the coupled product **9d** was very effective with IC_{50} value of 16.04 µM, than the coupling reactants **1a** and **3b** which showed IC_{50} values of 41.22 and 29.39 µM. Similarly, while the fused product **10d** exhibited IC_{50} value of 22.48 µM, the reactants **1a** and **4b** showed IC_{50} values of 41.22 and 33.39 µM. In the third case, the lignan **11d** displayed excellent IC_{50} value of 18.79 µM and the reactants **5b** and **1a** showed IC_{50} values of 68.03 and 41.22 µM, respectively. As in case of TNF-α and IL-1β, compound **11e** (IC_{50} value 13.29 µM), an acetate derivative of **11d** was found to be more active than **11d** (Table 5.2.8). Overall, the inhibition effect exhibited by coumarin-based lignans was more than the tested individual coumarin and cinnamate derivatives, especially the acetate derivative which validates the results of docking studies. Thus, the pro-inflammatory inhibition effect by the fused-cyclic coumarin-based lignans was found to be synergistic.

5.2.14 Structure activity relationship of fused-cyclic coumarin-based lignans

Based on the anti-inflammatory activity demonstrated by the newly synthesized compounds (**9d**, **10d**, **11d** and **11e)** and natural cleomiscosin A (**15**) under LPS-induced acute endotoxemia and carrageenan-induced animal models, the following deductions on structure activity relationships were arrived.

5.2.14.1 Structure activity relationship based on LPS-induced acute endotoxemia model

Evaluation of the percentage inhibition effect against LPS-induced TNF-α under mouse endotoxemia model (Table 5.2.6) revealed highly significant inhibition (62.56 %) by compound (**10d**) having two hydroxyl groups (C-4′ and C-3′) in the phenyl ring. If one of this –OH groups at C-3′ was removed/acetylated as in case of **9d/11e** or substituted with $–OCH_3$ as in **11d**, the activity was found to be decreased. Similar observations were found in case of inhibiting the release of IL-1β by LPS induction (Table 5.2.6). Compound **10d** having dihydroxy phenyl nucleus formed by coupling ethyl caffeate (**4b**) with 7,8-dihydroxy-4-methyl coumarin (**1a**) had shown highest percentage inhibition (67.95 %). If the –OH group at C-3′ was absent as in **9d** or substituted with $–OCH_3$ as in **11d**, the activity was found to be decreased. The reduction in the activity was not much if the substitution was an acetyl group as in **11e** (57.31 %).

On comparing the % inhibition effect exhibited by **9d** and **10d**, the activity was more if two hydroxyl groups in the phenyl ring were present as in the case of **10d**. However, the activity was found to be increased if one of this –OH group (at C-3′) was substituted with $–OCH_3$ as in **11d** and the activity was found to be increased if there were $-OCOCH_3$ and $–OCH_3$ substituted phenyl ring in the compound, for example **11e**.

Further, a higher percentage inhibition was exhibited by the new synthetic lignans compared to cleomiscosin A (**15**) (TNF-α - 15.7%, IL-1β – 41.08% and IL-6 – 28.35%) against all the three pro-inflammatory cytokines. The natural coumarinolignan cleomiscosin A (**15**) mimics **11d** partially and differ by having a primary alcohol group at C-8′ (instead of ethyl ester) and methoxyl group at C-6 (instead of methyl group at C-4) (Table 5.2.6).

5.2.14.2 Structure activity relationship based on Carrageenan-induced animal model

On analyzing the percentage inhibition of carrageenan-induced TNF-α and IL-1β production in plasma samples of mice treated with new synthetic lignans, the following deductions were made. Lignan having *p*-OH substituted phenyl ring (**9d**) exhibited remarkable inhibition of TNF-α with 88.63 %. The activity was found to be decreased if two –OH groups were introduced into the phenyl ring or other substituents such as -OH & -OCH_3 and –$OCOCH_3$ and –OCH_3 (Figure 5.2.31).

Similar trend in decrease in the activity was observed in case of inhibition of carrageenan-induced IL-1β secretions. Compound **9d** with mono-hydroxyl substitution at C-4′ position exhibited good activity (Figure 5.2.31 and 5.2.32). However, the activity was found to be reduced if there was an additional substituent at C-3′ (OH / OCH_3). The activity was observed to be retained or slightly increased if there was an acetyl group at C-3′ in addition to –OH group at C-4′ (Figure 5.2.32)

Overall, presence of -hydroxyl groups in the phenyl ring of coumarin-based lignans was identified to be essential for the anti-inflammatory activity. Further, the attempt of making novel 4-methyl substituted coumarinolignans having acid ester groups had been successful culminating potentially active therapeutic agents.

5.3 Developing glucoside of cleomiscosin A (15) as pro-inflammatory cytokines inhibitor

In view of the molecular docking results, in-vitro and in-vivo inhibition effect shown by cleomiscosin A (**15**), it was thought to make semisynthetic derivatives of the same. Cleomiscosin A (**15**) the first natural coumarinolignan had been isolated from various plant sources like *Cleome viscosa*, *Hyoscyamus niger*, *Rhododendron collettianum*, *Acer nikoense*, etc (Begum SA *et al*., 2010a). While **15** had been screened for several biological activities (Begum SA *et al*., 2010a), it encompassed significant hepatoprotective (Yadav NP *et al*., 2010) and anti-inflammatory potential (Begum S *et al*., 2010). Cleomiscosin A is an oxidative coupled product of fraxetin and coniferyl alcohol, found to be insoluble in water and soluble only in a mixture of methanol and chloroform. In view of the cytokine inhibitory potential exhibited by cleomiscosin A under in-vitro models (Sharma S *et al*., 2012) and its poor solubility issue, a polar glycosidic derivative was proposed to be synthesized and tested under cellular and animal models.

Cleomiscosin A glycoside (**15g**) was designed incorporating simple glucosidic linkage only to alcoholic hydroxyl at C-9 position keeping the phenolic group intact as it is essential for the activity (Yadav NP *et al*., 2010).

5.3.1 Synthesis and characterisation of cleomiscosin A glucoside

Preparation of cleomiscosin A glycoside (**15g**) comprised two steps. First step was the isolation of natural cleomiscosin A (**15**) from a plant source. The second step involved semisynthetic conversion of cleomiscosin A (**15**) to cleomiscosin A glycoside (**15g**).

5.3.1.1 Isolation and Characterization of cleomiscosin A (**15**)

As explained in the previous phase, cleomiscosin A was isolated from the methanolic extract of defatted seeds of *Cleome viscosa* following Scheme 5.8. The isolated compound was confirmed by co-TLC study with authentic sample and comparison of proton NMR data (Begum SA *et al*., 2010a). The ESI-MS and ^{1}H NMR spectra are presented in Figures 5.2.17 and 5.2.18. After authenticating the product, semisynthetic conversion to its glycoside was carried out.

5.3.1.2 Preparation and characterization of cleomiscosin A glycoside (15g)

Cleomiscosin-A-9′-*O*-glucoside (**15g**) was prepared using isolated cleomiscosin A (**15**). Briefly, a mixture of **15**, absolute pyridine and dry $CHCl_3$ was added drop wise to a solution of acetobromo-α-D-glucose in $CHCl_3$ and stirred at room temperature for 24 h under nitrogen atmosphere (Scheme 5.9). Pyridine used in this reaction promoted the selective glucosidation of alcoholic hydroxyl group. The product was recovered by de-protection and purified by prep-TLC. The purity of the prepared product (yield 15%) was ascertained through TLC studies over different solvent system ($CHCl_3$:MeOH; 1:1) and cleomiscosin A glucoside (**15g**) was confirmed by APCI-MS ($[M]^+$ 548.15 and $[M+Na]^+$ 571.10) (Figure 5.3.2) and ^{1}H NMR spectral analysis (Figure 5.3.1).

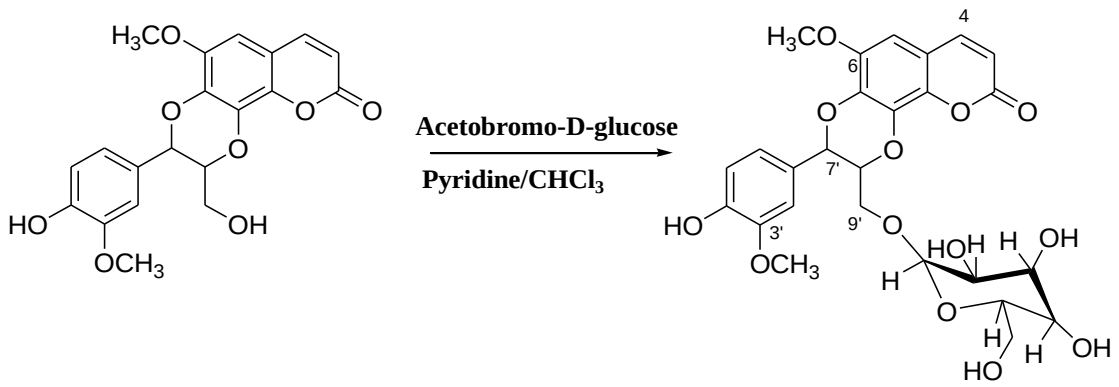

Cleomiscosin-A (15) **Cleomiscosin-A glucoside (15g)**

Scheme 5.9 Conversion of cleomiscosin A to its glucoside

The assignment of various signals discerned in the ^{1}H NMR spectra of cleomiscosin A (**15**) and cleomiscosin A glycoside (**15g**) along with their splitting pattern and coupling constant values are presented in experimental part. The formed product could possibly be an alpha-glucoside which was corroborated from the appearance of anomeric proton signal as a very narrow doublet (δ 4.90 ppm). Similar reaction using acetobromo-β-D-glucose and $BF_3.Me_2O$ had been reported for the synthesis of silybin-23-*O*-glucoside (Kren V *et al*., 1997).

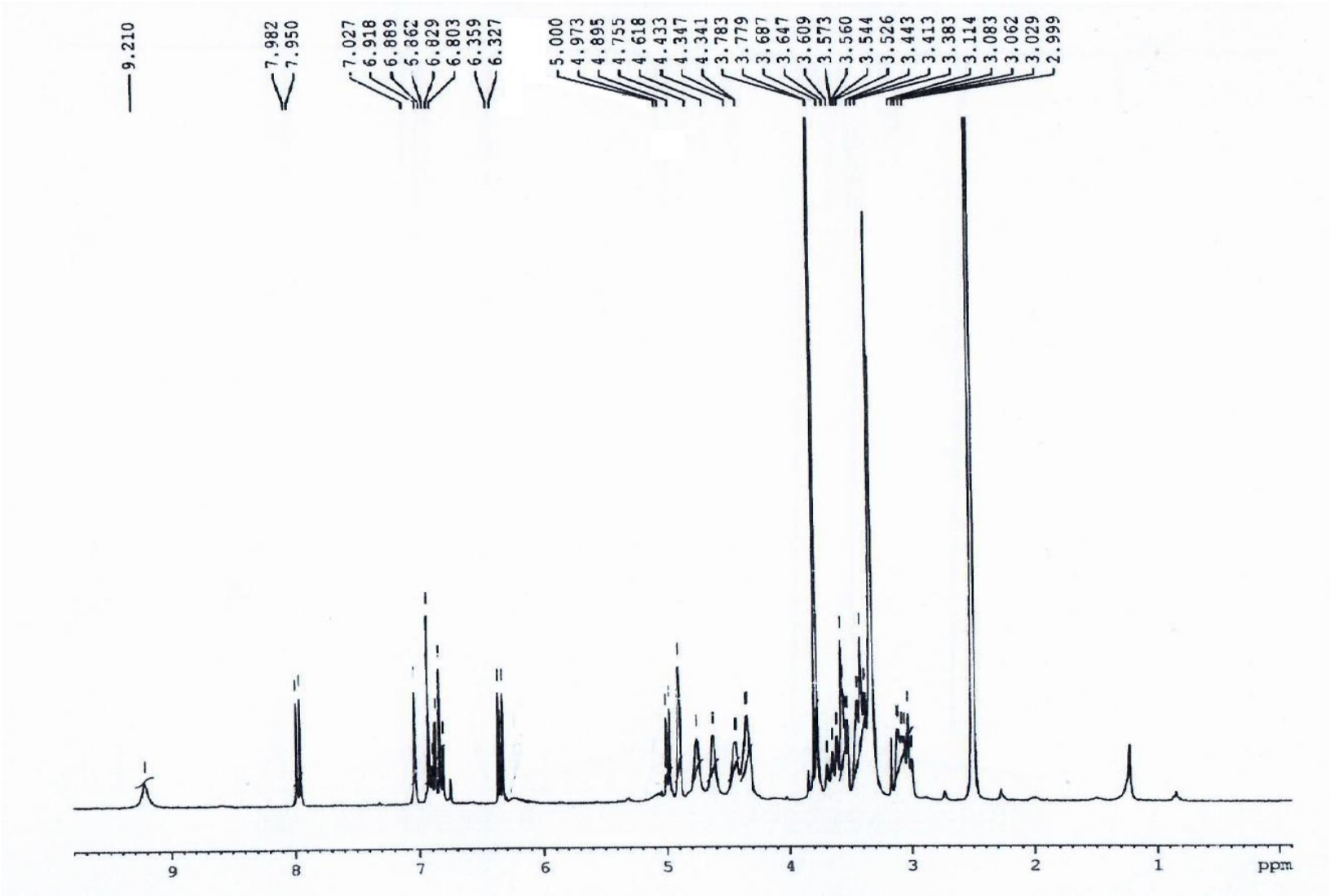

Figure 5.3.1 ^{1}H NMR spectrum of Cleomiscosin A glycoside (15g)

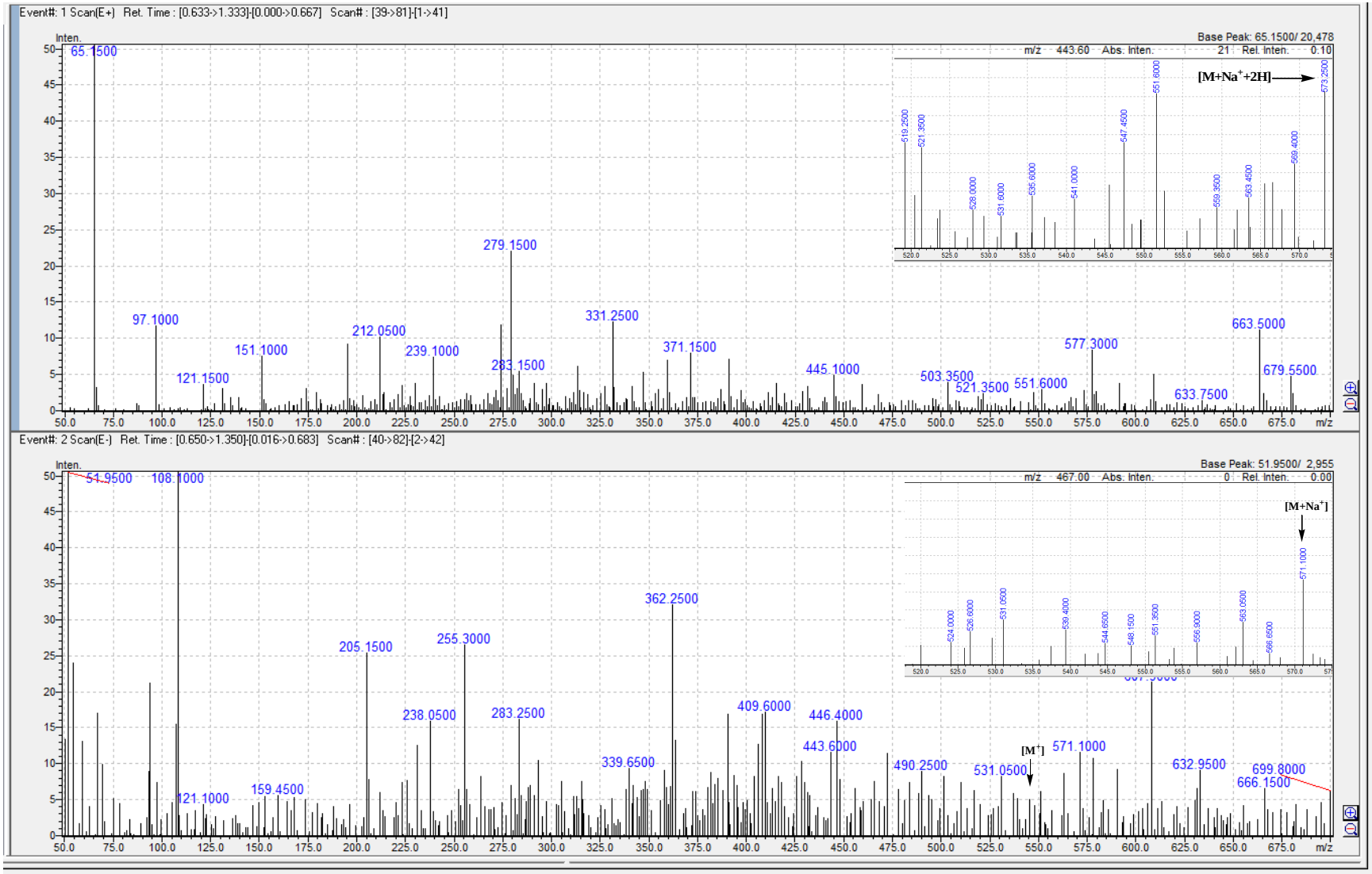

Figure 5.3.2 APCI mass spectrum of Cleomiscosin A glycoside (15g)

5.3.2 Effect of cleomiscosin A (15) and cleomiscosin A glycoside (15g) on LPS-induced TNF-α secretion using ELISA assay

Effect of cleomiscosin A (**15**) and cleomiscosin A glycoside (**15g**) on production of pro-inflammatory cytokines was evaluated using LPS-induced model in mouse macrophage RAW 264.7 cell lines and compared with standard drug prednisolone (**17**). LPS triggers the secretion of pro-inflammatory cytokines such as TNF-α, IL-1β and IL-6. The RAW 264.7 cell lines were pre-treated with 100 μM, 30 μM, 10 μM and 3 μM concentrations of the compounds. After compound treatment, cells were stimulated with 1 μg/ml LPS. Supernatant was collected after 6 h of incubation with LPS. Estimation of TNF-α was done using ELISA kit as per the manufacturer's instruction (Zhang H *et al*., 2008).

Both **15** and **15g** exhibited more than 50% inhibition at 100 μM concentration and the effect was found to be concentration dependent, demonstrating **15** (IC_{50} 39.89 μM) to be more potent than **15g** (IC_{50} 139.48 μM). Although the effect of compounds was comparatively less than the standard immunosuppressant drug, prednisolone (50.32 % inhibition at 10 μM), interestingly they were found to suppress TNF-α secretion even at a low concentration of 3 μM (Figure 5.3.3).

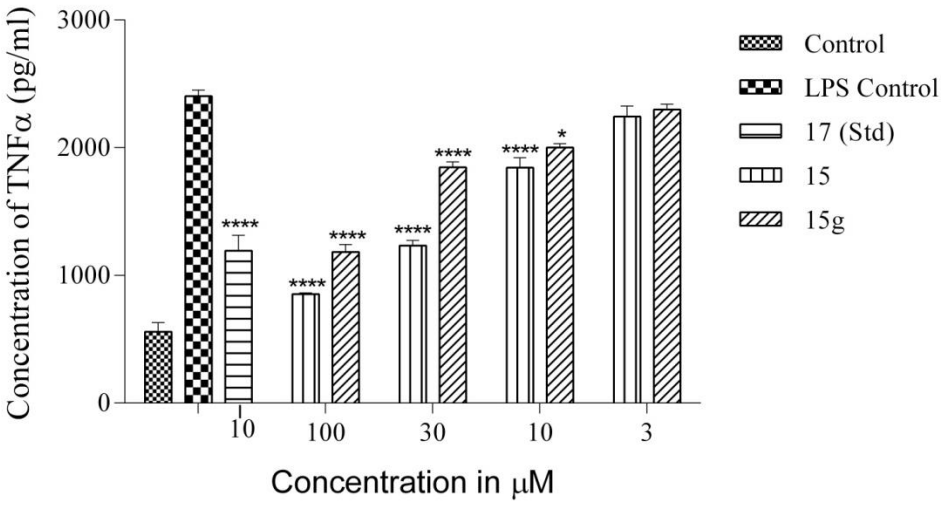

Figure 5.3.3 In-vitro TNF-α inhibitory effects of cleomiscosin A (15) and semi-synthesized cleomiscosin A glycoside (15g) on LPS induced RAW 264.7 cells using ELISA. Cells were pretreated with the indicated concentrations of compound **15**, **15g** and standard prednisolone (**17**) (10 μM) for 1 h and then incubated with LPS (1 μg/mL) for 6 h. TNF-α concentration was determined by ELISA kit. The values are presented as mean ± SEM from triplicate. ****P < 0.0001 vs LPS control *P < 0.05 vs LPS control.

5.3.3 Effect of cleomiscosin A (15) and cleomiscosin A glycoside (15g) under mouse endotoxemia model

In order to understand the in-vivo performance of **15** and **15g**, an acute endotoxemia study on mice was carried out. Compounds were administered orally at two dose levels (25 mg/kg and 50 mg/kg) followed by LPS (0.3 mg/kg) i.p. injection. The plasma TNF-α level was measured after 60 min using ELISA kit (Khan R *et al*., 2015). In control group, LPS injection caused approximately 30 fold increase in TNF-α concentration. This LPS-induced TNF-α secretion was found to be decreased in the treatment groups. Interestingly, cleomiscosin A glycoside (**15g**) was found to be significantly active and 5 times more active than cleomiscosin A (**15**), in attenuating the TNF-α production. **15g** exhibited 52.03 % and 29.23 % inhibition at 50 mg/kg and 25 mg/kg, respectively. On the other hand, only 10.77 % (50 mg/kg) and 5.61 % (25 mg/kg) inhibition effect was observed with administration of **15** (Figure 5.3.4). This five-fold increase in activity

of cleomiscosin A glycoside (**15g**) compared to cleomiscosin A (**15**) could be attributed to the newly added glucose moiety, which improved the solubility and oral bioavailability of the glycoside derivative.

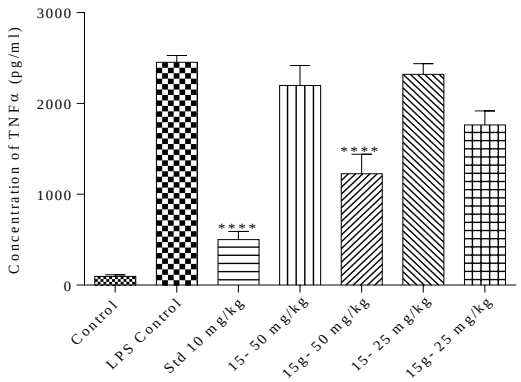

Figure 5.3.4 In-vivo screening of cleomiscosin A (15) and cleomiscosin A glycoside (15g) using LPS induced mouse endotoxemia model. Figure shows the inhibitory effect of compounds **15**, **15g** and standard prednisolone (**17**) at doses of 25mg/kg and 50mg/kg on TNF-α secretions induced by LPS in mice (The values are presented as mean ±SEM (n=6). ****P<0.0001 vs LPS control)

5.3.4 Effect of cleomiscosin A (15) and cleomiscosin A glycoside (15g) on LPS-induced IL-1β and IL-6 production using ELISA

Further, the study was extended to explore the inhibition property of cleomiscosin A glycoside (**15g**) to control the expression of other pro-inflammatory cytokines such as IL-6 and IL-1β which are important in neuroinflammation (Gray SM and Bloch MH., 2012; Spooren A *et al*., 2011) and renal injury (Mulay SR *et al*., 2013). Screening was done on LPS-stimulated RAW 264.7 macrophages using ELISA protein estimation method. Excitingly, the glucoside compound **15g** showed 98.11 % inhibition of IL-6 at 30 μM with IC_{50} value of 7.94 μM and this effect was higher than its parent molecule **15** (IC_{50} value 12.67 μM) (Figure 5.3.6). Alongside, **15g** was

effective in controlling IL-1β expression too with IC_{50} of 45.76 μM, which was better compared to **15** (IC_{50} value 57.7 μM) (Figure 5.3.5). Outcome of the ELISA assay proved the striking potentiality of glucoside derivative (**15g**) in downregulating IL-6 as well as IL-1β cytokines.

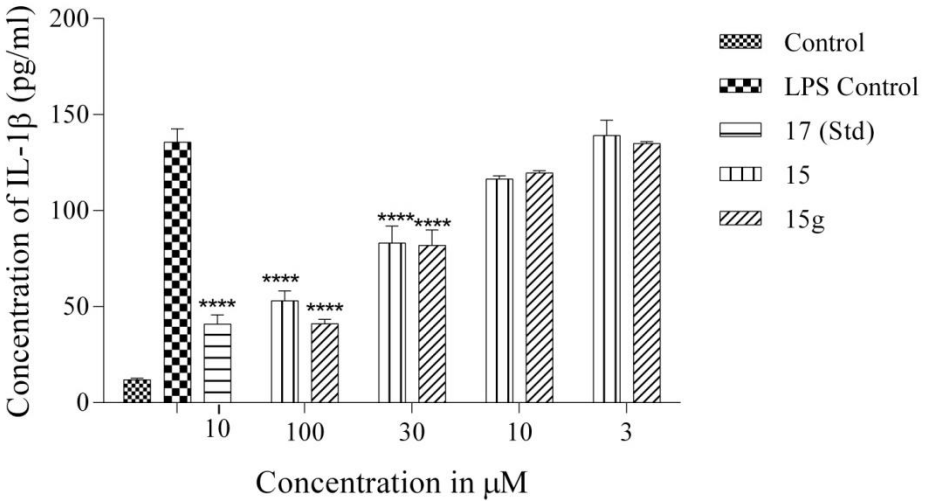

Figure 5.3.5 In-vitro IL-1β inhibitory effect of cleomiscosin A (15) and semi-synthetic cleomiscosin A glycoside (15g) on LPS induced RAW 264.7 cells using ELISA. Cells were pretreated with the indicated concentration of the compounds **15** and **15g** as well as with the standard prednisolone (**17**) (10μM) 1 h before the incubation with LPS (1 μg/mL) and oxalate crystals (250μg/ml). After 6 h of incubation supernatant was collected and subjected to ELISA assay for IL-1β estimations. The values are presented as mean ± SEM from triplicate. ****$P <$ 0.0001 vs LPS control.

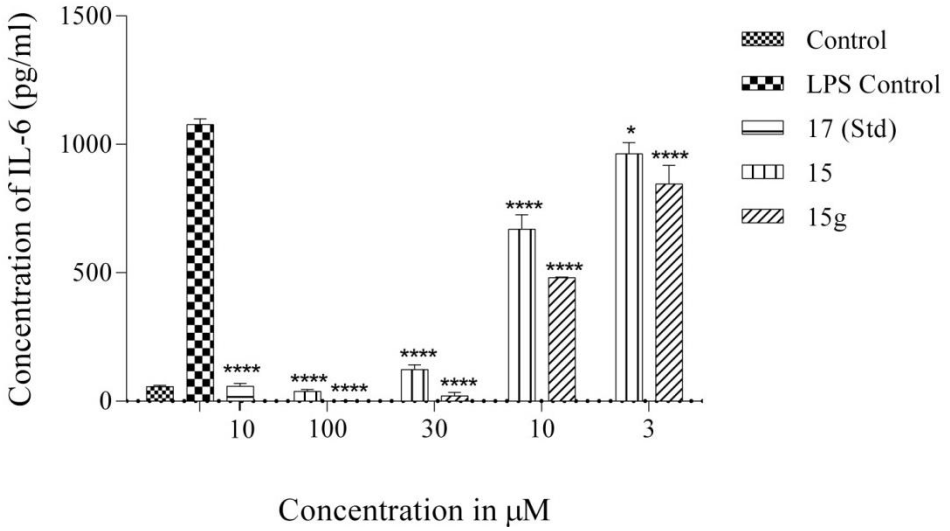

Figure 5.3.6 In-vitro IL-6 inhibitory effect of cleomiscosin A (15) and semi-synthetic cleomiscosin A glycoside (15g) on LPS induced RAW 264.7 cells using ELISA. Cells were treated with the indicated concentrations of compounds **15**, **15g** and standard prednisolone (**17**) (10μM) for 1 h and then incubated with LPS (1 μg/mL) for 6 h. Supernatant collected after incubation was used for estimating IL-6 levels using ELISA. The values are presented as mean ± SEM from triplicate. ****$P < 0.0001$ vs LPS control, *$P < 0.05$ vs LPS control.

5.3.5 Effect of cleomiscosin A (15) and cleomiscosin A glycoside (15g) on LPS-induced NO production

Additionally, the potentiality of **15g** onto nitric oxide (NO) production was measured using Griess method (Sun J *et al*., 2003). Macrophages when exposed to LPS produce NO by stimulating inducible nitric oxide synthase. Excessive production of NO will lead to host cell damage because of its cytotoxicity. **15g** and **15** at 100 μg/mL concentration significantly reduced the LPS-induced NO production by 50.99 and 56.53 %, respectively (Figure 5.3.7).

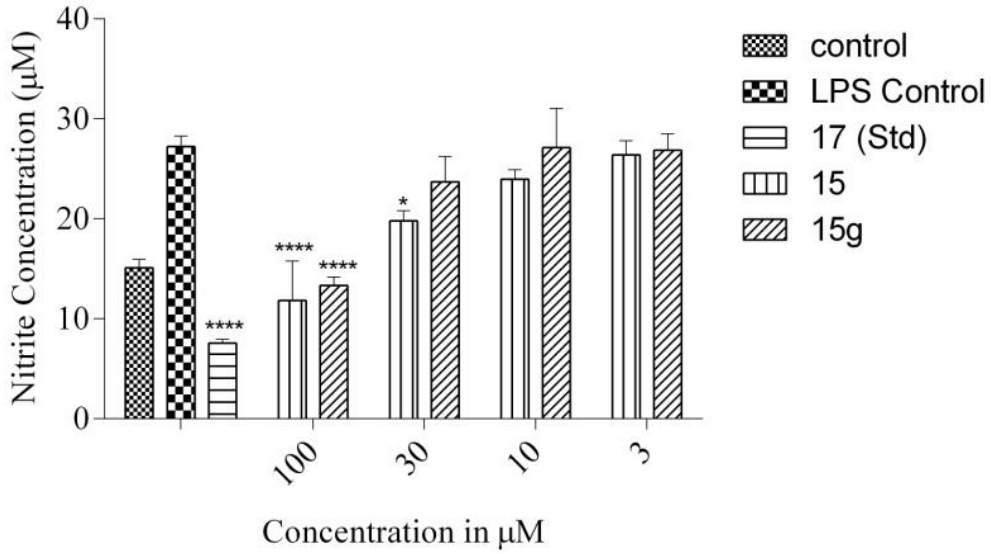

Figure 5.3.7 In-vitro NO production inhibitory effects of cleomiscosin A (15) and semi-synthesized cleomiscosin A glycoside (15g) on LPS induced RAW 264.7 cells. Cells were treated with the indicated concentration of compounds **15**, **15g** and standard prednisolone (**17**) (10 μM) for 1 h and then incubated with LPS (1 μg/mL) for 16 h. Supernatant collected was used for NO estimations using Griess method. The values are presented as mean ± SEM from triplicate. ****$P < 0.0001$vs LPS control, * $P < 0.05$ vs LPS control.

5.3.6 Cytotoxic effect of cleomiscosin A (15) and cleomiscosin A glycoside (15g)

Also, cytotoxicity of **15g** and **15** were tested in LPS-stimulated RAW 264.7 macrophages. Cell viability by treatment with various concentrations of the samples for 1 h followed by the addition of LPS and incubation for 24 h was analyzed by MTT assay (van Meerloo J *et al*., 2011). **15g** and **15** exhibited IC_{50} values of 187.90 and 257.58 μM, respectively (Figure 5.3.8).

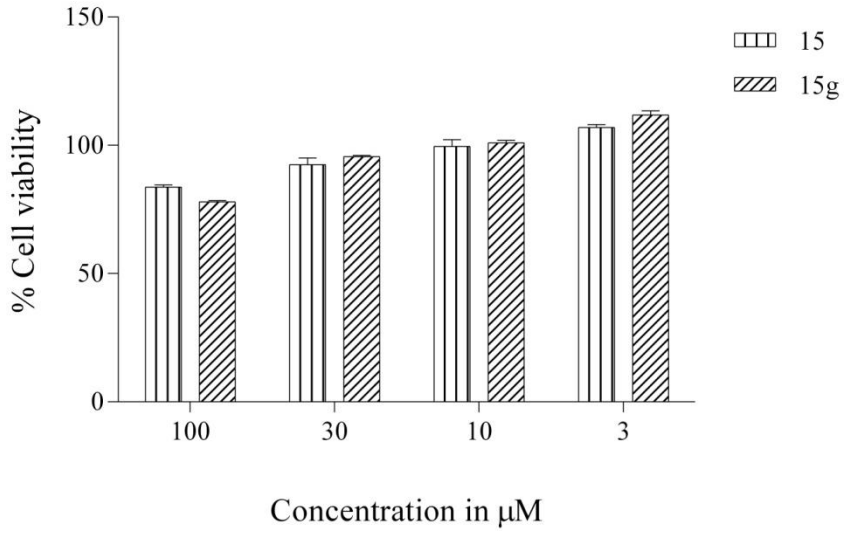

Figure 5.3.8 Cytotoxicity effects of cleomiscosin A (15) and semi-synthesized cleomiscosin A glycoside (15g). Figure shows the effect of treatment of cells with the indicated concentration of compounds **15** and **15g** for 24 h. The viability assay was carried out using MTT reagent. The values are presented as mean ± SEM from triplicate.

5.3.7 Molecular docking studies on cleomiscosin A glycoside (15g)

In order to have some insight into the binding pattern of cleomiscosin A glycoside (**15g**) over the active sites of inflammatory proteins, molecular docking studies were performed. Docking studies on the glucoside (**15g**) was carried out following the same procedure as mentioned earlier using GOLD 5.2 and compared with its parent compound cleomiscosin A (**15**).

5.3.7.1 Docking interactions with pro-inflammatory cytokine TNF-α

When docked with TNF-α, **15g** showed higher GOLDScore_fitness (61.466) than cleomiscosin A (**15**) and standard compounds (**16** and **17**). Interestingly, the GOLDScore_fitness of **15g** was found be the second highest among all the test ligands of the present study with compound **10e** possessing highest score of 62.3072.

On comparing the docking interaction map of cleomiscosin A glycoside (**15g**) with that of the standards, it was found to exhibit exactly the similar hydrophobic interaction pattern with TNF-α residues as that of prednisolone (Leu344, Tyr346, Ser347, Tyr406, Leu407, Gly408, Gly409, Ile442, Leu492, Tyr494, Ser495, Gln496, Tyr554, Leu555, Gly556 and Tyr586). However, **15g** was found to contain only one different interaction residue, i.e. His302. Further, cleomiscosin A glycoside (**15g**) exhibited the interesting π-π stacking interaction with Tyr346 as that of its parent compound, cleomiscosin A (**15**). Also, a distinct hydrogen bond interaction with Tyr438 was shown by this compound, which was not observed with any of the previously discussed molecules (Figure 5.3.9).

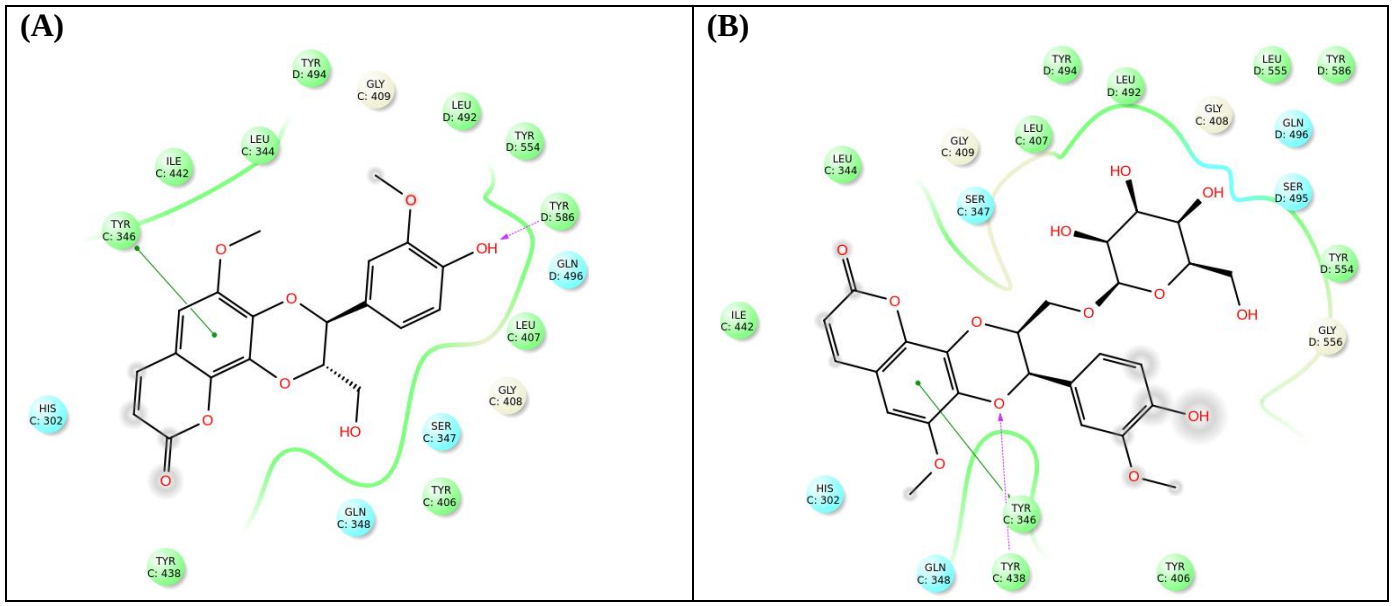

Figure 5.3.9 2D TNF-α docking interaction map displaying the binding and interactions of cleomiscosin A (15) (A) and cleomiscosin A glycoside (15g) (B)

5.3.7.2 Docking interactions with pro-inflammatory cytokine IL-1β

While docking with IL-1β, cleomiscosin A glycoside (**15g**) displayed GOLDScore_fitness (58.24) higher than the standard drugs (**16** and **17**), cleomiscosin A (**15**), dihydroxy methyl coumarin derivatives, phenylpropanoids and most of the coumarin-based lignan compounds (Table 5.1.3, 5.1.4, 5.1.6 and 5.1.7).

On comparing the IL-1β docking 2D picture, it was observed that cleomiscosin A glycoside (**15g**) exhibited a well-balanced interaction with IL-1β residues as seen in diclofenac sodium (**16**) [Arg10 (exactly similar fashion with two hydrogen bonding), Ile12, Ile22], prednisolone (**17**) (Ile12, Gln13, Val14, Ala20, Ile22, Tyr143) and natural molecule cleomiscosin A (**15**) (Asp7, Arg21, Phe104) (Figure 5.3.10). All these interactions have collectively made the molecule show high IL-1β GOLDScore_fitness.

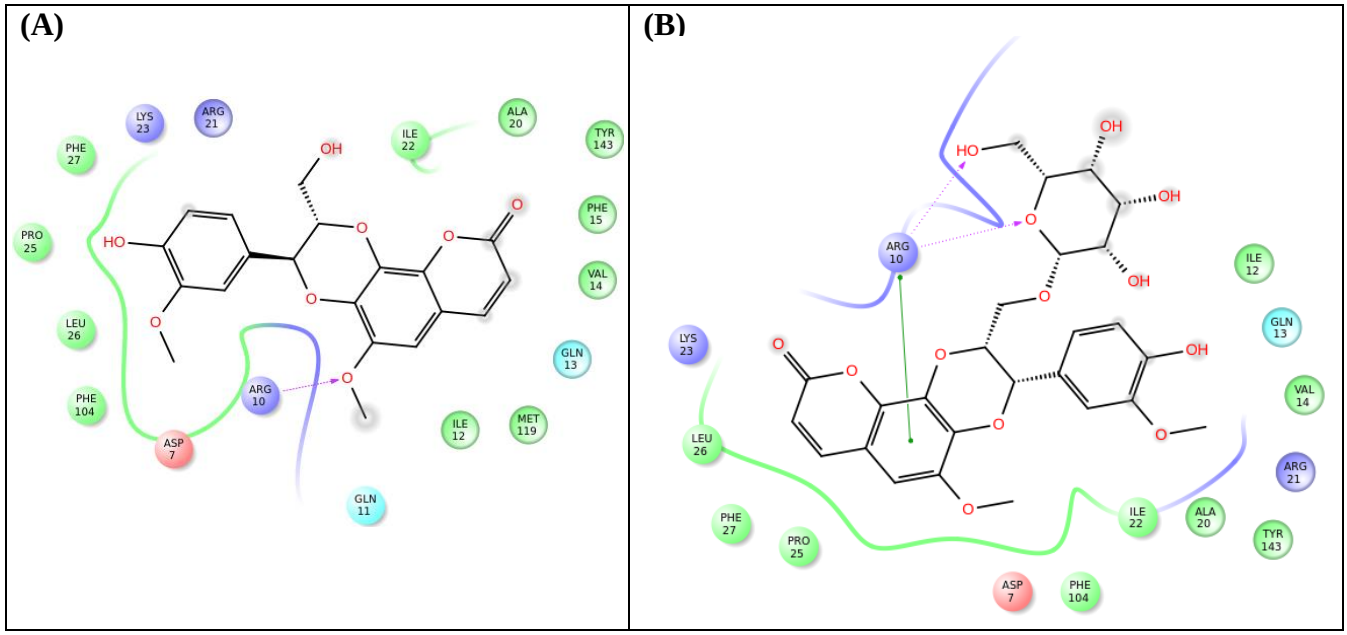

Figure 5.3.10 2D IL1-β docking interaction map displaying the binding and interactions of cleomiscosin A (15) (A) and cleomiscosin A glycoside (15g) (B)

5.3.7.3 Docking interactions with pro-inflammatory cytokine IL-6

Similar results were observed when cleomiscosin A glycoside (**15g**) was docked with IL-6 protein, displaying a high fitness score (GOLDScore_fitness, 44.84) than the standard compounds, dihydroxy methyl coumarin derivatives, phenylpropanoids and most of the fused compounds. However, the GOLDScore_fitness of **15g** was found to be lesser than cleomiscosin A (50.9474) (Table 5.1.3, 5.1.4, 5.1.6 and 5.1.7). On comparative analysis of the IL-6 docking 2D picture, this molecule showed some common hydrophobic residues observed in diclofenac (**16**) (Ser101, Phe103 and Glu286), prednisolone (**17**) (Lys105, Gln196 and Asp198 and one hydrogen bonding) and natural molecule cleomiscosin A (**15**) (Ser152, Lys154 and Ser224) as well. Interestingly, cleomiscosin A glycoside (**15g**) had one distinctly different hydrogen bond interaction with Glu114 residue (Figure 5.3.11). Overall the docking results disclosed cleomiscosin A glycoside (**15g**) as a better scaffold than cleomsicosin A (**15**). Thus, the study validated the above reported pro-inflammatory inhibition effect of novel semisynthetic cleomiscosin A glycoside (**15g**).

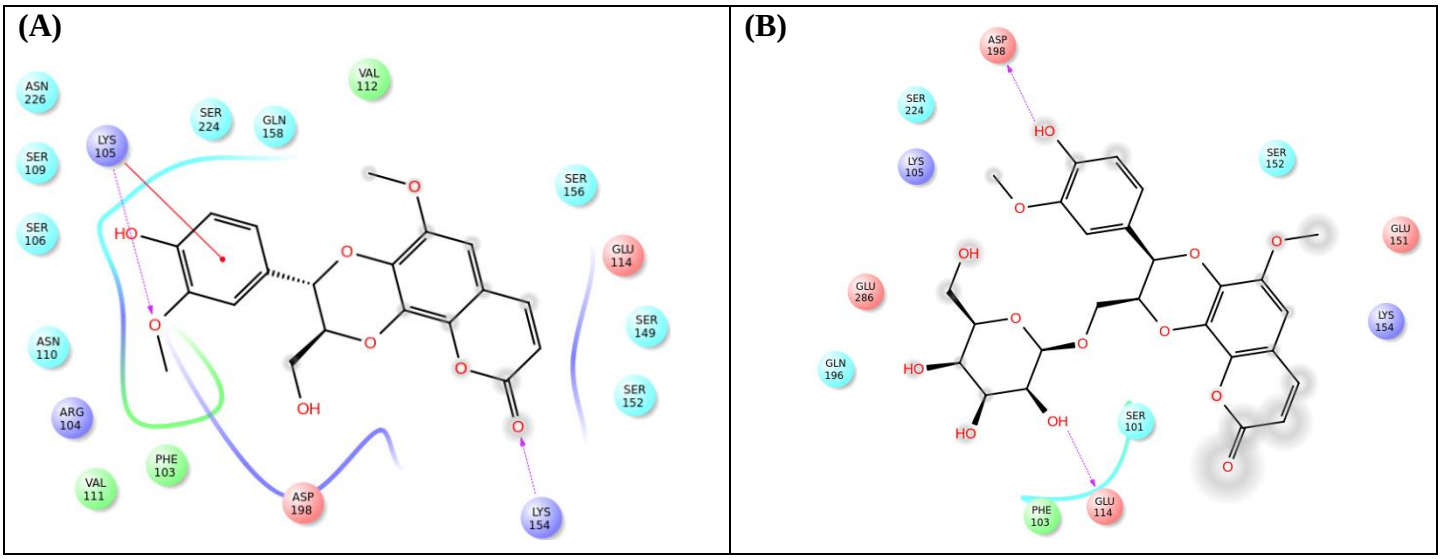

Figure 5.3.11 2D IL-6 docking interaction map displaying the binding and interactions of cleomiscosin A (15) (A) and cleomiscosin A glycoside (15g) (B)

5.3.8 Conclusion

Thus, the study concludes that the effect of cleomiscosin A glycoside (**15g**) could be because of hydrophilic group i.e. glucose attached to cleomiscosin A (**15**), which improved the solubility and bioavailability of the same. This is the first report of semisynthesis of a coumarinolignan glucoside. Although various donors and promoters were attempted (Yang Y *et al*., 2015; Mastihubová M and Poláková M., 2016), it was with acetobromo-α-D-glucose and pyridine, the preparation was achieved. Thus, results of in-vitro and in-vivo studies corroborated cleomiscosin A glycoside (**15g**) as a potentially active derivative of cleomiscosin A (**15**). Studying the pharmacokinetics of cleomiscosin A glycoside (**15g**), could lead to its development into anti-inflammatory drug candidate.

CHAPTER 6

SUMMARY AND FUTURE PERSPECTIVES

CHAPTER 6

SUMMARY AND FUTURE PERSPECTIVES

Phase I: Synthesis and in-vitro biological evaluations on methyl coumarin and phenyl propanoid derivatives followed by molecular docking studies towards developing novel coumarin-based pro-inflammatory cytokines inhibitors.

In Phase I, 7,8-dihydroxy-4-methyl coumarin (**1a**) and phenyl propanoid derivatives (**3b**, **4b** and **5b**) were synthesized and in-vitro assay was performed to test their inhibition effect on the lipopolysaccharide (LPS)-induced secretions of TNF-α, IL-1β, and IL-6 proteins using ELISA kits. The synthesized compounds **1a**, **3b**, **4b** and **5b** were characterized based on IR and Mass spectral analysis. Compound **5b** and **4b** exhibited IC_{50} values of 7.12 μM and 16.68 μM, respectively in inhibiting TNF-α protein. Phenyl propanoids **3b**, **4b** and **5b** showed significant inhibition (p<0.0001 at 100 μM) of LPS-induced IL-1β and IL-6 secretions with IC_{50} values ranging between 30 and 68 μM. Further these compounds were effective in controlling the LPS-induced NO levels and the compounds were found to be non-cytotoxic.

Further, molecular docking studies on the synthesized compounds and some of the designed structural analogues **(1a-7c)** of **1a**, **3b**, **4b** and **5b** were performed using Genetic Optimization Ligand Docking-GOLD 5.2 molecular docking mechanism. The interactions between the active sites of targeted proteins (TNF-α, IL-1β, and IL-6) and ligands were studied and compared with the binding patterns of clinically used drugs like diclofenac sodium (**16**) and prednisolone (**17**). Docking results of TNF-α claimed compound **4c** to show highest GOLDScore_fitness (GF score

52.3522) followed by compounds **5c** (GOLDScore_fitness, 48.4354) and **6a** (GOLDScore_fitness, 47.5894). In case of docking against IL-1β, compound **4a** (GOLDScore_fitness, 47.5829) showed highest fitness score followed by compounds **4c** (GOLDScore_fitness, 47.3047) and **5c** (GOLDScore_fitness, 43.9733). In case of docking against IL-6, compound **3a** (GOLDScore_fitness, 39.6625) showed highest fitness score followed by compounds **3** (GOLDScore_fitness, 36.8807) and **5a** (GOLDScore_fitness, 36.6038). The performance of the docked compounds in terms of GOLDScore_fitness and hydrophobic interaction residues were found to be comparable to that of the standard drugs diclofenac sodium (**16**) and prednisolone (**17**).

On witnessing the pro-inflammatory cytokine inhibitory effect demonstrated by the coumarin and phenyl propanoid derivatives under virtual and absolute cell-based studies, an idea of making fused-cyclic derivatives by coupling the coumarins (**1a** and **1b**) and phenyl propanoids (**2-7c**) of the training set emerged.

Around sixty fused-cyclic derivatives of coumarins and phenyl propanoid / cinnamoyl derivatives (**1a-7c**) in various combinations were designed, which mimicked coumarinolignans, known as a group of plant-derived secondary metabolites. Docking studies on those fused-cyclic lignan compounds (**8-13k**) were carried out along with a natural coumarinolignan, i.e. cleomiscosin A (**15**) as reference and the results were compared with the standard drugs, diclofenac sodium (**16**) and prednisolone (**17**). Docking results of TNF-α claimed compound **10e** (GF score 62.3072) to show highest GOLDScore_fitness followed by compound **10c** (GOLDScore_fitness, 61.1623) and **10g** (GOLDScore_fitness, 60.4847). In case of docking against IL-1β, compound **12d** (GOLDScore_fitness, 62.4274) showed highest fitness score followed by compound **10i** (GOLDScore_fitness, 61.5607) and **12e** (GOLDScore_fitness,

60.5262). In case of docking against IL-6, compound **11d** (GOLDScore_fitness, 48.0317) showed highest fitness score followed by compounds **10a** (GOLDScore_fitness, 47.1820) and **10g** (GOLDScore_fitness, 47.0590).

The GOLDScore_fitness, active site interactions, hydrogen bond interactions and π-π interactions of the fused-cyclic compounds were found to be distinctive than the natural coumarinolignan (**15**) and clinically used acute and chronic anti-inflammatory drugs like diclofenac sodium (**16**) and prednisolone (**17**). All these results yielded a positive indication to work further on this group of fused-cyclic coumarin-based lignan compounds to develop them as anti-inflammatory drugs.

Phase II: Synthesis of coumarin-based lignans followed by in-vitro and in-vivo pharmacological evaluations towards developing pro-inflammatory cytokines inhibitors

In phase II, some representative compounds from the fused-cyclic derivatives were selected for synthesis followed by testing them under in-vitro assays and in-vivo animal models. Compounds **9d**, **10d**, **11d** and **11e** were synthesized. Oxidative coupling of a coumarin derivative with corresponding cinnamic acid ester in the presence of diphenyl selenoxide yielded fused-cyclic compounds. The compounds were characterized using ^{1}H-, ^{13}C-NMR, HMBC and mass spectral analysis. The reference compound cleomiscosin A (**15**) was isolated from the seeds of *Cleome viscosa* and characterized by ^{1}H-NMR and Mass spectral analysis.

Results of in-vitro protein inhibition assay on RAW 264.7 cell lines displayed significant inhibition effect against TNF-α, IL-1β and IL-6 under LPS and crystal induction ($P < 0.0001$ at 100μM). The compound **10d**, exhibited IC_{50} values of 8.5 μM, 22.48 μM and 47.57 μM against TNF-α, IL-6 and IL-1β, respectively. Another compound **11e** showed IC_{50} values of 18.37 μM,

13.29 μM and 17.94 μM against TNF-α, IL-6 and IL-1β, respectively. Compound **11d**, exhibited IC_{50} values of 23.63 μM, 18.79 μM and 23.81 μM against TNF-α, IL-6 and IL-1β, respectively. Compound **9d**, exhibited IC_{50} values of 36.31 μM, 16.04 μM and 29.99 μM against TNF-α, IL-6 and IL-1β, respectively. The natural compound cleomiscosin A (**15)** showed IC_{50} values of 39.89 μM, 12.67 μM and 57.7 μM against TNF-α, IL-6 and IL-1β, respectively. The fused-cyclic synthetic coumarinolignan compounds were found to be potentially active than the natural coumarinolignan (**15**) and individual coumarin **1a** and cinnamate derivatives **3b, 4b** and **5b**. In addition all compounds effectively decreased the LPS-stimulated NO levels and were found to be non-cytotoxic against the macrophages.

Further, the molecules were tested under in-vivo animal models with various inflammatory inducers like LPS, carrageenan and oxalate crystals following standard protocols (BITS-Hyd/IAEC/2017/09 and BITS-Hyd/IAEC/2017/23). Under LPS-stimulated mouse endotoxemia model, all the tested compounds (**9d**, **10d**, **11d**, **11e and 15**) were found to be significantly reducing the expression of pro-inflammatory cytokines at an oral dose of 50 mg/kg ($P < 0.01$). The compound **10d** showed a striking 66.41 % inhibition of IL-1β, 62.56 % inhibition of TNF-α and 43.15 % of IL-6 concentration in plasma. Interestingly, all the synthesised compounds of fused-cyclic coumarin-based lignans exhibited more than 50 % inhibition of secretion of IL-1β. The tested compounds significantly reduced expression of IL-1β in peritoneal lavage also ($P < 0.0001$). There was a remarkable 67.95% reduction of LPS-induced IL-1β concentration in peritoneal lavage by compound **10d**, 63.57% reduction by **9d**, 57.31% reduction by compound **11e** and 50.80 % reduction by compound **11e**.

Further, the compound **10d**, which was found to exhibit highly significant activity against all the tested cytokines was subjected for a dose dependent study under mouse endotoxemia model.

Compound **10d**, demonstrated activity at 10 mg/kg (33.94% - IL-1β and 19.2% - TNF-α) and 30 mg/kg (48.38% - IL-1β, 33.36% - TNF-α, and 19.01%-IL- 6) body weight as well.

All the tested compounds at 50 mg/kg body weight were found to be effectively reducing the expression of pro-inflammatory cytokines in carrageenan inflamed-paw homogenates. The compound **10d** showed 50.03% inhibition of TNF-α and 36.58% inhibition of IL-1β levels in inflamed-paw homogenate. Compound **11e** displayed 54.90 % of TNF-α and 48.46% inhibition of IL-1β. Compounds **9d** and **11d**, respectively exhibited 88.63% and 45.18% of TNF-α and 43.42% and 43.84% inhibition of IL-1β in inflamed-paw homogenate.

Additionally, the compounds at 50 mg/kg body weight were found to be effectively reducing the paw volume when measured using digital plethysmometer. Compound **10d** controlled the induced edema for the early 2 h effectively. In the other case, animals injected with compound **11e**, were found to be effective after one hour of induction and the effect was sustaining for another two hours.

On observing the inhibition effect against IL-1β by the newly synthesized compounds, the study was directed to test the potency against renal inflammation through oxalate-induced animal model. Compound **10d** significantly reduced the elevated levels of blood urea nitrate (BUN) at a dose of 50 mg/kg ($P < 0.0001$ vs oxalate control), indicating the protection of renal function against the damage induced by oxalate nephropathy. The compound **10d** showed 49.95 % inhibition of elevated plasma BUN compared to oxalate nephropathy control group and 37.5 % inhibition of plasma IL-1β levels.

Further, compound **10d** attenuated renal injury as displayed by the reduction in the renal RNA expression of IL-1β, IL-6, TNF-α (pro-inflammatory markers) and KIM-1 (renal injury marker).

Also, compound **10d** exhibited protection of renal tissue as determined through histological analysis performed by H&E staining. The treatment with this compound significantly reduced tubular dilation, tubular necrosis and cast.

The outcome of the Phase II study disclosed compound **10d** as potentially active inhibitor under various inflammatory animal models showing dose dependent activity. Nevertheless other new compounds, **9d**, **11d** and **11e** were also found to be potentially active under in-vitro studies, LPS-induced mouse endotoxemia and carrageenan induced paw edema models. A structure activity relationship study revealed that the dihydroxyl groups in the phenyl ring of lignans are essential for the activity. Also, esterification of lignans and presence of 4-methyl substituent in coumarin has some role in enhancing the activity as observed by comparison of the activity with cleomiscosin A (**15**).

Phase III: Synthesis, in-vitro, in-vivo and docking studies on glucoside of cleomiscosin A, a natural coumarinolignan

In Phase III, attempts were made to improve the hydrophilic property and pro-inflammatory cytokine inhibitory effect of cleomiscosin A (**15**), a naturally occurring coumarinolignan derived from plants. In view of this, *O*-glucoside of cleomiscosin A (**15g**) was synthesized by reacting natural cleomiscosin A (isolated from *Cleome viscosa* seeds) with acetobromo-α-D-glucose and pyridine. The formed product was confirmed through APCI-MS and proton NMR analysis.

Inhibition effect of **15** and **15g** against TNF-α, IL-6 and IL-1β secretions was determined on LPS-induced RAW 264.7 cells using ELISA kits. Compound **15g** was potentially inhibitory against IL-6 and IL-1β secretions exhibiting IC_{50} values of 7.94 and 45.76 μM, respectively. Also, in-vivo (mouse endotoxemia model) performance of glucoside (oral administration) in

inhibiting TNF-α expression was significant ($P < 0.0001$) (52.03 % and 29.23 % at 50 and 25 mg/kg body weight, respectively), demonstrating five-fold increase in activity compared to its parent cleomiscosin A (**15**). In addition, **15g** reduced LPS-induced NO levels and was found to be weakly cytotoxic ($IC_{50} > 150$ μM).

Further, in order to understand the putative binding pattern of 9′-*O*-glucoside of cleomiscosin A (**15g**) over the pro-inflammatory proteins TNF-α, IL-1β and IL-6, docking studies were performed. Excellent GOLDScore_fitness was displayed by **15g** (TNF-α - 61.466, IL-1β - 58.24 and IL-6 - 44.84). This is the first report of semi-synthesis and pro-inflammatory cytokine inhibition effect of a coumarinolignan glucoside.

Thus the present research work explored some novel potentially active coumarin-based lignans which can be developed further as drugs for treating various chronic inflammatory diseases such as osteoarthritis, rheumatoid arthritis, crystal induced inflammation, ischemic injury, peripheral nerve damage and pain, progression of other autoimmune diseases, etc.

Future Perspectives

The anti-inflammatory activity of synthesized novel coumarin-based lignans and cleomiscosin A glucoside could be tested under other chronic inflammatory disease models to explore their efficacy further.

Pharmacokinetics of the synthesized novel coumarin-based lignans and cleomiscosin A glucoside could be evaluated.

Toxicity studies of these compounds could be performed

Oral Formulations for these compounds can be developed and evaluated.

These compounds can be used as lead molecules for synthesizing more active analogues in future.

REFERENCES

REFERENCES

Ahmad N, Zeb F, Ahmad I, Wang F (2009) Repenins A–D, four new antioxidative coumarinolignoids from *Duranta repens* Linn. Bioorg Med Chem Lett 19:3521-3524.

Ahn JH, Hwang BY, Lee MK (2013) Simultaneous quantitation of nine constituents of *Fraxinus rhynchophylla* using high performance liquid chromatography - diode array detector. Nat Prod Sci 19:236-241.

Ahn JH, Shin E, Liu Q, Kim SB, Choi KM, Yoo HS, Hwang BY, Lee MK (2012) Lignan derivatives from *Fraxinus rhynchophylla* and inhibitory activity on pancreatic lipase. Nat Prod Sci 18:116-120.

Aichour S, Haba H, Benkhaled M, Harakat D, Lavaud C (2014) Terpenoids and other constituents from *Euphorbia bupleuroides*. Phytochem Lett 10:198-203.

Allosterix pharma (2011) Novel TACE inhibitor [database on the Internet]. 2011 Feb. http://www.allosterixpharma.com/TACE_marketing_document_February_2011-1.pdf.

Arulselvan P, Fard MT, Tan WS, Gothai S, Fakurazi S, Norhaizan ME, Kumar SS (2016) Role of antioxidants and natural products in inflammation. Oxid Med Cell Longev 2016 doi: 10.1155/2016/5276130

Bai B, Gu XW, Chen Y, Guan FQ, Shan Y, Feng X (2015) Virginicin, a new naphthalene from *Kosteletzkya virginica* (Malvaceae). J Braz Chem Soc 26:1-9.

Barnes PJ (2013) New anti-inflammatory targets for chronic obstructive pulmonary disease. Nat Rev Drug Discov 12:543-559.

Barnes PJ (2018) Targeting cytokines to treat asthma and chronic obstructive pulmonary disease. Nat Rev Immunol. doi: 10.1038/s41577-018-0006-6

Bawankule DU, Chattopadhyay SK, Pal A, Saxena K, Yadav S, Faridi U, Darokar MP, Gupta AK, Khanuja SPS (2008) Modulation of inflammatory mediators by coumarinolignoids from *Cleome viscosa* in female swiss albino mice. Inflammopharmacology 16:272-277.

Beavers C, Adams A (2010) New and upcoming biological agents for rheumatoid arthritis Orthopedics 33 doi: 10.3928/01477447-20091124-18

Begum S, Sahai M, Suessmuth R, Asai T, Hara N, Fujimoto Y (2006) Hyosgerin, a new optically active coumarinolignan from the seeds of *Hyoscyamus niger*. Chem Pharm Bull 54:538-541.

Begum S, Saxena B, Goyal M, Ranjan R, Joshi VB, Rao CV, Krishnamurthy S, Sahai M (2010) Study of anti-inflammatory, analgesic and antipyretic activities of seeds of *Hyoscyamus niger* and isolation of a new coumarinolignan. Fitoterapia 81:178-184.

Begum SA (2010a) Bioactive non-alakloidal secondary metabolites of *Hyoscyamus niger* Linn. Research Journal of Seed Science 3:210-217.

Begum SA, Sahai M, Ray AB (2010) Non-conventional lignans: coumarinolignans, flavonolignans, and stilbenolignans. In: Kinghorn AD, Falk H, Kobayashi J (Eds.), Progress in the Chemistry of Organic Natural Products. Springer, Verlag/Wien, pp.1-70.

Belgi G, Friedmann PS (2002) Traditional therapies: glucocorticoids, azathioprine, methotrexate, hydroxyurea. Clin Exp Dermatol 27:546-554.

Bisht K, Wagner K-H, Bulmera AC (2010) Curcumin, resveratrol and flavonoids as anti-inflammatory, cyto- and DNA-protective dietary compounds. Toxicology 278:88-100.

Cao S, Brodie PJ, Callmander M, Randrianaivo R, Rakotobe E, Rasamison VE, Kingston DGI (2010) Saponins and a lignan derivative of *Terminalia tropophylla* from the Madagascar dry forest. Phytochemistry 71:95-99.

Chakraborti AK, Gulhane R (2003) Perchloric acid adsorbed on silica gel as a new, highly efficient, and versatile catalyst for acetylation of phenols, thiols, alcohols, and amines. Chem Commun 1896-1897.

Chan DS-H, Lee H-M, Yang F, Che C-M, Wong CCL, Abagyan R, Leung C-H, Ma D-L (2010) Structure-based discovery of natural-product-like TNF-α inhibitors. Angew Chem Int Ed 49:2860-2864.

Chen D-L, Li G, Liu Y-Y, Ma G-X, Zheng W, Sun X-B, Xu X-D (2018) A new cadinane sesquiterpenoid glucoside with cytotoxicity from *Abelmoschus sagittifolius*. Nat Prod Res doi: 10.1080/14786419.2018.1431635

Chen JJ, Wang TY, Hwang TL (2008) Neolignans, a coumarinolignan, lignan derivatives, and a chromene: Anti-inflammatory constituents from *Zanthoxylum avicennae*. J Nat Prod 71:212-217.

Chen QJ, Ouyang MA, Tan QW, Zhang ZK, Wu ZJ, Lin QY (2009) Constituents from the seeds of *Brucea javanica* with inhibitory activity of tobacco mosaic virus. J Asian Nat Prod Res 11:539-547.

Chen YF, Jobanputra P, Barton P, Bryan S, Fry-Smith A, Harris G, Taylor RS (2008) Cyclooxygenase-2 selective non-steroidal anti-inflammatory drugs (etodolac, meloxicam, celecoxib, rofecoxib, etoricoxib, valdecoxib and lumiracoxib) for osteoarthritis and rheumatoid arthritis: a systematic review and economic evaluation Health Technol Assess 12:1-278.

Cheng J-F, Chen M, Wallace D, Tith S, Arrhenius T, Kashiwagi H, Ono Y, Ishikawa A, Sato H, Kozono T, Satob H, Nadzana AM (2004) Discovery and structure–activity relationship of coumarin derivatives as TNF-a inhibitors. Bioorg Med Chem Lett 14:2411-2415.

Cheng L, Zhang X, Zhang M, Zhang P, Song Z, Ma Z, Cheng Y, Qu H (2009) Characterization of chemopreventive agents from the dichloromethane extract of *Eurycorymbus cavaleriei* by liquid chromatography–ion trap mass spectrometry. J Chromatogr A 1216:4859-4867.

Choi Y, Park SK, Kim HM, Kang JS, Yoon YD, Han SB, Han JW, Yang JS, Han G (2008) Histone deacetylase inhibitor KBH-A42 inhibits cytokine production in RAW 264.7 macrophage cells and in vivo endotoxemia model. Exp Mol Med 40:574-581.

Choy EH, Panayi GS (2001) Cytokine pathways and joint inflammation in rheumatoid arthritis. N Engl J Med, 344:907-916.

Coleman JW (2002) Nitric oxide: a regulator of mast cell activation and mast cell-mediated inflammation. Clin Exp Immunol 129:4-10.

Correa H, Valenzuela AL, Ospina LF, Duque C (2009) Anti-inflammatory effects of the gorgonian *Pseudopterogorgia elisabethae* collected at the islands of Providencia and San Andrés (SW Caribbean). J Inflamm (Lond) 6:5. doi: 10.1186/1476-9255-6-5

Das B, Ravikanth B, Reddy KR, Thirupathi P, Raju TV, Sridhar B (2008) Diterpenoids from *Jatropha multifida*. Phytochemistry 69:2639-2641.

Demirkiran O, Topcu G, Azarpira A, Choudhary MI (2014) Tyrosinase inhibitory activity of chemical constituents of *Euphorbia macrostegia*. Chem Nat Compd+ 50:810-813.

Dentener MA (2008) Effect of infliximab on local and systemic inflammation in chronic obstructive pulmonary disease: a pilot study. Respiration 76:275-282.

Dhimolea E (2010) Canakinumab. MAbs 2:3-13.

Dinarello CA (2000) Proinflammatory cytokines. Chest 118:503-508

Dinarello CA (2010) Anti-inflammatory agents: present and future. Cell 140:935-950.

Donfack ARN, Tala MF, Wabo HK, Jerz G, Zeng GZ, Winterhalter P, Tan NH, Tane P (2014) Two new anthraquinone dimers from the stem bark of *Pentas schimperi* (Rubiaceae). Phytochem Lett 8:55-58.

Drake VJ, Online Two faces of inflammation [database on the Internet]. Linus Pauling Institute Oregon State University. [updated May 2007]. http://lpi.oregonstate.edu/ss07/inflammation.html during wound healing. Cell Mol Life Sci 73:3861-3885.

Dzoyem JP, Donfack ARN, Tane P, McGaw1 LJ, Eloff JN (2016) Inhibition of nitric oxide production in LPS-stimulated RAW264.7 macrophages and 15 LOX activity by anthraquinones from *Pentas schimperi*. Planta Med. https://doi.org/10.1055/s-0042-104417

El-Haggar R, Al-Wabli RI (2015) Anti-inflammatory screening and molecular modeling of some novel coumarin derivatives. Molecules 20:5374-5391.

Ellis A, Bennett DLH (2013) Neuroinflammation and the generation of neuropathic pain. Br J Anaesth 111:26-37.

Erwin, Noor A, Soekamto NH, Altena IV, Syah YM (2014) Waltherione C and cleomiscosin from *Melochia umbellata* var. Degrabrata K. (Malvaceae), biosynthetic and chemotaxonomic significance. Biochem Syst Ecol 55:358-361.

Feng J, Wang Y, Yi X, Yang W, He X (2016) Phenolics from durian exert pronounced NO inhibitory and antioxidant activities. J Agr Food Chem https://doi.org/10.1021/acs.jafc.6b01580

Ferheen S, Rehman A-U, Rasool MA, Naqvi B, Imran M, Khan RA, Kalhoro MA, Malik A (2014) Anti-tuberculosis coumarinolignans from *Daphne mucronata*. Asian J Chem 26:7262-7264.

Fylaktakidou KC, Hadjipavlou-Litina DJ, Litinas KE, Nicolaides DN (2004) Natural and synthetic coumarin derivatives with anti-Inflammatory/antioxidant activities. Curr Pharm Des 10:3813-3833.

Godoy ME, Rotelli A, Pelzer L, Tonn CE (2000) Antiinflammatory activity of cinnamic acid esters. Molecules 5:547-548.

Gray SM, Bloch MH (2012) Systematic Review of proinflammatory cytokines in cbsessive-compulsive disorder. Curr Psychiatry Rep 14:220-228.

Grover J, Jachak SM (2015) Coumarins as privileged scaffold for anti-Inflammatory drug development. RSC Adv 5:38892-38905.

Han HE, Kim TK, Son HJ, Park WJ, Han PL (2013) Activation of autophagy pathway suppresses the expression of iNOS, IL6 and cell death of LPS-stimulated microglia cells. Biomol Ther 21:21-28.

He ZZ, Yan JF, Song ZJ, Ye F, Liao X, Peng SL, Ding LS (2009) Chemical constituents from the aerial parts of *Artemisia minor*. J Nat Prod 72:1198-1201.

Howard M, Muchamuel T, Andrade S, Menon S (1993) Interleukin 10 protects mice from lethal endotoxemia. J Exp Med 177:1205-1208.

Hsiao P-Y, Lee S-J, Chen I-S, Hsu H-Y, Chang H-S (2016) Cytotoxic cardenolides and sesquiterpenoids from the fruits of *Reevesia formosana*. Phytochemistry doi: org/10.1016/j.phytochem.2016.06.009

Iwalewa EO, McGaw LJ, Naidoo V, Eloff JN (2007) Inflammation: the foundation of diseases and disorders. A review of phytomedicines of South African origin used to treat pain and inflammatory conditions. Afr J Biotechnol 6:2868-2885.

Kan S, Chen G, Han C, Chen Z, Song X, Ren M, Jiang H (2011) Chemical constituents from the roots of *Xanthium sibiricum*. Nat Prod Res 25:1243-1249.

Kang YM, Lee NH (2011) A new isoflavone glycoside from the stems of *Tilia taquetii* Schneider. Bulletin of the Korean Chemical Society 32:1048-1050.

Katsori A-M, Hadjipavlou-Litina D (2014) Coumarin derivatives: an updated patent review (2012 -- 2014). Expert Opin Ther Pat 24:1323-1347.

Kaushik U, Aeri V, Mir SR (2015) Cucurbitacins – An insight into medicinal leads from nature. Pharmacogn Rev 9:12-18.

Khan R, Basha A, Ragavendra G, Rao PC, Tanemura Y, Fujimoto Y, Begum AS, (2015) Attenuation of TNF-α secretion by L-proline-based cyclic dipeptides produced by culture broth of *Pseudomonas aerugenosa*. Bioorg Med Chem Lett 25:5756-5761.

Klareskog L, Catrina AI, Paget S (2009) Rheumatoid arthritis. The Lancet 373:659-672.

Kren V, Kubisch J, Sedmera P, Halada P, Prikrylová V, Jegorov A, Cvak L, Gebhardt R, Ulrichová J, Simánek V (1997) Glycosylation of silybin. J Chem Soc Perkin Trans 1:2467-2474.

Kuang HX, Xia YG, Yang BY, Wang QH, Lü SW (2009) Lignan constituents from *Chloranthus japonicus* Sieb. Archives of Pharmacal Research 32:329-334.

Kuboki A, Maeda C, Arishige T, Kuyama K, Hamabata M, Ohira S (2008b) Total synthesis of cleomiscosin C via a regioselective cycloaddition reaction of o-quinone. Tetrahedron Lett 49:4516–4518.

Kuboki A, Yamamoto T, Taira M, Arishige T, Konishi R, Hamabata M, Shirahama M, Hiramatsu T, Kuyama K, Ohira S (2008a) Reversal of the regioselectivity in a cycloaddition of o-quinones by varying the position of alkoxy substituents. Tetrahedron Lett 49:2558–2561.

Kulkarni RG, Achaiah G, Sastry GN (2006) Novel targets for anti-inflammatory and anti-arthritic agents. Curr Pharm Des 12:2437-2454.

Lampiasi N, Montana G (2016) The molecular events behind ferulic acid mediated modulation of IL-6 expression in LPS-activated Raw 264.7 cells. Immunobiology 221:486-493.

Landskron G, la Fuente MD, Thuwajit P, Thuwajit C, Hermoso MA (2014) Chronic inflammation and cytokines in the tumor microenvironment. J Immunol Res Ther 2014:1-19.

Lee DM, Weinblatt ME (2001) Rheumatoid arthritis The Lancet 358:903-911.

Leung L, Cahill CM (2010) TNF-alpha and neuropathic pain–a review. J Neuroinflammation 7: 27 doi: 10.1186/1742-2094-7-27

Li D, Jiang YY, Jin ZM, Li HY, Xie HJ, Wu B, Wang KW (2016) Isolation and absolute configurations of diastereomers of 8α-hydroxy-T-muurolol and (1α,6β,7β)-cadinane-4-en-8α,10α-diol from *Chimonanthus salicifolius*. Phytochemistry 122:294-300.

Liu B, Xu YK (2015) Cytotoxicity and synergistic effect of the constituents from roots of *Aglaia odorata* (Meliaceae). Nat Prod Res. doi.org/10.1080/14786419.2015.1016940

Liu H-B, Zhang H, Yu J-H, Yue J-M (2016) New diterpenoids from *Sapium discolor*. J Asian Nat Prod Res https://doi.org/ 10.1080/10286020.2015.1119665

Li-Weber M, Giaisi M, Treiber MK and Krammer PH (2002) The anti-inflammatory sesquiterpene lactone parthenolide suppresses IL-4 gene expression in peripheral blood T cells. Eur J Immunol 32:3587-3597.

Maffo T, Melong R, Nganteng DND, Wafo P, Ali MS, Ngadjui BT (2018) Neomacrodione: a new degraded diterpenoid from the roots of *Neoboutonia macrocalyx* Beng (Euphorbiaceae). Nat Prod Res 32:85-90.

Maheswara M, Siddaiah V, Damu GLV, Rao YK, Rao CV (2006) A solvent-free synthesis of coumarins via Pechmann condensation using heterogeneous catalyst. J Mol Catal A- Chem 255: 49-52.

Mastihubová M, Poláková M (2016) A selective and mild glycosylation method of natural phenolic alcohols. Beilstein J Org Chem 12:524-530.

Mclnnes LB, Schett G (2011) The pathogenesis of rheumatoid arthritis. N Engl J Med 365:2205-2219.

Michael RD (1980) Oxidation of selenides and tellurides with positive halogenating species. J Org Chem 45:274-279.

Michalet S, Payen-Fattaccioli L, Beney C, Cegiela P, Bayet C, Cartier G, Noungoue-Tchamo D, Tsamo E, Mariotte AM, Dijoux-Franca MG (2008) New components including cyclopeptides from barks of *Christiana Africana* DC. (Tiliaceae). Helv Chim Acta 91:1106-1117.

Morris CJ (2003) Carrageenan-induced paw edema in the rat and mouse. In: Winyard PG, Willoughby DA (Eds.), Inflammation Protocols. Methods in Molecular Biology, Humana Press, pp. 115-121

Mosmann T (1983) Rapid colorimetric assay for cellular growth and survival: application to proliferation and cytotoxicity assays. J Immunol Methods 65:55-63.

Mulay SR, Kulkarni OP, Rupanagudi KV, Migliorini A, Darisipudi MN, Vilaysane A, Muruve D, Shi Y, Munro F, Liapis H (2013) Calcium oxalate crystals induce renal inflammation by NLRP3-mediated IL-1β secretion. J Clin Investig 123:236-246.

Nakashima KI, Oyama M, Ito T, Akao Y, Witono JR, Darnaedi D, Tanaka T, Murata J, Iinuma M (2012) Novel quinolinone alkaloids bearing a lignoid moiety and related constituents in the leaves of *Melicope denhamii*. Tetrahedron 68:2421-2428.

Nathan C, Ding A (2010) Nonresolving Inflammation. Cell 140:871-882.

Oka T, Aou S, Hori T (1994) Intracerebroventricular injection of interleukin-1 beta enhances nociceptive neuronal responses of the trigeminal nucleus caudalis in rats. Brain Res 656:236-244.

Ouyang X, Ghani A, Malik A, Wilder T, Colegio OR,. Flavell RA, Cronstein BN, Mehal WZ (2013) Adenosine is required for sustained inflammasome activation via the A2A receptor and the HIF-1a pathway. Nat Commun 4:1-9. doi: 10.1038/ncomms3909

Patel NK, Bhutani KK (2014) Suppressive effects of *Mimosa pudica* (l.) constituents on the production of LPS-induced pro-inflammatory mediators. EXCLI J 13:1011-1021.

Pavan R, Jain S, Shraddha, Kumar A (2012) Properties and therapeutic application of bromelain: A Review. Biotechnol Res Int 2012. doi: 10.1155/2012/976203

Ranjan R, Sahai M (2009) Coumarinolignans from the seeds of *Annona squamosa* Linn. E-J Chem 6:518-522.

Rasool MA, Khan R, Malik A, Bibib N, Kazmib SU (2010) Structural determination of daphnecin, a new coumarinolignan from *Daphne mucronata*. J Asian Nat Prod Res 12:324-327.

Ren K, Torres R (2009) Role of interleukin-1beta during pain and inflammation. Brain Res Rev 60:57-64.

Rubio-Perez JM, Morillas-Ruiz JM (2012) A review: inflammatory process in Alzheimer's disease, role of cytokines. Scientific World Journal 2012:1-15.

Scarpignato C, Lanas A, Blandizzi C, Lems WF, Hermann M, Hunt RH and For the International NSAID Consensus Group (2015) Safe prescribing of non-steroidal anti-inflammatory drugs in patients with osteoarthritis – an expert consensus addressing benefits as well as gastrointestinal and cardiovascular risks. BMC Med 13:55. doi: 10.1186/s12916-015-0285-8

Scott DL (2012) Biologics-based therapy for the treatment of rheumatoid arthritis. Clin Pharmacol Ther 91:30-43.

Scott DL, Wolfe F, Huizinga TW (2010) Rheumatoid arthritis. Lancet 376:1094-1108.

Sharma S, Chattopadhyay SK, Trivedi P, Bawankule DU (2010) Synthesis and anti-inflammatory activity of derivatives of coumarino-lignoid, cleomiscosin A and its methyl ether. Eur J Med Chem 45:5150-5156.

Sharma S, Chattopadhyay SK, Yadav DK, Khan F, Mohanty S, Maurya A, Bawankule DU (2012) QSAR, docking and *in vitro* studies for anti-inflammatory activity of cleomiscosin A methyl ether derivatives. Eur J Pharm Sci 47:952-964.

Sielinou VT, Vardamides JC, Nkengfack AE, Laatsch H (2012) Phenolic derivatives and an antifungal and cytototoxic labdane diterpenoid from the root bark of *Turraeanthus mannii*. Phytochem Lett 5:409-413.

Soh RF, Bankeu JK, Lenta BN, Mbaning BM, Ngouela S, Tsamo E, Sewald N (2009) Antibacterial ellagic acid derivatives and other constituents from *Pancovia pedicellaris*. Z Naturforsch B 64b:1070-1076.

Spooren A, Kolmus K, Laureys G, Clinckers R, Keyser JD, Haegeman G, Gerlo S (2011) Interleukin-6, a mental cytokine. Brain Res Rev 67:157-183.

Strand V, Burmester GR, Ogale S, Devenport J, John A, Emery P (2012) Improvements in health-related quality of life after treatment with tocilizumab in patients with rheumatoid arthritis refractory to tumour necrosis factor inhibitors: results from the 24-week randomized controlled RADIATE study. Rheumatology 51:1860-1869.

Sun J, Zhang X, Broderick M, Fein H (2003) Measurement of nitric oxide production in biological systems by using Griess reaction assay. Sensors 3:276-284.

Tan T, Luo Y, Zhong C-C, Xu X, Feng Y (2017) Comprehensive profiling and characterization of coumarins from roots, stems, leaves, branches, and seeds of *Chimonanthus nitens* Oliv. using ultra-performance liquid chromatography/quadrupole-time-of-flight mass spectrometry combined with modified mass defect filter. J Pharm Biomed Anal. http://dx.doi.org/ 10.1016/j.jpba.2017.04.016

Tanaka H, Ishihara M, Ichino K, Ito K (1988) Synthesis of natural coumarinolignans: Oxidative coupling of 7,8-dihydroxycoumarins and phenylpropenes in the presence of diphenyl selenoxide. Heterocycles 27: 2651-2658.

Tandon S, Chatterjee A, Chattopadhyay SK, Kaur R, Gupta AK (2010) Pilot scale processing technology for extraction of Cliv-92: A combination of three coumarinolignoids cleomiscosins A, B and C from *Cleome viscosa*. Ind Crops Prod 31:335-343.

Taniguchi K, Karin M (2018) NF‑κB, inflammation, immunity and cancer: coming of age. Nat Rev Immunol doi:10.1038/nri.2017.142

Tedgui A, Mallat Z (2001) Anti-inflammatory mechanisms in the vascular wall. Cir Res 88:877-887.

Testa B (2006) Prodrug objectives and design. In: Taylor JB, Triggle DJ (Eds.), Comprehensive Medicinal Chemistry II Volume 5: ADME-Tox Approaches. Elsevier, pp. 1009-1041.

Torres MCM, Braz-Filho R, Silveira ER, Diniz JC, Viana FA, Pessoa ODL (2010) Terpenoids from *Croton regelianus.* Helv Chim Acta 93:375-381.

Tsokos GC (2011) Systemic Lupus Erythematosus. N Engl J Med 365:2110-2121.

Turner MD, Nedjai B, Hurst T, Pennington DJ (2014) Cytokines and chemokines: At the crossroads of cell signalling and inflammatory disease. Biochim Biophys Acta. doi: 10.1016/j.bbamcr.2014.05.014

Uddin G, Ullah W, Siddiqui BS, Shah SQ (2013) Grewialin and optivanin new constituents from the stem bark of *Grewia optiva* Drummond ex Burret (Tiliaceae). Nat Prod Res 27:215-220.

van Meerloo J, Kaspers GJL, Cloos J (2011) Cell sensitivity assays: the MTT assay. In: Cree I (Eds.), Cancer Cell Culture. Methods in Molecular Biology (Methods and Protocols). Humana Press, pp. 237-245.

Wang H, Bloom O, Zhang M, Vishnubhakat JM, Ombrellino M, Che J, Frazier A, Yang H, Ivanova S, Borovikova L Manogue KR, Faist E, Abraham E, Andersson J, Andersson U, Molina PE, Abumrad NN, Sama A, Tracey KJ (1999) HMG-1 as a late mediator of endotoxin lethality in mice. Science 285:248-251.

Wang KW, Li D, Wu B, Cao XJ (2016) New cytotoxic dimeric and trimeric coumarins from *Chimonanthus salicifolius*. Phytochem Lett 16:115-120.

Xiang-Yun Z, Xiang-Hai C, Xiao-Dong L (2012) Chemical constituents of *Allophylus longipes*. Chin J Nat Med 10:36-39.

Xu JF, Feng ZM, Liu J, Zhang PC (2008) New hepatoprotective coumarinolignoids from *Mallotus apelta*. Chem Biodivers 5:591-597.

Yadav NP, Chanda D, Chattopadhyay SK, Gupta AK, Pal A (2010) Hepatoprotective effects and safety evaluation of coumarinolignoids isolated from *Cleome viscosa* seeds. Indian J Pharm Sci 72:759-765.

Yamada K, Subeki, Nabeta K, Yamasaki M, Katakura K, Matsuura H (2009) Isolation of antibabesial compounds from *Brucea javanica*, *Curcuma xanthorrhiza* and *Excoecaria cochinchinensis*. Biosci Biotechnol Biochem 73:776-780.

Yang J, Liu W, Li S, Ye H, Tang H, Chen L, Peng A (2014) Coumarinolignans isolated from the seeds of *Brucea javanica*. Helv Chim Acta 97:278-282.

Yang Y, Zhang X, Yu B (2015) O-Glycosylation methods in the total synthesis of complex natural glycosides. Nat Prod Rep 32:1331-1355.

Yim SH, Jung DW, Williams DR, Geckeler KE, Kim KK, Shin BA, Lee IS, Kim HJ (2015) Anti-proliferative effects of β-cyclodextrin inclusion complexes with coumarinolignans from *Acer mono*. Korean J Pharmacogn 46:133-139.

Yin HL, Li JH, Li J, Li B, Chen L, Tian Y, Liu SJ, Zhang T, Dong JX (2013) Four new coumarinolignoids from seeds of *Solanum indicum*. Fitoterapia 84:360-365.

Yoshikawa K, Kawahara Y, Arihara S, Hashimoto T (2011) Aromatic compounds and their antioxidant activity of *Acer saccharum*. J Nat Med 65:191-193.

Yuan G, Wahlqvist ML, He G, Yang M, Li D (2006) Natural products and anti-inflammatory activity. Asia Pac J Clin Nutr 15:143-152.

Zhang H, Song ZJ, Chen WQ, Wu XZ, Xu HH (2012) Chemical constituents from *Aglaia odorata* Lour. Biochem Syst Ecol 41:35-40.

Zhang H, Yan D, Shi X, Liang H, Pang Y, Qin N, Chen H, Wang J, Yin B, Jiang X, Feng W, Zhang W, Zhou M, Li Z (2008) Transmembrane TNF-alpha mediates "forward" and "reverse" signaling, inducing cell death or survival via the NF-kappaB pathway in Raji Burkitt lymphoma cells. J Leukoc Biol 84:789-797.

Zhang J-M, An J (2007) Cytokines, inflammation and pain. Int Anesthesiol Clin 45:27-37.

Zhang ML, Irwin D, Li XN, Sauriol F, Shi XW, Wang YF, Huo CH, Li LG, Gu YC, Shi QW (2012) PPARγ agonist from *Chromolaena odorata.* J Nat Prod doi: 10.1021/np300386d

Zhang X, Song Y, Ci X, An N, Ju Y, Li H, Wang X, Han C, Cui J, Deng X (2008) Ivermectin inhibits LPS-induced production of inflammatory cytokines and improves LPS-induced survival in mice. Inflamm Res 57:524-529.

Zhao M, Lau ST, Zhang XQ, Ye WC, Leung PS, Che CT, Lin ZX (2011) Bruceines K and L from the ripe fruits of *Brucea javanica*. Helv Chim Acta 94:2099-2105.

Zhou K, Chen D, Li B, Zhang B, Miao F, Zhou L (2017) Bioactivity and structure-activity relationship of cinnamic acid esters and their derivatives as potential antifungal agents for plant protection. PLoS ONE. doi.org/10.1371/journal.pone.0176189

APPENDIX

LIST OF PUBLICATION FROM THESIS WORK

Patent Filed

1. Ahil Sajeli Begum, Santosh Kumar S, Onkar P. Kulkarni and Kirti Hira. Indian Patent Application No. TEMP/E-1/18152/2018-DEL (Ref. No. 201811017168). Title: Compounds as Pro-inflammatory cytokine inhibitor (2018/05/07)

Articles

2. Ahil Sajeli Begum, S. Santhosh Kumar, SuryanarayanaGottapu, KirtiHira (2018) O-Glucoside of natural cleomiscosin-A: An attenuator of pro-inflammatory cytokine production. Phytochemistry Letters 26:83-87.
3. Santhosh Kumar S, Sajeli Begum A (2018) Advances in the chemistry and pharmacological potential of coumarinolignans. Topics in Current Chemistry – Springer. (Accepted)
4. S Santhosh Kumar, Ahil Sajeli Begum, Kirti Hira, Sarfaraj Niazi, B.R. Prashantha Kumar (2018) Molecular docking studies and implications on methyl coumarin and phenyl propanoid derivatives towards developing novel pro-inflammatory cytokines (TNF-α, IL-6 and IL-1β) inhibitors. (Communicated)

OTHER PUBLICATIONS

1. Ameer Basha, Sajeli Begum, Govardhanam Ragavendra, Mahibalan Senthi, Rukaiyya Khan, Ravi Sojitra, Santhosh Kumar, Asalla Srinivas, "Antifungal effect and protective role of ursolic acid and three phenolic derivatives in the management of Sorghum grain mold under field conditions" Chemistry and BioDiversity, 2016, 13(9), 1158-1164. doi: 10.1002/cbdv.201500515.

LIST OF POSTER PRESENTATIONS IN CONFERENCES

1. Synthesis of O-glucoside of natural cleomiscosin-A as TNF-α inhibitor. Presented at the 68th Indian Pharmaceutical Congress held at Andhra University, Vizag during 16thdec 2016 to 18thdec 2016.
2. Tumor necrosis factor-alpha inhibitory activity of *H. pinifolia*. Presented at 24th ISCB International conference held at Manipal University, Jaipur during 11th Jan 2018 to 13th Jan 2018.

BIOGRAPHY OF SANTHOSH KUMAR S

Santhosh Kumar. S completed his B.Pharm degree in the year 2008 from RVS College of Pharmaceutical Sciences, Sulur affiliated to The Tamil Nadu Dr. M.G.R. Medical University, Chennai. He completed his M.Pharm degree in the year 2010 from JSS College of Pharmacy, Ooty affiliated to JSS University, Mysore. He worked as lecturer for 2 years 2 months in Pharmaceutical Chemistry Department, SRM College of Pharmacy, Kattankulathur. Later he continued as lecturer in Quality Assurance Department, Siddaganga College of Pharmacy, Tumkur, Karnataka. In Sep 2012, he joined as research scholar and registered for Ph.D in BITS-Pilani Hyderabad Campus under supervision of Prof. A. Sajeli Begum. As a part of research achievements he has contributed to 5 international publications till date.

BRIEF BIOGRAPHY OF THE SUPERVISOR

Dr. Ahil Sajeli Begum is currently an Associate Professor in Department of Pharmacy, Birla Institute of Technology and Science, Pilani-Hyderabad Campus. She received her B.Pharm degree (1999) from The Tamilnadu Dr. M.G.R. Medical University, Chennai and M.Pharm degree (2001) in Pharmaceutical Chemistry from Institute of Technology-Banaras Hindu University (IT-BHU), Varanasi. She as awarded with Ph.D. degree (2005) by BHU for her thesis work on "Chemical Investigation of Solanaceous Plants". Prof. AS Begum is a recipient of the Deutscher Akademischer Austausch Dienst (DAAD) Fellowship (2004) to pursue research at Eberhard Karls University, Tubingen, Germany. Soon after completing her Ph.D. program, she joined in Department of Pharmaceutics at IT-BHU, Varanasi as an Assistant Professor and then moved to BITS-Pilani Hyderabad in mid-2010. She has 13 years of experience in teaching and research. She has successfully completed two research projects funded by University Grants Commission (UGC) – New Delhi and Council of Scientific and Industrial Research-New Delhi. Presently she is handling two sponsored projects granted by DST and ICMR-ICSSR-New Delhi. She has 36 publications to her credit and authored a book chapter in "Progress in the Chemistry of Organic Natural Products" published by Springer Wien New York. Prof AS Begum is a life time member of various scientific forums like Association of Pharmaceutical Teachers of India (APTI), Indian Pharmacy Graduates Association (IPGA), Indian Chemical Society, etc. She has successfully guided three Ph.D students and currently supervising four students for their doctoral thesis work.